



Cyclic strain-mediated regulation of
thrombomodulin expression and release
from human aortic endothelial cells

A dissertation submitted for the degree of Ph.D by

Fiona A. Martin, B.Sc

Under the supervision of Dr. Philip M. Cummins

August 2013

School of Biotechnology, Dublin City University, Dublin 9, Ireland

Declaration:

I hereby certify that this material, which I now submit for assessment on the programme of study is entirely my own work, that I have exercised reasonable care to ensure that the work is original, and does not to the best of my knowledge breach any law of copyright, and has not been taken from the work of others save and to the extent that such work has been cited and acknowledged within the text of my work.

Signature: _____

Student I.D: 58116699

Date: _____

Acknowledgements

Completing my Ph.D degree is probably the most challenging activity I have undertaken so far in my life. The best and worst moments of my doctoral journey have been shared with many people. It has been a great privilege to spend several years in the School of Biotechnology at Dublin City University, and its members will always remain dear to me.

First and foremost, I would like to express my sincere gratitude to my supervisor Dr. Philip Cummins for the continuous support of my Ph.D study and research, for his patience, motivation, enthusiasm, humour and immense knowledge. I could not have imagined having a better advisor and mentor for my Ph.D study.

Dr. Ronan Murphy, too, was critical to the Ph.D process, providing encouraging advice and ideas throughout the years. In addition, I have to give a special thanks to Dr. Gerardene Meade for putting up with our constant chatter in the lab! I would also like to thank my examiners, Dr. Christine Loscher and Dr. Patricia Maguire, who delivered uplifting and constructive feedback. It is no easy task, reviewing a thesis, and I am grateful for their thoughtful and detailed comments. Dr. Loscher in particular allowed me the opportunity to undertake this Ph.D in by coordinating and organising the Therapeutics and Theranostics Ph.D programme and I am deeply grateful for this.

Ph.D students often talk about loneliness during the course of their study but this is something, which I never experienced at DCU. A heartfelt thanks has to go out to both past and present members of our group, which made the “basement” a very enjoyable and inviting place to work. In particular, I am indebted to Tony, Anthony, Paul, Mishan and Andrew for showing me the ropes in the first year or so of the Ph.D. I also have a deep appreciation for the friendship I have made with the other Ph.D students with whom I have begun this journey with, especially Keith, Ciaran, Brian, Shan and Colin. I also have to thank new lab members including Alisha, Laura, Hannah and Rob and wish them every success in their projects.

On a personal note, I feel I have to mention my boyfriend, Vincent, who joined me in the last three years of this adventure. He has been a constant source of strength and inspiration. It would have been much more difficult to finish without his encouragement, as practical as it was heartfelt. I also feel obliged to mention the names of a few friends whose support meant beyond what they realize. I thank my cousin Laura and my best friend Susan for believing in me early on.

Finally, I would not have contemplated this road if not for my parents, Michael and Mary, who instilled within me the confidence to constantly achieve to the best of my ability. They invested so much in me – both emotionally and financially. To my parents, thank you. I hope to repay them when I’m rich and famous! My younger siblings, John and Niamh, have also been very supportive along the way

There is no doubt that this Ph.D would not have been possible without the support from both my immediate and extended family and friends.

Abstract

Introduction: Elevated cyclic strain often leads to vein graft rejection, which is correlated to increased thrombomodulin release. Limited in vitro and in vivo studies document this release but the pathway involved is still unclear. In this study, we examine thrombomodulin (TM) expression and release after elevated cyclic strain. We also look at how physiological levels of shear stress impact TM expression and release. We assess the effect that various inflammatory mediators (i.e., ox-LDL) have on this cyclic strain-induced TM response. We investigate a range of signalling components (i.e., eNOS) in the cyclic strain-mediated TM expression and release pathway. We finish on the possible microvesicle (MV) involvement in cyclic strain-induced TM release.

Hypothesis: Thrombomodulin (TM), an integral membrane protein involved in coagulation, is regulated by cyclic strain and plays a pivotal role in endothelial dysfunction.

Results: (i) Following cyclic strain (7.5%), TM expression was down-regulated in both protein and RNA but up-regulated release into the cell culture media. (ii) Physiological levels of shear stress (10 dynes/cm²) acted as a more potent stimulus for TM release (when compared to cyclic strain) and also increased TM mRNA expression. (iii) Both TNF- α and ox-LDL had a down-regulatory effect on TM expression in static HAECs whereas glucose has no effect. In addition, TNF- α or ox-LDL caused an additive increase in cyclic strain-induced TM release. By contrast, glucose was found to “attenuate” cyclic strain-mediated TM release. (iv) We established that inhibition of PTK and p38 MAPK increased cyclic strain-mediated TM expression (i.e., reverses the typical strain-dependent response), thus play a role in the cyclic strain-decrease TM pathway. (v) We showed that MMPs and ROS decreased cyclic strain-induced TM release (i.e., reverses the typical strain-dependent response), thus they are involved in the cyclic strain-induced TM release pathway. (vi) We also observed that inhibition of integrin $\alpha\beta 3$ causes an additional increase in TM release in both static and strained HAECs, suggesting that integrins serve as a cellular “brake” for the release of TM. (vii) We noted that cyclic strain-induced TM release has some microvesicle involvement with one third of the release on exosomes.

Conclusions: Cyclic strain regulates the release and expression of thrombomodulin in endothelial cells. TM release is regulated by MMPs and ROS, although a portion of release is due to microvesicle involvement.

Table of contents

Declaration	ii
Acknowledgements	iii
Abstract	iv
Table of contents	v
List of figures	xi
List of tables	xv
Abbreviations	xvi
Units	xxiii
Publications	xxiv
Posters/Abstracts	xxiv
Oral presentations	xxv
Chapter 1: Introduction	1
1.1 The vascular tree	2
1.1.1 The vascular endothelium	6
1.1.2 Endothelial dysfunction	7
1.1.3 Cardiovascular disease	8
1.1.4 Hemodynamic forces	10
1.1.5 Mechanotransduction	14
1.2 Thrombomodulin (TM)	17

1.2.1 TM Structure	17
1.2.2 Functions of TM	20
1.2.2.1 Anti-coagulant	20
1.2.2.2 Anti-fibrinolytic	22
1.2.2.3 Anti-inflammatory	23
1.2.3 Transcriptional regulation of TM	25
1.2.4 Post-transcriptional regulation of TM	30
1.2.5 Post-translational regulation of TM	32
1.2.5.1 Oxidation	32
1.2.5.2 Glycosylation	34
1.2.5.3 Proteolysis	35
1.2.6 Therapeutic consideration for TM	39
1.2.6.1 Soluble recombinant TM	39
1.2.6.2 Biomaterial coating and TM	43
1.2.6.3 Statins and TM	45
1.3 Rationale for project	46
1.4 Objectives	48
Chapter 2: Materials and Methods	49
2.1 Materials	50
2.2 Cell culture methods	52
2.2.1 Endothelial cells	52

2.2.1.1 Culture of human aortic endothelial cells (HAECs)	52
2.2.2 Trypsinisation of HAECs	53
2.2.3 Cryopreservation and recovery of cells	54
2.2.4 Cell counting	54
2.2.4.1 Hemocytometer	54
2.2.4.2 ADAM™ cell counter	55
2.2.5 Hemodynamic Force Studies	57
2.2.5.1 Cyclic strain: Flexercell® Tension Plus™ FX-4000T™ System	57
2.2.5.2 Laminar shear stress: Orbital rotation	58
2.2.6 Transendothelial permeability assay	59
2.2.7 Inhibitors and inflammatory mediators	61
2.2.8 Fluorescence Activated Cell Sorting (FACs) analysis	63
2.2.8.1 Vybrant™ Apoptosis Assay kit	64
2.2.9 Membrane vesicle analysis	65
2.2.9.1 Centrifugation techniques	65
2.2.9.2 Exosome isolation	66
2.2.9.3 Media concentration	67
2.3 mRNA preparation and analysis	69
2.3.1 An RNase-free environment	69
2.3.2 RNA preparation	69
2.3.3 The Nanodrop® ND-100 spectrophotometer	70
2.3.4 DNase treatment of mRNA	72
2.3.5 Reverse transcription	72

2.3.6 Polymerase chain reaction (PCR)	73
2.3.7 Quantitative real time PCR (qPCR)	74
2.3.8 Agarose gel electrophoresis	76
2.4 Immunodetection techniques	77
2.4.1 Western blotting	77
2.4.1.1 Preparation of whole cell lysates	77
2.4.1.2 Bicinchoninic acid (BCA) assay	78
2.4.1.3 Polyacrylamide gel electrophoresis (SDS-PAGE)	78
2.4.1.4 Electrotransfer to nitrocellulose membrane	80
2.4.1.5 Ponceau S staining	80
2.4.1.6 Immunoblotting and chemiluminescence band detection	81
2.4.1.7 Coomassie gel staining	82
2.4.2 ELISA	83
2.4.2.1 ELISA analysis	83
2.4.2.2 Thrombomodulin Human ELISA Kit	84
2.4.2.3 Human Thrombomodulin/BDCA-3 DuoSet [®] ELISA	84
2.4.2.4 Multiplex ELISA	85
2.4.2.4.1 Human proinflammatory-I ultra sensitive 96 well multi-spot [®] plate	86
2.4.2.4.2 Human vascular injury I 96-well multi-spot [®] plate	88
2.4.3 Immunocytochemistry	89
2.5 Statistical analysis	90

Chapter 3: Preliminary characterisation studies and investigation of the effects of cyclic strain on expression and release of thrombomodulin	91
3.1 Introduction	92
3.2 Results	93
3.2.1 Characterisation of endothelial cells	93
3.2.1.1 Endothelial cell markers	93
3.2.1.2 Endothelial cell morphology	94
3.2.2 Viability studies	94
3.2.3 Effect of elevated cyclic strain on biomarker levels in HAECs	95
3.2.4 Constitutive expression and release of TM in “static” HAECs	97
3.2.5 Effect of cyclic strain on TM expression levels in HAECs	97
3.2.6 Effect of cyclic strain on TM release from HAECs	99
3.2.7 Effect of laminar shear stress on TM expression and release	99
3.3 Table and Figures	100
3.4 Discussion	120
Chapter 4: Investigation into the molecular mechanisms involved in cyclic-strain mediated thrombomodulin release and expression	128
4.1 Introduction	129
4.2 Results	132
4.2.1 Inflammatory mediators	132

4.2.2 Signaling components	133
4.2.2.1 Signalling components and TM expression	134
4.2.2.2 Signalling components and TM release	135
4.3 Tables and Figures	136
4.4 Discussion	149
Chapter 5: Further studies on the dynamics of cyclic strain-mediated TM “release” from HAECs	163
5.1 Introduction	164
5.2 Results	168
5.2.1 Microvesicle (MV) analysis	168
5.2.3 Molecular size of sTM	169
5.2.4 Functional efficacy of sTM	170
5.2.5 Paracrine release of sTM	170
5.3 Table and Figures	172
5.4 Discussion	181
Chapter 6: Final summary	188
6.1 Final Summary	189
Bibliography	195
Appendix	a-h

List of figures

Figure 1.1: The entire human vascular tree.

Figure 1.2: The aortic vasculature with a cross-section exposing the multi-layer structure.

Figure 1.3: Three-layer structure of the blood vessel.

Figure 1.4: Mechanical forces; frictional shear stress (τ) and cyclic circumferential stretch (ρ), acting on the vessel wall.

Figure 1.5: How biomechanical forces affect endothelial cells.

Figure 1.6: Mechanotransduction mechanisms used by endothelial cells.

Figure 1.7: The mechanotransduction pathways activated inside endothelial cells in response to shear stress.

Figure 1.8: Structure of TM consisting of five domains.

Figure 1.9: The binding of TM with thrombin to convert endogenous Protein C into activated Protein C (APC).

Figure 1.10: Thrombin/TM or plasmin can activate TAFI (60 kDa) yielding TAFIa (35kDa).

Figure 1.11: Promoter region of the TM gene with predicted response elements.

Figure 1.12: Shear stress regulation of Krüppel-like factor 2 (KLF2).

Figure 1.13: The smallest active fragment of TM.

Figure 1.14: Soluble TM is shed and/or proteolysed from the membrane as a result of endothelial injury.

Figure 1.15: Putative role of rhomboids (RHBDL2) in the release of bioactive molecules (e.g., TM) and remodeling of cell-cell contact points.

Figure 1.16: Mechanism of action of ReomodulinTM (ART-123).

Figure 1.17: The PECAM-1 (CD31) protein domain structure and sites of molecular binding interactions.

Figure 1.18: Photographs of the luminal surface of expanded polytetrafluoroethylene (ePTFE) covered stent grafts explanted at 4 weeks.

Figure 2.1: HAECs are isolated from the human ascending (thoracic) and descending (abdominal) aorta.

Figure 2.2: The haemocytometer, indicating the counting grid.

Figure 2.3: The ADAMTM counter and loading of an AccuChip and reading.

Figure 2.4: Flexercell[®] Tension PlusTM FX-4000TTM system.

Figure 2.5: Transendothelial permeability assay.

Figure 2.6: Amicon[®] Ultra-2 centrifugal filter device.

Figure 2.7: The NanoDrop[®] machine (A) and typical graph readouts for (B) RNA and (C) DNA.

Figure 2.8: Wet transfer cassette assembly used to transfer electrophoresed proteins from an SDS-PAGE gel to the nitrocellulose membrane.

Figure 2.9: Principles of sandwich-based immunoassays.

Figure 2.10: Human ProInflammatory I 4-Plex Multi-Spot[®] Plate.

Figure 2.11: Human Vascular Injury I 96-well Multi-Spot[®] Plate.

Figure 3.1: Characterisation of HAECs.

Figure 3.2: Endothelial cell morphological alterations in response to shear stress compared to static control cells.

Figure 3.3: VybrantTM Apoptosis FACs Assay.

Figure 3.4: Trypan blue and ADAMTM cell counter viability studies.

Figure 3.5: IFN- γ biomarker data.

Figure 3.6: IL-1 β biomarker data.

Figure 3.7: IL-6 biomarker data.

Figure 3.8: TNF- α biomarker data.

Figure 3.9: siCAM-3 biomarker data.

Figure 3.10: E-selectin biomarker data.

Figure 3.11: P-selectin biomarker data.

Figure 3.12: Thrombomodulin (TM) biomarker data.

Figure 3.13: Thrombin-treated and untreated controls for the Pro-Inflammatory Injury and Vascular Injury Panels.

Figure 3.14: Fluorescent and confocal imaging of TM immunoreactivity in static HAECs.

Figure 3.15: Constitutive expression and release of TM in static HAECs.

Figure 3.16: Dose-dependent effect of cyclic strain on cellular TM protein levels as monitored by Western blotting.

Figure 3.17: Dose- and frequency-dependent effects of cyclic strain on cellular TM protein levels in HAECs as monitored by ELISA.

Figure 3.18: Effect of cyclic strain on TM mRNA levels in HAECs as monitored by qRT-PCR.

Figure 3.19: Dose-, time- and frequency-dependent effects of cyclic strain on TM release.

Figure 3.20: Shear stress regulates TM expression and release.

Figure 4.1: Effect of TNF- α on TM expression and release.

Figure 4.2: Effect of oxLDL on TM mRNA expression and release.

Figure 4.3: Effect of glucose on TM expression and release.

Figure 4.4: Effect of MMPs and serine proteases on cyclic strain-dependent TM protein expression.

Figure 4.5: Effect of eNOS on cyclic strain-dependent TM protein expression.

Figure 4.6: Effect of Rac1 on cyclic strain-dependent TM protein expression.

Figure 4.7: Effect of NADPH oxidase on cyclic strain-dependent TM protein expression.

Figure 4.8: Effect of kinase proteins on cyclic strain-dependent TM protein expression.

Figure 4.9: Effect of MMPs, cyclic RGD peptide integrins and serine proteases on cyclic strain-induced TM release.

Figure 4.10: Effect of eNOS on cyclic strain-induced TM release.

Figure 4.11: Effect of Rac1 on cyclic strain-induced TM release.

Figure 4.12: Effect of NADPH oxidase on cyclic strain-induced TM release.

Figure 4.13: Effect of kinase proteins on cyclic strain-induced TM release.

Figure 5.1: Cellular microvesicle (MV).

Figure 5.2: The steps involved in processing microvesicles (MVs) from cell culture media.

Figure 5.3: Microvesicles and TM release.

Figure 5.4: Microvesicle and TM release from BAECs.

Figure 5.5: Impact of increasing centrifugation conditions.

Figure 5.6: The steps involved in enriching exosomes from cell culture media.

Figure 5.7: Exosome enrichment.

Figure 5.8: Detection of TM in cell lysates and media supernatants.

Figure 5.9: Functional efficacy of sTM.

Figure 5.10: Paracrine TM release.

List of tables

Table 1.1: The functions of each of the five domains of TM.

Table 1.2: Current literature documenting the effect of hemodynamic forces on TM expression and release.

Table 2.1: Inflammatory mediator and concentrations used in HAECs.

Table 2.2: Pharmacological inhibitors blocking specific cellular targets and concentrations used in HAECs.

Table 2.3: 0.5 volumes of Total Exosome Isolation reagent (Invitrogen, The Netherlands) was added to the appropriate volume of cell culture media.

Table 2.4: Primer sequences, product size and annealing temperature used for both PCR and qPCR.

Table 2.5: SDS-PAGE gel formations.

Table 2.6: Optimized primary and secondary antibody dilutions for proteins monitored by Western blots.

Table 2.7: Optimized primary and secondary antibody dilutions for proteins monitored by immunocytochemistry.

Table 3.1: The effects of elevated levels of cyclic strain (12.5%) on the expression of each biomarker measured in both total cell lysates and cell media.

Table 4.1: Inflammatory conditions tested in the absence or presence of cyclic strain.

Table 4.2: Signalling components tested in the absence or presence of cyclic strain.

Table 6.1: My contribution demonstrating the effect of hemodynamic forces on TM expression and release.

Abbreviations

1°	Primary
2°	Secondary
Ab	Antibody
ADAM	Advanced detection and accurate measurement
Akt	Protein kinase B
AP-1	Activator protein-1
APC	Activated protein C
APS	Ammonium persulphate
BAEC	Bovine aortic endothelial cell
BCA	Bicinchoninic acid
BDCA-3	Blood dendritic cell antigen-3
BSA	Bovine serum albumin
CABG	Coronary artery bypass graft surgery
cAMP	Cyclic adenosine monophosphate
Cdc42	Cell division control protein 42 homolog
cDNA	Complementary DNA
CHD	Coronary heart disease
CHL-1	Close homolog of L1
COOH	Carboxyl group
CVD	Cardiovascular disease
CPB2	Procarboxypeptidase B2

CPU	Carboxypeptidase U
CS	Chondroitin sulphate
DAPI	4',6-diamidino-2-phenylindole
DCI	Dichloroisocoumarin
DEPC	Diethylpyrocarbonate
DES	Drug eluting stents
DIC	Disseminated intravascular coagulation
dH ₂ O	Distilled water
DNA	Deoxyribonucleic acid
dNTP	Deoxyribonucleotide triphosphate
DMSO	Dimethyl sulphoxide
E-box	Enhancer box
EC	Endothelial cell
ECL	Enhanced chemiluminescence
ECM	Extracellular matrix
E. coli	Escherichia coli
EDTA	Ethylenediaminetetraacetic acid
EGF	Epidermal growth factor
ELISA	Enzyme-linked immunosorbent assay
EMP	Endothelial microparticle
eNOS	Endothelial nitric oxide synthase
EPCR	Endothelial protein C receptor
ePTFE	Expanded polytetrafluoroethylene

ERK	Extracellular signal-related kinase
FACs	Flow cytometry
FBS	Fetal bovine serum
FCS	Fetal calf serum
FDA	Food and drug administration
FITC	Fluorescein isothiocyanate
GAG	Glycosaminoglycan
GAPDH	Glyceraldehyde 3-phosphate dehydrogenase
GPCR	G-protein coupled receptor
GPI	Glycosylphosphatidylinositol
H ₂ O	Water
H ₂ O ₂	Hydrogen peroxide
HAAECs	Human abdominal aortic endothelial cells
HAEC	Human aortic endothelial cell
HASMCs	Human aortic smooth muscle cells
Hepes	4-(2-hydroxyethyl)-1-piperazineethanesulfonic acid
HMGB1	High-mobility group box 1
HRP	Horseradish peroxidase
HSF1	Heat shock factor protein 1
HUS	Hemolytic-uremic syndrome
HUVEC	Human umbilical vein endothelial cells
ICAM-1	Intercellular adhesion molecule-1
IFN- γ	Interferon-gamma

IgG	Immunoglobulin G
IKK	I κ B kinase
IL	Interleukin
ITGA5	Integrin alpha-5
KLF2	Krüppel-like factor 2
LLD	Lectin like domain
L-NAME	L-ng-nitroarginine methyl ester
LPA	Lysophosphatidic acid
LPS	Lipopolysaccharide
LSS	Laminar shear stress
MAPK	Mitogen-activating protein kinase
MCP-1	Monocyte chemoattractant protein-1
Met	Methionine
MHC	Major histocompatibility complex
miR	MicroRNA
MMP	Matrix metalloproteinase
MP	Microparticle
mRNA	Messenger ribonucleic acid
MSD®	Meso scale discovery
MV	Microvesicle
MW	Molecular weight
NADPH	Nicotinamide adenine dinucleotide phosphate
NF κ B	Nuclear factor kappa-light-chain-enhancer of activated B cells

NH ₂	Amine group
NMWL	Nominal molecular weight limit
iNOS	Inducible nitric oxide synthase
nNOS	Neuronal nitric oxide synthase
NO	Nitric oxide
NOS	Nitric oxide synthase
NOS-3	Nitric oxide synthase-3
NSCLC	Nonsmall cell lung cancer
O	Oxygen
OXLDL	Oxidized low density lipoprotein
PAGE	Polyacrylamide gel electrophoresis
PAI-1	Plasminogen activator inhibitor-1
PAR1	Protease-activated receptor 1
PBS	Phosphate buffer saline
PC	Protein C
PCPB	Plasma carboxypeptidase
PCR	Polymerase chain reaction
PECAM-1	Platelet endothelial cell adhesion molecule
PF-1	Platelet factor-4
<i>P. gingivalis</i>	<i>Porphyromonas gingivalis</i>
pH	Power of the hydrogen ion
PI	Phosphate inhibitor
PI	Propidium iodide
PI3K	Phosphoinositide 3-kinase

PKC	Protein kinase C
PMA	Phorbol ester
PN-1	Protease nexin-1
PTFE	Polytetrafluoroethylene
qPCR	Quantitative real time polymerase chain reaction
RCF	Relative centrifugal force
RHBDL2	Rhomboid-like 2
RIPA	Radioimmunoprecipitation assay
RNA	Ribonucleic acid
ROS	Reactive oxygen species
RT-PCR	Reverse transcription polymerase chain reaction
S18	40S ribosomal protein S18
SARS	Severe acute respiratory syndrome
scFv	Single chain variable fragment
SDS	Sodium dodecyl sulphate
SDS-PAGE	Sodium dodecyl sulphate polyacrylamide gel electrophoresis
Ser	Serine
siCAM-3	Soluble intercellular adhesion molecule-3
SIRS	Systemic inflammatory response syndrome
SIRT1	Sirtuin 1
SMC	Smooth muscle cell
SOD	Superoxide dismutase
Spred1	Sprout-related ECH1 domain-containing protein 1

sTM	Soluble thrombomodulin
TAFIa	Activated thrombin activable fibrinolysis inhibitor
TAFIai	Inactivated thrombin activable fibrinolysis inhibitor
TAFI	Thrombin activable fibrinolysis inhibitor
TBS	Tris buffered saline
TEMED	Tetramethylethylenediamine
TF	Tissue factor
TF	Transcription factor
TNF- α	Tumour necrosis factor-alpha
TGF- β 1	Transforming growth factor- β 1
TMB	3,3',5,5'-Tetramethylbenzidine
TM	Thrombomodulin
TTP	Tristetraprolin
UT	Untreated
UTR	Untranslated region
UV	Ultraviolet
VCAM-1	Vascular adhesion molecule-1
VE-cadherin	Vascular endothelial cadherin
VEGF	Vascular endothelial growth factor
vWF	Von Willebrand Factor
WHO	World Health Organisation

Units

aa	Amino acids
bp	Base pairs
cm	Centimeters
g	Grams
hrs	Hours
kDa	Kilo daltons
kg	Kilogram
L	Litre
M	Molar
mg	Milligrams
min	Minute
ml	Millilitre
mm	Millimetre
mM	Millimolar
ng	Nanogram
N/m ²	Newton meter squared
°	Degree celsius
Pa	Pascal
rpm	Revolution per minute
sec	Seconds
µg	Microgram

μl	Microlitre
μM	Micromolar
V	Volts
v/v	Volume per volume
w/v	Weight per volume
yr	Year

Publications

Martin FA, Murphy RP, Cummins PM. Thrombomodulin and the vascular endothelium: insights into functional, regulatory and therapeutic aspects. *American Journal of Physiology Heart Circulatory Physiology* 2013; doi: 10.1152/ajpheart.00096.2013.

Martin FA, Rochfort KR, Davenport C, McLoughlin A, Murphy RP, Cummins PM. Regulation of thrombomodulin expression and release in human aortic endothelial cells by cyclic strain. *Arterioscler Thromb Vasc Biol* 2013; In Preparation.

Posters/Abstracts

Fiona A Martin, Anthony F Guinan, Andrew Murphy, Ronan P Murphy and Philip M Cummins. Cyclic strain induced thrombomodulin release: putative role in macrovascular endothelial injury. *(Bio)pharmaceutical & Pharmacological Sciences research day 2011*, Dublin City University.

Fiona A Martin, Anthony F Guinan, Andrew Murphy, Ronan P Murphy and Philip M Cummins. Cyclic strain induced thrombomodulin release: putative role in macrovascular endothelial injury. *School of Biotechnology: 3th Annual Research Day 2011*, Dublin City University.

Fiona A Martin, Keith D Rochfort, Colin Davenport, Anthony F Guinan, Andrew Murphy, Ronan P Murphy and Philip M Cummins. Cyclic strain-induced release of thrombomodulin from human aortic endothelial cells. *School of Biotechnology: 4th Annual Research Day 2011*, Dublin City University.

Fiona A Martin, Keith D Rochfort, Colin Davenport, Anthony F Guinan, Andrew Murphy, Ronan P Murphy and Philip M Cummins. Cyclic strain-induced release of thrombomodulin from human aortic endothelial cells. *Arteriosclerosis, Thrombosis, and Vascular Biology Scientific Sessions 2012*, Hilton Chicago, Illinois.

Oral presentations

Fiona A Martin, Keith D Rochfort, Colin Davenport, Anthony F Guinan, Ronan P Murphy and Philip M Cummins. Cyclic strain-mediated regulation of thrombomodulin expression and release from human aortic endothelial cells. *School of Biotechnology: 5th Annual Research Day 2013*, Dublin City University.

Chapter 1:

Introduction

This chapter is an overview of the cardiovascular system, specifically concentrating on endothelial cells where we discuss their function in maintaining vascular haemostasis, and the after effects if they become dysfunctional. Endothelial cells have the capacity to sense and respond to alterations in shear and pulsatile blood flow, which is crucial for both arterial wall remodeling and vasoregulation. However, the deviation of endothelial cells from normal physiology plays a central role in the initiation of vascular disease. Mechanosensors, present in the vascular wall, have the ability to convert physical forces into biochemical signals. This mechanoregulation influences signalling pathways which are imperative for endothelial homeostasis as these pathways control the expression and function of many bioactive molecules including an endothelial cell membrane protein, thrombomodulin (TM), the main focus of this project.

1.1 The vascular tree

The rhythmic beat of the human heart keeps blood flowing through the body. It is one of the most important organs in the entire body as it is responsible for the circulation of blood for the cellular exchange of nutrients and gases in place of wastes and metabolic by-products (Fig 1.1). It is basically a pump the size of your fist, composed of muscle which beats approximately 72 times per minute of our lives keeping the blood flowing through it's 60,000 miles of blood vessels. The endothelium lines the entire vasculature, having first point of contact with the blood and thus, is crucial to the homeostasis of the circulatory system.

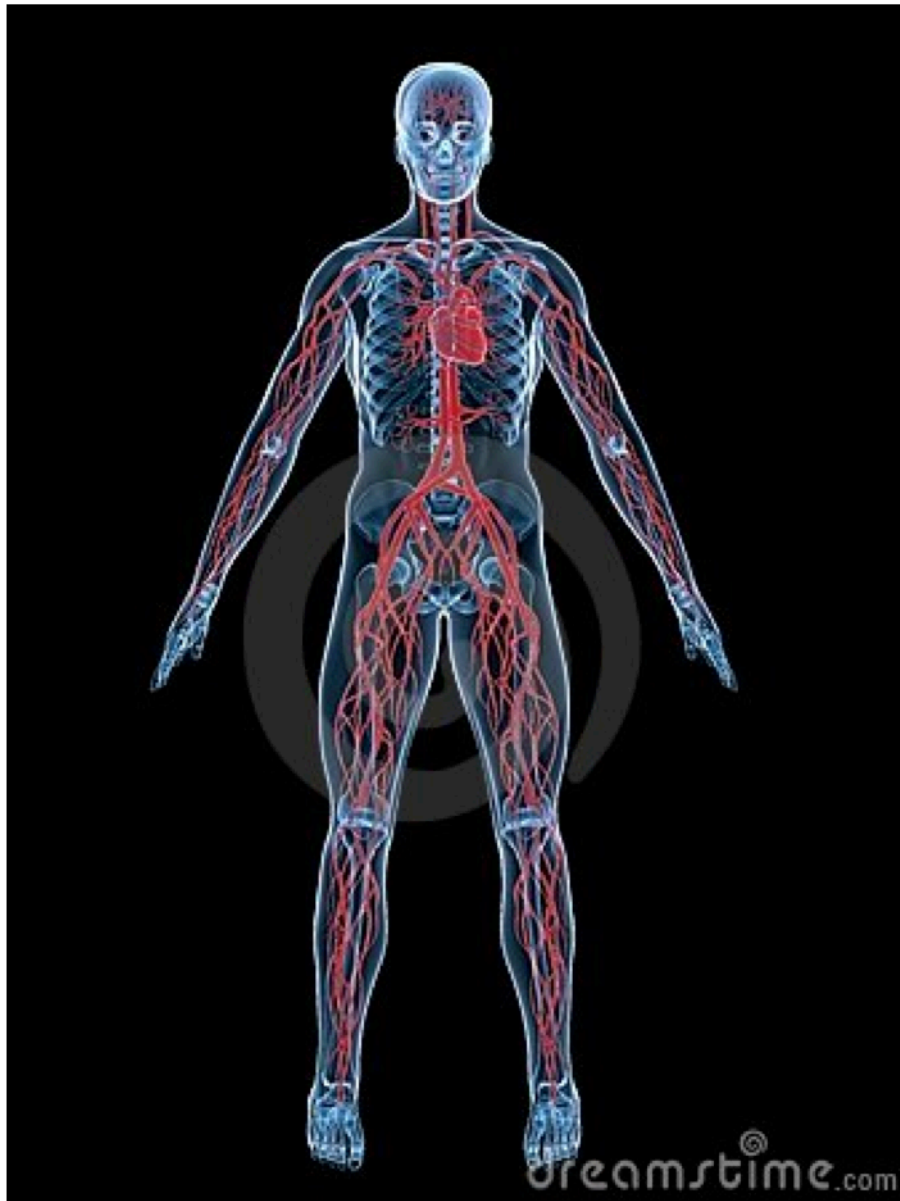


Figure 1.1: The entire human vascular tree (<http://nl.dreamstime.com/royalty-vrije-stock-foto-s-vasculair-systeem-image6730718>).

The circulatory system is composed of both the microvasculature and the macrovasculature. The microvasculature is that portion of the vasculature made up of small

vessels including capillaries, arterioles and venules. The macrovasculature is that portion of the circulatory system containing large vessels such as arteries and veins (diameters measuring greater than 100 microns) (Fig 1.2).

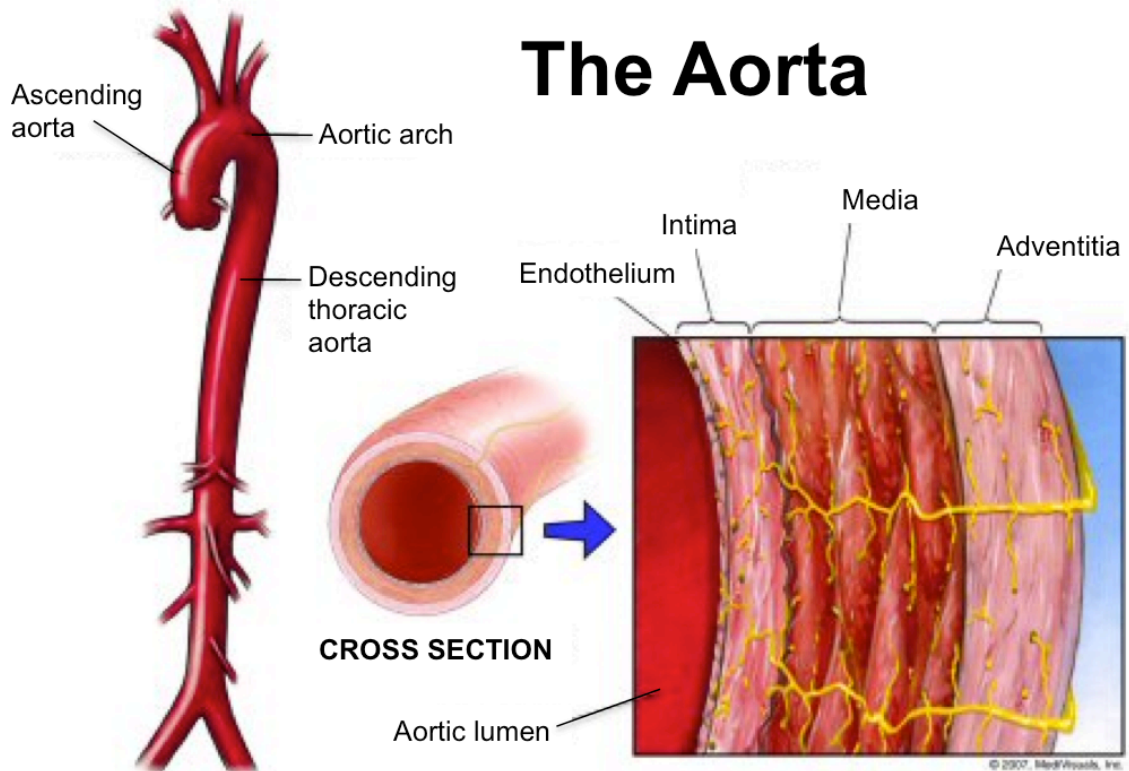


Figure 1.2: The aortic vasculature with a cross-section exposing the multi-layer structure (<http://www.hearts.vcu.edu/clinical/aortic/index2.html>).

Every one of these blood vessels in the vasculature, apart from capillaries, shares a common three layered structure (Fig 1.3). These three layers are known as: (i) tunica adventitia; (ii) tunica media and (iii) tunica intima;

(i) Tunica adventitia

The tunica adventitia is the outermost layer of the blood vessel that links it to the adjacent tissue and is made up of elastic and collagen fibres. It also provides larger blood vessels with nerves and collateral vessels to aid blood supply for the surrounding tissues (Corselli et al., 2012).

(ii) Tunica media

The tunica media or middle coat is composed principally of smooth muscle cells and large amounts of elastic fibres organised in roughly spiral layers. It is responsible for controlling vascular tone and function via smooth muscle cell circular orientation around the vessel, perpendicular to the direction of blood flow (Liddy et al., 2011).

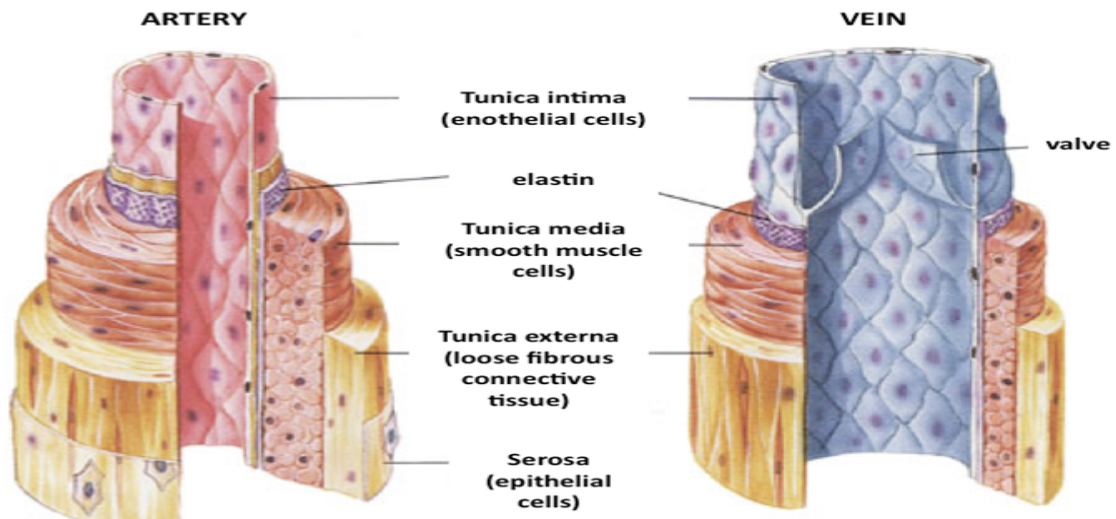


Figure 1.3: Three-layer structure of the blood vessel (McKinley and O'Loughlin, 2006).

(i) Tunica intima

The tunica intima is the innermost layer consisting of a simple, squamous layer surrounded by a connective tissue basement membrane with elastic fibres. The whole luminal surface itself, collectively known as the endothelium, is essentially a monolayer of endothelial cells. The endothelium is in direct contact with the blood as it flows through the lumen of the blood vessel and acts as the main focus of this thesis (Vanhoutte et al., 2007).

1.1.1 The vascular endothelium

The vascular endothelium, a continuous monolayer of flattened endothelial cells that forms the luminal lining of all blood vessels, separates circulating blood from the vascular wall and surrounding tissues and is vital to the health and homeostatic responsiveness of the mammalian circulatory system (for review see Michiels, 2003). Within the adult human, it comprises up to 6×10^{13} cells (or an exchange surface area of up to 350 m^2), and it exhibits considerable phenotypic heterogeneity across different vascular beds (Pries et al., 2000; Aird, 2007).

As the central theme of several thousand publications over the last few decades, the highly dynamic nature and functional complexity of the endothelium have been well documented. Under normal physiological conditions, its prime function is to regulate systemic blood flow and tissue perfusion rates through adjustment of vessel diameter and vascular tone (closely interacting with the underlying smooth muscle cells and pericytes), with a vasodilatory phenotype predominating in healthy vessels (Furchgott and Zawadzki, 1980). The endothelium also acts as a highly selective barrier controlling the paracellular

(and transcellular) exchange of fluids, ions and diverse nutrient macromolecules between circulating blood and tissues (Balda and Matter, 1998), a homeostatic function maintained by the coordinated interaction of inter-endothelial adherens and tight junction complexes (Taddei et al., 2008).

In a further dimension to this barrier role, endothelial cells (which normally maintain an anti-inflammatory phenotype) can mediate the recruitment and extravasation of pro-inflammatory leukocytes to areas of tissue damage and infection via the luminal expression/release of cell adhesion molecules (selectins, integrins, platelet & endothelial cell adhesion molecule type-1/PECAM-1) and cytokines (tumor necrosis factor- α /TNF- α , IL-1, IL-6, monocyte chemoattractant protein type-1/MCP-1) (Cotran and Pober 1990; Ebnet and Vestweber, 1999). Finally, the luminal surface of the healthy endothelium expresses a wide variety of molecules that serve to down-regulate platelet and thrombotic mechanisms, thereby creating an anti-coagulant surface for blood flow and preventing thrombus formation (Cines et al., 1998; Pearson, 1999). One of these anti-coagulant molecular targets, thrombomodulin (TM), represents the focus of this thesis and will be discussed in more detail below.

1.1.2 Endothelial dysfunction

As discussed already, the vascular endothelium is essential for maintaining the homeostatic integrity of the blood vessel via its ability to monitor and respond to acute/chronic changes in circulatory parameters. During pathological conditions, endothelial cells become “activated” due to a combination of one or more stimuli such as altered flow hemodynamics, injury, hypoxia, or the action of blood-borne constituents, eliciting

dysfunction of the endothelium with consequences for vessel remodeling. Importantly, endothelial dysfunction only transpires if the activation of endothelial cells is long-term. So short-term activation of endothelial cells that may occur (e.g., during exercise) does not irreparably impair endothelial function. Impairment in endothelial function not only changes endothelial cell morphology and phenotype, but also causes initiation and progression of cardiovascular diseases (Aird, 2007; Cines et al., 1998; Deanfield et al., 2007).

Due to the architecture of the vasculature tree, certain areas, such as arterial bifurcations or curvatures are characterised by attenuated levels and patterns of shear stress and cyclic strain (e.g., atherosclerosis). Moreover, certain vascular conditions lead to locally and globally elevated levels of shear and strain (e.g., hypertension, vein graft bypass) with supraphysiological shear near lesions. These haemodynamic alterations can lead to endothelial dysfunction and enhance the progression of vascular dysfunction and diseases (Han et al., 2010; Matsushita et al., 2001). These forces will be discussed in more detail below in Section 1.1.4.

1.1.3 Cardiovascular disease

It is evident that when endothelial cells become dysregulated it can lead to cardiovascular disease (CVD). CVD is an umbrella term for any disease of the heart or circulatory system encompassing atherosclerosis, congenital heart disease, heart failure, coronary artery disease, peripheral vascular disease, cerebrovascular disease and hypertension. Atherosclerosis is a common inflammatory response affecting arterial blood vessels. It is characterised by plaque deposition and thrombosis at atheroprone sites. Endothelial dysfunction is a hallmark of

atherosclerosis and can initiate an inflammatory cascade and endothelial barrier break down. This can lead to plaque build-up which if ruptured can cause a myocardial infarction (Tineli et al., 2007; Hahn and Schwartz, 2009).

According to the World Health Organisation (WHO) 17.3 million people died from CVDs in 2008 with over 80% of these deaths occurring in low and middle-income countries. They predict that by 2030 more than 23 million people will die annually from CVDs. In Ireland, about 10,000 people die each year from CVD which is 36% of all deaths (Irish Heart Foundation).

Dysfunction of the circulatory system stems from both *fixed* and *modifiable* risk factors. The fixed risk factors that may make you susceptible to CVD include;

- Gender (higher risk in males)
- Age (risk increases as you age)
- Genetic make-up (family history of heart disease)
- Race (African Americans, American Indians and Mexican Americans are more likely to develop heart disease than Caucasians).

However, there are numerous lifestyle changes you could make to lower the risk of developing CVD. These modifiable risk factors include;

- Smoking
- Stress
- Physical inactivity
- Hypertension (high blood pressure)
- Obesity (more than 20% over one's ideal body weight)
- Unhealthy diet and high cholesterol

➤ Type-2 diabetes

The risk factors listed above play a crucial role in initiating or worsening the outcomes of CVD shown by an array of studies on stroke, atherosclerosis or the mediation of blood flow-associated hemodynamic forces and blood pressure.

1.1.4 Hemodynamic forces

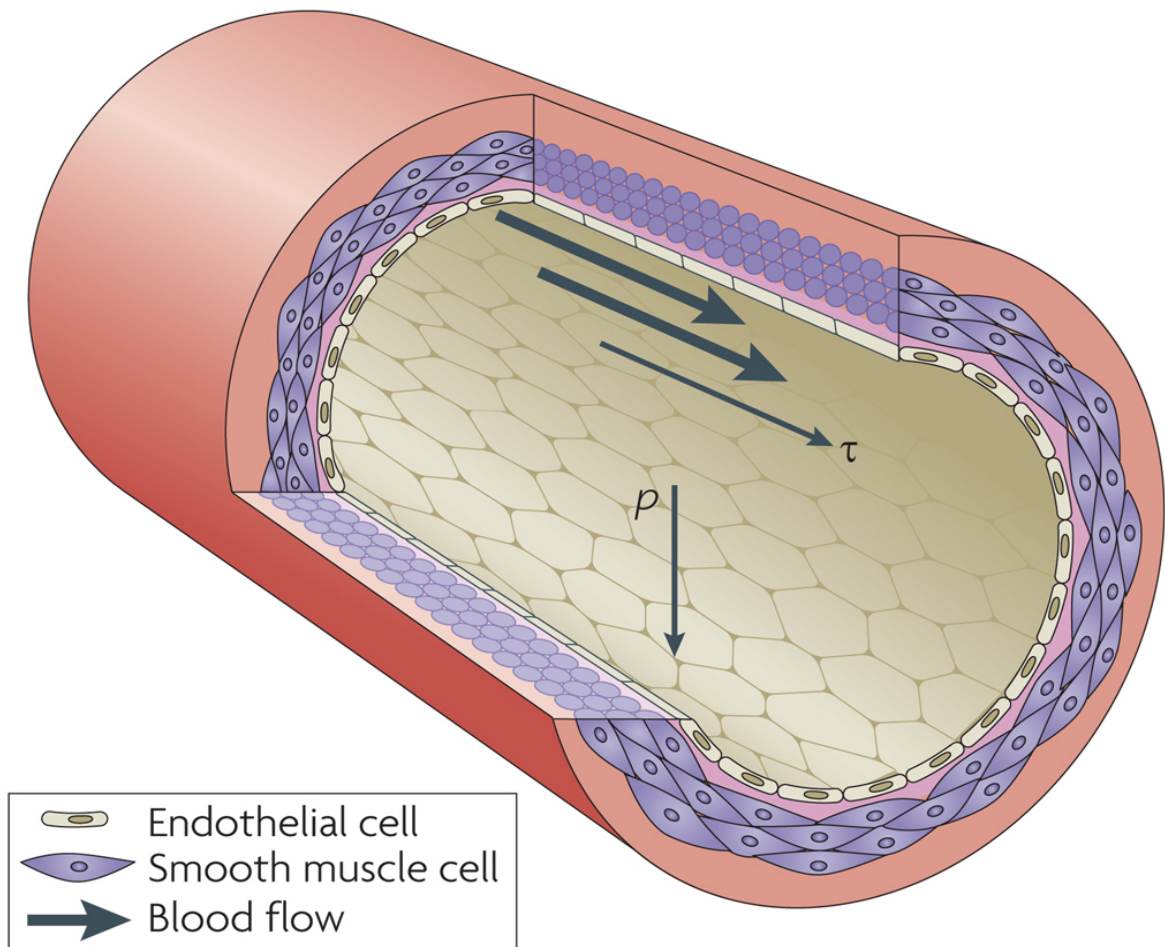


Figure 1.4: Mechanical forces; frictional shear stress (τ) and cyclic circumferential stretch (ρ), acting on the vessel wall (Hahn and Schwartz, 2009).

The endothelium exists within a pressurized fluid environment in direct contact with the circulating blood and blood-borne components. Blood flow-associated hemodynamic forces, namely pulsatile shear stress and cyclic circumferential strain (Fig 1.4), exert a profound influence on endothelial cell fates, gene expression and signaling (Ando and Yamamoto, 2011). The latter force, cyclic strain, will be the chief focus of this PhD thesis.

Shear stress is the tangential frictional force exerted by blood flow as it drags across the endothelial surface, causing cells to ‘flatten’ and morphologically align in the direction of flow (Ando and Yamamoto, 2011; Ensley et al., 2012; Malek and Izumo, 1994). Laminar shear stress (LSS), as used throughout this thesis, is well known to have an “atheroprotective” effect on endothelial cells (Traub and Berk, 1998).

Shear stress is expressed in units of force / unit area (Newton per meter squared [N/m²] or Pascal [Pa] or dynes/cm²; 1 N/m² = 1 Pa = 10 dynes/cm²). In normal physiological circumstances, the endothelium is subjected to shear ranges of 10-70 dyne/cm². For laminar flow, vessel shear can be expressed as follows;

$$\tau = \frac{4\mu Q}{\pi r^3}$$

Where τ = shear stress, μ = blood viscosity, Q = flow rate and r = vessel radius.

Physiologically, flow rate is highest at the centre of the vessel lumen and reduces towards the endothelium.

Cyclic strain, the principal emphasis of this work, describes the repetitive circumferential stretching of the vessel wall in synchronization with the cardiac cycle (Fig 1.5) (Awolesi et al., 1995; Cummins et al., 2007; Chen et al., 2008; Chien, 2007). This mechanical force, generated by the periodic contraction of the heart, impacts both the endothelial and underlying smooth muscle cells in macrovessels (Fig 1.4 above). The measure of cyclic strain is proportionally related to vessel diameter and blood pressure as large arteries such as the aorta enlarge at the peak of this blood pressure cycle (systole) and then slowly collapse as pressure from the heart drops (diastole) to pump blood downstream. Cyclic strain studies carried out *in vitro*, including the work in this thesis, replicate the effects of cyclic strain on cellular signal transduction in endothelial cells using vacuum based technologies to deform flexible-bottom culture plates (Awolesi et al., 1995; Chen et al., 2008; Collins et al., 2006; Han et al., 2010). In response to cyclic strain, the blood vessel wall thickens or thins so that force per unit of wall is constant (Schiffrin, 1992), which is portrayed by Laplace's Law (Laplace, 1899), as shown below;

$$T = \frac{Pr}{h}$$

Where T = wall tension (or force per unit length of the vessel), P = blood pressure, r = radius and h = the thickness of the vessel wall.

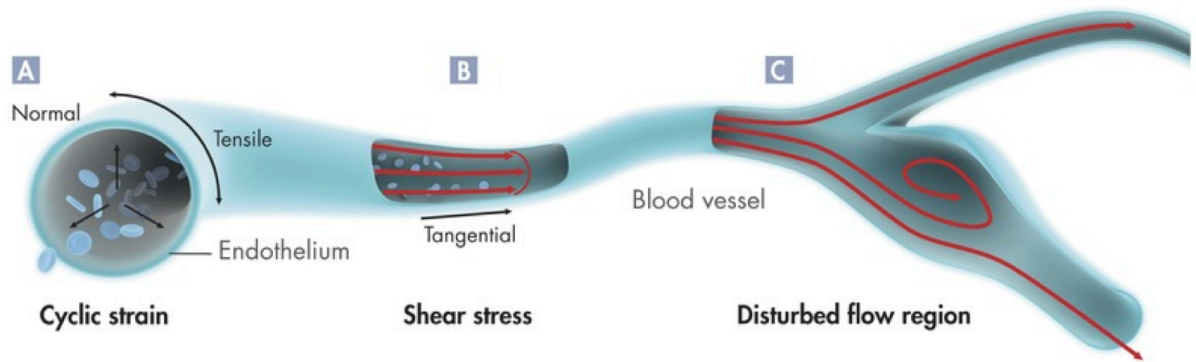


Figure 1.5: How biomechanical forces affect endothelial cells. **(A)** Cyclic strain, which is felt principally in larger arterial vessels. **(B)** Laminar shear stress, which is sensed predominantly in straight sections of the vasculature. **(C)** Disturbed shear, which is found in areas of high curvature or downstream of bifurcations (<http://www.qiagen.com/Knowledge-and-Support/Resource-Center/Resource-Search/Lab-and-Scientific-Knowledge/Newsletters-and-Magazines/Articles/Reviews-online-mechanotransduction/>).

Under physiological conditions, arterial diameters can remodel according to changes in fluid flow (Schaper, 2009). Conversely, vessels with high blood pressure need denser walls to be mechanically stable. If this pressure remains high, which may happen in pathological conditions such as hypertension, the vessel walls ability to remodel will be compromised. This eventually affects vessel elasticity and reduces the capacity of the artery to modulate blood flow in response to unexpected changes in blood pressure (Hahn and Schwartz, 2009).

According to the literature, there is a strong link between endothelial dysfunction and pathological levels of cyclic strain, which will be main focus of this thesis (Cummins et al., 2007; Chen et al., 2008; Collins et al., 2006; Han et al., 2010; Matsushita et al., 2001; Von

Offenberg et al., 2004). The focus of this thesis is to understand how the hemodynamic environment, and specifically cyclic strain, impacts thrombomodulin dynamics within human vascular cells in vitro. The rationale for this will be outlined towards the end of this chapter. The ability of the endothelial cell to convert these biomechanical forces into molecular responses is known as mechanotransduction and will be discussed in more detail in the next section.

1.1.5 Mechanotransduction

Endothelial cells possess diverse mechanoreceptor mechanisms (Fig 1.6) that allow them to sense their hemodynamic environment and transduce mechanical signals into appropriate cellular responses (e.g., nitric oxide release, gene expression), thus enabling blood vessels to structurally adapt their architecture (i.e., diameter, wall thickness, barrier function) to suit circulatory parameters (Wang and Thampatty, 2006). This process is known as mechanotransduction. Within this context, physiological ranges of laminar shear stress and cyclic strain of endothelial cells promote anti-proliferative, anti-coagulant and anti-thrombotic characteristics consistent with an atheroprotective phenotype (i.e., manifesting healthy endothelial function and atherosclerotic resistance) (Wu et al., 1995; Traub and Berk, 1998; Akimoto et al., 2000). Moreover, chronic dysregulation of endothelial responsiveness to hemodynamic stimuli (e.g., in arterial oscillatory flow zones or in vein graft regions of impaired endothelial function) has very serious clinical implications ranging from endothelial

dysfunction to atherosclerosis, intimal hyperplasia, thrombosis and stroke (Tinelli et al., 2007; Hahn and Schwartz, 2009).

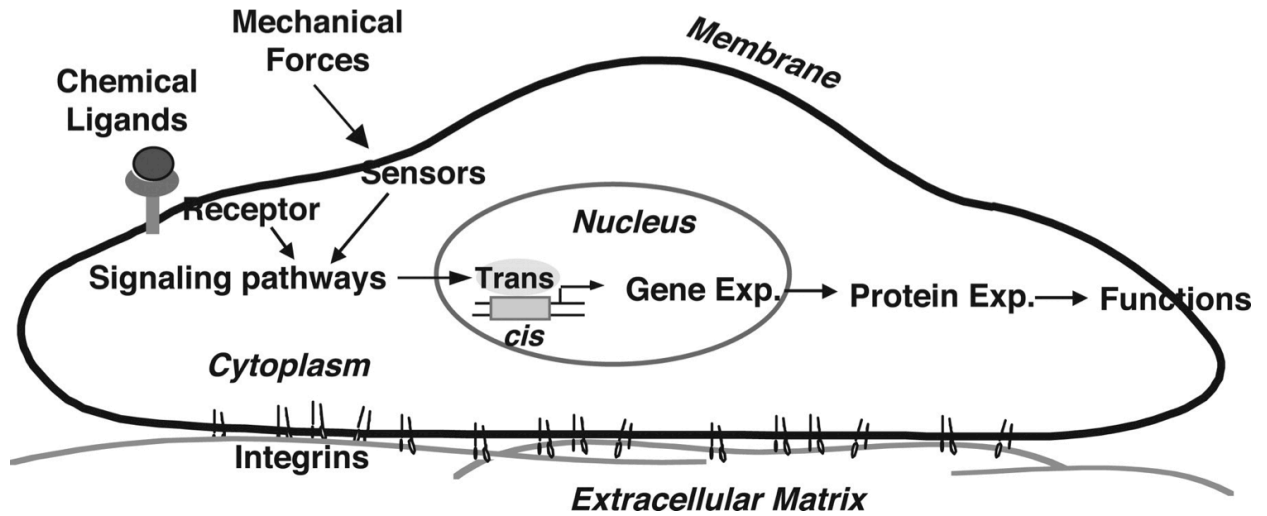


Figure 1.6: Mechanotransduction mechanisms used by endothelial cells (Chien, 2007).

It is clear from the many publications that hemodynamic forces influence the expression and/or activation of various signaling pathways (Fig 1.7) (Chen et al., 2008; Cheng et al., 2001; Takada et al., 1994). For instance, shear stress effects the gene expression of endothelial nitric oxide synthase (eNOS), endothelin-1, and thrombomodulin in human retinal microvascular endothelial cells (Ishibaza et al., 2011). Also, cyclic strain was shown to induce reactive oxygen species production through an endothelial NAD(P)H oxidase (Matsushita et al., 2001). An understanding of which signalling pathways putatively mediate the cyclic strain-dependent regulation of TM will therefore undertaken in this thesis.

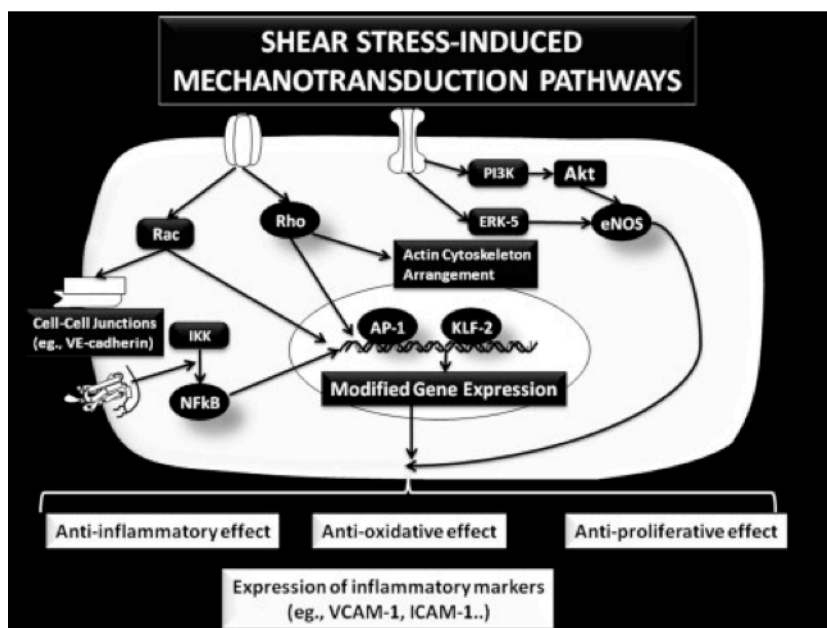


Figure 1.7: The mechanotransduction pathways activated inside endothelial cells in response to shear stress (El-Hamamsy et al., 2010). Key: Akt, protein kinase B; AP-1, activator protein-1; eNOS, endothelial nitric oxide synthase; ERK-5, extracellular signal-regulated kinase-5; ICAM-1, intercellular adhesion molecule-1; IKK, IκB Kinase; KLF-2, krüppel-like factor-2; NFκB, nuclear factor kappa-light-chain-enhancer of activated B cells; PI3K, phosphoinositide 3-kinase; VCAM-1, vascular adhesion molecule-1; VE-cadherin, vascular endothelial cadherin.

1.2 Thrombomodulin (TM)

1.2.1 TM structure

Thrombomodulin (THBD, CD141, BDCA3, fetomodulin), discovered and first named in 1982 by Esmon *et al.* (for review see Esmon and Owen, 2004), is a multi-domain integral membrane protein constitutively expressed on the luminal surface of vascular endothelial cells at a density of 50,000-100,000 molecules per cell (Suzuki *et al.*, 1988). In addition to coating the endothelium throughout all vascular beds, TM expression has been widely detected in several other tissues suggesting multi-functionality beyond its widely established anti-coagulation and anti-inflammatory roles (Van de Wouwer *et al.*, 2004). It has also been identified in human gestational tissues such as placenta and myometrium (Uszyński *et al.*, 2000), the gingival epithelium (Matsuyama *et al.*, 2000), keratinocytes (Senet *et al.*, 1997), polymorphonuclear neutrophils (Conway *et al.*, 1992), monocytes (Tsai *et al.*, 2010), dendritic cells (Yerkovich *et al.*, 2009), osteoblasts (Maillard *et al.*, 1993), and even platelets (Suzuki *et al.*, 1988). Furthermore, TM has also been detected in a variety of cultured cells including smooth muscle cells (Soff *et al.*, 1991), A549 small cell lung cancer cells (Fujiwara *et al.*, 2002) and NIH 3T3 cells (Dittman *et al.*, 1988), whilst soluble variants have been detected in human urine (Nakano *et al.*, 1998) and serum (Zycinska *et al.*, 2009).

Domain	Amino Acid Residue	Function
1. N-terminal lectin-like domain	1-226	<ul style="list-style-type: none"> • Receptor endocytosis • Anti-inflammatory activity <ul style="list-style-type: none"> – Helps regulate tumour growth – Mediates endothelial inflammation by down-regulating nuclear factor κB (NF-κB) and mitogen-activating protein kinase (MAPK) pathways – Essential role in cell-to-cell adhesion
2. EGF-like domain (1-6 repeats):	227-462	<ul style="list-style-type: none"> • Thrombin binding and protein C activation • Anti-fibrinolytic activity • Activation of thrombin activable fibrinolysis inhibitor (TAFI)
➤ EGF repeat 3	311-344	<ul style="list-style-type: none"> • TAFI activation
➤ EGF repeat 4	351-386	<ul style="list-style-type: none"> • Essential for Protein C activation • TAFI activation
➤ EGF repeat 5	390-407	<ul style="list-style-type: none"> • Thrombin binding and Protein C activation • TAFI activation
➤ EGF repeat 6	427-462	<ul style="list-style-type: none"> • Involved in thrombin binding and Protein C activation • TAFI activation
3. Ser/Thr-rich domain	463-497	<ul style="list-style-type: none"> • Required for full cofactor activity • The attached chondroitin sulfate (CS) moiety regulates anti-coagulant functions; <ul style="list-style-type: none"> • Increases affinity of TM for thrombin • Enhances anti-thrombin III ability to inhibit thrombin • Allows binding of platelet factor 4 (PF-4) to increase its activation • Attachment site for the malaria pathogen
4. Transmembrane domain	498-521	<ul style="list-style-type: none"> • Signalling function
5. Cytoplasmic domain	522-557	<ul style="list-style-type: none"> • Activates endothelial nitric oxide (NO) synthase 3 (NOS-3) • Regulates G protein-coupled signalling

Table 1.1: The functions of each of the five domains of TM.

The human TM gene, separately cloned by Wen *et al.* (Wen et al., 1987) and Suzuki *et al.* (Suzuki et al., 1988) from a human cDNA library, is an intronless gene localized to chromosome 20p12-cen (Espinosa et al., 1989). It codes for a protein of 575 amino acids (processed to 557 amino acids following removal of the N-terminal signal peptide) and has been widely reported as having a MW ranging from 70-100 kDa. TM is structurally organized into five domains (Table 1.1): (D1) an N-terminal C-type lectin domain (CTLTD); (D2) a chain of six extracellular EGF-like repeats; (D3) an extracellular serine/threonine (ser/thr) rich region; (D4) a transmembrane spanning region; and (D5) a short cytoplasmic tail (Fig 1.8).

Over the last two decades, a multitude of studies have uncovered the complex functional heterogeneity of these domains (Table 1.1), ranging from mediating TM interaction with anti-coagulant cofactors such as thrombin, protein C and thrombin-activatable fibrinolysis inhibitor (D2.D3) (Ito and Maruyama, 2011; Kokame et al., 1998), to TM internalization and regulation of inflammatory responses (D1) (Conway et al., 1994; Kokame et al., 1998). For a highly comprehensive overview of the structural properties of TM, the reader is directed to a recent review by Conway (Conway, 2011).

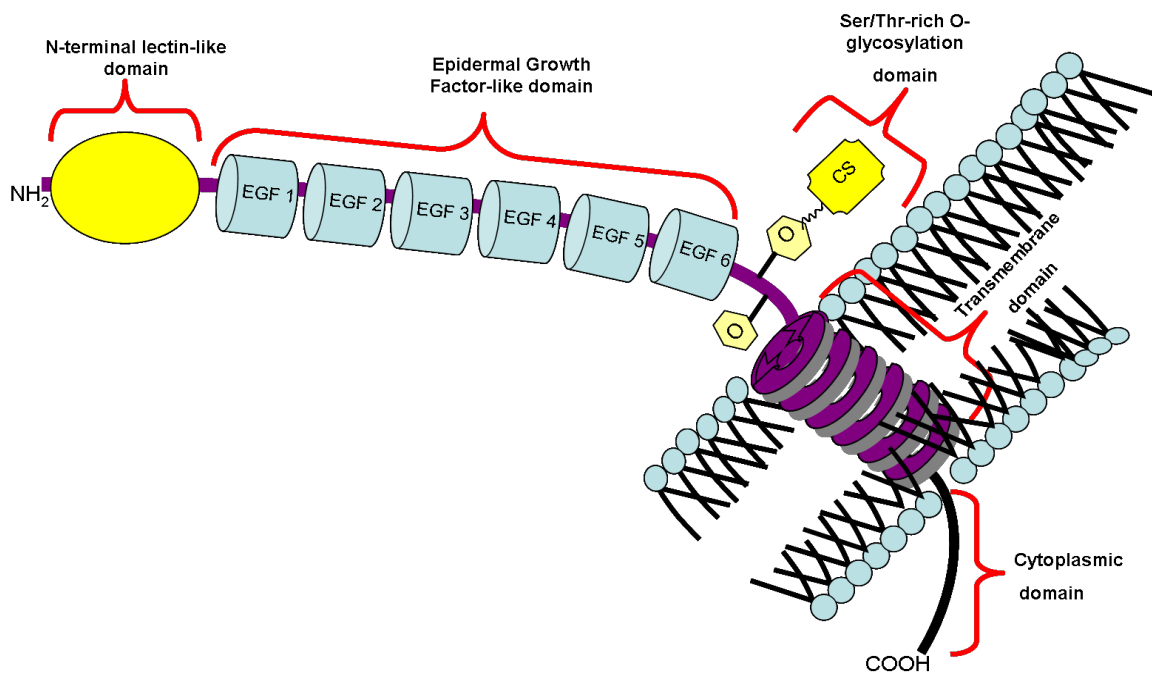


Figure 1.8: Structure of TM consisting of five domains; N-terminal lectin-like domain, epidermal growth factor-like domain, ser/thr-rich domain, transmembrane domain and cytoplasmic domain. Key: COOH, carboxyl group; CS, chondroitin sulphate; EGF, epidermal growth factor-like domain; O, oxygen; NH₂, amine group.

1.2.2 Functions of TM

TM exerts a vasculoprotective function in endothelial cells by inhibiting both coagulation (Weiler and Isermann, 2003) and fibrinolysis (Bajzar, 2000), whilst suppressing inflammation (Esmon and Owen, 2004). These roles substantively overlap and compliment each other and will be described below:

1.2.2.1 Anti-coagulant

The first characterized function of TM revolved around its role in the coagulation cascade (Fig 1.9). The ability to bind the serine protease thrombin and potentiate its role within the protein C (PC) activation cascade is often viewed as the archetypal function of TM. Numerous knock-out studies have shown that TM is essential for life. Indeed, mouse models of TM gene mutation (TM^{pro/pro} mouse) and endothelial cell-specific gene deletion (TMLox⁻ mouse) both exhibit greatly reduced ability to generate activated protein C (APC) within the circulation, leading to thrombosis and a hypercoagulable state (Isermann et al., 2001; Rijneveld et al., 2004). Coagulation is regulated by two main mechanisms; (i) the heparin-antithrombin mechanism, which inhibits coagulation proteases and (ii) the anti-coagulant pathway of protein C (PC) which will be discussed in slightly more detail (Califano et al., 2000). TM has a high affinity for binding to thrombin (K_d ~0.5 nmol L⁻¹), with bound thrombin subsequently going on to generate activated protein C (APC) (Weiler and Isermann, 2003).

Thrombin, known to regulate thrombosis and homeostasis, is a pro-coagulant disulphide-bonded protease dimer (Freedman, 2001). Thrombin binds to the TM EGF5-6 repeat domains and also, with lower affinity, to the TM CS moiety within the ser/thr-rich domain via the thrombin anion binding exosite I and II regions, respectively (Light et al., 1999; Ye et al., 1993). Upon binding to TM, this ultimately induces endocytosis and degradation of the TM-thrombin complex in lysosomes, a mechanism inhibited by PC but not by APC (Okamoto et al., 2012). The TM binding also alters thrombin's conformation allowing it to activate PC (Freedman, 2001). The action of TM binding therefore converts thrombin from a pro-coagulant protease to an anti-coagulant enzyme by shielding the pro-coagulant exosite I of thrombin (Esmon, 2003).

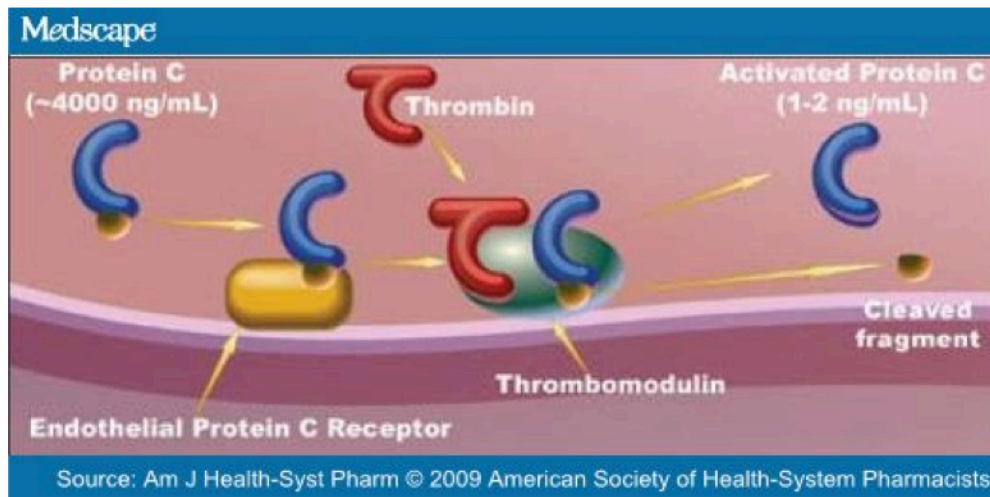


Figure 1.9: The binding of TM with thrombin to convert endogenous Protein C into activated Protein C (APC) (Mann HJ et al., 2009).

The binding of thrombin with TM has the effect of blocking the interaction of thrombin with circulating pro-coagulant substrates (e.g., fibrinogen) and enhancing its specificity for PC, leading to a substantially elevated rate of PC activation (over 1000-fold relative to unbound thrombin) (Adams and Huntington, 2006). Thrombin cleaves PC to cause the release of a dodecapeptide activation sequence and yield activated PC (APC), a disulphide-linked heterodimer, an event that is significantly enhanced if PC is bound to endothelial protein C receptor (EPCR) (Stearns-Kurosawa et al., 1996). Once dissociated from EPCR, APC elicits potent anti-coagulant effects primarily through the proteolytic inactivation of factor Va and factor VIIIa (Dahlbäck and Villoutreix, 2005). This is a fundamental anti-coagulant mechanism that inhibits the amplification of thrombin generation and catalyzes the proteolytic activation of PC.

1.2.2.2 Anti-fibrinolytic

In conjunction with its anti-coagulant function, TM also has an anti-fibrinolytic role. Thrombin binding to TM enhances the substrate specificity of the latter towards thrombin-activable fibrinolysis inhibitor (TAFI), a plasminogen-bound zymogen, to yield TAFIa (Adams and Huntington, 2006; Nesheim et al., 1997). TAFIa - also known as procarboxypeptidase B2 (CPB2), carboxypeptidase U (CPU), and plasma carboxypeptidase (pCPB) - exhibits carboxypeptidase-like activity towards C-terminal lysine residues from partially degraded fibrin (Leung et al., 2008; Zhao et al., 2003), thereby serving as a negative regulator of fibrinolysis (Fig 1.10). This enhances the stabilization of fibrin clots ensuring greater injury localization during vascular inflammatory events. Interestingly, selective

blockade of the TM/thrombin-mediated generation of TAFIa (e.g., using monoclonal antibodies) represents a valid approach to the development of pro-fibrinolytic therapies to reduce clot lysis time (Mishra et al., 2011).

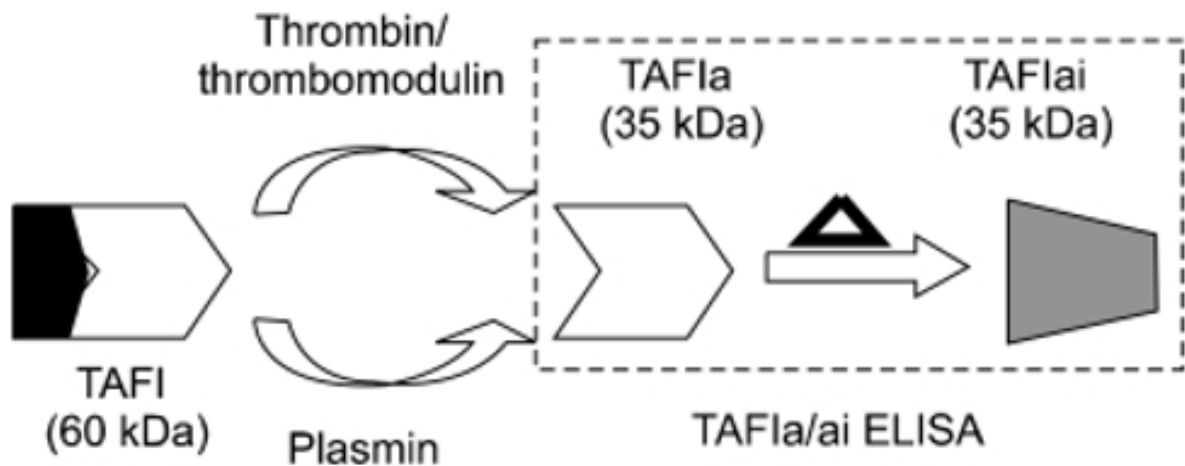


Figure 1.10: Thrombin/TM or plasmin can activate TAFI (60 kDa) yielding TAFIa (35kDa). Consequently, TAFIa is heat inactivated (triangle) to form TAFIai (shaded). All TAFI isoforms are found in plasma. TAFIa/ai-specific ELISA measured only TAFIa and TAFIai, not TAFI (Park et al., 2010).

1.2.2.3 Anti-inflammatory

The anti-inflammatory properties of TM have also been well documented (Van de Wouwer et al., 2004). The N-terminal C-type lectin-like domain (LLD) of TM was found to have a direct role in regulating inflammation. A relatively recent study by Nara *et al.* (Nara et al., 2006) for example describes how treatment of human endothelial cells with an anti-TM

monoclonal antibody elicits inflammatory signalling mechanisms (e.g., NF- κ B stimulation, IL-6 secretion) leading to endothelial activation, whilst Takagi and co-workers report that the C-type lectin domain of TM is a modulator of dendritic cell-mediated immunostimulatory events (Takagi et al., 2011). Whilst bound to EPCR for example, thrombin-generated APC can suppress monocyte-dependent cytokine production (Grey et al., 1994) and induce a cytoprotective endothelial gene expression profile (Joyce et al., 2001). EPCR-bound APC can also switch the signalling specificity of protease-activated receptor 1 (PAR1), which serves to orchestrate cellular responses to coagulation proteases such as thrombin from a pro-inflammatory to an anti-inflammatory response (Cheng et al., 2003; Rezaie, 2001; Riewald et al., 2003). Similarly, both *in vitro* (Leung et al., 2008) and *in vivo* (Beppu et al., 2010; Mao et al., 2005) studies have shown that thrombin-generated TAFIa can proteolytically inactivate a number of endogenous pro-inflammatory mediators such as bradykinin, osteopontin, and the complement-derived anaphylotoxins C3a and C5a via cleavage of their C-terminal arginine residues (Fig 1.10). TM can also negatively regulate the complement system by accelerating factor I-mediated inactivation of C3b. In this respect, missense mutations in TM can lead to a diminished ability to protect against activated complement – a feature of ~5% of potentially fatal atypical hemolytic-uremic syndrome (HUS) cases (Delvaeye et al., 2009). It should also be noted that circulating thrombin itself has several potent pro-inflammatory properties within the vascular endothelium - from induction of pro-inflammatory molecule expression (e.g., IL-6, IL-8, E-selectin, and MCP-1) (Anrather et al., 1997; Stanková et al., 1995) and nitric oxide production (Motley et al., 2007), to activation of NF- κ B signalling and monocyte/endothelial adhesion (Delekta et al., 2010). Thrombin is also known to potentiate endothelial activation by TNF- α (Anrather et al., 1997). Thus, by reducing circulating levels of thrombin as well as

switching its substrate specificity towards PC and TAFI (to yield anti-inflammatory APC and TAFIa), TM functions as an anti-inflammatory molecule, rendering it both a pivotal player in the progression of inflammatory diseases and a viable target for therapeutic intervention.

Evidently, TM plays a pivotal role in endothelial homeostasis by accelerating APC production, inhibiting coagulation and fibrinolysis (Nesheim, 2003) and mediating inflammation via its lectin-like domain (LLD) (Conway, 2011). This gives the endothelium protection against apoptosis, inflammation, fibrinolysis and thrombosis (Morser et al., 2010).

1.2.3 Transcriptional regulation of TM

The 5'-untranslated promoter region of the TM gene displays numerous response elements conferring transcriptional sensitivity to various stimuli (Fig 1.11) (Tazawa et al., 1993; Yao et al., 1999). Oxidative stress (Kumar et al., 2009), hypoxia (Ogawa et al., 1990), oxidized LDL (Ishii et al., 2003), C-reactive protein (Nan et al., 2005), phorbol esters (PMA) (Grey et al., 1994), cyclic adenosine monophosphate (cAMP) (Grey et al., 1998) and TNF- α (Grey et al., 1998) tend to down-regulate endothelial TM expression, whilst an up-regulatory effect has been attributed to thrombin (Séguin et al., 2008), VEGF (Calnek and Grinnell, 1998), retinoic acid (Marchetti et al., 2003) and heat shock (Fu et al., 2008).

In view of so many competing influences, basal endothelial TM levels typically reflect a balance between up- and down-regulatory forces. For example, p66Shc-mediated cellular oxidative stress leading to transcriptional repression of Krüppel-like factor 2 (KLF2), a transcription factor positively regulating the TM promoter, can lead to down-regulation of TM expression (Kumar et al., 2009), whilst up-regulation of KLF2 by antioxidant laminar shear

stress has the opposite effect (Dekker et al., 2002; Ishibazawa et al., 2011) – a particular aspect of TM regulation discussed in greater detail in the next section (post-transcriptional regulation).

Similarly, TNF- α dependent suppression of endothelial TM levels via NF- κ B activation has been well documented (Lin et al., 2010, Sohn et al., 2005), an effect that can be counter-balanced by all-trans retinoic acid treatment (Marchetti et al., 2003), laminar shear stress (Jun et al., 2009), and statins (Bergh et al., 2012). Interestingly, the TM promoter does not actually contain a classic NF- κ B consensus motif, but NF- κ B can mediate cytokine-induced repression of TM expression by competing for binding to p300, a transcriptional coactivator essential for TM expression (Sohn et al., 2005). An intriguing study by Takeda *et al.* (Takeda et al., 2007) also reports that endothelial TM levels are subject to circadian variation (an important variable in CVD event occurrence) via TM promoter transactivation involving CLOCK/BMAL-2 heterodimer binding to the promoter E-box region (-CANNTG-).

Endothelial TM expression also displays sensitivity to blood flow-associated laminar shear stress, a hemodynamic force known to impart an atheroprotective phenotype to the endothelium (Traub and Berk, 1998). In view of the anti-coagulant and anti-inflammatory characteristics of this phenotype, the observation that shear stress is a positive regulator of TM expression in most studies is therefore unsurprising. Shear-dependent up-regulation of TM expression under both acute and chronic treatment paradigms has been reported in human retinal microvascular endothelial cells (Ishibazawa et al., 2011), primate peripheral blood-derived endothelial outgrowth cells (Ensley et al., 2012), HUVECs (Bergh et al., 2009; Takada et al., 1994; Wu et al., 2011), human abdominal aortic endothelial cells (HAAECs)

(Rossi et al., 2010), and even in a mouse transverse aortic constriction model of flow-dependent remodeling (Li et al., 2007).

```

CCCTGATCTCTGAACCATACAACACTTGCACGACATTCTCAAGCAACTAGATAGGTCTGG
                                E-Box
CCTTGGCGATGCCTGCCCAAGATCAGGGGATTGCTGTCCAGATGTCAGAATGGAGAAGAA
                                E-Box
TGGAGAAGGCTTTGAGGTTATTAGACCACTCCATCCTCTTGCTGCCCTAGTATAATTTCC
GGCCTCTTCTAAGGTCATTTGGGACCCAACCCCTCTGCTAGTCACAGCAGCCAGGCTTCC
                                Retinoic Acid
TGAGCTCCCATCAGGGATCTAGCTAATCCTTCTCAGAGTCTTGCAAGTTTCAGACACACC
                                KLF-2
CTCTACCAGACTCTTCCTTTTTTTTCCCCCTGCCCAACTACCAGGCCATCCTCCAAACT
CTGGTAGCATCTATAGGGAAGTGTGTGTGTACGTGTGCGTTTGCTTGTGTACGTGTGTAG
                                HIF-1
AGGTTTAAAGACAGGCTACCCGTGGGCTATACCGGAGAGTCTGGGACGGGAAGTGTGCAC
                                ETS-1
TTGCTGACACAAATTCAGTTCGTGGTGGCGCCTGCAGGCCACGCCCTAGGGCCTCCCTAC
                                AP-1
GCCCCGACAGTGTTTTTAACTCTTCGCACAGAGGTGATCCAGGCTGGAGGGCGGGCCACA
                                CRE                                SP-1
AGGCGTCCGGAGAACCAGTAATCCGAGAACGCAGCATCAGCCCTTCCCCTAGGCACTT
                                GRE
CCTTCCTTTTCCCGAACCTCCAGAGAGGGAGGGCCGCGCATTTATAAACTGGAGCCTCAG
                                TATA Box
CTGAGTGGCATGTCAGAGGCTGCCTCGCAGGGACTACGAACCTGGGCTAGAAAAGTCTAG
GCTGAGACAGAGGCTAACTGCTGTCGCCGCAGACGTACGAACCTCTGCCGGGACTGGGT
GCCTGCACCATCGCAGTGCTAGCGTTTCTCGTAGCTTGCACGGTGTCTCCTGAACAGCA
TG

```

Figure 1.11: Promoter region of the TM gene with predicted response elements. Consensus motifs and corresponding response element are highlighted. Key: KLF-1, Krüppel-like factor-2; HIF-1, hypoxia inducible factor-1; ETS-1, v-Ets E26 erythroblastosis; AP-1, activating protein-1; CRE, cAMP response element; SP-1, specificity protein-1, GRE, glucocorticoid response element; *N*, any base. Sequence shown is for rat thrombomodulin promoter (GenBank AF022742.1) Promoter 1-708; ATG start site, 900-902.

The ability of shear stress to offset the down-regulatory impact of TNF- α treatment on TM expression in HUVECs has also been reported (Jun et al., 2009). In stark contrast to these studies, an early publication by Malek *et al.* (Malek et al., 1994) has reported that endothelial TM expression exhibits a mild transient increase followed by a (reversible) decrease to just 16% of baseline levels within 9 hrs of flow onset in bovine aortic endothelial cells (BAECs). One should probably regard this early observation as somewhat atypical however, in light of the volume of recent studies reporting the opposite effect. The use of BAECs for this study (as opposed to human/primate/mouse models) may serve as a possible explanation. Interestingly, the same authors also report that TM is similarly regulated in BAECs by both laminar *and* turbulent shear, although they suggest that this unusual observation should be interpreted with caution due to the arbitrary nature of the chosen shearing conditions (i.e., may not reflect the true *in vivo* situation).

Whilst studied to a lesser extent, contrasting observations also accompany reports on the regulation of TM expression by cyclic strain, the repetitive mechanical deformation of the vessel wall as it rhythmically distends and relaxes with the cardiac cycle. Using a rabbit autologous vein graft model, Sperry *et al.* (2003) have demonstrated that the substantially reduced TM expression in vein grafts (observed both acutely and chronically) occurs as a direct consequence of outward vessel wall distension and, interestingly, not elevated vessel shear rates or local inflammatory response - leading them to conclude that strain-mediated elevation of endothelial thrombogenicity is a principal cause of occlusive thrombosis preceding autologous vein graft failure. In an apparent contrast to this observation, slightly earlier paired studies by Golledge *et al.* (1999) and Gosling *et al.* (1999) employing *ex vivo* human saphenous vein segments within a validated *in vitro* flow circuit, report that exposure

of vein grafts to arterial flow significantly reduces endothelial TM expression in a cyclic strain-independent manner (although stretch-activated calcium ion channels appear to be involved). One explanation for this difference may possibly be attributed to ineffective external stenting used in the earlier studies to block out cyclic strain influences, with up to $7\pm 2\%$ pulsatile expansion still possible with external polytetrafluoroethylene (PTFE) stents. Another explanation may stem from the fact that the later (Sperry et al., 2003) and earlier (Gosling et al., 1999; Golledge et al., 1999) studies reflect chronic (weeks) versus acute (45-90 mins) observations, respectively.

Using both vein graft and *in vitro* vascular cell culture models, recent studies by Kapur and co-workers into the mechanism of endothelial thromboresistance in vein grafts convincingly demonstrate that cyclic strain-dependent induction and release of transforming growth factor- $\beta 1$ (TGF- $\beta 1$) within the medial smooth muscle cell layer could decrease endothelial TM expression in a paracrine manner (Kapur et al., 2011), albeit via an unknown signaling mechanism. Using a pan-neutralizing TGF- $\beta 1$ antibody (1D11), these authors were able to block TM down-regulation, preserve levels of activated protein C, and reduce thrombus formation in a rabbit vein graft model. In stark contrast to these observations however (and indeed to those above), a recent paper by Chen et al. (2008) demonstrates a sustained increase in TM protein expression in HUVEC cultures following 21% (but not 15%) cyclic strain, with a nitric oxide (NO) signaling mechanism strongly implicated in these events. The authors of this study suggest that as TM promoter activity was not induced by cyclic strain of HUVECs, the observed increase in protein expression may putatively be attributed to NO-mediated stabilization of TM protein via S-nitrosylation. In the absence of further data however, and considering the supra-physiological levels of strain applied, the

relevance of this study remains questionable and possibly highlights a limitation of cell culture models in addressing the regulatory impact of cyclic strain on TM expression. Finally, a study by Feng and co-workers report a 2.6 fold down-regulation of TM expression in human aortic smooth muscle cells (HASMCs) following 4% equibiaxial cyclic strain for 24 hrs (1999), however the physiological relevance of this result is questionable in view of the fact that vascular SMCs do not appear to express TM protein or mRNA in vessel walls (Soff et al., 1991) (again highlighting a limitation of cell culture models). The focus of this thesis will try to address the limitation in cell culture models in relation to cyclic strain and TM.

1.2.4 Post-transcriptional regulation of TM

MicroRNAs (miRNAs) are endogenously expressed non-coding RNA molecules (18-24 bases) that post-transcriptionally regulate gene expression within eukaryotic genomes, a mechanism that involves miRNA hybridization with the 3'-untranslated mRNA region of target genes leading to gene silencing and translational repression of protein synthesis (Bonauer et al., 2010; Hussain, 2012). The vascular endothelium is now a confirmed source of several dozen miRNAs that collectively facilitate regulation of endothelial gene expression and cell fate (Staszal et al., 2011; Suarez et al., 2007).

Recent findings on the flow-dependent regulation of Krüppel-like factor 2 (KLF2), a vasoprotective transcription factor known to positively regulate endothelial genes including TM (Fig 1.12) (Gracia-Sancho et al., 2011), provide the most compelling evidence thus far that endothelial TM expression is influenced *albeit indirectly* by miRNA. Inhibition of miR-92a, a member of the miR-17-92 cluster predicted to bind the 3'-UTR of the KLF2 transcript

(Bonauer and Dimmeler, 2009), was found to increase protein and mRNA levels for both KLF2 and TM in HUVECs (Irani, 2011; Wu et al., 2011). The same study also demonstrates that miR-92a is down-regulated by atheroprotective laminar shear to induce KLF2 and TM levels, consistent with earlier shear studies (Dekker et al., 2002; Ishibazawa et al., 2011). Thus, shear-dependent suppression of miR-92a in endothelial cells likely enhances expression of KLF2 leading to transactivation of the TM promoter. Consistent with these observations, atheroprone endothelial sites (e.g., aortic arch) that exhibit non-laminar shear flow pattern, manifest elevated miR-92a leading to decreased levels of KLF2 (and, one would assume, TM) (Fang and Davies, 2012).

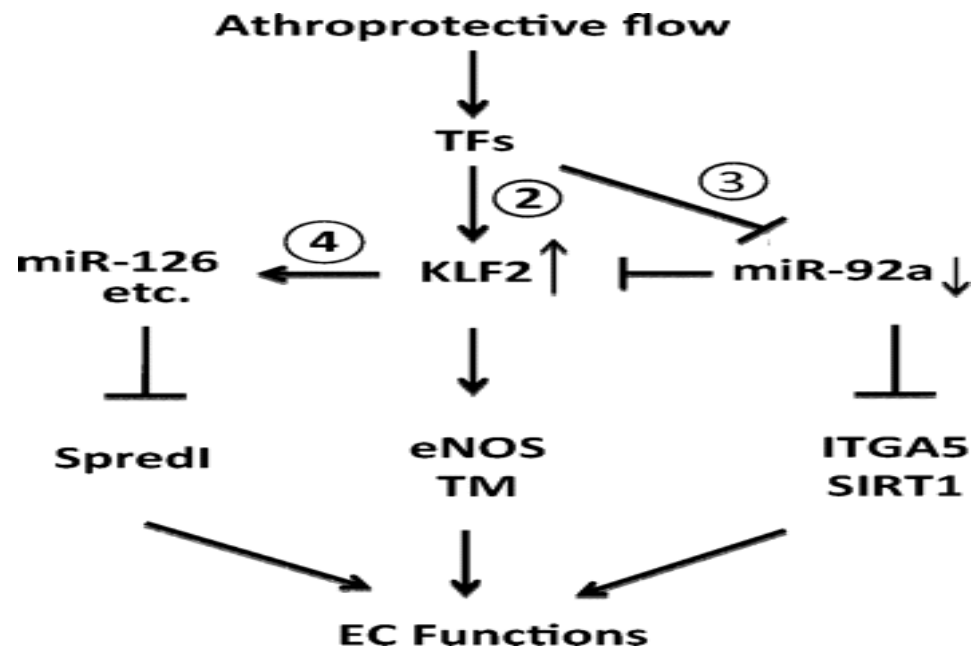


Figure 1.12: Shear stress regulation of Krüppel-like factor 2 (KLF2). Key: EC, endothelial cell; eNOS, endothelial nitric oxide synthase; ITGA5, integrin alpha-5; miR, microRNA; SIRT1, sirtuin 1; Spred1, sprout-related ECH1 domain-containing protein 1; TF, transcription factor; TM, thrombomodulin (Wu et al., 2011).

MicroRNAs are now established therapeutically viable targets in the regulation of vascular inflammation and senescence (e.g., miR-146a, miR-217, miR-34a, miR-126, miR-21, miR-210, miR-181b) (Qin et al., 2012; Sun et al., 2012; Vasa-Nicotera et al., 2011; Voellenkle et al., 2012), tumour angiogenesis (miR-19b-1) (Yin et al., 2012), and in vascular diseases such as hypertension (miR-125a/b-5p) (Li et al., 2010) and atherosclerosis (miR-92a, miR-27, miR-10a) (Chen et al., 2012; Fang and Davies, 2012; Fang et al., 2010). In view of the established roles for TM in the regulation of inflammatory and thrombotic processes within the vascular wall, in conjunction with its indirect regulation by miR-92a via KLF2 (Fang and Davies, 2012, Wu et al., 2011), one can anticipate future studies detailing approaches to modulating TM levels *in vivo* using miRNA-targeting strategies.

1.2.5 Post-translational regulation of TM

As with many regulatory proteins, TM can undergo an assortment of post-translational modifications that can lead to alterations in its size, structural orientation, amino acid side chain chemistry, and localization, ultimately modulating its vascular homeostatic properties to reflect the tissue environment.

1.2.5.1 Oxidation

Early work by Glaser *et al.* (1992) demonstrated that endothelial TM could be almost completely inactivated by oxidation of methionine-388 located within the fifth EGF-like repeat domain (which mediates thrombin binding and anti-coagulant function). These authors

present evidence pointing to polymorphonuclear neutrophil-derived NADPH oxidase as a probable source of the biological oxidants that cause the TM inactivation typically observed in inflamed tissues. Oxidation of met-388 (Fig 1.13) leads to lessening of TM functions (Wang et al., 2000; Wood et al., 2003; Wood et al., 2005), whilst ROS-dependent inactivation of TM has been reported in a mouse model of vascular dysfunction and thrombosis (Adams et al., 2011). Furthermore, a relatively recent article by Stites and Froude (2007) proposes that the elevated oxidative stress associated with smoking and diabetes is responsible for the pro-thrombotic state of these conditions by virtue of increased TM met-388 oxidation and the subsequent decrease in circulating activated protein C levels. Also noteworthy, cellular reducing agents have been shown to modify TM disulphide bonds, rendering the molecule more susceptible to serine protease-mediated cleavage and its subsequent shedding (Menschikowski et al., 2010).

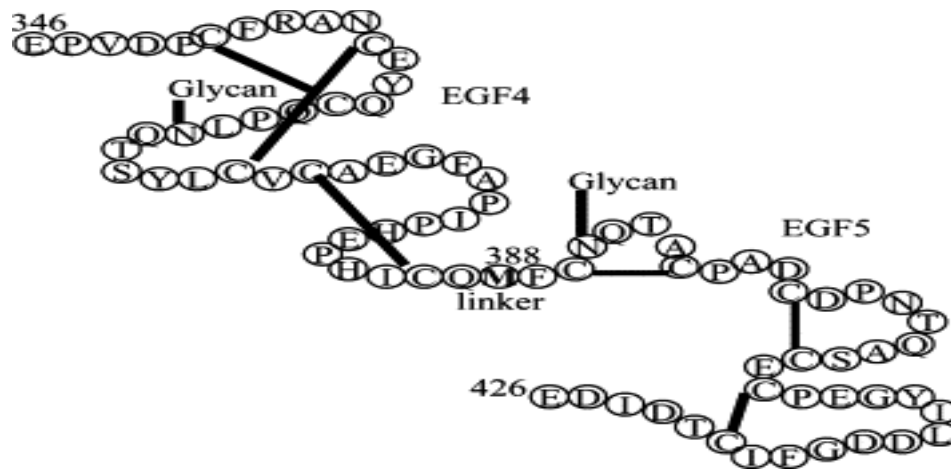


Figure 1.13: The smallest active fragment of TM. Key: amino acids, single letter code; Met 388, in bold; disulphide bonding pattern between cysteine residues, solid lines; two N-linked glycosylation sites, flags (Wood et al., 2005).

1.2.5.2 Glycosylation

As with many transmembrane proteins boasting an ecto-domain, TM is a glycoprotein likely displaying tissue-, organ- and species-specific glycosylation phenotypes, thus enabling regulatory flexibility with respect to TM:thrombin function in different vascular beds. N-linked glycosylation at asparagine residues has been reported for urinary TM (Edano *et al.*, 1998; Wakabayashi *et al.*, 2001). Early studies also report the presence of a TM-associated O-linked glycosaminoglycan (GAG) chain, showing cell-dependent modification of TM at Ser-474 (Lin *et al.*, 1994). Interestingly, both Edano *et al.* and Lin *et al.* also report GAG modification at Ser-472 in C127 mammary tumour cells and CHL-1 melanoma cells, respectively (Edano *et al.*, 1998; Lin *et al.*, 1994). This O-linked GAG modification mediates TM interactions with exogenous GAGs and modulates its thrombin-binding and anti-coagulant activities (Koyama *et al.*, 1991). Indeed, treatment of rabbit TM with chondroitin ABC lyase to remove O-linked GAGs substantially reduced its thrombin-binding capacity (Koyama *et al.*, 1991), whilst Ye *et al.* (1993) report that the chondroitin sulphate (CS) moiety of TM allows it to bind a second molecule of thrombin. The relevance of the O-linked GAG chain in TM is further clarified in a relatively recent study by Bouton and co-workers (2007), who demonstrate in HAECs that the TM CS moiety facilitates complexation with protease nexin-1 (PN-1), a thrombin-inhibiting serpin secreted by endothelial cells. The resultant TM/PN-1 complex has markedly increased inhibitory capacity towards thrombin activity and thrombin-induced fibrinogen clotting in comparison to either unbound TM or PN-1. Importantly, this study is consistent with an earlier paper by Koyama *et al.* (1991) demonstrating how TM can modulate thrombin inactivation by other heparin-activated serpins

(i.e., heparin cofactor II and antithrombin III) as a function of its O-linked CS phenotype in conjunction with the presence or absence of exogenous GAGs (e.g., heparin or dermatan sulphate).

1.2.5.3 Proteolysis

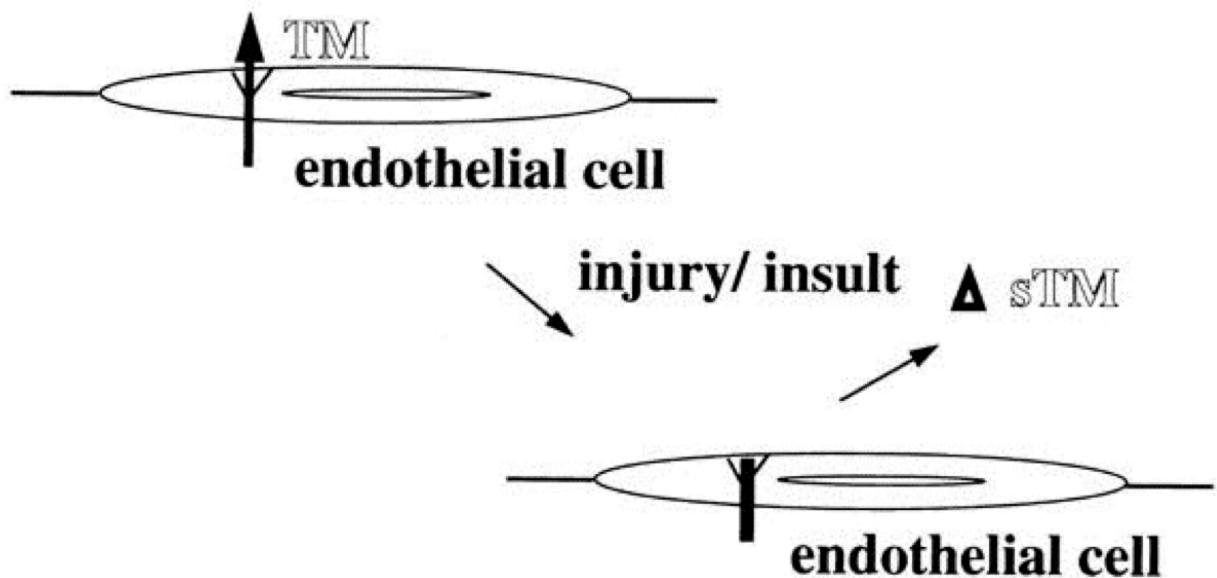


Figure 1.14: Soluble TM is shed and/or proteolysed from the membrane as a result of endothelial injury (Spanier et al., 1996).

Much attention has been devoted to the subject of endothelial TM as a cellular substrate for proteolytic cleavage, frequently leading to its shedding as a soluble variant (sTM) (Fig 1.14). In this respect, sTM has been observed in biological fluids ranging from serum (Oida et al., 1990) and urine (Jackson et al., 1994) to synovial fluid (Conway and

Nowakowski, 1993). A study by Abe *et al.* (1994) demonstrated that following incubation of HUVECs with either granulocyte elastase or cathepsin G, both leukocyte-derived lysosomal proteases, cellular TM activity was respectively decreased by 90% and 80%, with a concomitant increase in soluble TM variants within the media fraction. Other early studies further confirm likely roles for neutrophil-derived elastase and cathepsin G in the reduction of endothelial cell surface TM activity and elevated TM shedding as causative elements of vascular injury in models of *E.coli*-induced sepsis, TNF α -induced endothelial activation, and adult respiratory distress syndrome (ARDS) (Boehme *et al.*, 1996; Kobayashi *et al.*, 1998; MacGregor *et al.*, 1997; Redl *et al.*, 1995). Moreover, a recent study by Matsuyama *et al.* (2008) has implicated neutrophil-derived enzymes in the proteolytic release of TM from gingival epithelial cells during periodontitis. Other enzymes have also been implicated in TM proteolysis and subsequent shedding. Wu *et al.* (2008) report that LPA-induced shedding of the TM lectin-like domain in HUVECs is MMP-dependent. Moreover, *P.gingivalis*-derived cysteine proteases (arginine- and lysine-specific gingipains) have been shown to elicit TM degradation and release from the microvascular endothelium in patients with periodontitis, leading to vascular coagulation and inflammation (Inomata *et al.*, 2009). Studies have also confirmed TM cleavage by rhomboids, a family of evolutionarily conserved intramembrane serine proteases originally characterized based on their proteolytic specificity towards *Drosophila* “Spitz-like” substrates. The TM transmembrane domain can be cleaved by RHBDL2-like rhomboids to release soluble TM, a process mediated through the TM cytoplasmic domain (Lohi *et al.*, 2004). Whilst intriguing however, the relationship between rhomboids and TM has thus far only been studied in non-vascular cells and dermal wound models (Fig 1.15) (Cheng *et al.*, 2011; Lohi *et al.*, 2004; Bergbold and Lemberg, 2013).

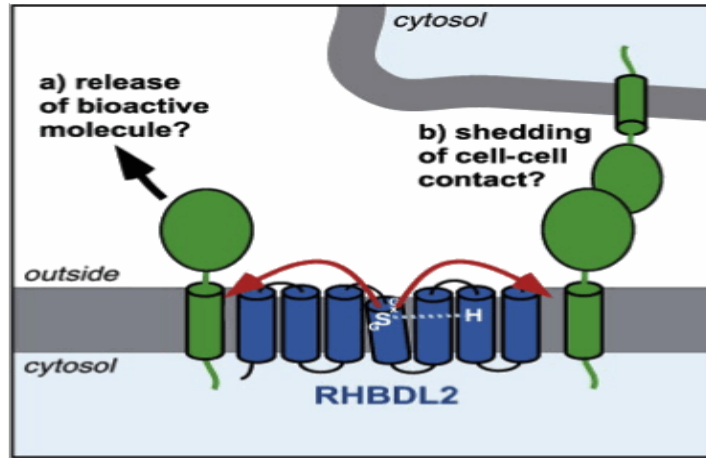


Figure 1.15: Putative role of rhomboids (RHBDL2) in the release of bioactive molecules (e.g., TM) (**A**) and remodeling of cell-cell contact points (**B**) (Bergbold and Lemberg, 2013).

Non-proteolytic mechanisms causing loss of TM from the cell surface are also worth mentioning. Early studies using A549 and hemangioma cells demonstrated how TM/Thrombin binding could lead to internalization of surface TM with evidence for partial TM degradation and recycling (Maruyama and Majerus, 1985; Dittman et al., 1988). Later studies go on to demonstrate that TM cell surface levels can be regulated by endocytosis via non-clathrin coated pits, an internalization process directed by TM's extracellular lectin-like domain (Conway et al., 1994; Conway et al., 1997). TM shedding from activated endothelium via endothelial microparticles (and exosomes) has also been suggested. These heterogeneous microvesicles facilitate the inter-cellular exchange of signalling components such as miRNAs, coagulant molecules, and receptors (Andriantsitohaina et al., 2012). Early work by Satta and co-workers for example has demonstrated that LPS treatment increases TM activity on monocyte-derived MPs by up to 80% (Satta et al., 1997). Co-elevated TM and MP levels in

serum have also been observed during systemic inflammatory response syndrome (SIRS) in humans and during heatstroke in baboons (Bouchama et al., 2008; Ogura et al., 2004), whilst recent work by Duchemin points to an influence of circulating MPs on the “TM-resistance” of patients suffering from myeloproliferative neoplasm (Duchemin et al., 2010). Importantly, the putative role of MPs/exosomes as vehicles for TM release from HAECs will be further investigated in this thesis.

Circulating levels of TM are typically in the low ng/ml range in healthy human subjects, with pathology frequently causing a moderate, but significant, 1.5-2.0 fold increase in patient plasma TM levels (Dharmasaroja et al., 2012; Lin et al., 2008; Mok et al., 2010; Rousseau et al., 2009; Welters et al., 1998). Whilst these TM levels are probably too low to have a significant impact on coagulation processes, the consistent elevation in circulating TM levels during pathologies is now widely regarded as an important circulatory biomarker for endothelial dysfunction and vascular risk assessment (Boehme et al., 1996). Consistent with this notion, elevated plasma TM levels have been found to correlate with atherosclerosis (Pawlak et al., 2010; Taylan et al., 2012), cardioembolic stroke (Dharmasaroja et al., 2012), obesity (Urban et al., 2005), *Lupus erythomatosus*-associated metabolic syndrome (Mok et al., 2010), pre-eclampsia (Rousseau et al., 2009), sepsis-associated disseminated intravascular coagulation (DIC) (Lin et al., 2008), and severe acute respiratory syndrome (SARS) (Liu et al., 2005). Significantly elevated plasma TM levels have also been observed in patients following coronary artery bypass graft (CABG) surgery (Arazi et al., 1998; Kokame et al., 1998). By contrast, several clinical studies report on vascular pathologies manifesting reduced sTM levels. For example, an inverse relationship between sTM and disease risk has been reported for type-2 diabetes (Thorand et al., 2007) and coronary heart disease (Salomaa et al.,

1999; Wu et al., 2003), whilst lower levels of sTM have been reported in the serum of patients suffering from acute cerebral infarction (Nomura et al., 2004). Indeed, the more recent MONICA/KORA study demonstrates a lack of any association between sTM levels and CHD risk (Karakas et al., 2011). The incongruity within these collective observations therefore illustrates the need for greater understanding of the precise functional relevance and action of sTM in serum and reinforces the importance of co-analysing sTM levels with other thrombotic/coagulation markers (e.g., factor VIII, PAI-1) during vascular risk assessment and cohort stratification (Aleksic et al., 2008).

1.2.6 Therapeutic considerations for TM

1.2.6.1 Soluble recombinant TM (sTM)

An improved understanding of the regulation and functions of TM within the vascular endothelium has enabled researchers to better exploit its therapeutic potential. The *vasculoprotective* properties of various soluble TM preparations (which have been shown to effectively bind circulating thrombin and generate activated protein C) have received particular attention, with studies ranging from animal models to human clinical trials (for review see Morser et al., 2012). An early study by Li *et al.* (Li et al., 2004) for example demonstrates how recombinant sTM infusion could reduce neointimal hyperplasia following balloon injury in a rabbit femoral artery model - a therapeutic mechanism that likely encapsulates the anti-coagulant and anti-inflammatory properties of the recombinant sTM domains. The ability of sTM to effectively reverse the inflammatory phenotype of the renal

microvascular endothelium in rat and murine models of acute ischemic kidney injury and chronic kidney disease, respectively, has also been reported (Rajashekhar et al., 2012; Sharfuddin et al., 2009). As further testament to its vasculoprotective properties, the therapeutic benefits of recombinant sTM administration towards recovery from severe inflammatory disorders such as heatstroke and radiation toxicity have again been demonstrated in rat and murine models, respectively (Geiger et al., 2012; Hagiwara et al., 2010), the former study highlighting an sTM mechanism involving a decrease in high-mobility group box 1 (HMGB1) serum levels in conjunction with blockade of NO over-production. A human recombinant TM comprising the six EGF-like repeats (domain 2) and ser/thr-rich section (domain 3), subsequently referred to as TMD23, has also been reported to have vasculoprotective properties in animal models. Shi *et al.* (2005) illustrate the pro-angiogenic potential of TMD23 in rat corneal implants, whilst Wei *et al.* (2011) demonstrate the ability of TMD23 to reduce both neointimal formation (C57BL/6 mouse carotid ligation model) and atherosclerotic lesion formation (ApoE^{-/-} mouse model).

The beneficial effects of soluble TM have also been reported in human clinical trials (Saito et al., 2007). Approved in 2008 for human therapy in Japan, ART-123 (thrombomodulin alpha, ReomodulinTM) is a recombinant human soluble TM comprising extracellular domains 1-3, which are essential for the anti-inflammatory and anti-coagulant actions of the molecule. ART-123 has been reported to be extremely effective in the rapid resolution of DIC (Fig 1.16) (Ito and Maruyama, 2011; Kawano et al., 2011; Ogawa et al., 2012), proving safer and more effective as an inhibitor of the propagation of coagulation than traditional low-dose heparin therapy (Nakashima et al., 1998). ART-123 has also been used to successfully treat microangiopathies stemming from transplantation-associated sepsis (Sakai

et al., 2010) and *Lupus*-induced thrombosis (Suarez et al., 2007), as well as reversing the capillary leakage that accompanies ‘inflammatory engraftment syndrome’ in individuals undergoing hematopoietic stem cell therapy (Ikezoe et al., 2010).

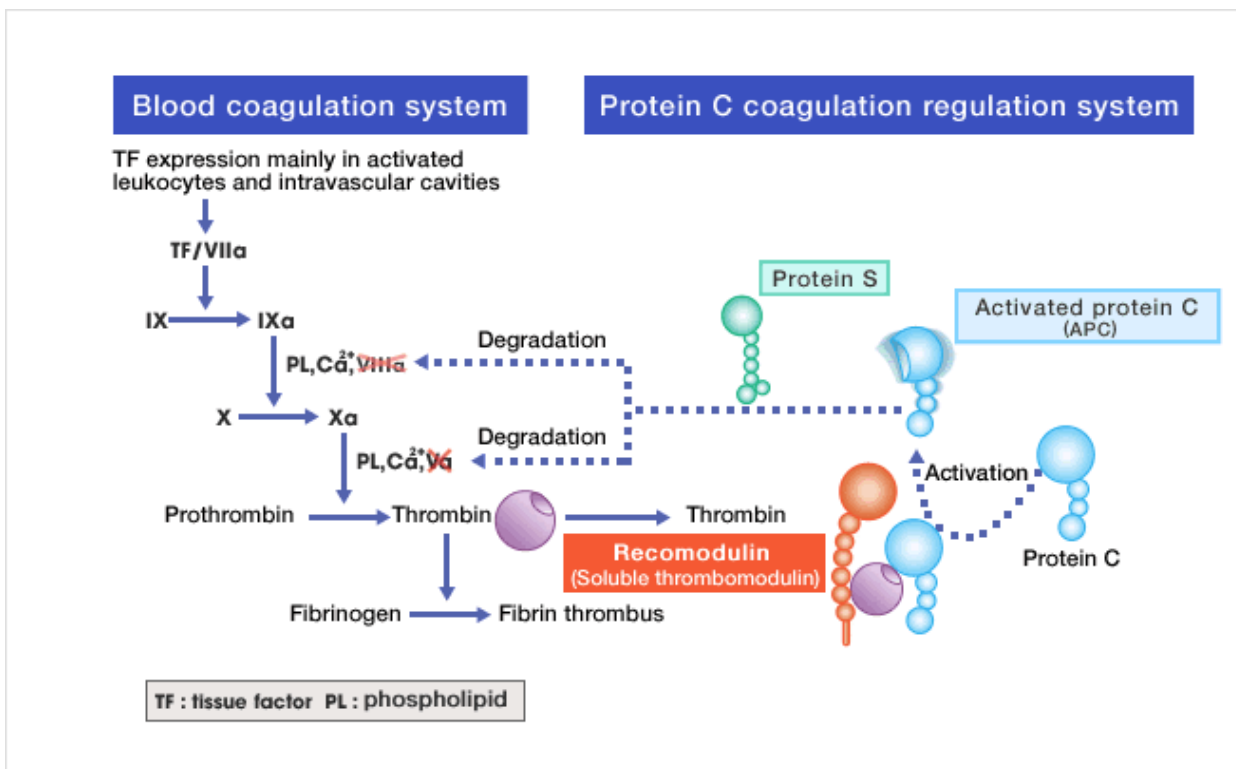


Figure 1.16: Mechanism of action of Recomodulin™ (ART-123). It activated protein C by binding to thrombin (<http://www.recomodulin.com/en/recomodulin/mechanism.html>).

Solulin® (sothrombomodulin alpha) is another human recombinant sTM analogue that has recently undergone a Phase 1 human clinical trial (Van Iersel et al., 2011). Solulin comprises the same soluble extracellular structure as ART-123, but with specific modifications to further enhance the pharmacokinetic and pharmacodynamic properties of the molecule. These include a series of N-/C-terminal amino acid deletions and up to four single

amino acid exchanges to enhance resistance to oxidation, improve cellular export, and prevent attachment of chondroitin sulphate - collectively improving the stability, homogeneity, and plasma elimination half-life of sTM (Van Iersel et al., 2011). The efficacy of Solulin in reducing infarct volume during acute ischemic stroke in rats has been attributed to its thrombin binding anti-coagulant properties (Su et al., 2011), as well as its ability to down-regulate inflammatory cytokine gene expression (Ryang et al., 2011), whilst its anti-fibrinolytic properties are evident in clot stability assays performed on whole blood drawn from hemophilic human and canine subjects (Foley et al., 2012).

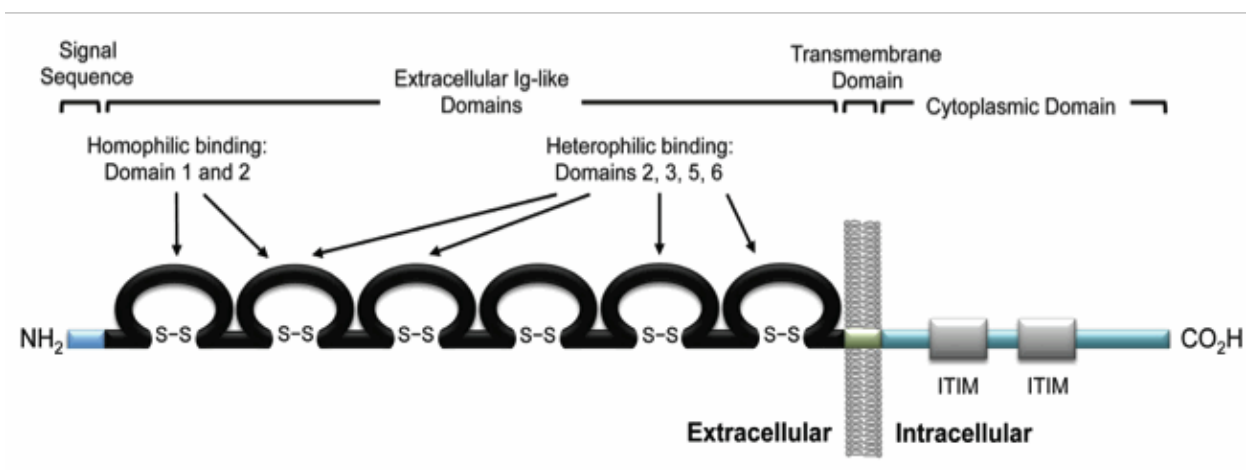


Figure 1.17: The PECAM-1 (CD31) protein domain structure and sites of molecular binding interactions (Chacko et al., 2012).

Finally, strategies to improve sTM targeting and therapeutic efficacy offer a means of enhancing the clinical value of recombinant soluble TM. Early work by Wang and co-workers for example demonstrated that fusing a tissue factor (TF) single chain antibody to an active TM fragment generated a novel fusion protein, Ab(TF)-TM, with a dual mechanism of action

- namely, anti-coagulant TM-mediated enhancement of protein C activation in conjunction with blockade of pro-thrombotic TF/factor VIIa-mediated activation of factor IX/X. The fusion protein subsequently demonstrated significantly higher fold efficacy in the resolution of DIC in rats than either sTM or Ab(TF) alone (Wang et al., 2006). Similarly, linking a PECAM-1-directed antibody single chain fragment (scFv) to TM recently yielded a fusion protein, scFv (PECAM-1)-TM, for enhanced vascular immunotargeting of TM in mice (Fig 1.17) (Chacko et al., 2012). Moreover, fusion of TM to a red blood cell-directed scFv was recently shown to prolong the circulation time and bioavailability of soluble TM (Zaitsev et al., 2012).

1.2.6.2 Biomaterial coating and TM

The use of recombinant human TM to modulate the surface thromboresistance of blood-contacting biomaterials represents another important therapeutic application. Workers have recently demonstrated for example that coating of ART-123 onto dialyzer membranes can effectively prevent clot formation during dialysis, thereby providing a safe alternative to the drawbacks of heparin administration (Matsusaki et al., 2008; Omichi et al., 2010). Moreover, recent evidence demonstrating incomplete endothelialization and low TM expression levels among existing FDA-approved drug eluting stents (DES) has prompted scientists to re-consider the influence of DES agents on endothelial thromboresistance leading to stent thrombosis (Joner et al., 2008). Paclitaxel, an anti-proliferative DES agent used to prevent neointimal hyperplasia, has been shown to cause TNF- α -induced release of tissue factor leading to endothelial TM down-regulation and thereby contributing to a pro-

thrombotic intimal stent surface (Wang et al., 2011; Wood et al., 2010). Re-engineering of stents to avoid such thrombogenic complications is now being undertaken. Wong et al. have demonstrated for example that stenting with recombinant human TM-coated PTFE stents (Fig 1.18) could significantly reduce balloon angioplasty-induced neointimal hyperplasia in a pig carotid artery model (Wong et al., 2008). Long term studies however need to be conducted to ascertain the resilience of this and other related stent coating improvements for the prevention of arterial thrombosis and graft stenosis following balloon angioplasty and CABG, respectively.

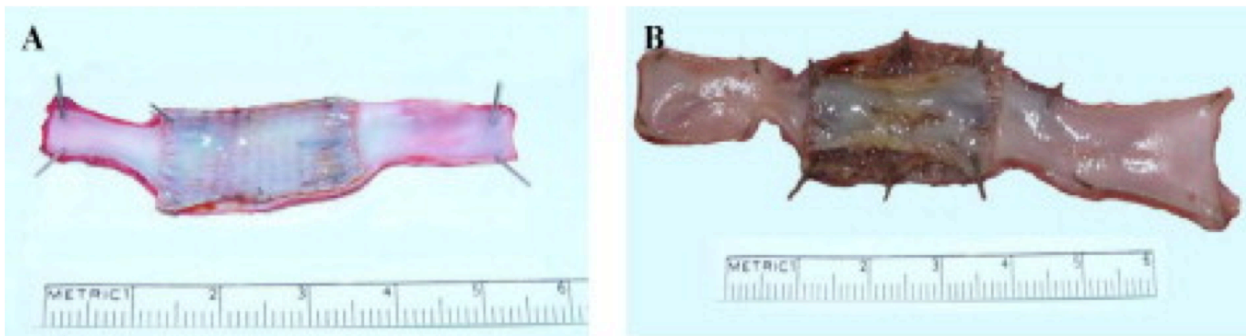


Figure 1.18: Photographs of the luminal surface of expanded polytetrafluoroethylene (ePTFE) covered stent grafts explanted at 4 weeks. **(A)** The recombinant TM-coated ePTFE stent graft is covered with a smooth, gleaming white thin layer with minimum surface deposition. **(B)** The uncoated ePTFE stent graft is covered with an uneven thick yellow-brown layer with scattered blood clots (Wong et al., 2008).

1.2.6.3 Statins and TM

Statins reduce endogenous cholesterol biosynthesis through selective inhibition of 3-hydroxy-3-methylglutaryl co-enzyme A reductase (Krukemyer and Talbert, 1987), and so are widely prescribed for the treatment of dyslipidemias associated with cardiovascular disease and diabetes. Statins also exhibit a multitude of beneficial pleiotropic (non-lipid) effects, of which the vascular endothelium is a key target. Statin-mediated up-regulation of eNOS for example has well known anti-inflammatory and anti-coagulant effects (Takemoto and Liao, 2001). Induction of endogenous TM production leading to anti-inflammatory effects constitutes a further pleiotropic benefit of statins, albeit originally unforeseen for this class of drug (and quite distinct from the pre-designed therapeutic modality of recombinant soluble TM). Various studies have documented the up-regulation of TM expression in endothelial cells in response to either atorvastatin or simvastatin treatment and demonstrate the anti-inflammatory ability of statins to counteract the suppressive effects of TNF- α (and thus, NF- κ B) on TM expression (Bergh et al., 2012; Lin et al., 2009; Shi et al., 2003). The induction of TM expression and protein C activation in irradiated HUVECs has also recently been reported to be a protective effect of atorvastatin (Ran et al., 2010). The statin-mediated induction of TM expression has been attributed to transcriptional mechanisms involving both the up-regulation of KLF2 expression and the NO-dependent dissociation of HSF1 from heat shock protein 90, with subsequent nuclear translocation of both factors to Kruppel-like factor and heat shock elements within the TM promoter, respectively (Fu et al., 2008; Sen-Banerjee et al., 2005). With respect to KLF2, researchers have also reported that atheroprotective laminar shear stress, through suppression of miR-92a, can up-regulate endothelial TM via KLF2-

dependent transactivation of the TM promoter (Dekker et al., 2002; Wu et al., 2011). Interestingly, the pleiotropic up-regulation of endothelial TM by statins was only observed under atheroprotective shearing conditions (consistent with miR-92a suppression and KLF2 induction), and not under conditions of atherogenic oscillatory shear (Rossi et al., 2011). These collective observations suggest that statin-mediated pleiotropic effects on TM are restricted to shear-protected regions of the endothelium and putatively involve suppression of miR-92a. They also lead one to speculate that anti-miR-92a-driven TM up-regulation, used in conjunction with statins, may be a potentially viable future therapeutic approach for the improved treatment of vascular pathologies manifesting elevated endothelial thrombogenicity.

1.3 Rationale for project

Circumferential cyclic strain is an important moderator of the biochemical and physical properties of the endothelium and the entire vasculature in general (Cheng et al., 2001; Howard et al., 1997; Matsushita et al., 2001). Dysregulation of cyclic strain (e.g., attenuated, elevated, altered pulsatility) can affect vessel wall health and normal remodeling processes (Chen et al., 2008). It can also lead to endothelial dysfunction and cardiovascular diseases including hypertension (Li et al., 2010), atherosclerosis (Hahn and Schwartz, 2009), coronary heart disease (Tinelli et al., 2007) and vein graft rejection (Sperry et al., 2003). Thrombomodulin is clearly critical to endothelial function (Adams and Huntington, 2006; Conway, 2011; Esmon, 2003). Interestingly, elevated levels of cyclic strain have been correlated to increased thrombomodulin release (Kim et al., 2002). However, extremely limited in vitro and in vivo studies document this release (Chen et al., 2008; Feng et al., 1999;

Golledge et al., 1999; Gosling et al., 1999; Kapur et al., 2011; Sperry et al., 2003), whilst the pathway involved still remains unclear. Furthermore, there are limited studies on the effect of cyclic strain on TM expression.

Biomechanical force	TM expression	TM release
Shear stress	↑ (Takada 1994; Bergh 2009; Wu 2011)	?
Cyclic strain	↑ <i>in vitro</i> (Chen et al., 2008) ↓ <i>in vivo</i> vein grafts (Sperry et al., 2003)	?
Soluble TM (sTM)	NA	↑ in DIC, hypertension (Lin et al., 2008; Lopes et al., 2002) ↓ in type-2 diabetes, coronary heart disease (Thorand et al., 2007; Wu et al., 2003)

Table 1.2: Current literature documenting the effect of hemodynamic forces on TM expression and release. The symbols used represent the following; ↑, increased; ↓, decreased; +/-CS, in the absence or presence of cyclic strain; NA, not applicable.

1.4 Objectives

With this in mind, a clearer understanding of how cyclic strain modulates TM production and release within the vascular endothelium is warranted. Our basic objectives are:

1. To understand how cyclic strain regulates thrombomodulin release and expression
2. To identify the signalling components mediating strain-dependent regulation of thrombomodulin
3. To understand how inflammatory mediators (e.g., TNF- α) influence strain-induced regulation of thrombomodulin
4. To investigate microvesicle involvement in cyclic strain-mediated thrombomodulin release whilst more clearly clarifying whether thrombomodulin is released from the membrane via exosomes or microparticles

The data presented in the subsequent chapters investigates; (i) the regulatory effect of equibiaxial cyclic strain on TM in cultured HAECs; (ii) the role played by inflammatory mediators (e.g., TNF- α and ox-LDL) on the strain-mediated regulation of TM expression and release; a range of signalling mechanisms were also studied to determine their involvement in both cyclic strain-mediated regulation of TM expression and release; and (iii) the putative role of both MPs and exosomes as microvesicular vehicles for TM release in response to strain.

Chapter 2:

Materials & Methods

2.1 Materials

Abcam (MA, USA): Mouse anti-thrombomodulin monoclonal IgG antibody, human thrombomodulin ELISA kit

Acris antibodies (Herford, Germany): Rabbit anti-human CD141/THBD

Aktiengesellschaft and Company (Numbrecht, Germany): T25/75/175 tissue culture flasks, 1.5 ml micro tube with safety cap, 6-well and 96-well tissue culture plates, 2 ml blowout pipette, 2 ml, 5 ml, 10 ml and 25 ml serological pipettes, 10, 20 and 1000 µl pipette tips, 15 ml and 50 ml falcons, 50 ml flat-bottom falcons, cryovials, cell scrapers, P100 tissue culture dishes.

Applied Biosystems (CA, USA): Fast optical 96-well reaction plates (with adhesive covers), high capacity cDNA reverse transcription kit

BioRad (CA, USA): Coomassie stain, Precision Plus protein marker, thick mini trans-blot filter paper

Bio-Sciences Ltd (Dun Laoghaire, Ireland): F96 immuno plate II maxisorp

Biotrend Chemikalien GmbH (Köln, Germany): Oxidized low-density lipoprotein

Calbiochem (San Diego, CA): Apocynin

Corriell Cell Repository (NJ, USA): Bovine aortic endothelial cells (BAECs)

Dunn Labortechnik GmbH (Germany): Bioflex[®] plates (Pronectin[®] -coated)

eBioscience (CA, USA): Il-6 ELISA kit

Enzo Life Sciences (NY, USA): GM6001

Eurofins MWG Operon (Ebersburg, Germany): Human primer sets: eNOS, GAPDH, KLF2, S18, Thrombomodulin

Fermentas (York, UK): Green Taq, DNA ladder 100 bp and 1 Kb, dNTPs, 10X Buffer, MgCl₂

GE-Healthcare (Bucks, UK): ECL secondary antibodies; donkey anti-rabbit, sheep anti-mouse

Gibco (Scotland, UK): UltraPUR[™] Distilled water DNase-/RNase-free

Invitrogen (Bio-Sciences) (Groningen, The Netherlands): Propidium iodide (PI), SyberSafe[®], Total exosomes isolation reagent, Trizol[®] reagent, Vybrant[™] FACs apoptosis assay kit #2, ultra pure water

Labtech (East Sussex, UK): ADAM[™] counter kit

Merck Millipore (MA, USA): Rabbit anti-sheep IgG HRP-conjugated secondary antibody

Meso Scale Discovery (MD, USA): K15009C-1 MS2400 Human Pro-inflammatory panel 1, Ultrasensitive ELISA kit, K15135C-1 MS2400 Human vascular injury panel I, Ultrasensitive ELISA kit

Millipore (MA, USA): Amicon Ultra 2ml 30K 24PK, Luminata[™] Crescendo Western HRP Substrate, tumour necrosis factor- α (TNF- α)

PALL Corporation (Dun Laoghaire, Ireland): Acrodisc 32 mm syringe filter with 0.2 μ M super membrane, biotrace nitrocellulose membrane

Promocell (Heidelberg, Germany): Cryo-SFM, Endothelial cell growth media MV, Human aortic endothelial cells (HAECs)

R&D Systems (MN, USA): Human thrombomodulin/BCDA-3 DuoSet ELISA, sheep anti-human thrombomodulin antibody

Roche Diagnostics (Basel, Switzerland): FastStart universal SYBR green (ROX), protein and phosphatase inhibitor cocktail

Sigma-Aldrich (Dorset, UK): Autoradiography Kodak developing and fixer solutions, acetone, agarose, ammonium persulfate, β -mercaptoethanol, bisacrylamide, bromophenol blue, chloroform, CL-Xposure film 125 mm X 175 mm, dimethyl sulfoxide, DNase amplification kit, EDTA, glucose, glycerol, glycine, HEPES, hydrochloric acid, Lauryl sulfate (i.e., SDS), magnesium sulphate, methanol, PBS tablets, penicillin-streptomycin (100X), Ponceau S, potassium chloride, potassium phosphate, potassium phosphate-dibasic trihydrate, potassium hydroxide, sodium chloride, sodium deoxycholate, sodium fluoride, sodium orthovanadate, sodium phosphate, sucrose, superoxide dismutase, tetramethylethylenediamine (TEMED), 3,3',5,5'-tetramethylbenzidine liquid substrate, trypsin-EDTA solution (10X), Triton[®] X-100, trizma base, tryptone, Tween[®] 20.

Qiagen (West Sussex, UK): SYBR Green[®] PCR kit

Technoclone GmbH (Vienna, Austria): Technozym[®] von Willebrand factor:Ag ELISA kit

Thermo Fisher Scientific (Leicestershire, UK): BCA protein assay kit, bovine serum albumin (BSA), Taq DNA Polymerase, isopropanol, trizma base, weigh boats, Supersignal West Pico chemiluminescent substrate, restore Western blot stripping buffer, RNase Away

2.2 Cell culture methods

All cell culture procedures were carried out in a clean and sterile environment using a Holten Lamin-Air laminar flow cabinet. Cells were examined daily for growth and morphology characteristics using a Nikon Eclipse TS100 phase-contrast microscope.

2.2.1 Endothelial cells

2.2.1.1 Culture of human aortic endothelial cells (HAECs)

Differentiated human aortic endothelial cells (HAECs) were obtained from PromoCell GmbH (Heidelberg, Germany). The cells were isolated from a 22 year old female donor. Cells were cultured in Endothelial cell growth medium MV supplemented with antibiotics (100 U/ml penicillin and 100 µg/ml streptomycin) and a separate Supplement Mix® of growth factors containing fetal calf serum (FCS) (0.05 ml/ml), endothelial cell growth supplement (0.004 ml/ml), epidermal growth factor (10 ng/ml), heparin (90 µg/ml), and hydrocortisone (1 µg/ml). Cells between passages 5-11 were used for experimental purposes and were stored in a humidified atmosphere of 5% CO₂/95% air at 37°C (Fig 2.1).

2.2.2 Trypsinisation of HAECs

HAECs are an adherent cell line so trypsinisation is necessary for their sub-culture. Growth media was removed from the flasks and the cells were washed X3 sterile PBS to remove α -macroglobulin, a trypsin inhibitor present in FCS. An appropriate volume of trypsin/EDTA (10% volume in sterile PBS) was subsequently added to the cells and incubated at 37°C for 1-2 mins until the cells begin to detach from the flask surface. Trypsin was inactivated by the addition of complete growth media containing FCS and the cells were removed from suspension by centrifugation at 0.1 rcf for 5 min. Cells were resuspended in growth medium (or freeze medium) and counted using either a Neubauer chamber haemocytometer or ADAM™ Counter. HAECs were routinely split at a 1:3 or 1:4 ratios for either further sub-culturing or to be cryopreserved.

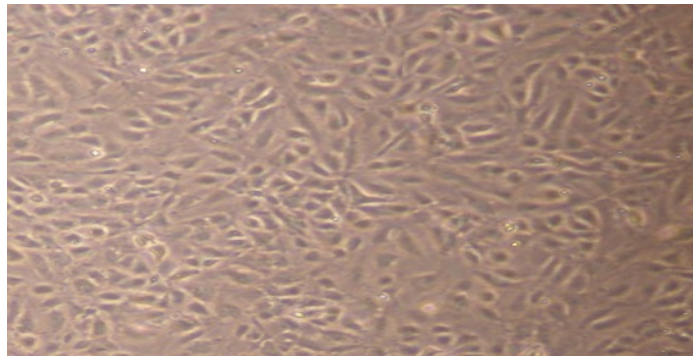


Figure 2.1: HAECs are isolated from the human ascending (thoracic) and descending (abdominal) aorta. They have a “cobblestone” morphology when static, as shown above.

2.2.3 Cryopreservation and recovery of cells

For long-term storage, cells were maintained in a liquid nitrogen cryo-freezer unit (Taylor-Wharton, USA). Following trypsinisation, cells to be stored were centrifuged at 0.1 rcf for 5 min at room temperature and the resultant pellet was resuspended in HAEC media containing 20% (v/v) FBS, 10% (v/v) dimethylsulphoxide (DMSO) and 1% (v/v) penicillin/streptomycin. 1.5 ml aliquots were transferred to sterile cryovials and frozen in a –80°C freezer at a rate of –1°C/minute using a Mr Freeze[®] cryo-freezing container. Following overnight freezing at –80°C, the cryovials were transferred to the cryo-freezer unit.

For recovery of cells, cryovials were thawed rapidly in a 37°C water bath and added to a cell culture dish containing pre-warmed (37°C) growth medium to dilute the DMSO. After 24 hrs the medium was removed, the cells were washed in PBS and fresh growth medium added.

2.2.4 Cell counting

2.2.4.1 Haemocytometer

To aid in reproducibility of experiments, cells were seeded at precise numbers and densities. This was done using a Neubauer chamber haemocytometer following trypan blue staining for cell viability (Fig 2.2). 20 ml of trypan blue was added to 100 ml of cell suspension and the mixture left to incubate for 2 min. 20 ml of this mixture was loaded into the counting chamber of the haemocytometer and cells visualized by light microscopy (Fig

2.1). Viable cells excluded the dye, whilst dead cells stained blue due to compromise of the cell membrane. Cells that touch the top and right lines of a square were not counted, while cells on the bottom and left side were counted. The number of cells was calculated using the following equation:

$$\text{Average Cell No.} \times \text{Dilution Factor} \times 1 \times 10^4 \text{ (area under cover slip mm}^3\text{)} = \text{Viable cells/ml}$$

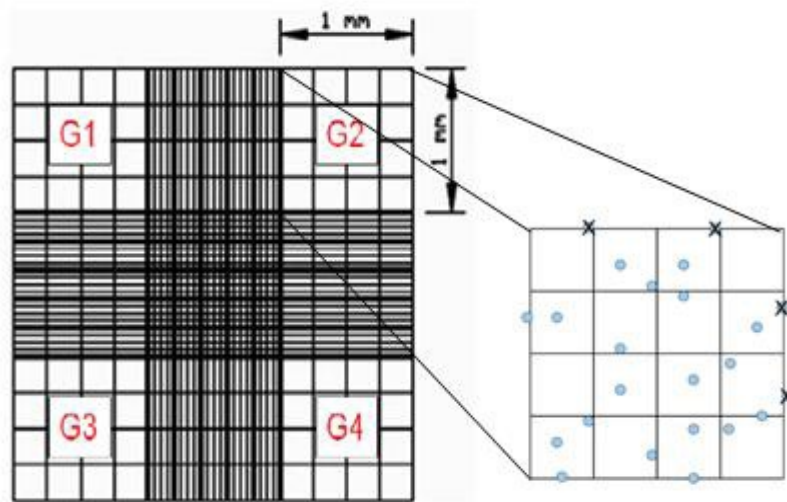


Figure 2.2: The haemocytometer, indicating the counting grid.

2.2.4.2 ADAM™ cell counter

Cell counts were also made using an Advanced Detection and Accurate Measurement (ADAM™) cell counter (Digital Bio, Korea) that utilises fluorescent cell staining to determine total and viable cell count in a given sample (Fig 2.3). Cells are mixed with two solutions; Solution N, containing propidium iodide (PI), a fluorescent dye that will intercalate with DNA, but which cannot enter cells with intact membranes. Therefore, only non-viable cells

will fluoresce with PI alone. The second, Solution T, contains PI and a detergent that will disrupt viable cell membranes allowing PI to stain both viable and non-viable cells. ADAM™ contains both laser optics and image analysis software that allows parallel determination of both total and viable cell numbers in a sample from these two staining methods.

Two 12 µl aliquots of a cell sample were taken; one aliquot was mixed with 12 µl of Solution N accustain and the second with 12 µl Solution T accustain. 20 µl of each cell mixture was then loaded into the appropriate labelled chamber in an AccuChip. The AccuChip was then loaded into the ADAM™ counter where 40-60 images were taken of the cell chambers and average cell number and viability calculated using the integrated image analysis software (Fig 2.3).

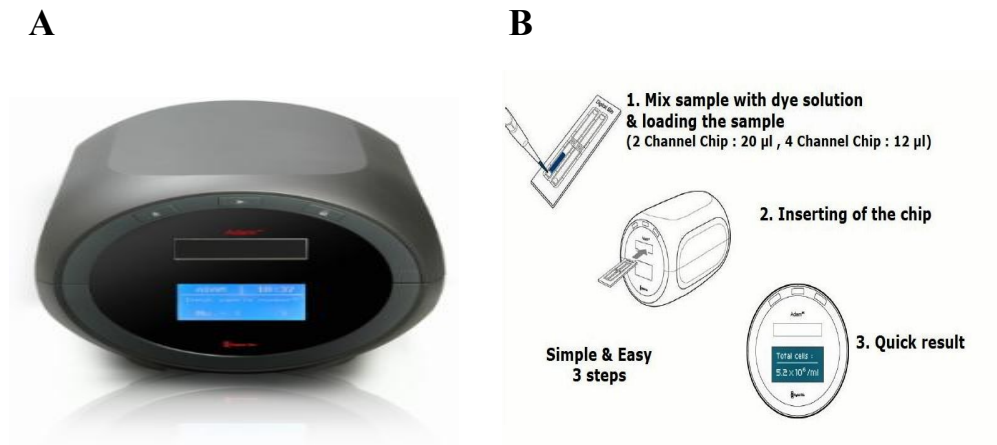


Figure 2.3: The ADAM™ counter (A) and loading of an AccuChip and reading (B).

2.2.5 Hemodynamic force studies

2.2.5.1 Cyclic strain: Flexercell[®] Tension Plus[™] FX-4000T[™] System

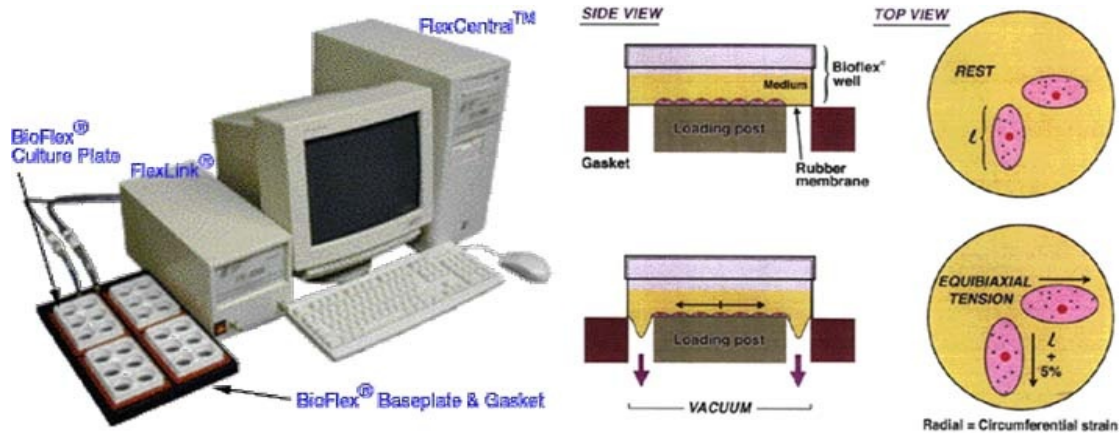


Figure 2.4: Flexercell[®] Tension Plus[™] FX-4000T[™] system.

For cyclic strain studies, HAECs were seeded onto 6-well Bioflex[®] plates at the appropriate seeding density (300,000 – 500,000 cells/well). Bioflex[®] plates have a flexible Pronectin[®]-coated silicon membrane bottom which can be deformed by microprocessor-controlled vacuum (Fig 2.4) (Dunn Labortechnik GmbH, Germany). Before the experiment, media is replenished and cells are then exposed to equibiaxial cyclic strain. A Flexercell[®] Tension Plus[™] FX-4000T[™] system (Flexercell International Corp., Hillsborough, NC) was used to apply physiological equibiaxial cyclic strain to each plate (0-12.5% strain, 60 cycles/min, 0-48 hr, cardiac waveform) as previously described (Collins et al., 2006; von Offenbergs Sweeney et al., 2004). Post-strain, media supernatants, cell lysates, and mRNA

samples were harvested for analysis. Media supernatants were harvested per each individual well whereas 2-3 wells were frequently pooled for each cell lysate or mRNA sample.

Both dose-response and time-course studies were carried out. Control plates containing “unstrained” endothelial cells were also seeded into Bioflex[®] plates in the same manner and kept in the same incubator as the strained cells. Following cyclic strain experiments, cells were either; (i) harvested for Real-Time PCR measurement of mRNA; (ii) harvested for ELISA measurement of secreted protein concentration in the supernatant or; (iii) harvested for Western blotting to determine protein expression levels.

2.2.5.2 Laminar shear stress: Orbital Rotation

For laminar shear stress studies, orbital rotation was applied as described in other publications (Fitzpatrick et al., 2009; Colgan et al., 2007). HAECs were seeded at 300,000 cells/well onto 6-well plates and grown to confluency. Culture medium was removed and replenished with 4 ml of fresh medium. Cells were then exposed to laminar shear stress (0-10 dynes/cm², 0-24 hr) using an orbital rotator (Stuart Scientific Mini Orbital Shaker, Staffordshire, UK), with shear determined by the following equation (Hendrickson et al., 1999);

Control plates containing un-sheared “static” endothelial cells were cultured in the same incubator but on a different shelf to avoid vibrations caused by the orbital rotator. Studies were carried out for differing periods of time (0-48 hrs, 0–10 dynes/cm²). Following shearing experiments, cells were either; (i) harvested for Real-Time PCR measurement of

mRNA expression levels or; (ii) harvested for ELISA measurement of secreted protein concentration in the supernatants.

$$\text{Shear Stress} = \alpha \sqrt{\rho n (2 \pi f)^3}$$

Where α = radius of rotation in cm

ρ = density of liquid in g/l

f = rotation per second

n = liquid viscosity 7.5×10^{-3} dynes/cm² @ 37°C

2.2.6 Transendothelial permeability assay

To measure permeability, HAECs were trypsinised and re-plated at high density (500,000 cells/well) into Millicell hanging cell culture inserts (6-well format, 0.4 μ m pore size, 24 mm filter diameter). After 24 hrs, cells were attached to the surface of the membrane and transendothelial permeability was analysed as previously described (Collins et al., 2006). Fluorophore media was prepared with 1 ml of media and 5 mg (0.0050 g) of FITC-Dextran. A working solution of FITC-Dextran was prepared as follows;

$$250 \mu\text{g/ml}/5000 \mu\text{g/ml} = 0.05 \text{ ml} = 50 \mu\text{l}$$

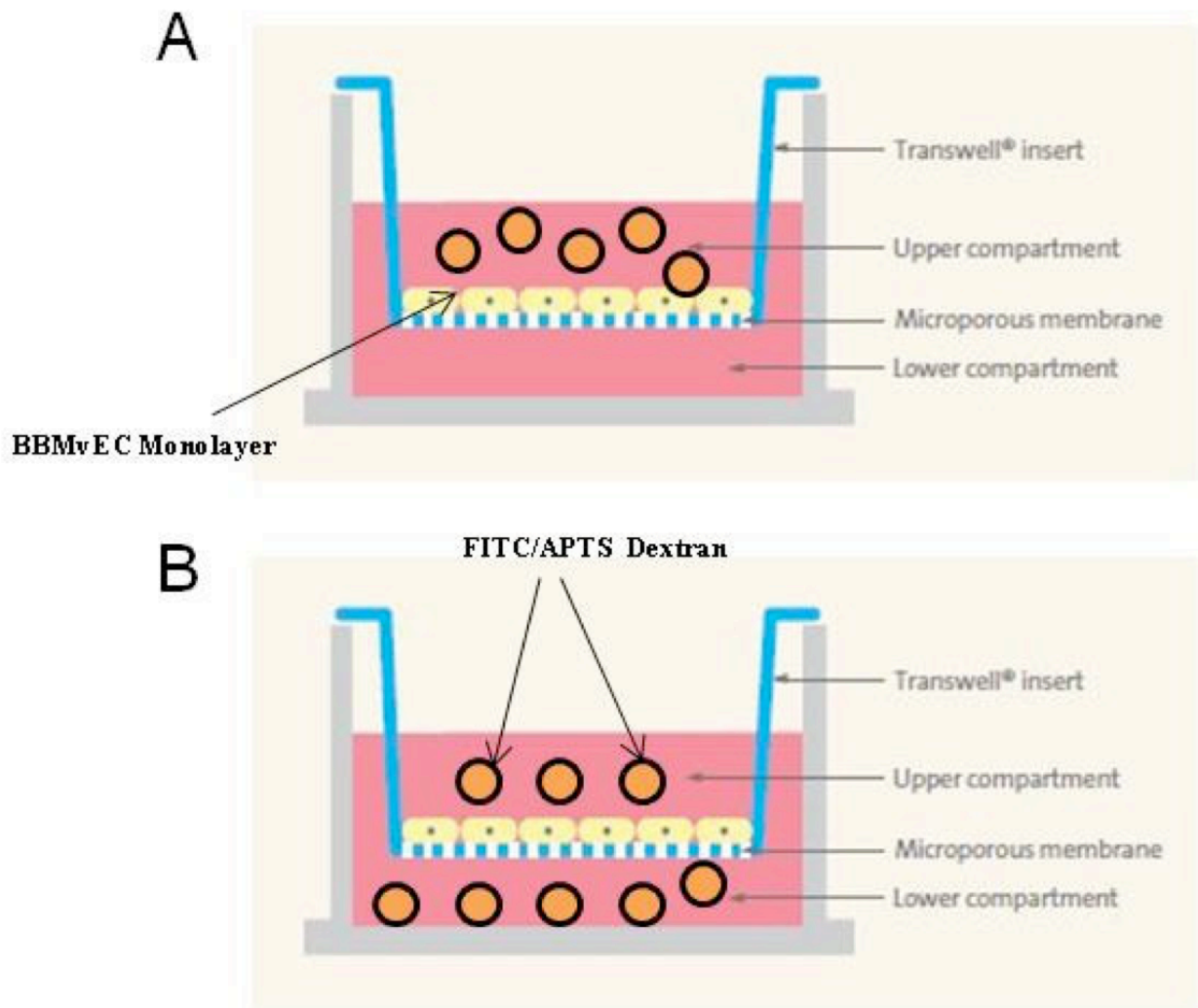


Figure 2.5: Transendothelial permeability assay. **(A)** Shows FITC-labelled dextran in the upper (abluminal) compartment at $t=0$, which diffuses through the HAEC monolayer and semi-permeable membrane, into the lower (subluminal) compartment **(B)**, from which samples are collected every 30 min over 3 hrs.

The final volume is per ml of solution that you are working with, so you need to multiply by 2 (for each insert) and then by the numbers of wells you intend to use (i.e., 2

mls*number of wells + 1). The FITC-Dextran solution was sterilized before application to cells using a syringe fitted with a sterile filter. Fresh culture media was added to the upper (abluminal) and lower (subluminal) chambers of the Millicell insert within the 6- well dish (e.g., 2 ml: upper, 4ml: lower). For the purpose of testing for functional sTM, the upper (abluminal) chambers were “spiked” with 250 µg/ml of concentrated media (described in more detail in Section 5.2.1.5) in the presence or absence of thrombin (1 unit) for 30 mins at 37°C. Subsequently, the media is aspirated and replaced with 4 mls of fresh media in the subluminal chamber and 2 mls of fluorophore media in the abluminal chamber. Transwell diffusion was allowed to advance (Fig 2.5).

Medium samples (28 µl) were collected every 30 min from the subluminal compartment (for up to 3 hrs), diluted to a final volume of 400 µl with complete medium, and examined for FITC-dextran fluorescence (as 3x100 µl replicates in a 96-well fluorescence microplate). Using a TECAN Safire 2 fluorospectrometer (Tecan Group, Switzerland), excitation and emission wavelengths of 490 and 520 nm, respectively, were chosen. % Transendothelial exchange (%TE) of FITC-dextran 40 kDa is expressed as the total subluminal fluorescence at a given time point (from 0-180 min) expressed as a percentage of total abluminal fluorescence at t=0 min.

2.2.7 Inhibitors and inflammatory mediators

In order to probe the signaling pathway putatively mediating the effects of cyclic strain on TM expression and release, inhibitor studies were performed on HAECs in the

absence or presence of cyclic strain. We also investigated the effect of inflammatory mediators on cyclic strain mediated TM expression and release. Prior to treatment with pharmacological inhibitors or inflammatory mediators, HAECs were grown to 80% confluency on Bioflex[®] plates for cyclic strain studies or 6-well dishes for static cell studies, after which growth medium was removed and cells were washed twice in sterile PBS. Inflammatory mediators (Table 2.1) or inhibitors (Table 2.2) were re-constituted in a suitable diluent. Working concentrations were made up in Endothelial Cell Growth Medium MV with addition of antibiotics and Supplement Mix[®]. Cells were then exposed to inhibitors for 1 hr prior to, and for the duration of, hemodynamic challenge. Inhibitor concentrations used in experiments were taken from recent literature and manufacturer's recommendations.

For inflammatory mediator studies (Table 2.1), cells were incubated in culture media containing;

Inflammatory component	Type	Conc. Used
TNF- α	Pro-inflammatory cytokine	0-100 ng/ml
Ox-LDL	Atherogenic lipid	0-145.7 μ g/ml
Glucose	Hyperglycemia	5-30 mM

Table 2.1: Inflammatory mediator and concentrations used in HAECs.

For inhibitor studies (Table 2.2), cells were incubated in culture media containing;

Target	Inhibitor	Conc.
MMPs	GM6001	10 μ M
Integrin α v β 3	Cyclic RGD integrin inhibitor	130 μ M
Rhomboids	DCI	10 μ M
eNOS	L-NAME	1mM
Rac1	NSC23766	50 μ M
NADPH oxidase	Apocynin SOD	10 μ M 100 U/ml
Erk 1/2	PD98059	10 μ M
p38	PD169316	10 μ M
PI3K	PI3K- α In.	2 μ M
Protein Tyr Kinase	Genistein	2 μ M

Table 2.2: Pharmacological inhibitors blocking specific cellular targets and concentrations used in HAECs.

2.2.8 Fluorescence Activated Cell Sorting (FACs) analysis

Flow cytometry is a process used to characterize the properties of fluorescently labelled cells. It gives information about cell size, granularity, and the phenotypic expression of protein markers on or in a particular cell, as well as the proliferative, apoptotic and necrotic state of cells in response to different experimental treatments.

2.2.8.1 Vybrant™ Apoptosis Assay Kit

A Vybrant™ Apoptosis Kit #2 was used to monitor apoptosis in HAECs following cyclic strain experiments. The kit contains an Alexafluor488-conjugated recombinant Annexin V and a red-fluorescent Propidium Iodide (PI) nucleic acid-binding dye. The Alexafluor488 dye is an almost perfect match to Fluorescein IsoThioCyanate (FITC), but it creates brighter and more photostable conjugates. PI stains necrotic cells (but not live apoptotic cells) with red fluorescence, binding tightly to the nucleic acids in the cell. After staining a cell population with Alexafluor488-conjugated Annexin V and PI in the provided binding buffer, apoptotic cells show green fluorescence, dead cells show red and green fluorescence, and live cells show little or no fluorescence. These populations can easily be distinguished using a flow cytometry with the spectral line of an argon-ion laser set for 488 nm excitation.

HAECs were seeded onto Bioflex® plates and allowed to grow for 24 h. Cyclic strain was applied to cells as described above for 24 h. After the treatment, HAECs were washed in PBS three times and harvested by trypsinisation. Cell counts were carried out on each well using both the haemocytometer and Adam™ Cell counter. Afterwards, cell suspensions were pelleted by centrifugation (700 rcf for 5 min) and washed again in 1 ml PBS (containing 0.1% BSA) and re-suspended by gentle pipetting. Cells were subsequently pelleted by centrifugation and re-suspended in 200 µl of 1X Annexin-binding buffer. Propidium Iodide (0.4 µl from 100 µg/ml working solution) and 1 µl Alexafluor488 Annexin V were added to the cell suspension and incubated at room temperature for 15 min. Cells were then placed on ice pending flow cytometry analysis using a Becton Dickinson FACSCAN flow cytometer (NJ, USA).

2.2.9 Membrane vesicle analysis

Cells are known to secrete or shed a large variety of vesicles such as microparticles and exosomes into the extracellular space in normal physiology as well as in activated or disease states (Izumi, 2012). These microvesicles are now emerging as new diagnostic biomarkers with possible roles in mediating inflammation and immunological processes. They have the unique ability to allow the horizontal transfer of bioactive molecules such as proteins, RNAs and microRNAs, to neighbouring cells via outward budding and fission of the plasma membrane of the host cell (Cocucci et al., 2009).

Microparticles (MPs), also referred to as microvesicles, particles, shedding vesicles or ectosomes, are small complex membrane-enclosed structures (measuring 100 nm to 1 μ m) that can be “shed” from the plasma membrane of activated or apoptotic endothelial cells. In contrast, exosomes are small intracellularly derived vesicles (30-120 nm) containing RNA and protein that are “secreted” by a wide variety of cell types and detected in body fluids including blood, saliva, urine and breast milk. Both the type of stimulus and the originating cell determine the vesicle composition (Fleissner et al., 2012). Levels of these vesicles were measured in response to cyclic strain using a combination of centrifugation and isolation techniques described below.

2.2.9.1 Centrifugation techniques

Post-cyclic strain, media supernatants were harvested per well as before. All media samples were spun at 98 rcf for 5 mins at 4°C to remove cellular debris. 110 μ l of each sample

was transferred to a fresh eppendorf for ELISA analysis. The media samples were then spun at 700 rcf for 15 mins at 4°C to further eliminate cellular debris, then at centrifugation speeds ranging from 14,400-20,000 rcf for 20 and 40 minutes, respectively. The supernatants were collected for analysis and the pellets (containing microparticle fractions) were re-suspended in 1 ml or 110 µl of 1X PBS for downstream analysis. All samples were monitored for thrombomodulin using a Human Thrombomodulin/BDCA-3 DuoSet[®] ELISA kit (R&D Systems, MN USA). The steps used to process microvesicles are illustrated by a flow-chart in Fig 5.2.

2.2.9.2 Exosome isolation

Culture media	Reagent
1 mL	500 µl
10 mL	5 mL

Table 2.3: 0.5 volumes of Total Exosome Isolation reagent (Invitrogen, The Netherlands) was added to the appropriate volume of cell culture media.

Post cyclic strain, media supernatants were harvested per well as before. Samples were initially spun at 98 rcf for 5 mins at 4°C, followed by a further spin at 2000 rcf for 30 mins to remove cells and debris. The clear cell-free supernatant was transferred to a new eppendorf. Total Exosome Isolation (Invitrogen, The Netherlands) reagent was then added in 0.5 volumes to the cell culture media (Table 2.3). This reagent forces less-soluble components (i.e.,

exosomes) out of solution, allowing them to be collected after brief, low-speed centrifugation. After this, the eppendorfs were vortexed several times and incubated overnight with Total Exosome Isolation reagent at 2 °C to 8 °C. After incubation, 120 µl of media, now known as “pre-spin” media, was transferred to a fresh eppendorf. The remaining media was centrifuged at 10,000 rcf for 1 hour at 2°C to 8°C. Following this spin, the supernatant, now known as “post-spin” media, was transferred to a new eppendorf for further analysis. Exosomes were contained in the pellet (not visible) at the bottom of the tube and then re-suspended in 25 – 100 µl 1X PBS. TM concentration was measured in the re-suspended pellet, the post- and pre-spin media using the Human Thrombomodulin/BDCA-3 DuoSet[®] ELISA kit (R&D Systems, MN USA). The steps used to process microvesicles are illustrated by a flow-chart in Fig 5.4.

2.2.9.3 Media concentration

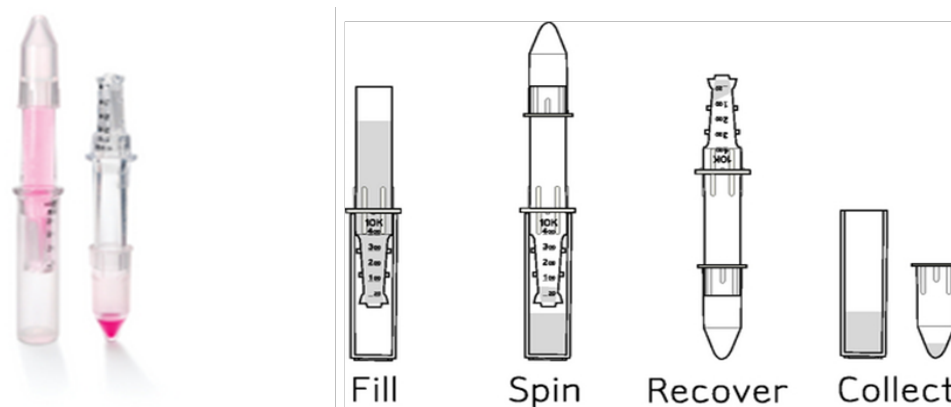


Figure 2.4: Amicon[®] Ultra-2 centrifugal filter device (Millipore, MA, USA).

In order to further investigate TM release, we concentrated serum-free cell culture media for analysis via Western blotting. Post-cyclic strain, serum-free cell culture media was harvested as before and then concentrated using Amicon[®] Ultra-2 30K Centrifugal Filter Devices (Millipore, MA USA) according to the manufacturer's instructions (Fig 2.6). This device processed volumes up to 2 mls with a 30K (30,000 NMWL) cutoff point, thus not allowing biomolecules with molecular weights lower than 30 kDa to pass through. Firstly, the empty filter device, filtrate collection tube and concentrate collection tube are separately weighed before use. After addition of approximately 2 mls cell culture media, the assembled unit is re-weighed. The filter device is centrifuged for 20 mins in a swinging bucket rotor at 3220 rcf. The filter device is then removed from the centrifuge and the Amicon[®] Ultra filter unit is separated from the filtrate collection tube. To recover the concentrated solute, invert the filter unit and concentrate collection tube, and spin for 2 mins at 1000 rcf to transfer the concentrated sample from the filter device to the tube. After the spin, the filter unit is removed from the concentration collection tube and the filtrate and collection tube are weighed again. The weight of the empty device/tubes is subtracted from this new value in order to calculate weights of the starting material, filtrate and concentrate. This direct weighing procedure allowed us to quantify recoveries. This concentrated media (approximately 30-40 μ l) was also analysed for protein concentration via a Bicinchoninic acid (BCA) assay, and subsequently employed for Western blotting.

2.3 mRNA Preparation and Analysis

2.3.1 An RNase-free environment

As RNA is susceptible to degradation by ubiquitous RNases, standard procedures were utilised to avoid this potential hazard (Sambrook et al., 1989). Before working with RNA, any apparatus or surfaces to be used were treated with RNase AWAY spray (Thermo Fisher, Leicestershire, UK) to remove RNases. As hands are a major source of RNase contamination, gloves were used at all times and changed regularly. Pipette tips, eppendorfs, PBS and buffers were also autoclaved to avoid RNase contamination.

2.3.2 RNA preparation

Following cyclic strain or shear stress experiments, mRNA is harvested. Trizol[®] is a ready-to-use reagent for the isolation of total RNA, DNA and/or protein from cells and tissues based on the technique developed by Chomczynski and Sacchi in 1987. Trizol[®] maintains the integrity of the RNA whilst disrupting cells and dissolving subcellular components.

Following the treatment, cells are lysed directly in Bioflex[®] culture plates by the addition of 1 ml of Trizol[®] per 10 cm². A volume less than this can result in contamination of the RNA with DNA. To ensure complete homogenization, cells were lysed by scraping the plate with a cell scraper and samples were then incubated for 5 min at room temperature to allow complete dissociation of nucleoprotein complexes. 0.2 ml of chloroform was added per 1 ml of Trizol[®] reagent used, then mixed for 15 sec before being incubated for 15 min at room

temperature. Samples were then centrifuged at 7969 rcf for 15 min at 4°C. The mixture separated into a lower red phenol-chloroform phase, an interphase and an upper colourless aqueous phase, which is entirely RNA. The aqueous phase was carefully removed and transferred into a fresh, sterile eppendorf. The RNA was then precipitated out of solution by the addition of 0.5 ml of isopropanol per 1 ml of Trizol[®] used. Samples were inverted 5-8 times and incubated for 10 min at room temperature and then centrifuged at 7969 rcf for 10 min at 4°C. The RNA precipitate forms a gel-like pellet on the side of the tube. The supernatant was removed and the pellet washed in 1 ml of 75% ethanol per ml of Trizol[®] used followed by centrifugation at 7969 rcf for 5 min at 4°C. The resultant pellet was air-dried for 5-10 min before being re-suspended in DEPC-treated water. This was then incubated for 10 min at 60°C, to homogenize the sample prior to quantification. The concentration of total RNA was determined using a NanoDrop[®], as outlined below. The sample was then stored at –80°C until used.

2.3.3 The NanoDrop[®] ND-1000 Spectrophotometer

The NanoDrop[®] ND-1000 Spectrophotometer was used to measure nucleic acid sample concentrations. An undiluted 1.2 µl sample was pipetted onto the end of a fibre optic cable (the receiving fibre). A second fibre optic cable (the source fibre) was then brought into contact with the liquid sample causing the liquid to bridge the gap between the fibre optic ends. (The gap is controlled to both 1 mm and 0.2 mm paths by the computer). A pulsed xenon flash lamp generated the light source and a spectrometer was used to analyse the light

after passing through the sample. The instrument was controlled by special software run from a PC, and the data were logged in an archive file on the PC.

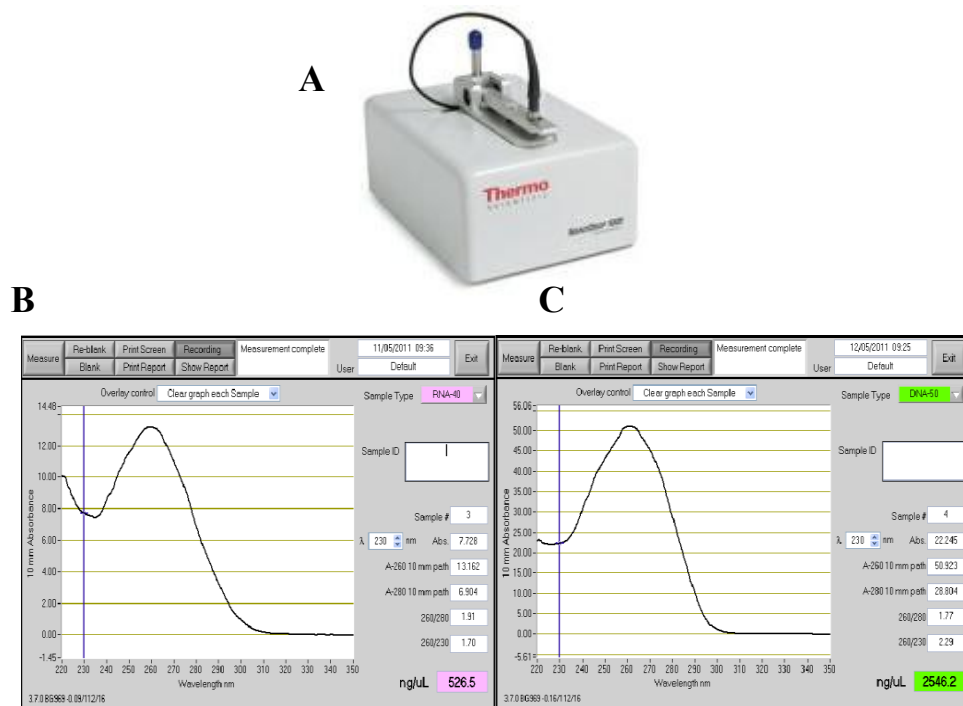


Figure 2.7: The NanoDrop[®] machine (A) and typical graph readouts for (B) RNA and (C) DNA are shown.

The NanoDrop[®] automatically calculates the purity of the nucleic acid samples by reading the absorbance at 260 nm and the absorbance at 280 nm and then determining the ratio between the two (A_{260}/A_{280}) (Fig 2.7). Pure DNA which has no protein impurities has a ratio of 1.8 whereas pure RNA has a ratio of 2.0. Lower ratios signify the presence of proteins, higher ratios imply the presence of organic reagents. Purification of RNA samples was achieved using a DNase treatment kit (Sigma-Aldrich, Dorset, UK) as described below.

2.3.4 DNase treatment of mRNA

The RNA sample for analysis was digested with 1 μ l RNase-free DNase I along with 1 μ l 10X DNase Buffer and incubated for 15 min at 37°C. 1 μ l DNase stop solution was added to the reaction mixture and was incubated for a further 10 min at 70°C to denature the DNase enzyme. The sample is then incubated for 5 mins on ice and the RNA could then be synthesised to cDNA.

2.3.5 Reverse transcription

In this procedure, mRNA was transcribed into cDNA by the enzyme reverse transcriptase. A high capacity cDNA reverse transcription kit (Applied Biosystems, CA, USA) was used as described below:

Reactions were made up as follows;

RT Buffer (10X)	2 μ l
dNTP mix (100 mM)	0.8 μ l
Random primers (10X)	2 μ l
MultiScribe Reverse Transcriptase	1 μ l
<u>Nuclease-free H₂O</u>	<u>4.2 μl</u>
Final volume	10 μ l

This mixture was added to a 0.2 ml PCR tube containing 1000 ng RNA diluted in nuclease-free water to 10 μ l to give a final volume of 20 μ l. Samples were spun down briefly in a centrifuge and then placed into a PCR machine and run at 25°C for 10 min, 37°C for 120

min, and finally 85°C for 5 min. cDNA products were then quantified on a NanoDrop® (Section 2.3.3) to check concentration and purity of samples.

2.3.6 Polymerase chain reaction (PCR)

PCR was used to optimize primer sets (Table 2.3) and to rule out primer-dimerisation before their use in quantitative Real-Time PCR (qRT-PCR). PCR reaction mixtures were prepared as follows:

Forward primer (10 µM)	1 µl
Reverse primer (10 µM)	1 µl
cDNA sample	1 µl
Reaction buffer (10X)	2.5 µl
dNTP (10 mM)	2 µl
MgCl ₂ (25 mM)	1.5 µl
Taq Polymerase	0.25 µl
RNase free water	15.75 µl
Final volume	25 µl

The mixture was then placed into an MJ Mini thermal cycler with hot-lid (Bio-Rad, CA, USA). Samples were then subjected to the following cycling conditions:

Denature		95°C	5 min	} 40 cycles
Cycling	Denature	95°C	15 sec	
	Annealing	55-60°C	30 sec	
	Extension	72°C	15 sec	
	Extension	72°C	5 min	
	Hold	4°C	Forever	

2.3.7 Quantitative Real-Time PCR (qRT-PCR)

Target gene	Primer sequence	Product size	Annealing temp
eNOS	For: 5'-GCTTGAGACCCTCAGTCAGG-3' Rev: 5'-GGTCTCCAGTCTTGAGCTGG-3'	300 bp	61.4°C
KLF2	For: 5'-GCACGCACACAGGTGAGAA-3' Rev: 5'-ACCAGTCACATTTGGGAGG-3'	200 bp	57°C
S18	For: 5'-CAGCCACCCGAGATTGAGCA-3' Rev: 5'-TAGTAGCGACGGGCGGTGTG-3'	250 bp	62°C
GAPDH	For: 5'-GAGTCAACGGATTTGGTCGT-3' Rev: 5'-TTGATTTTGGAGGGATCTCG-3'	238 bp	56°C
TM (Chen et Hsu, 2006)	For: 5'-ACCTTCCTCAATGCCAGTCAG-3' Rev 5'-GCCGTCGCCGTTTCAGTAG-3'	107 bp	60°C

Table 2.4: Primer sequences, product size, and optimal annealing temperature used for both PCR and qRT-PCR. All primer sets were produced from human sequences and annealing temperatures varied, as they were specific to each primer set. GAPDH and S18 act as endogenous housekeeping gene controls, which may be used to normalise all experimental data. During primer optimization, a negative control with no reverse transcriptase (RT) and template controls (i.e., no cDNA) was also run with each primer to rule out any cDNA contamination of mRNA samples.

Following optimisation of primers (Table 2.4) by routine PCR, they were subsequently employed in qRT-PCR. This technique follows the general principle of RT-PCR with amplified DNA quantified in real-time as it accumulates in the reaction. The reaction uses SYBR green, a dye that fluoresces only when bound to the minor groove of double stranded DNA. A laser then reads this fluorescence at the end of every cycle and the amount

of cDNA product formed during the PCR cycles can be quantified and graphically visualised in real time.

To normalise the optical system involved in real-time analysis, ROX, a passive dye, is incorporated into the SYBR mastermix. This is achieved by the reporter dye's (SYBR) signal being measured against the passive reference dye (ROX) signal to normalise for non-PCR-related fluorescence fluctuations occurring from well to well. The threshold cycle represents the refraction cycle number at which a positive amplification reaction was measured and was set at 10 times the standard deviation of the mean baseline emission calculated for PCR cycles 3 to 15. The results were analysed according to the Comparative CT method ($\Delta\Delta CT$) as described by (Livak and Schmittgen, 2001). An Applied Biosystems 7900HT Fast real-time PCR system was used for qPCR. Each reaction was set up in triplicate as shown below:

Forward primer (10 μM)	1.0 μl
Reverse primer (10 μM)	1.0 μl
cDNA	2.0 μl
SYBR Green	11.5 μl
RNase free water	9.5 μl
<hr/>	
Total volume	24 μl

Samples were then subjected to an initial denaturation step of 95°C for 10 min followed by 40 cycles of 95°C for 15 sec and a primer-specific temperature of between 55-60°C for 1 min. Data were collected during the annealing step. Quantification of cDNA target was normalised for differences across experiments/samples using endogenous S18/GAPDH housekeeper controls as active reference genes.

Routinely, melt curve analysis was carried out to ensure single product formation and to rule out possible contamination of product by non-specific binding and primer dimerisation.

Samples from both RT-PCR and qRT-PCR reactions were then visualized on 1% agarose gels as described below.

2.3.8 Agarose gel electrophoresis

Agarose gels were prepared by boiling 1 g of agarose in 100 ml of 1X TAE buffer (40 mM Tris-Acetate pH 8.2, 1 mM EDTA) to make a 1% gel. After adequate cooling (~60°C), 10 µl of SYBR Safe (Invitrogen, The Netherlands) was added to the gel, mixed by swirling and then poured into a casting rig. A comb was inserted for formation of wells. The gel was allowed to cool and polymerise before filling the chamber with 1X TAE and removing the comb.

As the 10X buffer in the RT-PCR reaction already contained a loading and tracking dye 15 µl of RT-PCR product was loaded directly to the gel. A 1 Kb or 100 bp DNA ladder was also added to one well as a molecular weight marker for reference. The gel was run at constant voltage (5 V/cm, usually 100 V) for 1 to 2 hrs. Samples were then visualised using the transilluminator settings on a G:BOX (Syngene, UK). Images could then be saved for later densitometric analysis.

2.4 Immunodetection techniques

2.4.1 Western Blotting

2.4.1.1 Preparation of whole cell lysates

After strain experiments, confluent HAECs were harvested from 6-well Bioflex® plates for analysis by cell lysis via the radioimmunoprecipitation assay protocol (Alcaraz et al., 1990). On ice, culture media was removed by aspiration and then cells were washed three times in chilled PBS. Following complete aspiration of PBS, cells were harvested using a cell scraper in radioimmunoprecipitation assay (RIPA) lysis buffer (64 mM HEPES pH 7.5, 192 mM NaCl, 1.28% w/v Triton X-100, 0.64% w/v sodium deoxycholate, 0.128% w/v sodium dodecyl sulfate SDS, supplemented with 0.5 M sodium fluoride, 0.5 M EDTA pH 8.0, 0.1 M sodium phosphate, 10 mM sodium orthovanadate, and 1X protease and phosphatase inhibitor cocktail) and transferred into a pre-chilled micro-centrifuge tube. Continuous lysate rotation was applied for 1hr at 4°C, prior to lysate clarification by centrifugation at 10,000 for 20 min at 4°C to sediment any triton-insoluble material. Clarified lysates were subsequently aliquoted into fresh tubes and were either stored at -80°C for future analysis or immediately subjected to a BCA assay and used for Western blot.

2.4.1.2 Bicinchoninic acid (BCA) assay

The BCA assay is a biochemical assay used to quantify the amount of protein in solution (Smith et al., 1985). In this assay, Cu^{2+} reacts with protein under alkaline conditions to produce Cu^+ , which in-turn reacts with BCA to produce a coloured product. Two separate reagents were supplied in the commercial kit (Thermo Fisher Scientific); (A) an alkaline bicarbonate solution and; (B) a copper sulfate solution. 1 part solution B is mixed with 49 parts solution A. 200 μl of this mixture is then added to 10 μl of protein lysate or BSA standards (standard curve in the range 0-2 mg/ml). The 96-well plate is incubated at 37°C for 30 minutes and the absorbance read at 562 nm using a Bio-TEK[®] ELx800 microtitre plate reader. The intensity of the coloured reaction product is a direct function of protein amount that can be determined by comparing its absorbance value to a BSA standard curve.

2.4.1.3 Polyacrylamide gel electrophoresis (SDS-PAGE)

SDS-PAGE was carried out on HAECs using 10% polyacrylamide gels as described by (Laemmli, 1970). Gels were prepared as outlined below in Table 2.5. SDS-PAGE was performed using the Mini-PROTEAN Tetra Cell[®] system (BioRad, CA, USA). The resolving gel was poured first, overlaid with distilled water and allowed to polymerize for 20 min. The distilled water was removed and the stacking gel was poured over the resolving gel, a comb inserted and the gel allowed to polymerize for 15 min. Combs, clamps and gaskets were then removed and the gel plates inserted into the electrophoresis chamber. The chamber is then filled with the reservoir buffer (25 mM tris, 192 mM glycine, 0.1% SDS, pH 8.3).

Component	Resolving gel (10%)	Stacking gel (5%)
1.5M Tris-HCL, ph 8.8	1.5 ml	
0.5M Tris-HCL, ph 6.8		750 µl
40% acrylamide stock	1.5 ml	375 µl
Distilled water	3 ml	1.85 ml
10% w/v SDS	60 µl	30 µl
10% w/v ammonium persulphate	30 µl	15 µl
TEMED	7 µl	7 µl
Final volume	6.097 ml	3.027 ml

Table 2.5: SDS-PAGE gel formations: Resolving gel buffer and stacking gel buffers have a pH of 8.8 and 6.8, respectively.

Protein concentration of each sample was determined by BCA assay to allow for equal protein loading/well. 6X loading buffer (6 g SDS, 30 ml glycerol, 3 ml β mercaptoethanol, 0.06 g bromophenol blue and 17 ml 1.5 M Tris-HCL, made up to final volume of 50 ml, pH 6.8) was added to volume - adjusted samples (final volume of sample was 30 µl), which were then boiled at 95°C for 5 min and immediately placed on ice. Samples were then loaded onto the gel into the appropriate lanes with 3 µl Precision Plus[®] protein molecular weight marker (BioRad). Both samples and protein markers were separated electrophoretically at 100V for 120 min.

2.4.1.4 Electrotransfer to nitrocellulose membrane

The wet or tank transfer method (Towbin et al., 1979) was utilized for electrotransfer of proteins to a nitrocellulose membrane. This was accomplished using a Mini PROTEAN[®] Trans Blot Module (BioRad) according to the manufacturer's instructions. Following electrophoresis, the gel was removed and soaked for 10 min in transfer buffer (25 mM tris pH 8.3, 192 mM glycine, 20% methanol and 0.1% w/v SDS) to remove any SDS complexes that might be bound to the gel. Nitrocellulose membrane and Whatmann filter paper were cut to the same size as the gel and also soaked in transfer buffer for 5 min. Following the gel and membrane pre-soakings, the transfer cassette accompanying the Mini-PROTEAN[®] electrophoresis system (BioRad, CA, USA) was assembled as in Fig 2.8. Once assembled, the cassette was checked to be free of air bubbles by rolling a 15 ml test tube over the cassette while submerged in transfer buffer to remove any residual bubbles. The cassette was then placed in the Trans Blot Module with the correct orientation and subjected to 100 V for 2 hrs at room temperature or 40 V overnight at 4°C.

2.4.1.5 Ponceau S staining

Following transfer completion, membranes were soaked in Ponceau S solution for 3 min with constant agitation to visually confirm uniform transfer of protein. Ponceau S is a negative stain, which binds to positively charged amino acid groups of protein. Transferred proteins were detected as red bands on a white background. The stain was subsequently

removed by gentle washing in dH₂O until all the stain has been washed away. The membrane was then used for immunological probing.

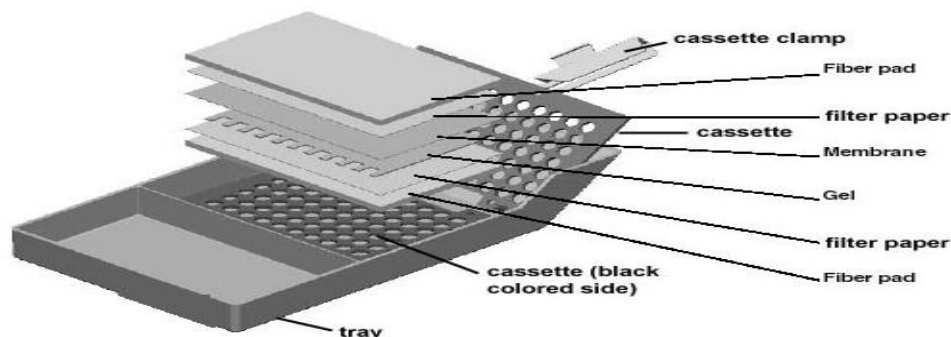


Figure 2.8: Wet transfer cassette assembly used to transfer electrophoresed proteins from an SDS-PAGE gel to the nitrocellulose membrane. The black coloured side is assembled face down, overlaid with a fibre pad, filter paper, resolved gel, nitrocellulose membrane, filter paper, and fibre pad, and sealed using the cassette clamp.

2.4.1.6 Immunoblotting and chemiluminescence band detection

Following removal of the Ponceau stain, membranes were blocked for 60 min in blocking solution (5% w/v milk in TBS, 10 mM Tris pH 8.0, 150 mM NaCl) and then incubated overnight at 4°C with primary antibody (Table 2.6) and gentle agitation. Following completion of primary incubations, membranes were washed 3 times for 10 min (30 min in total) in wash buffer. Membranes were subsequently incubated with the appropriate secondary antibody in TBST (5% milk w/v) for 2 hr with gentle agitation at room temperature. Membranes were then washed again using the same conditions described above.

Luminata™ Crescendo Western HRP Substrate (Millipore, MA USA) was the chemiluminescent substrate used for detection of horseradish peroxidase (HRP)-conjugated secondary antibodies. Resulting immunoblots were scanned and densitometric analysis was performed using NIH Image v1.61 software to obtain relative comparisons between bands.

1° Ab	Species	1° dilution	2° Ab	2° dilution
GAPDH polyclonal (Santa Cruz)	Rabbit monoclonal IgG	1 µg/ml	Anti-rabbit-HRP conjugated	1:3000
TM (Abcam)	Mouse polyclonal IgG	10 µg/ml	Anti-mouse HRP-conjugated	1:3000
TM (Acris)	Rabbit polyclonal IgG	1 µg/ml	Anti-rabbit-HRP conjugated	1:3000

Table 2.6: Optimized primary and secondary antibody dilutions for proteins monitored by Western blots.

2.4.1.7 Coomassie gel staining

Coomassie gel staining was routinely used to visualise protein bands on an SDS-PAGE gel. This is a useful technique to ensure that the transfer method worked as expected. In brief, the SDS-PAGE gel was treated with filtered (0.25 µM) coomassie solution whilst rocking for approximately 4 hrs. The gel was then de-stained, whilst rocking, in a methanol:acetic acid (50:50) solution until the protein bands appeared clear and distinct with no background staining, changing the de-stain solution regularly.

2.4.2 ELISA

2.4.2.1 ELISA analysis

The enzyme linked immunosorbent assay (ELISA) is used for the detection and quantification of cellular proteins and proteins secreted by activated cells in culture into the tissue culture media. A protein-specific capture antibody is immobilized onto a high protein binding capacity ELISA plate which enables the capture of the target protein (Fig 2.9). The captured protein is detected by a biotinylated antibody, which recognizes a distinct epitope. The sandwiched target protein is then quantified using a colourimetric reaction based on activity of avidin-horseradish peroxidase (bound to the biotinylated secondary antibody) on a specific soluble substrate. The coloured end product is read by a spectrophotometer. All ELISA's outlined below were sandwich-based immunoassays and were carried out according to manufacturer's instructions.

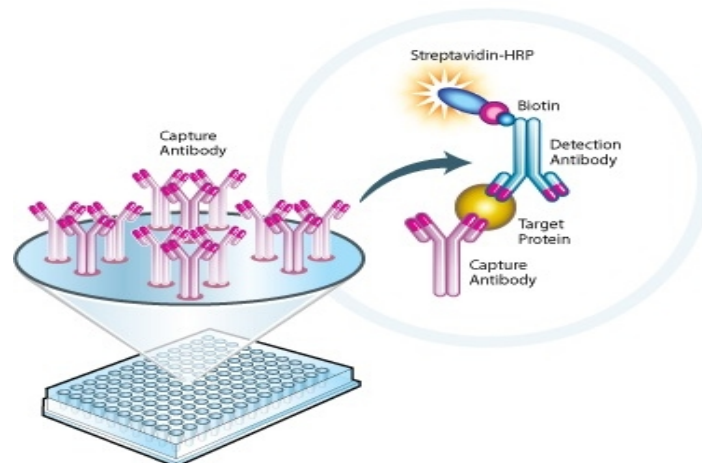


Figure 2.9: Principles of sandwich-based ELISA immunoassays.

2.4.2.2 Thrombomodulin Human ELISA Kit

The Thrombomodulin Human ELISA Kit (Abcam, MA USA) was used for the determination of thrombomodulin protein released into culture media. This assay has the ability to recognize both natural and recombinant thrombomodulin variants.

2.4.2.3 Human Thrombomodulin/BDCA-3 DuoSet[®] ELISA

The Human Thrombomodulin/BDCA-3 DuoSet[®] ELISA kit (R&D Systems, MN USA) contains the basic components necessary for the development of sandwich ELISA to measure both natural and recombinant human thrombomodulin in cell culture supernatants and lysates. The protocol followed was provided by the manufacturer and each step is followed by a wash/aspiration step as described in the manual (not including before the addition of the stop solution). Media supernatants and cell culture lysates were harvested for ELISA analysis from each well of all 6-well Bioflex[®] plates.

F96 maxisorp Nunc-Immuno 96-well plates (Bio-Sciences Ltd, Ireland) were coated with 50 µl of the capture antibody per well and incubated overnight at room temperature. The plate was then blocked by adding 150 µl of Reagent Diluent to each well and incubated for 1 hour at room temperature. Cell culture lysates were diluted 1:20 in 25% FCS in 1X PBS before addition to ELISA. Subsequently, 50 µl of the sample (undiluted media supernatants or diluted cell lysates) or TM standard were added to each well in duplicate and incubated for 2 hours at room temperature. The standards range from 31.25 to 2000 pg/ml of human thrombomodulin. 50 µl of the detection antibody was added to each well and then incubated

for 2 hours at room temperature. Following this, 50 µl of streptavidin-HRP was dispensed to each well and incubated for 20 minutes at room temperature in the dark. 50 µl of substrate solution was added to each well and incubated for 20 minutes at room temperature in the dark. With the addition of 25 µl of stop solution to each well, the reaction was terminated and the plate read using at both plate reader at both 570 and 450 nm. Wave correction is used to subtract the readings at 570 nm from 450 nm (corrects for optical imperfections in the plate). The reaction generates a coloured product, which is a direct function of the total measured TM concentration (media samples or cell lysates) that can be determined by comparing its absorbance value to a standard curve.

2.4.2.4 Multiplex ELISA

Multi-Array[®] Technology (Meso Scale Discovery, MD USA) is a multiplex immunoassay system that enables the measurement of biomarkers using electrochemiluminescent detection. In an MSD[®] assay, specific capture antibodies for the analytes are coated in arrays in each well of a 96-well carbon electrode plate surface. The detection system uses patented SULFO-TAG[™] labels, which emit light upon electrochemical stimulation initiated at the electrode surfaces of the Multi-Spot[®] plates. The electrical stimulation is decoupled from the output signal, which is light, to generate assays with minimal background. MSD labels, which are stable and non-radioactive, can be conveniently conjugated to biological molecules. Additionally, only labels near the electrode surface are detected, enabling non-washed assays.

The MSD assays only require minimal sample volume as compared to a traditional ELISA (which is limited by its inability to measure more than one analyte). With an MSD assay, four different biomarkers can be analyzed simultaneously using as little as 10-25 μ l of sample. These assays have high sensitivity, up to five logs of linear dynamic range, and excellent performance in complex biological matrices. This allows the measurement of native levels of biomarkers in normal and diseased samples without multiple dilutions. In order to investigate the effect of elevated cyclic strain on vascular and proinflammatory biomarkers, we used two custom-made plates; a human proinflammatory panel (measuring IFN- γ , IL-1 β , IL-6 and TNF- α) and a human vascular injury panel (measuring sICAM-3, E-selectin, P-selectin and TM).

2.4.2.4.1 Human ProInflammatory-I Ultra-Sensitive 96-Well Multi-Spot[®] Plate

The Human ProInflammatory I 4-Plex Assay detects proinflammatory targets in a sandwich immunoassay format (Meso Scale Discovery, MD USA). This assay consists of a plate, which is pre-coated with four capture antibodies on spatially distinct spots specific for IFN- γ , IL-1 β , IL-6 and TNF- α (Fig 2.10).

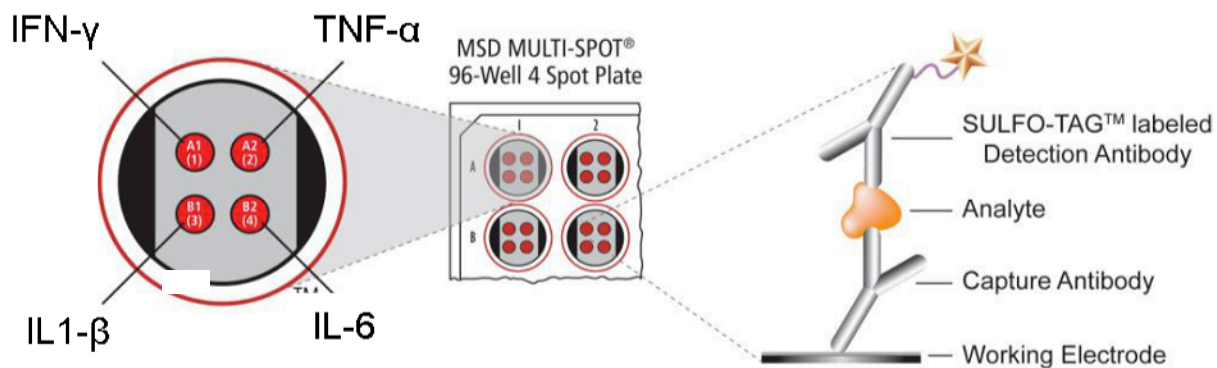


Figure 2.10: Human ProInflammatory I 4-Plex Multi-Spot® Plate.

Firstly, the plate was blocked by dispensing 25 μ l of the diluent into each well and then incubating for 30 minutes with vigorous shaking (9-98 rpm) at room temperature. The sample, either media supernatant or cell lysate, was diluted 1:2 with Endothelial Cell Growth Media MV. 25 μ l of each calibrator and diluted sample is added to each well in triplicate and duplicate respectively. The calibrators used a range from 0.61 to 10,000 pg/ml and contain labelled detection antibodies for anti-IFN- γ , anti-IL-1 β , anti-IL-6 and anti-TNF- α , labelled with an electrochemiluminescent compound, MSD SULFO-TAG™. The plate was then incubated for 2 hours with vigorous shaking (9-98 rcf) at room temperature. Analytes in the samples bind to capture antibodies immobilized on the working electrode surface. Subsequently, 25 μ l of the detection antibody was added to each well and left to incubate for 2 hours with vigorous shaking at room temperature. Target analytes subsequently bound to the labelled detection antibodies to complete the sandwich. 150 μ l of MSD read buffer was added to each well, which provides the necessary chemical environment for electrochemiluminescence. The plate was loaded onto the MSD SECTOR® instrument where a voltage applied to the plate electrodes caused the labels bound to the electrode surface to emit

light. The instrument measured the intensity of emitted light to give a quantitative measure of IFN- γ , IL-1 β , IL-6 and TNF- α present in the sample.

2.4.2.4.2 Human Vascular Injury I 96-Well Multi-Spot® Plate

The Human Vascular Injury I 4-plex ELISA detects soluble intercellular adhesion molecule-3 (sICAM-3), E-selectin, P-selectin and thrombomodulin (TM) (Fig 2.11) in a sandwich immunoassay format (Meso Scale Discovery, MD USA). This immunoassay is conducted in the same manner as the Human ProInflammatory Multi-Spot® plate as already described above.

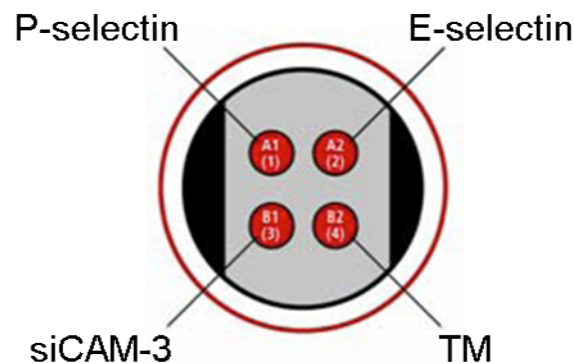


Figure 2.11: Human Vascular Injury I 96-well Multi-Spot® Plate.

2.4.3 Immunocytochemistry

Immunocytochemical techniques, as previously described by Groarke *et al.*, were employed to visually monitor the expression and/or subcellular localization of thrombomodulin (Groake, et al. 2001). Firstly, cell culture media was aspirated from the dish. HAECs were washed 3 times in PBS and fixed with 3.7% (v/v) formaldehyde for 20 minutes. Cells were subsequently washed in PBS 3 times; at this point samples could be stored in PBS for up to 2 days at 4°C. Cells were then blocked for 30 min in PBS containing 5% (w/v) BSA solution. After blocking, cells were washed 3 times in PBS and then incubated with a 50 µl solution of Thrombomodulin primary antibody (Table 2.7) for 1 hour at room temperature or on ice (Abcam, MA, USA; Acris Antibodies, Germany). Again cells were washed 3 times in PBS after which, they were incubated with 1:1000 Alexa Fluor 488 anti-rabbit (TM) or anti-mouse secondary antibody in 5% BSA for 1 hour in the dark at room temperature. Again cells were washed 3 times in PBS after which, nuclear DAPI staining was performed by incubating cells with propidium iodide (PI) for 3 min. Samples were then washed for a final time and mounting medium was added to the cells. Samples were visualised by standard fluorescent microscopy (Nikon Eclipse Ti, Tokyo, Japan).

Primary antibody/stain	Dilution
PI	1:2000
TM (Abcam)	1:50
TM (Acris)	1:50

Table 2.7: Optimized primary and secondary antibody dilutions for proteins monitored by immunocytochemistry.

2.5 Statistical analysis

Results are expressed as mean±sem. Unless otherwise indicated, all experiments were conducted in triplicate (n=3). Statistical comparisons between controls versus treated groups were made by ANOVA in conjunction with a Dunnett's post-hoc test for multiple comparisons. A Student's unpaired *t*-test was employed for pairwise comparisons. A value of $P \leq 0.05$ was considered significant.

Chapter 3:

Investigation of the effects of cyclic strain on the expression and release of thrombomodulin

3.1 Introduction

The primary aim of this project was to characterize an *in vitro* endothelial cell model focusing on the effects of elevated cyclic strain on macrovascular endothelial phenotype with respect to TM expression and release. Cyclic strain, the rhythmic distension of the blood vessel wall in time with the cardiac cycle, was to be applied to human aortic endothelial cells (HAECs) using a FlexerCell[®] Tension Plus[™] FX-4000T[™] System (Dunn Labortechnik GmbH, Germany) in conjunction with Pronectin[®]-coated Bioflex[®] plates. It has been well documented that when cyclic strain is pathologically elevated, vascular complications may result (i.e., vein graft rejection, hypertension) (Goch et al., 2009; Weiß et al., 2009). Cyclic strain induces both short- and long-term changes in cell signalling, protein synthesis, protein secretion/degradation, rate of cell division and energy metabolism (Chien, 2007). In addition, cyclic strain up-regulates the production of adhesion molecules and pro-inflammatory cytokines in endothelial cells (Sasmoto et al., 2005). HAECs are ideal for this model as large arteries are the most susceptible location for strain- and shear-based hemodynamic injury, as well as being translationally relevant to human CVD. Basic studies were carried out initially in bovine aortic endothelial cells (BAECs) due to their rapid doubling time and ease of use. This allowed techniques to be optimized and validated before proceeding to work with HAECs.

Initially, to ensure that our results were not due to excessively compromised cell viability following strain treatments, a number of cell viability assessments were conducted. In characterising this hemodynamic model, we were subsequently interested in assessing the range of inflammatory damage that could be elicited in endothelial cells by elevated levels of

cyclic strain. Following this, our goal was to focus in on one relatively unstudied but physiologically crucial target, thrombomodulin (TM), in order to define more clearly how it was responding to cyclic strain *in vitro*. TM is a cell membrane protein predominantly known for its involvement in the coagulation cascade (Cines et al., 1998; Pearson, 1999). Additionally, TM has beneficial antifibrinolytic and anti-inflammatory outcomes for the vessel wall (Conway, 2012), which would indicate the importance of TM to vascular homeostasis. The impact of cyclic strain on the expression/release of TM has received very little attention within *in vitro* models, highlighting the importance of understanding how strain regulates this physiologically and therapeutically relevant molecule. In this chapter, dose-, time- and cyclic frequency-dependency studies were conducted to investigate how cyclic strain mediates TM expression and release levels in HAECs. We also extended these studies to include another highly relevant biomechanical force, namely shear stress, to determine if it regulates TM in the same manner as cyclic strain. Initially, importance basic endothelial characterisation was performed.

3.2 Results

3.2.1 Characterisation of endothelial cells

3.2.1.1 Endothelial cell markers

Endothelial cells have specific biomarkers such as von Willebrand factor (vWF) and endothelial nitric oxide synthase (eNOS) that can be identified and measured to guarantee the

validity of the commercially-sourced HAECs. vWF and eNOS mRNA was detected in HAECs by RT-PCR (Fig 3.1).

3.2.1.2 Endothelial cell morphology

HAECs were grown to confluency and monitored daily by phase-contrast microscopy for characteristic growth patterns and typical “cobblestone” shaped morphology. Using the orbital flow system, low shear stress (10 dynes.cm², 24 hrs) was applied to HAECs, which realign in the direction of flow (Fig 3.2).

3.2.2 Viability studies

Viability studies on HAECs prior to treatment with cyclic strain were carried out using a range of methods to ensure that there were sufficient viable cells available for each experiment. Further viability checks were done *post-strain* experimentation for both normalisation purposes and to determine if cell viability was significantly affected by the strain treatment. Viability assessments were performed using;

- (i) The Vybrant™ apoptosis flow cytometry (FACs) assay was carried out post-cyclic strain (2.5% vs 12.5% for 24 hrs). R1, R2, R3 and R4 represent total, live, necrotic and apoptotic cells, respectively (Fig 3.3E). Since the four images are nearly identical, it is clear that the 12.5% cyclic strain treatment does not significantly reduce cell viability.

This quantitatively illustrates the strain-dependent change in HAEC viability (Fig 3.3F).

- (ii) Trypan blue was also used to measure the viability status of cells in each Bioflex[®] well after treatment with cyclic strain (2.5% vs 12.5% for 24 hrs). As before, virtually no difference was observed in cell viability between the 2.5% and 12.5% treatments with cyclic strain (Fig 3.4A).
- (iii) The ADAM[™] cell counter was used routinely to measure cell number and viability after every cyclic strain experiment. The graphs (Fig 3.4B and C) show that cell viability is nearly identical after two different 24 hrs cyclic strain ranges were applied (2.5% vs 12.5% and 0% - 7.5%).

3.2.3 Effect of elevated cyclic strain on biomarker levels in HAECs

Multiplex ELISA technology was employed to analyse levels of multiple cellular targets in both HAEC lysates and media supernatants. Samples were harvested from individual Bioflex[®] wells after treatment with low (2.5%) and high (12.5%) cyclic strain for 24 hrs at 60 cycles/min (routine frequency used throughout thesis). This ELISA measured levels of established pro-inflammatory and vascular injury markers using custom multiplex ELISA MSD[®] panels. For control studies, untreated cells were also compared to thrombin-treated cells (1.0 U/ml for 24 hrs).

The MSD[®] pro-inflammatory injury panel measured the concentration of four biomarkers; Interferon- γ (IFN- γ), interleukin-1 β (IL-1 β), interleukin-6 (IL-6) and tumour necrosis factor- α (TNF- α). We observed no difference in IFN- γ concentration in media yet it

was significantly decreased in cell lysates after 12.5% cyclic strain (Fig 3.5). Moreover, there was no significant change in IL-1 β levels in either media or cell lysates following 12.5% cyclic strain (Fig 3.6). IL-6 was notably up-regulated in both media and cell lysates after treatment with 12.5% cyclic strain (Fig 3.7). TNF- α was down-regulated in cell lysates but increased slightly in media following 12.5% cyclic strain (Fig 3.8).

The MSD[®] vascular injury panel quantified the concentration of four injury biomarkers; soluble intercellular adhesion molecule-3 (siCAM-3), E-selectin, P-selectin and thrombomodulin (TM). There was no significant difference in siCAM-3 concentration in media but a considerable decrease in cell lysates after 12.5% cyclic strain (Fig 3.9). A small increase was observed in E-selectin levels in media with a significant decrease in cell lysates following 12.5% strain (Fig 3.10). No significant changes were detected in the concentrations of P-selectin in media or cell lysates post 12.5% strain (Fig 3.11). Finally, TM levels were significantly up-regulated in media in parallel with a reduction in cellular lysates following 12.5% cyclic strain (Fig 3.12) Given the pathophysiological significance of TM, and the very limited *in vitro* data of TM with respect to cyclic strain, this target was selected for a further detailed study as the main focus of this thesis. These results are summarised in Table 3.1.

Thrombin (a pro-inflammatory molecule that also binds to TM) was employed as a control for treating cells and monitoring biomarker levels with both the Pro-Inflammatory and Vascular Injury MSD[®] panels. The Pro-Inflammatory Injury panel shows no significant difference in cytokine concentration between the thrombin-treated and untreated samples in media, although slight to moderate increases in cellular levels of cytokine expression were noted (particularly for IL-6) (Fig 3.13A-B). The Vascular Injury panel shows that thrombin-treated media samples have reduced release of both E-selectin and P-selectin. Moreover, TM

was the only biomarker that was significantly up-regulated intracellularly in thrombin-treated HAECs (Fig 3.13C-D).

3.2.4 Constitutive expression and release of TM in “static” HAECs

For the remainder of the thesis, specific focus will be placed on the vascular injury target, TM. Initially, we wanted to confirm both expression and constitutive release of TM in static HAECs. Fluorescent and confocal imaging of TM immunoreactivity was carried out to visualise constitutive cellular distribution of TM in HAECs under static conditions (Fig 3.14). Samples were visualised by standard fluorescent microscopy (Nikon Eclipse Ti, Tokyo, Japan) and confocal microscopy (Zeiss Axioskop FS, USA). TM mRNA expression was confirmed in static HAECs using standard RT-PCR (Fig 3.15A). TM protein expression was also confirmed in HAECs by Western blotting (Fig 3.15B). Time-dependent constitutive release of TM was observed between 24 – 72 hrs in HAECs (Fig 3.15C). For all subsequent experiments monitoring TM release from HAECs, the TM/BCDA-3 Duoset ELISA (R&D Systems, MN USA) was employed (Fig 3.15D).

3.2.5 Effect of cyclic strain on TM expression levels in HAECs

To further investigate this, a number of experiments were conducted with respect to different doses and frequencies of cyclic strain on HAECs *in vitro*. Dose-response studies were carried out on HAECs to examine the effect of cyclic strain on TM protein and mRNA expression levels. For protein expression studies, three Bioflex[®] wells were harvested and

pooled per sample after varying levels of cyclic strain (0%, 2.5% and 7.5%) were applied and then analysed by Western blotting (Fig 3.16). It can be noted that 7.5% was used as the upper level of strain for all subsequent experiments as the higher strain levels of up to 12.5% frequently caused significant cellular detachment from the Bioflex[®] membrane during stretch experiments (i.e., due to over-stretching of the membrane). 7.5% cyclic strain is still quite elevated for the endothelium *in vivo* but causes less cell detachment from the membrane. For technical ease, the control strain condition was selected as 0% (as opposed to 2.5%), which allows us to model the effect of cyclic strain on TM dynamics in endothelial cells (i.e. 0% versus 7.5%), as opposed to modeling a particular pathology manifesting elevated strain (i.e. 2.5% normal versus 7.5% elevated). In agreement with the MSD[®] multi-plex ELISA result, the Western blots showed an almost 75% down regulation in TM cellular expression in response to cyclic strain.

Next, cellular TM levels in response to changes in cyclic strain dose and frequency were monitored using ELISA. A similar downward trend in cellular TM levels was confirmed in response to cyclic strain treatment (Fig 3.17A). Frequency-response studies were also carried out in HAECs to examine the effect on TM protein expression of varying the strain frequency (30 – 120 cycles/min) whilst maintaining the amplitude (7.5%). Relative to the physiological norm of 60 cycles/min TM expression was slightly decreased following elevation of strain frequency to 120 cycles/minute (Fig 3.17B).

Finally, for mRNA studies, two Bioflex[®] wells were harvested and pooled per sample following cyclic strain (0% and 7.5%), and analysed using qRT-PCR with a 7900HT Fast real-time PCR system (Applied Biosystems, CA USA) (Fig 3.18). A decrease in TM mRNA levels of approximately 40% was observed after 7.5% cyclic strain.

3.2.6 Effect of cyclic strain on TM release from HAECs

Cyclic strain-dependent TM release from HAECs into media was measured following dose-, time- and frequency-dependent cyclic strain studies. Media samples were harvested from individual wells for the TM assay of 6 replicates per plate. In response to increasing cyclic strain (0-12.5%), TM release was elevated in a dose-dependent manner (by almost 8-fold) with no significant difference in release observed between 7.5% and 12.5% cyclic strain (Fig 3.19A). Moreover, when HAECs were exposed to 7.5% cyclic strain over a 48hr period, significant TM release was not observed until between 12 - 24 hrs, with levels increasing significantly up to 48 hrs (Fig 3.19B). Finally, in response to changing cyclic strain frequency from physiological level (60 cycles/min) to lower (30 cycles/min) or higher levels (120 cycles/min) whilst maintaining the amplitude (7.5%) of cyclic strain, we observed a very significant increase in TM release at elevated frequency (Fig 3.19C).

3.2.7 Effect of laminar shear stress on TM expression and release

Shear stress, the atheroprotective frictional force of the blood acting tangentially on the endothelium, was also briefly investigated as part of this study. Laminar shear stress (0 versus 10 dynes/cm², 0 - 48 hrs) was applied to HAECs, after which cells were harvested for either TM mRNA analysis or cell culture media for monitoring TM release.

TM mRNA levels were increased almost two-fold in response to physiological levels of shear stress (Fig 3.20A). TM release was also strongly up-regulated by shear stress, with TM release apparent after just 3-6 hrs of shear (Fig 3.20B).

3.3 Table and Figures

Biomarker	Cell Function	Media	Cell Lysates
Interferon- γ (IFN- γ)	Innate and adaptive immunity	–	↓
Interleukin-1 β (IL-1 β)	Inflammatory response	–	–
Interleukin-6 (IL-6)	Acute phase response	↑	↑
Tumour necrosis factor- α (TNF- α)	Acute phase response	↑	↓
Soluble intercellular adhesion molecular-3 (siCAM-3)	Cell adhesion	–	↓
E-selectin	Recruitment of leukocytes	–	↓
P-selectin	Recruitment of leukocytes	–	–
Thrombomodulin (TM)	Activates Protein C, inflammation and fibrinolysis	↑	↓

Table 3.1: The effects of elevated levels of cyclic strain (12.5%) on the expression of each biomarker measured both in total cell lysates and cell media. The symbols used represent the following; ↑, ↓ and – denotes up-regulation, down-regulation and no effect, respectively.

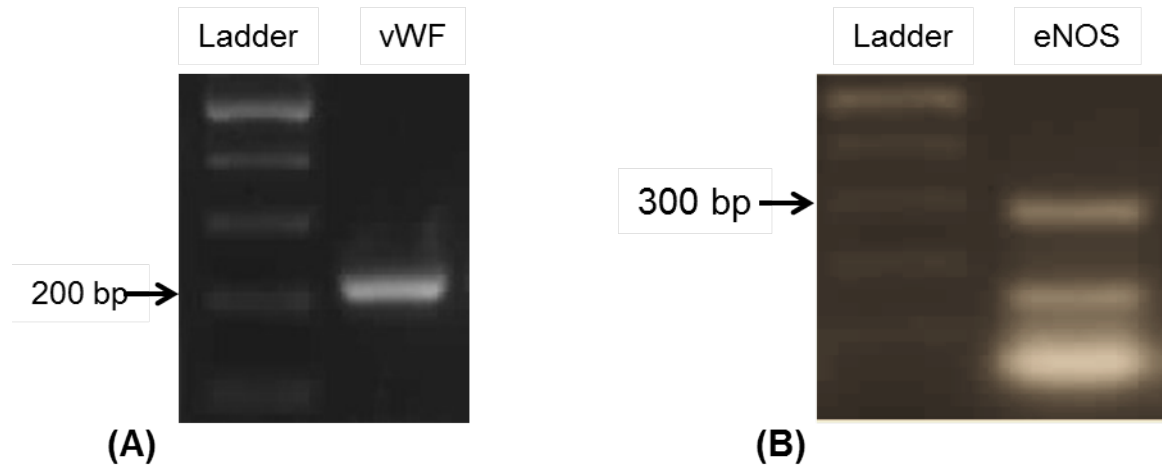


Figure 3.1: Characterisation of HAECs. **(A)** Shows the presence of the endothelial-specific marker vWF, in HAECs as detected by RT-PCR. **(B)** Shows the presence of endothelial-specific marker, eNOS, in HAECs as detected by RT-PCR. Blots are representative of 3 replicates.

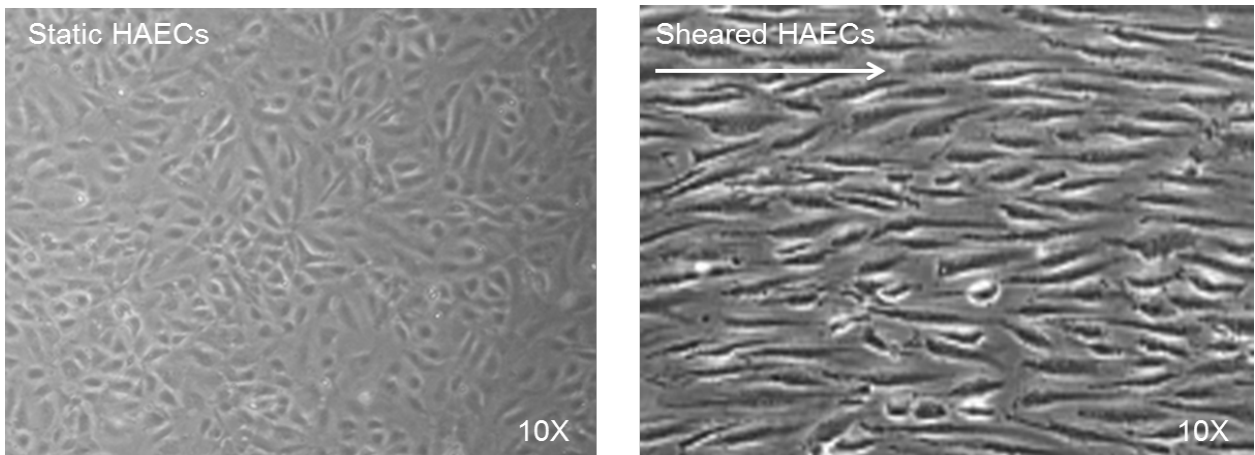


Figure 3.2: Endothelial cell morphological alterations in response to shear stress compared to static control cells. HAECs were sheared using the ibidi system. White arrow indicates the direction of the shear flow. Images are representative.

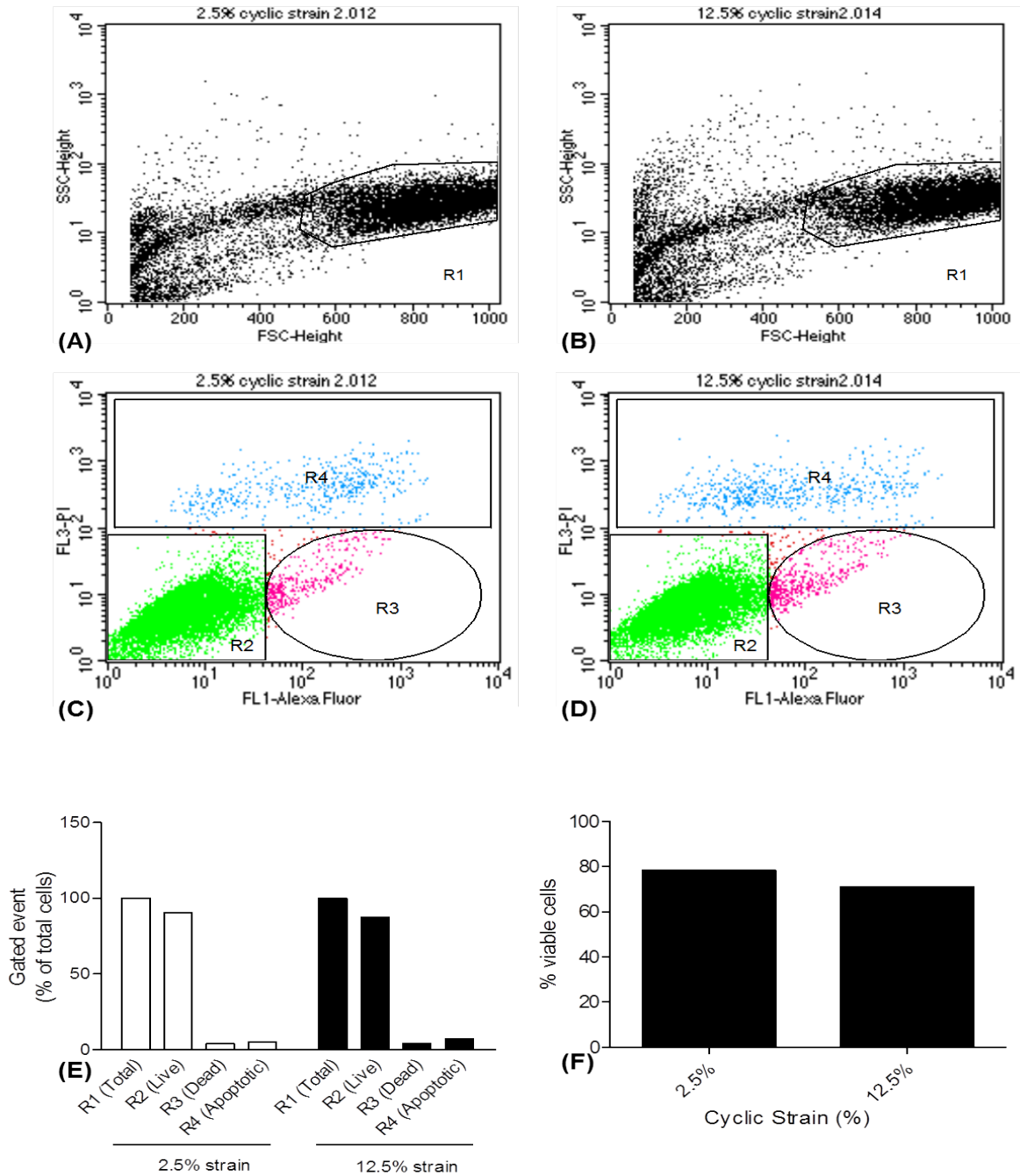


Figure 3.3: Vybrant™ Apoptosis FACS Assay. Cell viability was measured after treatment with either 2.5% (A - B) or 12.5% (C - D) cyclic strain for 24 hrs. (E) Gated events of viability assay. (F) Average values of cell viability per strain group (n=2). Key: R2, live cells; R3, necrotic cells; R4, apoptotic cells.

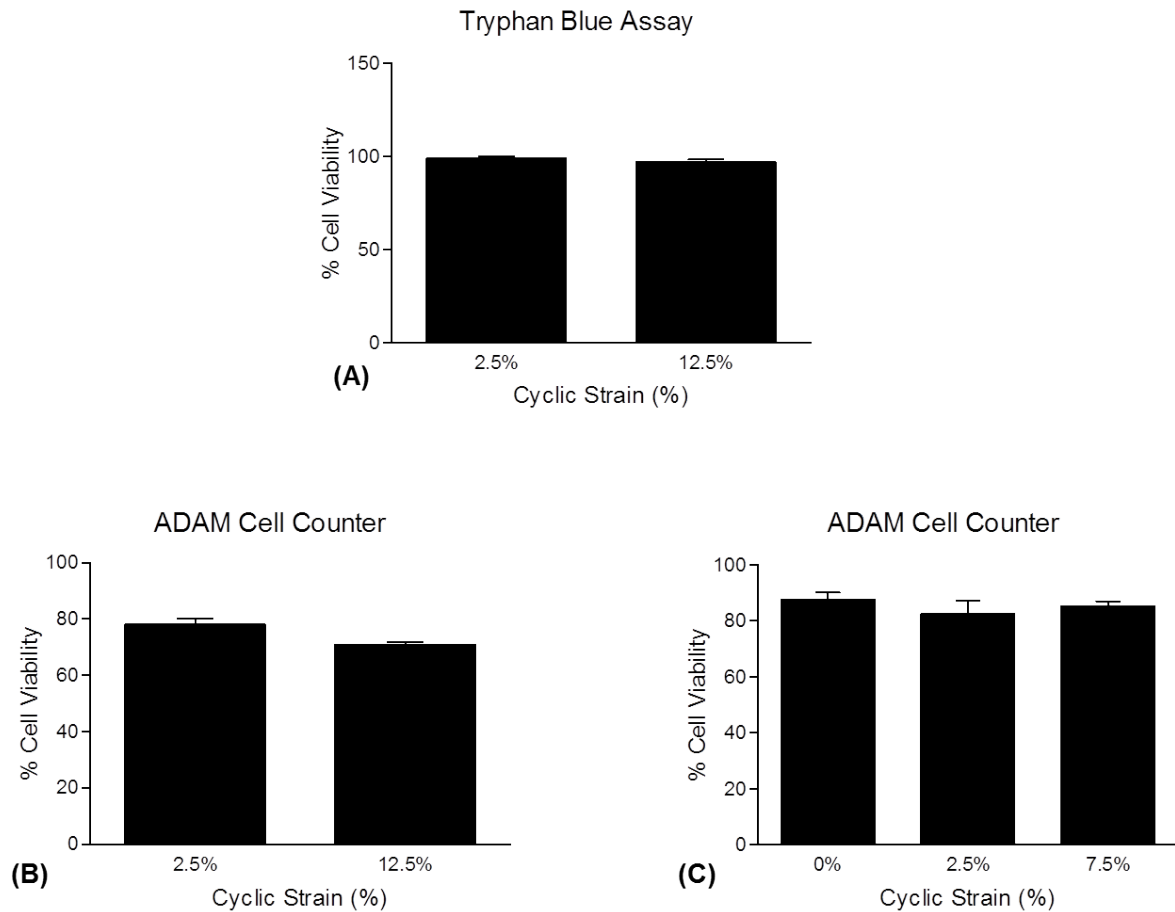


Figure 3.4: Trypan blue and ADAMTM cell counter viability studies. Trypan blue and the ADAMTM cell counter was used to analyse cell viability post-treatment with cyclic strain for 24 hrs. **(A)** Illustrates the percentage of viable cells post-treatment with either 2.5% or 12.5% cyclic strain for 24 hrs (n=6). **(B)** Employs the ADAMTM cell counter to assess the viability of the HAECs post-strain with 2.5% vs 12.5% strain for 24 hrs (n=6). **(C)** Employs the ADAMTM cell counter to assess cell viability from 0 – 7.5% strain (n=6).

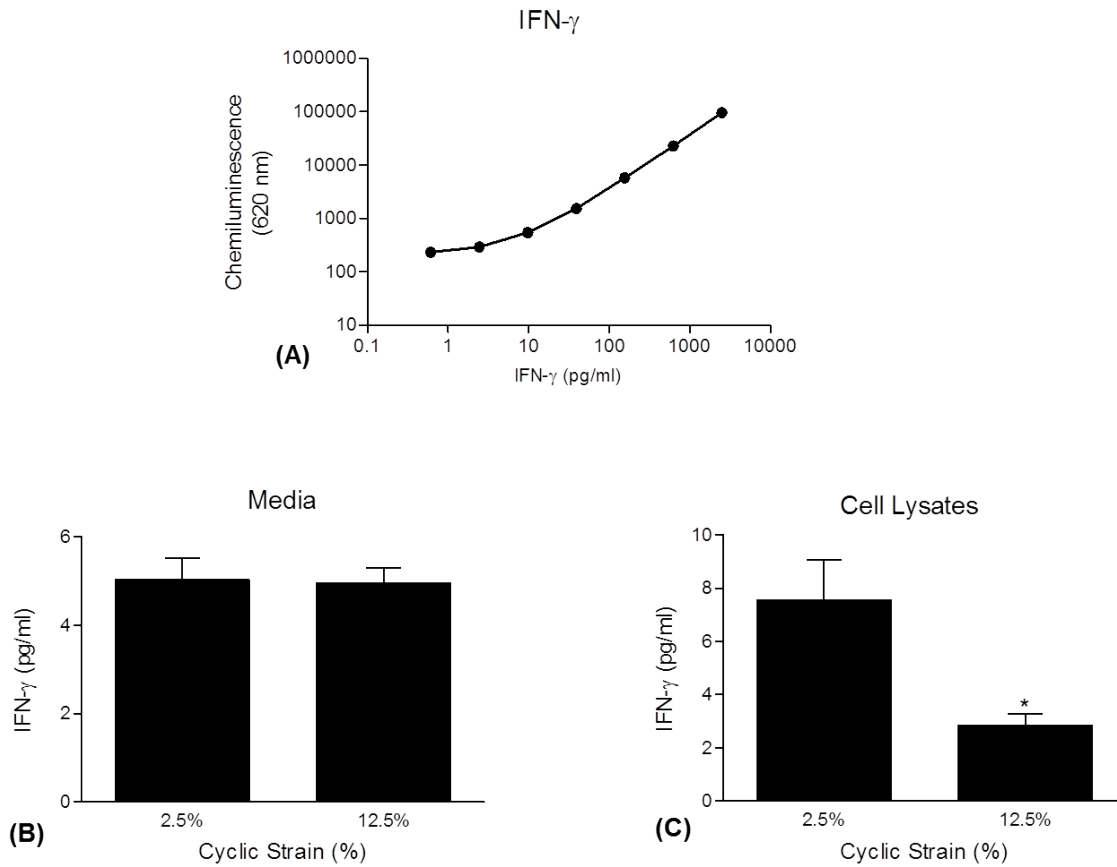


Figure 3.5: IFN- γ biomarker data. IFN- γ standard curve from ELISA is shown in (A). IFN- γ concentration (pg/ml) was measured in media supernatants (B) and cell lysates (C) that were previously treated with either 2.5% or 12.5% cyclic strain for 24 hrs ($*P \leq 0.05$ versus 2.5% determined using 1-way ANOVA and post-hoc Dunnett's test, $n=6$).

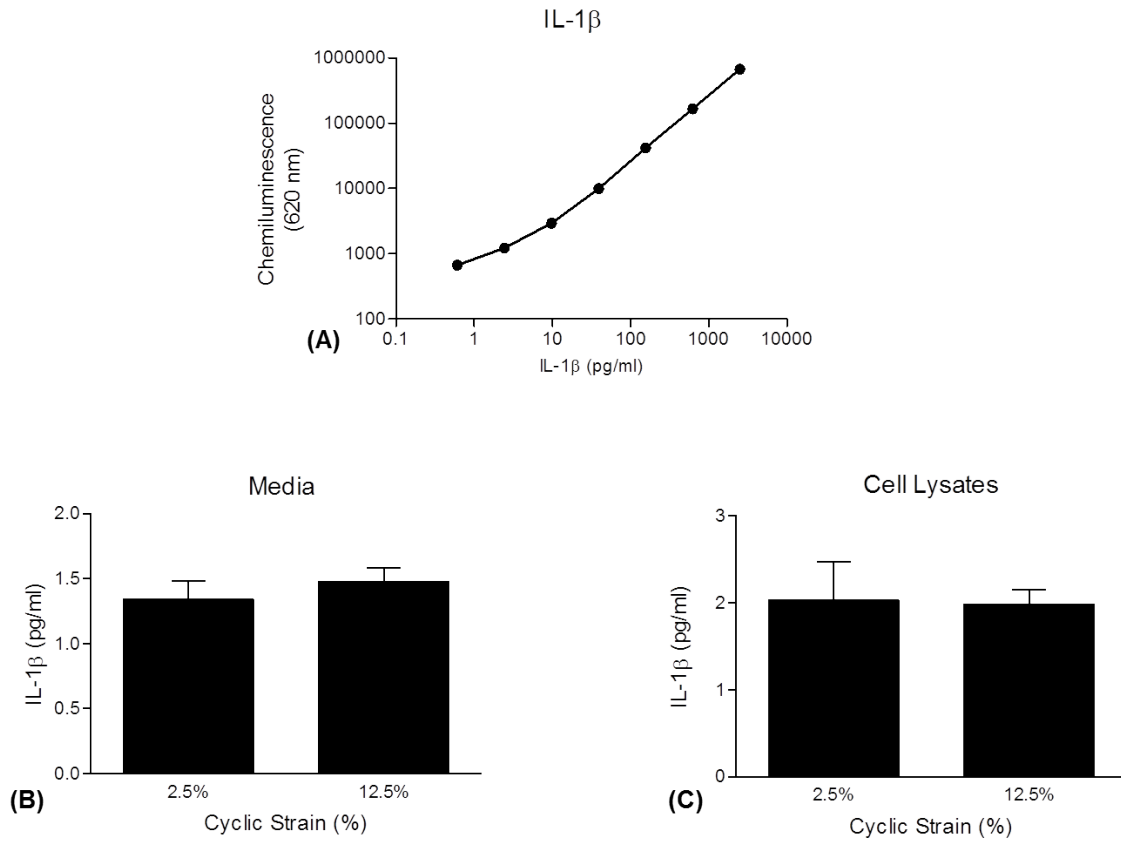


Figure 3.6: IL-1 β biomarker data. IL-1 β standard curve from ELISA is shown in (A). IL-1 β concentration (pg/ml) was measured in media supernatants (B) and cell lysates (C) that were previously treated with either 2.5% or 12.5% cyclic strain for 24 hrs (n=6).

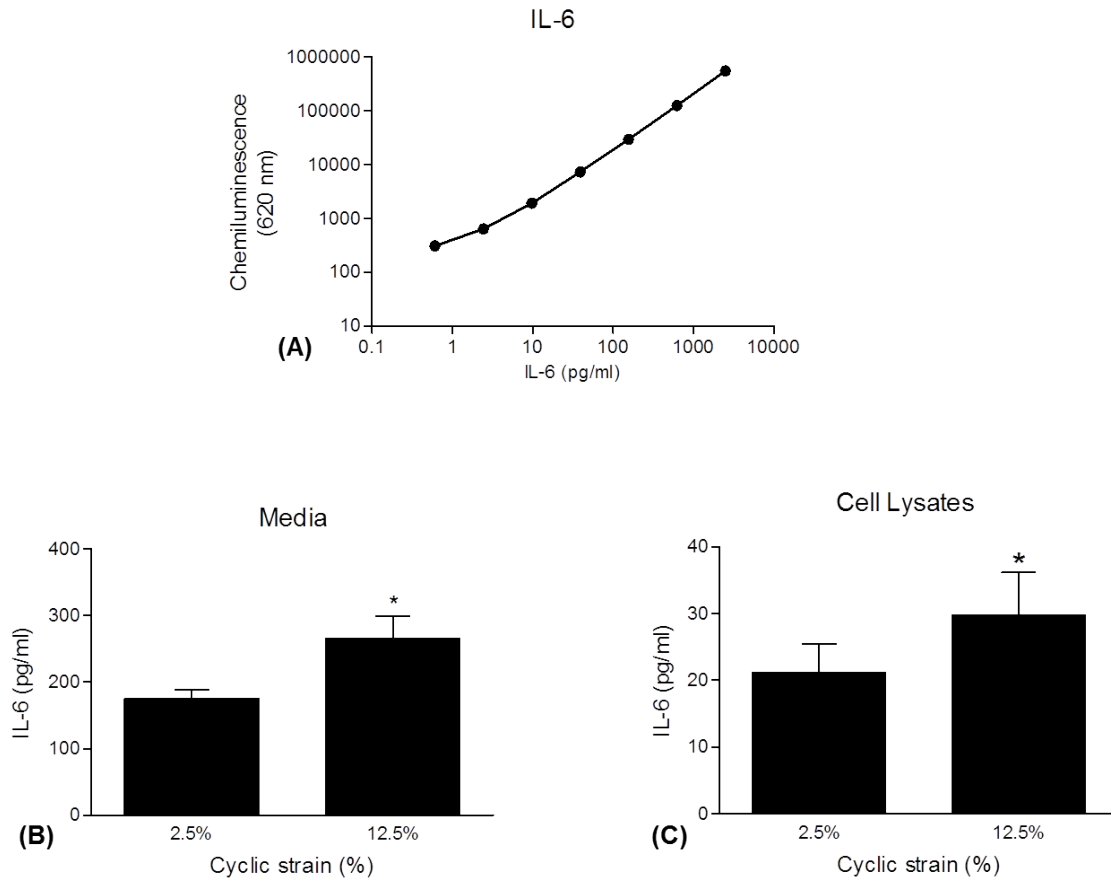


Figure 3.7: IL-6 biomarker data. IL-6 standard curve from ELISA is shown in (A). IL-6 concentration (pg/ml) was measured in media supernatants (B) and cell lysates (C) that were previously treated with either 2.5% or 12.5% cyclic strain for 24 hrs ($*P \leq 0.05$ versus 2.5% determined using 1-way ANOVA and post-hoc Dunnett's test, $n=6$).

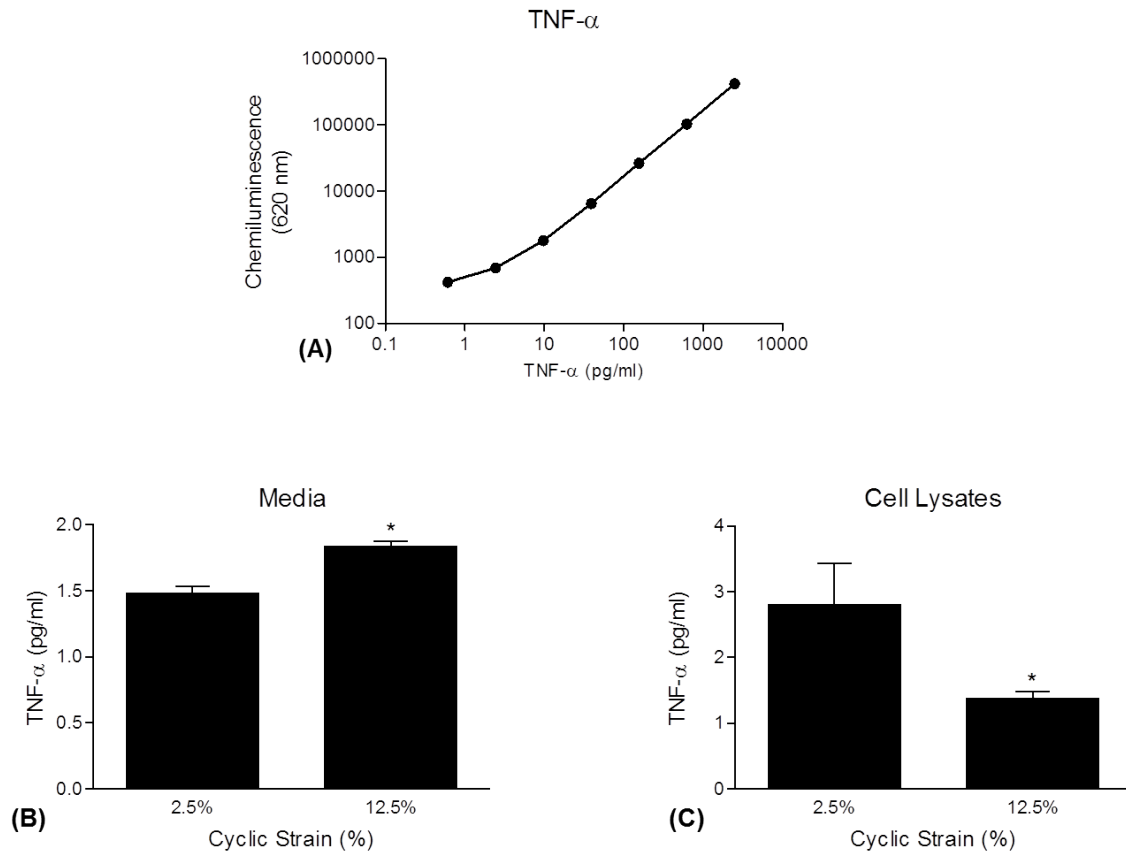


Figure 3.8: TNF- α biomarker data. TNF- α standard curve from ELISA is shown in (A). TNF- α concentration (pg/ml) was measured in media supernatants (B) and cell lysates (C) that were previously treated with either 2.5% or 12.5% cyclic strain for 24 hrs (* $P \leq 0.05$ versus 2.5% determined using 1-way ANOVA and post-hoc Dunnett's test, n=6).

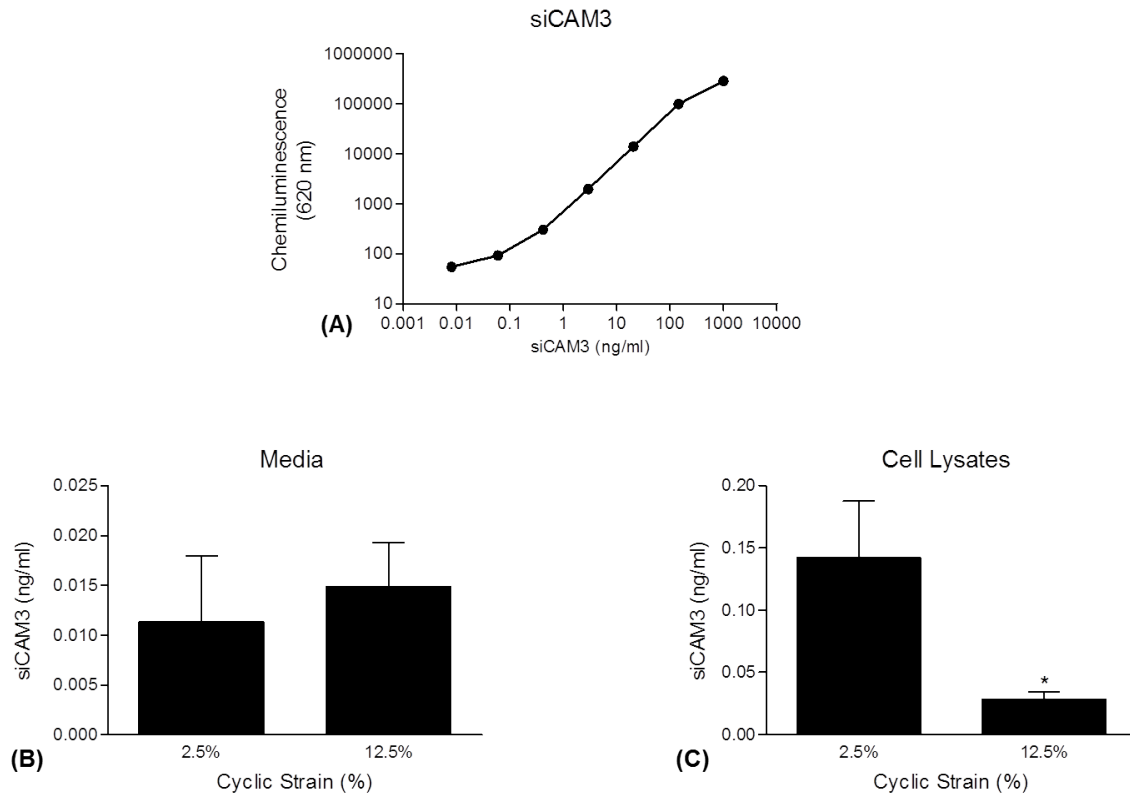


Figure 3.9: siCAM-3 biomarker data. siCAM-3 standard curve from ELISA is shown in (A). siCAM-3 concentration (ng/ml) was measured in media supernatants (B) and cell lysates (C) which were previously treated with either 2.5% or 12.5% cyclic strain for 24 hrs ($*P \leq 0.05$ versus 2.5% determined using 1-way ANOVA and post-hoc Dunnett's test, $n=6$).

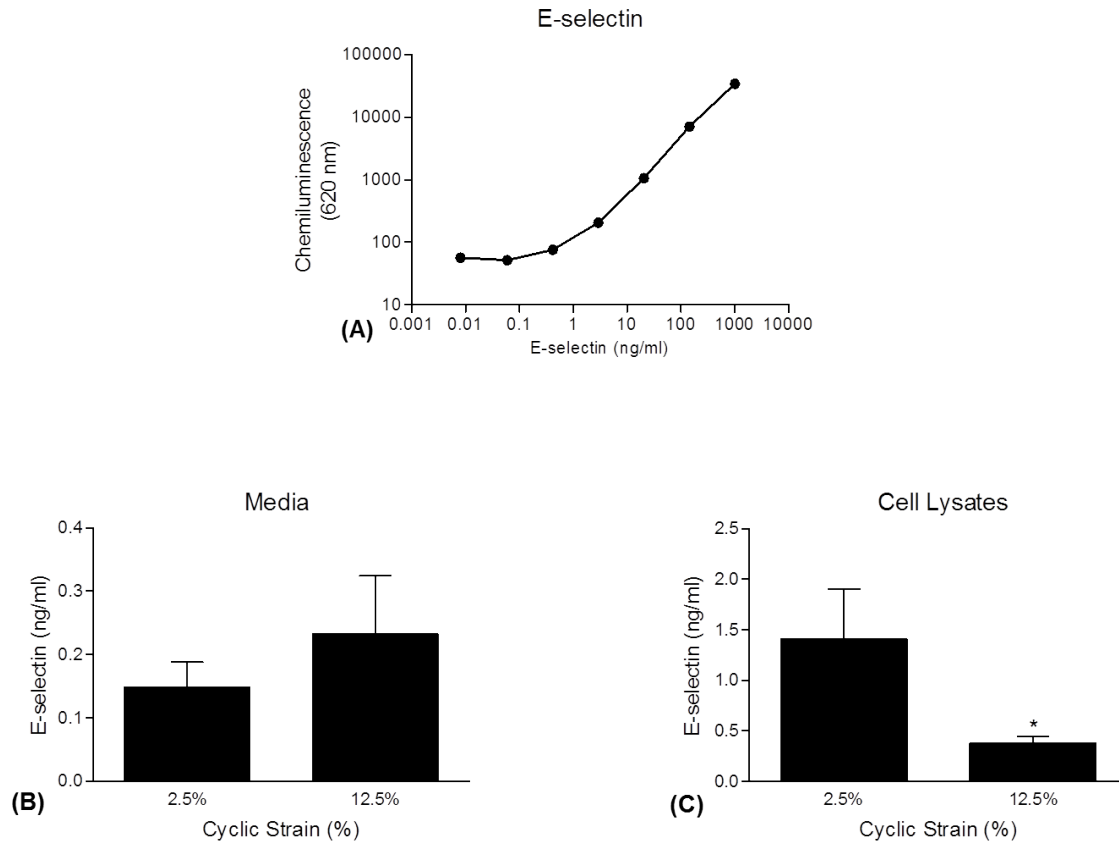


Figure 3.10 E-selectin biomarker data. E-selectin standard curve from ELISA is shown in (A). E-selectin concentration (ng/ml) was measured in media supernatants (B) and cell lysates (C) that were previously treated with either 2.5% or 12.5% cyclic strain for 24 hrs ($*P \leq 0.05$ versus 2.5% determined using 1-way ANOVA and post-hoc Dunnett's test, $n=6$).

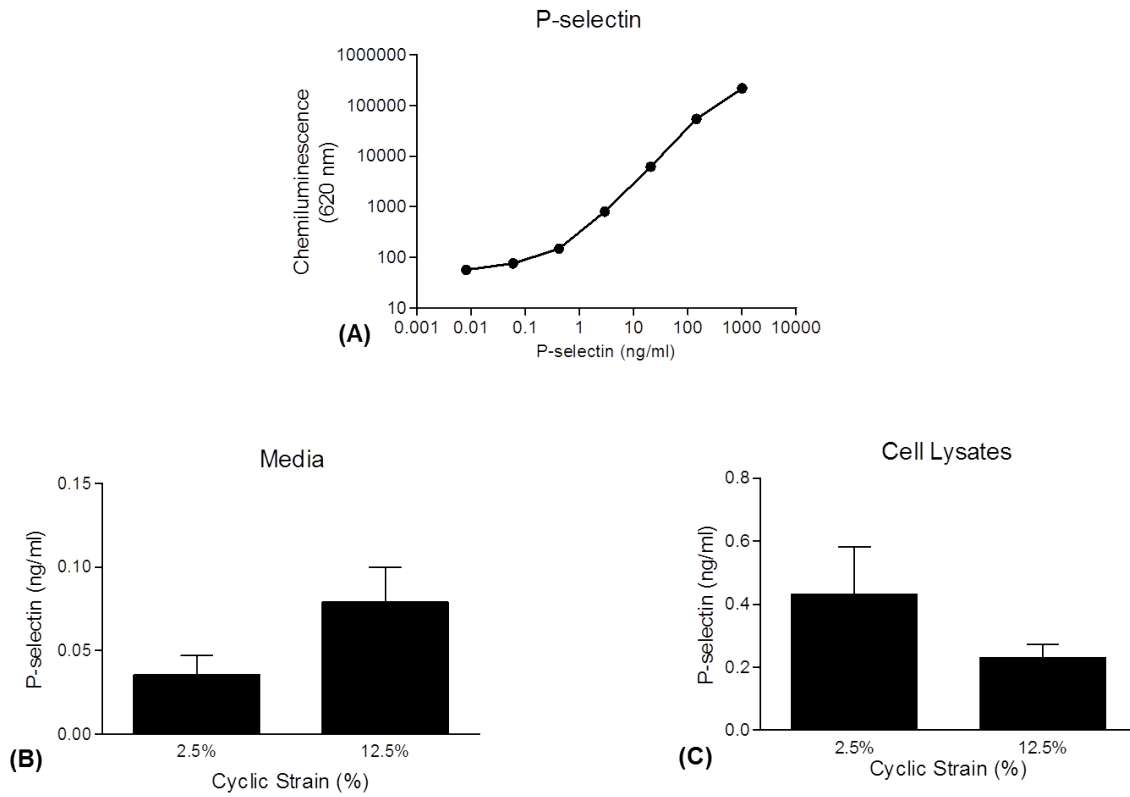


Figure 3.11: P-selectin biomarker data. P-selectin standard curve from ELISA is shown in (A). P-selectin concentration (ng/ml) was measured in media supernatants (B) and cell lysates (C) that were previously treated with either 2.5% or 12.5% cyclic strain for 24 hrs (n=6).

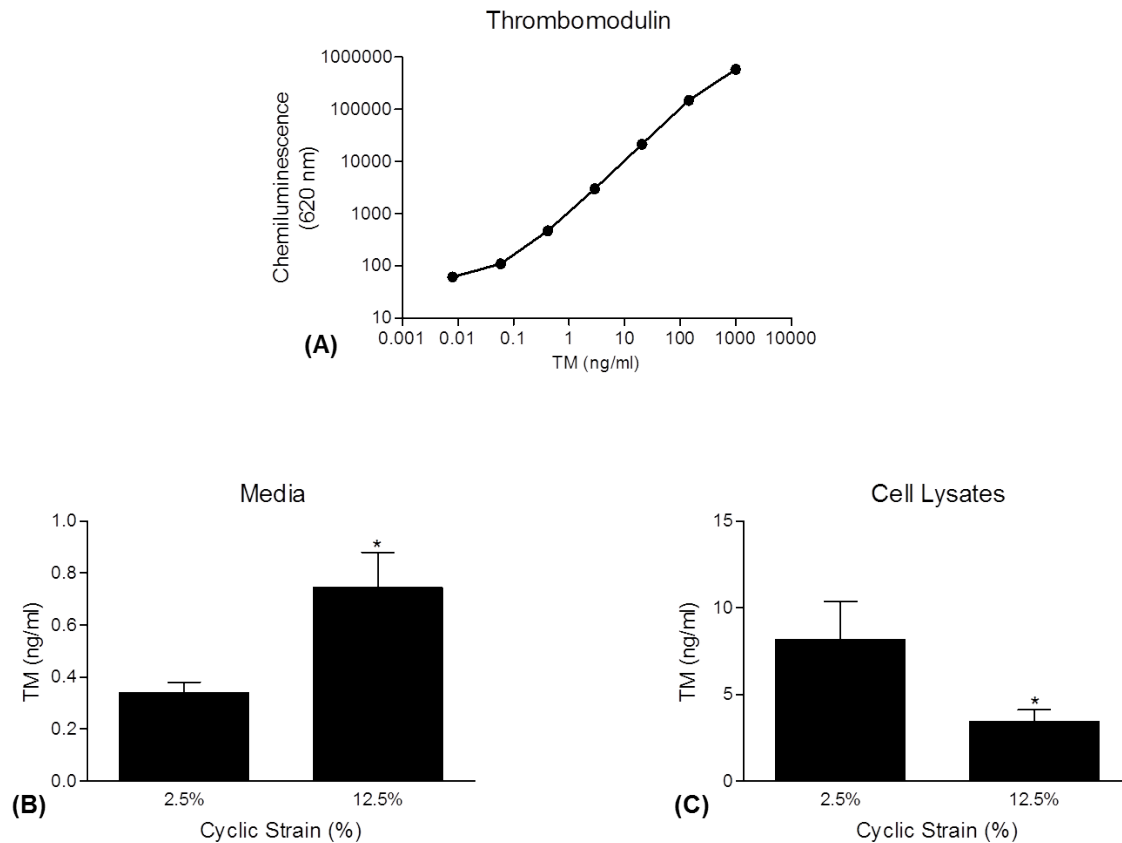


Figure 3.12: Thrombomodulin (TM) biomarker data. TM standard curve from ELISA is shown in (A). TM concentration (ng/ml) was measured in media supernatants (B) and cell lysates (C) that were previously treated with either 2.5% or 12.5% cyclic strain for 24 hrs ($*P \leq 0.05$ versus 2.5% determined using 1-way ANOVA and post-hoc Dunnett's test, $n=6$).

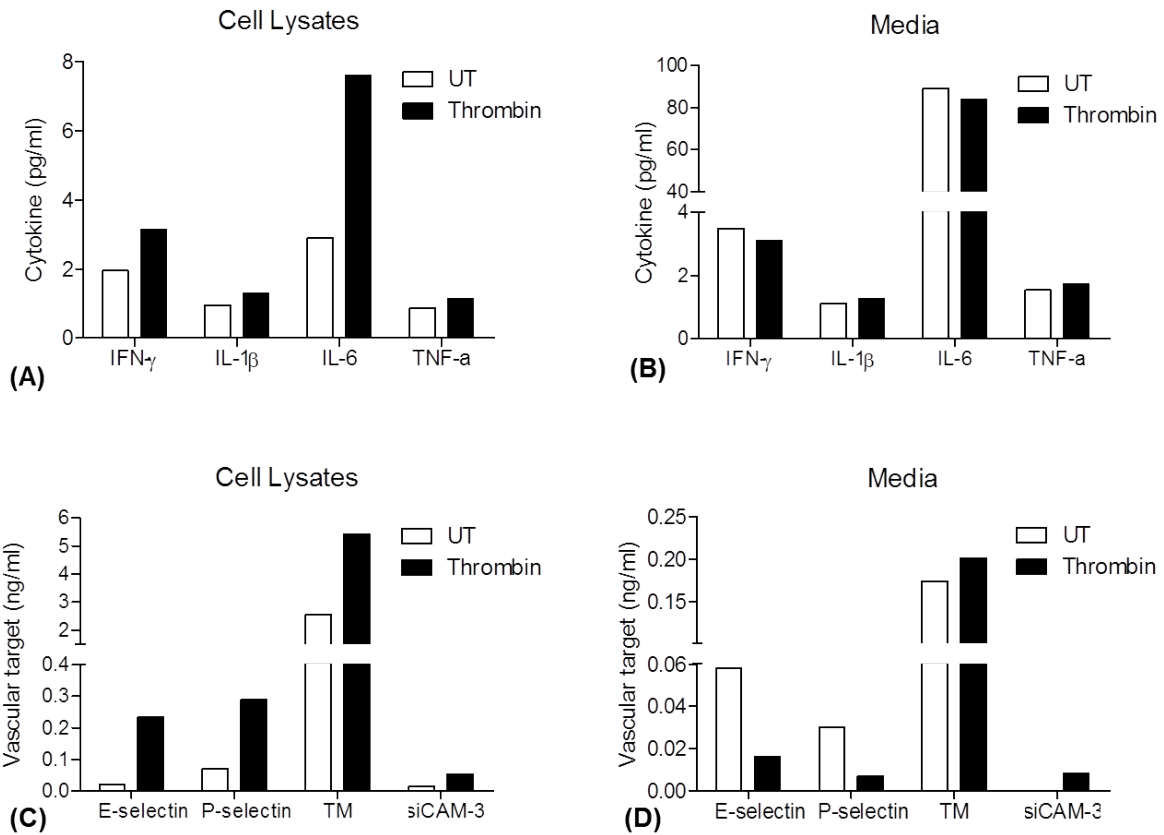


Figure 3.13: Thrombin-treated and untreated controls for the Pro-Inflammatory Injury and Vascular Injury Panels. Cell lysates (A and D) and media supernatants (B and D) were harvested from HAECs either untreated (UT) or treated with thrombin (1.0 U/ml for 24 hrs) and then measured for cytokine and vascular target levels (n=1).

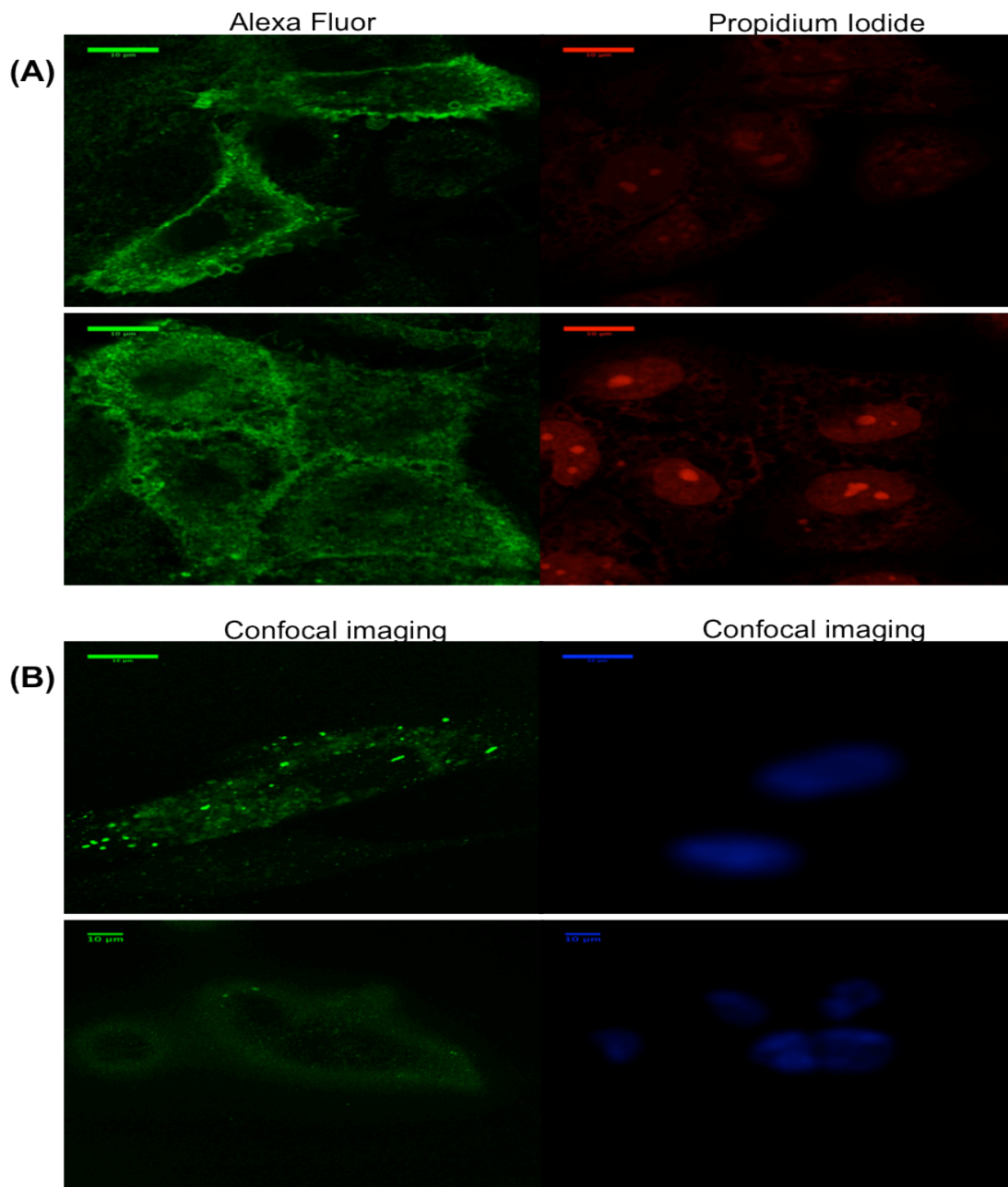


Figure 3.14: Fluorescent and confocal imaging of TM immunoreactivity in static HAECs. **(A)** TM is visualised (in green) along the cellular membrane. Propidium iodide, used for nuclear staining (in red). Intercellular TM is also shown. **(B)** Confocal imaging of TM immunoreactivity in static HAECs. TM is visualised (in green) both intracellularly and along the cellular membrane. All images are representative.

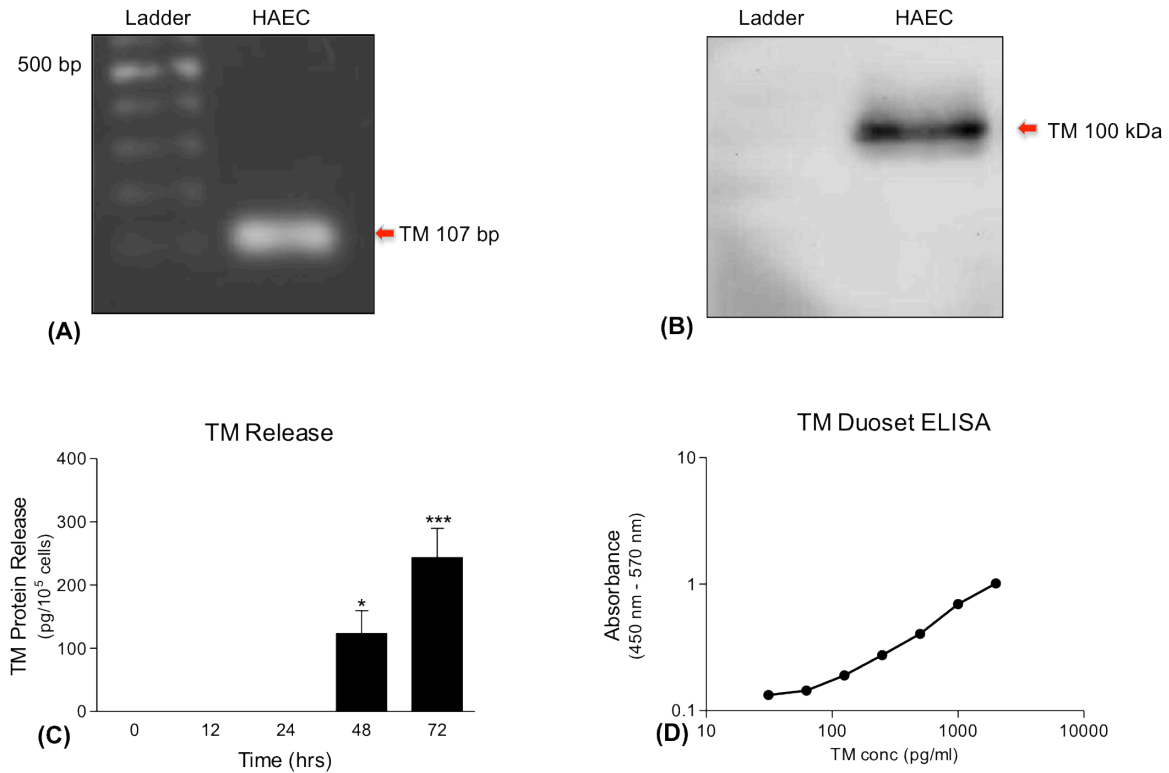


Figure 3.15: Constitutive expression and release of TM in static HAECs. **(A)** TM mRNA expression was measured by RT-PCR. Blots are representative of 3 replicates. **(B)** TM protein expression was observed by Western blotting. Blots are representative of 3 replicates. **(C)** Time-dependent release of TM from static HAECs into culture media was measured at different time points up to 72 hrs. (* $P \leq 0.05$ and *** $P \leq 0.001$ versus 0% determined using 1-way ANOVA and post-hoc Dunnett's test, $n=6$). **(D)** TM standard curve for the Duoset TM ELISA (R&D Systems, MN USA).

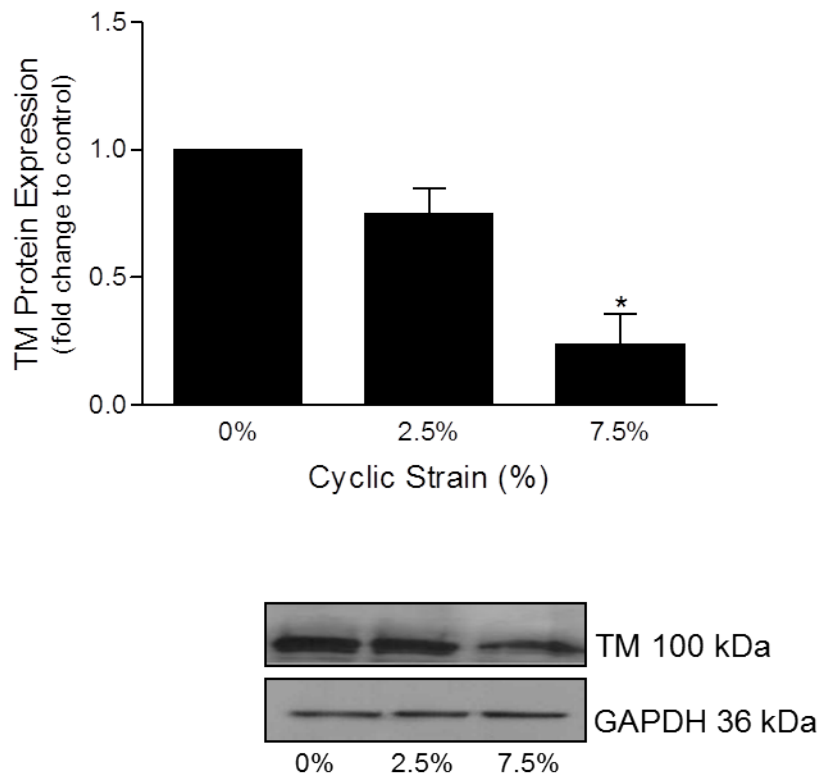


Figure 3.16: Dose-dependent effect of cyclic strain on cellular TM protein levels as monitored by Western blotting. Following application of cyclic strain (0%, 2.5% and 7.5% for 24 hrs) to HAECs, cell lysates were harvested and monitored for changes in both TM and GAPDH protein expression by Western blotting. The histogram illustrates scanning densitometry carried out on the Western blots to quantitate the fold change of TM relative to GAPDH (i.e., relative TM expression) (* $P \leq 0.05$ versus 0% determined using 1-way ANOVA and post-hoc Dunnett's test). Blots are representative of 3 replicates.

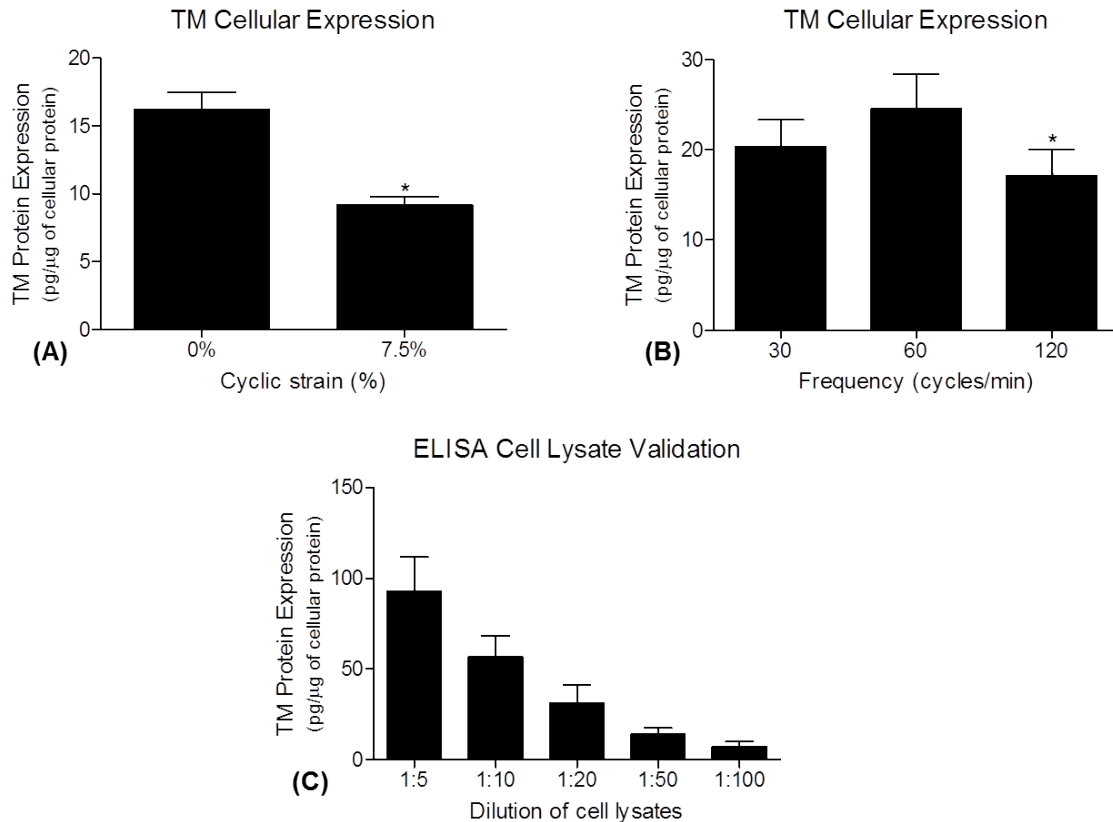


Figure 3.17: Dose- and frequency-dependent effects of cyclic strain on cellular TM protein levels in HAECs as monitored by ELISA. **(A)** Following application of cyclic strain (0% and 7.5% at 60 cycles/min for 24 hrs) to HAECs, cell lysates (typically diluted 1:20) were harvested and monitored for changes in TM protein expression by DuoSet ELISA ($*P \leq 0.05$ versus 0% determined using 1-way ANOVA and post-hoc Dunnett's test, $n=57$). **(B)** TM was measured in cellular lysates after 7.5% cyclic strain at frequencies of 30, 60 and 120 cycles per minute ($*P \leq 0.05$ versus 60 cycles/min determined using 1-way ANOVA and post-hoc Dunnett's test, $n=6$). **(C)** The DuoSet TM ELISA (designed primarily for measuring TM release into cell culture media) was validated to measure TM in cell lysates by preparing different dilutions of cellular lysates in 1X PBS (with 25% FCS) and subsequently measuring TM levels ($n=3$).

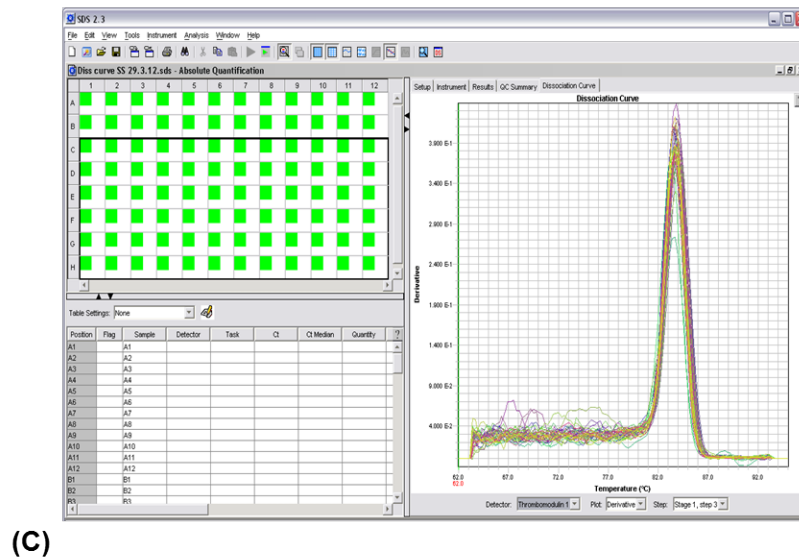
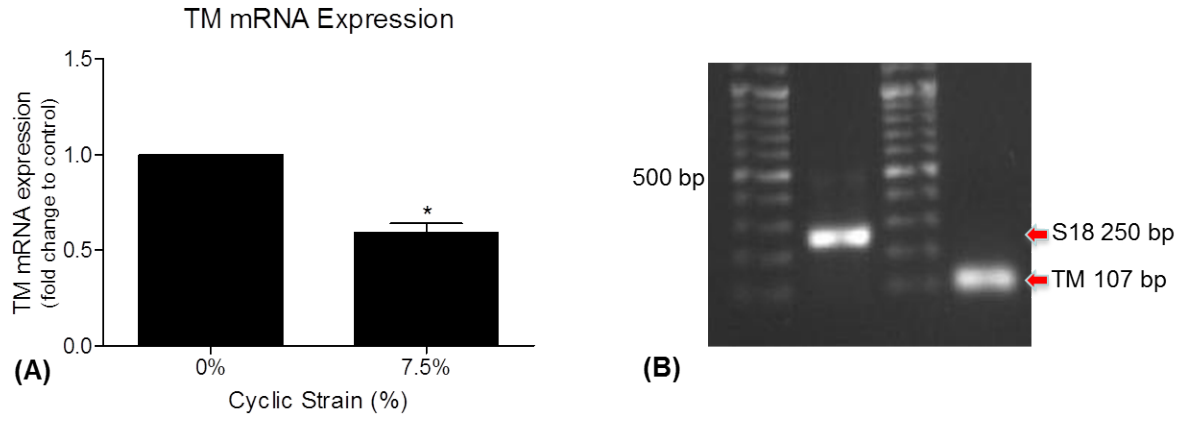


Figure 3.18: Effect of cyclic strain on TM mRNA levels in HAECs as monitored by qRT-PCR. (A) Following application of cyclic strain (0% and 7.5% for 24 hrs) to HAECs, mRNA samples were harvested and monitored for TM and S18 (endogenous control) expression by qRT-PCR ($*P \leq 0.05$ versus 0% determined using 1-way ANOVA and post-hoc Dunnett's test, $n=16$). (B) Primers for TM and S18 were initially optimized using standard PCR and then visualized on an agarose gel. Blots are representative of 3 replicates. (C) Melt curve analysis was carried out on the TM primers to determine their specificity.

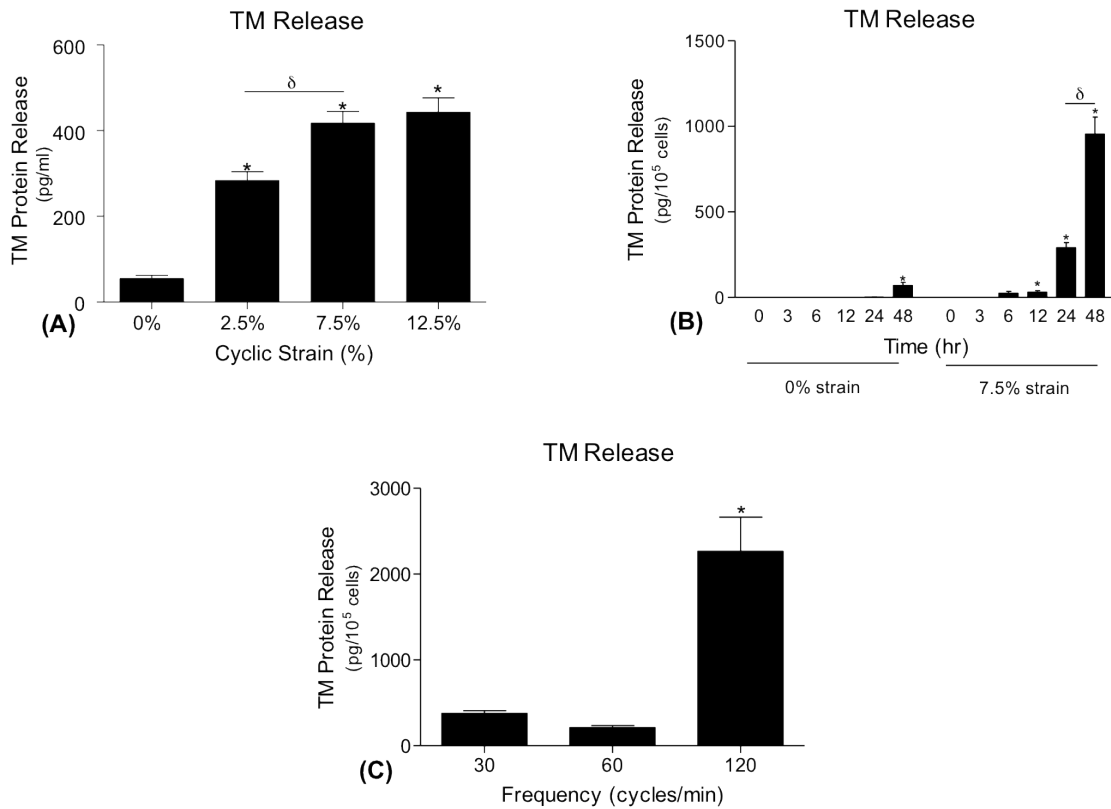


Figure 3.19: Dose-, time- and frequency-dependent effects of cyclic strain on TM release. **(A)** Different doses of cyclic strain, 0%-12.5% for 24 hrs were applied to HAECs and TM release into media was subsequently measured by ELISA ($*P \leq 0.05$ versus 0%, $\delta P \leq 0.05$ determined using 1-way ANOVA and post-hoc Dunnett's test, $n=6$). **(B)** TM release was also measured at different time points up to 48 hrs during the application of cyclic strain (0% and 7.5%) ($*P \leq 0.05$ versus 0 hrs, $\delta P \leq 0.05$ determined using 1-way ANOVA and post-hoc Dunnett's test, $n=6$). **(C)** The effect of cyclic strain frequency (7.5% strain at 30, 60, 120 cycles/min) on TM release from HAECs was measured by ELISA ($*P \leq 0.05$ versus 60 cycles/min determined using 1-way ANOVA and post-hoc Dunnett's test, $n=6$).

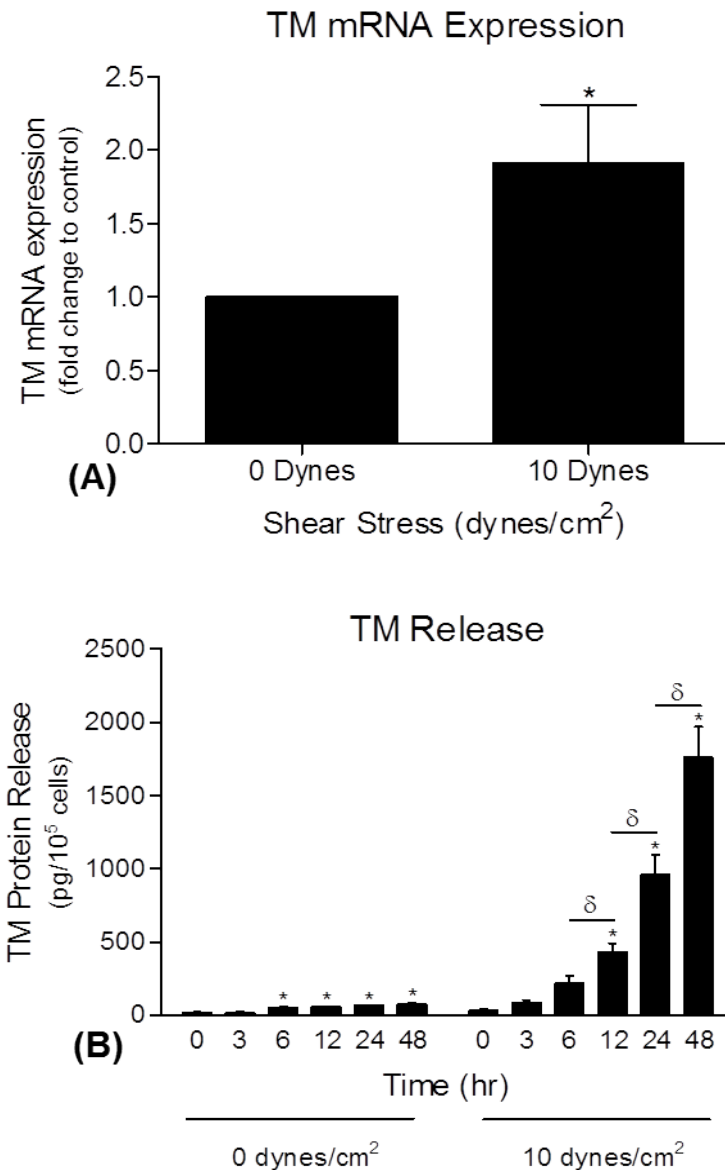


Figure 3.20: Shear stress regulates TM expression and release. HAECs were exposed to shear stress (0-10 dynes/cm², 0-48 hrs) and monitored for TM mRNA expression and TM release. **(A)** Shear stress-dependent up-regulation of TM mRNA levels (* $P \leq 0.05$ versus 0 dynes/cm² determined using 1-way ANOVA and post-hoc Dunnett's test, $n=9$). **(B)** Time-dependent increase in TM release in response to shear stress (* $P \leq 0.05$ versus 0 hrs, $\delta P \leq 0.05$ determined using 1-way ANOVA and post-hoc Dunnett's test, $n=6$).

3.4 Discussion

One of the main objectives for this project was to further understand how elevated cyclic strain impacts vascular injury biomarkers including thrombomodulin (TM) in endothelial cells. Cyclic strain is a biomechanical force that contributes to endothelial homeostasis and vascular health (Cheng et al., 2001). Thus, when cyclic strain becomes dysregulated, endothelial dysfunction leading to cardiovascular diseases such as atherosclerosis and hypertension may result (Hahn and Schwartz, 2009). TM has evident physiological importance to the endothelial cell, indicated by its functions in coagulation, inflammation and fibrinolysis (Martin et al., 2013). There is a shortage of studies (and particularly *in vitro* studies) investigating the effects of cyclic strain on TM expression and release. This lack of information on TM regulation by this potent hemodynamic force has therefore framed the resultant thesis.

Our initial MSD[®] Multiplex ELISA study identified a profile of pro-inflammatory and vascular injury molecules that were responsive to elevated cyclic strain. We looked at a range of pro-inflammatory cytokines, as they are known to play an imperative role in the formation and development of atherosclerotic lesions. We found that elevated cyclic strain reduced cellular expression of IFN- γ but had no effect on release. There were no available studies on IFN- γ , a dimerized soluble cytokine involved in innate and adaptive immunity (Theofilopoulos et al., 2001) in relation to cyclic strain for comparison. Subsequently, we observed that elevated strain had no effect on IL-1 β expression or release. This was in agreement with an earlier study showing that IL-1 β expression or release was not affected following 24 hrs cyclic strain (15.1%) (Okada et al., 1998). Next, we showed IL-6, a pro-inflammatory cytokine, was up-regulated in cell lysates and media following elevated cyclic

strain indicating the pro-inflammatory nature of this stimulus on endothelial cells. This is not surprising as IL-6 expression has already been reported to be increased following cyclic strain in smooth muscle cells (Zampetaki et al., 2005). Additionally, increased plasma concentration of IL-6 was observed in subjects with high blood pressure, which also concurs with our result (Chae et al., 2001). TNF- α , another cytokine involved in systemic inflammation was shown to be increased in media and decreased in cell lysates following cyclic strain. This is in contrast with an earlier study where its levels were not affected after elevated cyclic strain in endothelial cells isolated from human umbilical veins (Okada et al., 1998).

We also examined a range of known vascular injury markers in relation to elevated cyclic strain. Firstly, we found that siCAM-3 levels were decreased in cell lysates with no change noted in media, following elevated cyclic strain. siCAM-3 has not been linked to cyclic strain in the literature in respect to either expression or release making this result difficult to interpret. It is noteworthy however that siCAM-1, a member of the same cell adhesion family, has been reported to be up-regulated in the plasma of men with increased blood pressure (Chae et al., 2001). Subsequently, we went on to investigate the effect cyclic strain had on E-selectin and P-selectin, which are involved in the recruitment of leukocytes. We found that elevated cyclic strain had no significant effect on P-selectin levels in either media or cell lysates, whereas E-selectin was decreased in cell lysates with no change in media following cyclic strain. This is in contrast with an earlier study showing E-selectin substantially up-regulated after strain when compared to control cells under static conditions (Yun et al., 1999). This group used a “supraphysiological” level of 25% maximal strain at 30 cycles/min for 24 hrs, which renders this result somewhat questionable.

Of particular interest were the observations in relation to TM, a known injury marker for endothelial cells. Intracellular protein levels for TM were found to be significantly down-regulated by high cyclic strain, whilst its release from HAECs was increased (Martin et al., 2013). Further studies involving Western blotting and qRT-PCR both confirmed the dose-dependent reduction of TM protein and mRNA expression levels following elevated cyclic strain of HAECs. Moreover, further ELISA studies using a single-plex Duoset ELISA demonstrated how TM release/shedding was increased in response to cyclic strain in a dose-, frequency- and time-dependent manner. The increased release and reduced expression of TM would indicate that the endothelial cells are “losing” TM which would mean the endothelium would exhibit decreased anti-coagulant and anti-inflammatory properties (i.e., leading to a more pro-inflammatory and pro-coagulant endothelium). Conversely, the increased release of TM could be cardioprotective for the endothelium, as functional efficacy has been attributed to circulating sTM variants (Lin et al., 2008; Lopes et al., 2002). The assortment of viability studies employed concludes that the elevated strain conditions were not excessively detrimental to HAEC viability.

The current literature has contradicting reports on the regulation of TM by cyclic strain, the repetitive mechanical deformation of the vessel wall as it rhythmically distends and relaxes within the cardiac cycle. Consistent with our *in vitro* results demonstrating reduced TM expression levels induced by cyclic strain, substantially decreased *in vivo* mRNA and protein TM expression in response to outward vessel wall distension was previously reported in vein grafts using a rabbit autologous vein graft model (Sperry et al., 2003). Importantly, this group also claimed that wall tension was a more important regulator of TM gene expression than shear stress, which they demonstrated by ligating the distal carotid artery to

alter blood flow and pressure-induced vessel wall distension. Two somewhat older paired reports disagree with this aforementioned vein graft study; by using *ex vivo* human saphenous vein segments inside an external flow circuit, they describe how exposure of vein grafts to arterial flow significantly reduced endothelial TM expression in a cyclic strain-independent manner (Golledge et al., 1999; Gosling et al., 1999). One justification for this contradiction in results may perhaps be due to the insufficient external stenting used in the earlier studies (Golledge et al., 1999; Gosling et al., 1999) to prevent any cyclic strain influences, with up to $7\pm 2\%$ pulsatile expansion still possible with external polytetrafluoroethylene (PTFE) stents. Another reason for this difference may be because that the later (Sperry et al., 2003) and earlier (Golledge et al., 1999; Gosling et al., 1999) studies represent chronic (weeks) versus acute (45-90 mins) observations, respectively. A further additional study using *ex vivo* vein graft and *in vitro* vascular cell culture models persuasively demonstrate that cyclic strain-dependent induction (10% stretch at 1Hz for 16 hours) and release of transforming growth factor- $\beta 1$ (TGF- $\beta 1$) within the medial smooth muscle cell layer of the vessel could decrease endothelial TM expression in a *paracrine* manner (Kapur et al., 2011). Using a pan-neutralizing TGF- $\beta 1$ antibody (1D11), this group succeeded in blocking TM down-regulation, thereby conserving levels of activated protein C and decreasing thrombus formation in a rabbit vein graft model. A lone report that contradicted these studies (and indeed other studies including our own results) demonstrated a sustained *increase* in TM protein expression in HUVEC cultures after application of 21% (but not 15%) cyclic strain, with a role for NO signalling mechanisms strongly implicated (Chen et al., 2008). These authors suggest that the prolonged increase in protein expression may putatively be attributed to NO-mediated stabilization of TM protein via S-nitrosylation as the TM promoter activity was not induced

by cyclic strain of HUVECs. However, there is no further data to back-up these observations and taking into account the supra-physiological levels of strain applied, the significance of this study remains uncertain. Finally, a 2.6 fold down-regulation of TM expression in human aortic smooth muscle cells (HASMCs) following 4% equibiaxial cyclic strain for 24 hrs was reported (Feng et al., 1999). Again, the physiological relevance of this result is also open to debate, as SMCs do not express TM protein or mRNA within the vessel wall *in vivo*.

The previous studies emphasise the limitation of cell culture models in addressing the regulatory impact of cyclic strain on TM expression. In fact, this thesis is the first time TM expression and release has been shown to be negatively mediated by cyclic strain in an *in vitro* model, observations that are consistent with *in vivo* and *ex vivo* studies. Almost all the *ex vivo* and *in vivo* work mentioned above concur with our observations that TM expression is reduced in endothelial cells following elevated cyclic strain treatment, apart from the debatable studies by Chen et al. in 2008.

We also examined the effect of varying the frequency of cyclic strain, whilst maintaining the same amplitude (7.5%), on TM expression and release from HAECs. Endothelial cells are typically exposed to elevated frequencies of cyclic strain due to long-term increased blood pressure, intense exercise, and also sustained stress and anxiety (Laughlin et al., 2008). Evidently, permanent exposure to elevated blood pressure is detrimental to the endothelium whilst short-term increases (e.g., physical activity) in cyclic strain frequency have beneficial effects for the arterial endothelial cell, allowing it to sustain a normal phenotype (Hambrecht et al., 2003). To date, there are no reports on the impact of elevated strain frequency on either TM expression or release in endothelial cells, which would again highlight the deficiency of *in vitro* data regarding cyclic strain-dependent regulation of

TM. Relative to the physiological level of 60 cycles/min, we found that TM expression was only slightly decreased following 120 cycles/minute at the same 7.5% amplitude, although TM release was very substantially elevated. The reduction in TM protein expression combined with the elevated release of TM suggests that elevated strain amplitude (7.5%) and frequency (120 cycles/min) may have a profoundly deleterious effect on the endothelium thrombogenicity in the long term. Moreover, it also suggests that released TM (sTM) may be a novel biomarker for elevated blood pressure and endothelial dysfunction in general, possibly acting as an “SOS” signal for damaged endothelial cells to communicate with adjacent healthy cells.

Our data also demonstrates how TM expression and release from HAECs is up-regulated by elevated laminar shear stress, a hemodynamic component of blood flow known to convey an *atheroprotective* phenotype to the endothelium (Traub and Berk, 1998). TM has a shear stress response element (-GAGACC-) within its promoter region, which would partly explain the sensitivity of TM expression to laminar shear stress. We found that TM mRNA expression is increased by shear stress, which is in accordance with the current literature (Malek et al., 1994; Takada et al., 1994). The majority of studies show that shear stress is a positive regulator of TM expression, which is not surprising when one considers the anti-coagulant and anti-thrombotic properties of TM. Shear-dependent up-regulation of TM expression under both acute and chronic treatment paradigms has been observed in a wide range of models including a mouse transverse aortic constriction model of flow-dependent remodelling (Li et al., 2007), HUVECs (Takada et al., 1994; Bergh et al., 2009; Wu et al., 2011), human abdominal aortic endothelial cells (HAAECs) (Rossi et al., 2011), human retinal microvascular endothelial cells (Ishibazawa et al., 2011), and also in primate

peripheral blood-derived endothelial outgrowth cells (Ensley et al., 2012). Shear stress has also been reported to offset the down-regulatory influence of TNF- α treatment on TM expression in HUVECs (Jun et al., 2009). In contrast to these studies (and our own observations), endothelial TM expression showed a mild transient increase followed by a (reversible) decrease to just 16% of baseline levels within 9 hrs of flow onset in BAECs (Malek et al., 1994). However, this observation should be regarded with caution due to both the volume of studies reporting the opposite effect and the authors use of BAECs (as opposed to human/primate/mouse models).

In addition to expression, it is interesting to note that shear stress was also found to up-regulate TM release in a temporal manner. Indeed, shear was a significantly more potent stimulus for TM release, with higher amounts of sTM (i.e., soluble/release TM) measured in media when compared to cyclic strain. By contrast, cyclic strain causes a reduction of expression whilst temporally (and moderately) up-regulating release of TM. Although the reasons for this difference are unknown, it is possible to speculate. Levels of shear stress used in this study (up to 10 dynes/cm²) are considered healthy and atheroprotective for the endothelium whereas elevated strain (7.5%) is potentially patho-physiological. The increased TM release following shear stress may be having cardioprotective functions in the endothelium *in vivo*, thus helping to maintain homeostasis. In addition, it is important to note that the endothelium is not losing TM in this circumstance as cellular expression of TM is increased by healthy levels of shear. Elevated cyclic strain on the other hand is decreasing TM expression whilst increasing release so the endothelium would become more susceptible to endothelial dysfunction. Long-term elevated levels of strain may consequently be a contributor to the initiation of CVD. This may explain the elevated production of TM under

shear stress and the reduced production of TM under cyclic strain. Moreover, both haemodynamic stimuli are almost certainly eliciting distinct signalling pathways mediating expression and release of TM. Both shear and strain may also differentially activate transcription factors known to modulate TM expression (e.g., KLF-2). With this in mind, we next decided to examine the signalling pathway(s) putatively mediating the cyclic strain effects on TM. We also decided to examine how elevated cyclic strain impacts TM release in both the absence and presence of other inflammatory/atherogenic mediators.

Chapter 4:

**Investigation into the signalling
mechanisms underlying cyclic strain-
mediated thrombomodulin
expression and release**

4.1 Introduction

The previous chapter dealt with characterising the impact of cyclic strain on TM expression and release in HAECs. So far, we have observed that TM release is increased and cellular expression is reduced in response to elevated levels of cyclic strain. In this chapter, we extend our investigations by exploring the molecular mechanisms putatively involved in mediating the strain-induced modulation of TM expression and release from endothelial cells, which is as yet poorly defined in the literature.

In Section 4.2.1, we first looked at the effect that inflammatory mediators such as tumour necrosis factor- α (TNF- α), oxidized low density lipoprotein (ox-LDL) and elevated glucose have on TM expression and release from HAECs in the both absence and presence of cyclic strain (as inflammatory events *in vivo* usually involve a combination of humoral and biomechanical events, again an area relatively unexplored in the literature). It is widely accepted that TNF- α , a pro-inflammatory cytokine, is a negative regulator of TM expression (Bergh et al., 2009; Boehme et al., 1996; Grey et al., 1998; Lin et al., 2011; Soff et al., 1991). Oxidation of low density lipoprotein (LDL) is thought to play a crucial role in plaque development during atherosclerosis (Cominacini et al., 2000). It has also been reported that ox-LDL down-regulates TM expression (Ishii et al., 2003), yet there are no studies measuring how these inflammatory mediators impact TM release when combined with elevated cyclic strain. Hyperglycemia (i.e., toxic high glucose levels typically observed during type-2 diabetes) is another established cause of endothelial dysfunction during metabolic syndrome (Nakagami et al., 2005), yet there is nothing reported about how glucose may affect either TM

expression or release from the endothelium. As such, we also included this in our investigations.

In Section 4.2.2, we look at known signaling pathways activated by cyclic strain in an effort to identify the signaling mechanism(s) mediating the effects of strain on TM dynamics.

GM6001, a generic inhibitor of matrix metalloproteinases, was employed to ablate matrix metalloproteinase (MMP) activity. MMPs are known to be up-regulated by cyclic strain (Cummins et al., 2007; Hasaneen et al., 2005) and have previously been shown to mediate lysophosphatidic acid (LPA)-induced TM lectin-like domain shedding (Wu et al., 2008). We also utilised a specific serine protease inhibitor, 3,4-dichloroisocoumarin (DCI). Whilst there is no study thus far linking serine proteases to TM protein expression, they have been shown to specifically cleave TM (Cheng et al., 2011). Additionally, rhomboids, a family of intramembrane proteases sensitive to DCI inhibition, were previously reported to cleave TM from the membrane (Lohi et al., 2004) facilitating its release into media.

Another signaling component examined was endothelial nitric oxide synthase (eNOS) as it is up-regulated by cyclic strain in BAECs (Awolesi et al., 1995). eNOS, as its name suggests, produces nitric oxide (NO) in blood vessels which regulates vascular tone by inhibiting smooth muscle contraction and platelet aggregation (Vanhoutte PM, 2009). L-NAME (L-N^G-Nitroarginine methyl ester) was therefore employed to inhibit eNOS in strain experiments in order to observe its influence on TM expression and release from HAECs. Similarly, NSC23766 was employed to block Rac1 GTPase, a member of the Rho protein family. An earlier study showed that pravastatin could regulate TM expression in HAECs by inhibiting the activation of Rac1/Cdc42 and NFκB (Lin et al., 2007). Furthermore, cyclic

mechanical strain is known to be partly transduced via activation of Rac1 GTPase (Kumar et al., 2004). However, nothing in the literature associates Rac1 with TM release.

The putative role of NADPH oxidase (a superoxide-generating enzyme) was also investigated in our model because of its known mechano-sensitivity to cyclic strain (Cheng et al., 2001; Howard et al., 1997; Matsushita et al., 2001). There are no reports of a direct link between NADPH oxidase activation and TM regulation. Apocynin and superoxide dismutase (SOD) were therefore incorporated into strain experiments to selectively block NADPH oxidase activation and to degrade reactive oxygen species (ROS), respectively.

We also explored a number of kinase cascades; Protein tyrosine kinase (PTK), phosphoinositide 3-kinase (PI3K) and mitogen activated protein kinases (MAPKs) - p38 and Erk-1/2. A previous study has reported that the activation of PI3K/Akt causes a reduction in TM expression in a non-small cell lung cancer (NCLC) A549 cell line (Liu et al., 2010). In addition, it was shown *in vivo* using transgenic mice that MAP kinase pathways were dampened by the lectin-like domain of TM (Conway et al., 2002). Cyclic strain also elicits regulatory effects via various kinase cascades including protein tyrosine kinase (Yano et al., 1996), PI3K (Han et al., 2010), MAPK p38 (Shyu et al., 2010) and Erk-1/2 (Cheng et al., 2001). However, there is no study directly investigating the link between these kinases and the cyclic strain-mediated regulation of TM expression or release from endothelial cells.

Finally, we investigated integrins, heterodimeric mechanotransduction receptors known to be activated by strain (Wilson et al., 1995). In this regard, we employed a cyclic RGD peptide inhibitor into strain experiments to observe any integrin involvement in our TM model.

4.2 Results

4.2.1 Inflammatory mediators

HAECs were subjected to a range of atherogenic inflammatory conditions and the impact on TM expression (mRNA and protein) and release into cell culture media were assessed in the absence and presence of cyclic strain (7.5% equibiaxial, 60 cycles per min). Post-experiment, cells were harvested for total cellular protein (Western blotting), mRNA (qRT-PCR), and media (ELISA) for TM analysis. The inflammatory mediators and conditions employed are listed below;

- i. TNF- α : 0 versus 10 ng/ml (protein expression) or 0 - 100 ng/ml (mRNA analysis and TM release) for 24 hrs
- ii. ox-LDL: 0 - 50 μ g/ml (mRNA analysis and TM release) for 24 hrs
- iii. Glucose: 5 - 30 mM (mRNA analysis and TM release) for 24 hrs

The reagent concentrations for each condition were chosen to best imitate the *in vivo* situation. For example, the ox-LDL experiment employed 0, 10 and 50 μ g/ml of ox-LDL with 10 μ g/ml being normal and 50 μ g/ml being high normal - early atherogenic.

In the first study, TNF- α moderately decreased TM protein and mRNA expression in static HAECs (Fig 4.1A-B) whilst having no effect on TM release from static HAECs. TNF- α was seen to potentiate the strain-mediated induction of TM release from HAECs at 100 ng/ml (Fig 4.1C).

With respect to ox-LDL treatment, TM mRNA expression exhibits a statistically insignificant increase (at 10 µg/ml) followed by a significant decrease at higher oxLDL concentrations (50 µg/ml) (Fig 4.2A). Moreover, ox-LDL had no significant effect on TM release when used on static HAECs, but was seen to strongly potentiate cyclic strain-induced TM release at concentrations up to 50 µg/ml (Fig 4.2B).

With respect to glucose levels, TM mRNA expression was initially increased (statistically insignificant) after 15 mM glucose application followed by a return to baseline conditions after 30 mM in static HAECs (Fig 4.3A). Elevated glucose levels (15 - 30 mM) had no significant effect on TM protein expression in static endothelial cells (Fig 4.3B). Finally, elevated glucose (15 – 30 mM) was found to strongly reduce cyclic strain-induced TM release (Fig 4.3C). Table 4.1 summarises the results from this study.

4.2.2 Signalling components

Pharmacological inhibitors were chosen to selectively attenuate a range of different signalling components that were known to be strain-sensitive and putatively associated with strain-dependent changes in gene expression and cell function. Inhibitors towards a range of different signalling pathways were incubated with HAECs in the presence and absence of cyclic strain (7.5% equibiaxial, 60 cycles per min for 24 hrs). Post-treatment, cells were harvested for total cellular protein and cell culture media for TM analyses. The signalling components employed for the TM expression and release studies are listed below;

- i. GM6001, a broad-spectrum inhibitor of MMPs (e.g., MMP-1, 2, 3, 8, and 9) (25 µM for 24 hrs).

- ii. 3,4-dichloroisocoumarin (DCI), serine protease and rhomboid inhibitor (10 μ M for 24 hrs).
- iii. L-NAME, an eNOS inhibitor (1 mM for 24 hrs).
- iv. NSC23766, a Rac1 inhibitor (50 μ M for 24 hrs).
- v. Apocynin, a selective NADPH oxidase inhibitor (10 μ M for 24 hrs).
- vi. SOD, superoxide radical scavenger (100 U/ml for 24 hrs).
- vii. PI3K- α inhibitor (2 μ M for 24 hrs).
- viii. PD98059, Erk1/2 inhibitor (10 μ M for 24 hrs).
- ix. PD169316, p38 inhibitor (10 μ M for 24 hrs).
- x. Genistein, protein tyrosine kinase inhibitor (50 μ M for 24 hrs).
- xi. Cyclic RGD peptide, integrin inhibitor (130 μ M for 24 hrs).

4.2.2.1 Impact of signal pathway blockade on TM cellular expression

The TM BDCA-3 Duoset ELISA was routinely used to monitor TM protein levels in HAECs for these signalling studies. These results are outlined between Fig 4.4 and 4.6. Firstly, application of genistein or PD169316 to block protein tyrosine kinase or p38, respectively, significantly reversed the cyclic strain-mediated reduction in TM cellular expression (Fig 4.6A-B). Application of either NSC23766 (Fig 4.4B) or PI3K α (Fig 4.6D) did not exhibit a statistically significant effect on the strain-induced reduction in TM protein

levels. Lastly, experiments using either L-NAME (Fig 4.4A), apocynin (Fig 4.5A), SOD (Fig 4.5B) or PD98059 (Fig 4.6C) unfortunately lacked any clear statistical relevance (unknown reasons). The results are summarised in Table 4.2.

4.2.2.2 Impact of signal pathway blockade on TM release

This section investigated the impact that blockade of signalling components may have on cyclic strain-mediated TM release. These results are outlined between Fig 4.7 and 4.11. Firstly, application of GM6001 to inhibit MMPs moderately decreased (statistically significant) the cyclic strain-mediated increase in TM release (Fig 4.7A). Conversely, blockade of rhomboids with DCI had the opposite effect by moderately increasing the strain-induced TM release (Fig 4.7B). We also observed a strong decrease in cyclic strain-induced TM release following the addition of SOD to inhibit ROS (Fig 4.10B), although inhibition of NADPH oxidase using apocynin did not have an effect on the elevated TM release (Fig 4.10A). Interestingly, we observed a very significant increase in TM release under both static and strained conditions following the addition of cyclic RGD peptide (to inhibit $\alpha\beta3$ integrin), whilst PD169316 (for p38 inhibition) increased TM release under strain conditions (Fig 4.8 and 4.11B). Finally, the addition of either L-NAME (Fig 4.9A), NSC23766 (Fig 4.9B), genistein (Fig 4.11A), PD98059 (Fig 4.11C) or PI3K- α inhibitor (Fig 4.11D) had no statistically significant effect on the cyclic strain-induced increase of TM release from HAECs. Details of the signaling components tested are summarised in Table 4.2.

4.3 Tables and Figures

Inflammatory component	Conc. Used	TM mRNA expression	TM protein expression	TM release	
				- CS	+ CS
TNF- α	0-100 ng/ml	↓	↓	NE	↑ (100 ng/ml)
Ox-LDL	0-50 μ g/ml	↓	ND	NE	↑ (10-50 μ g/ml)
Glucose	5-30 mM	NE	NE	NE	↓ (15-30 mM)

Table 4.1: Inflammatory conditions tested in the absence or presence of cyclic strain. Details of the inflammatory components tested. The symbols used represent the following; ↑, significant increase; ↓, significant decrease; +/-CS, in the absence or presence of cyclic strain; ND, not determined; NE, no effect.

Target	Inhibitor	Conc.	Thrombomodulin	
			<i>Expression</i>	<i>Release</i>
MMPs	GM6001	10 μ M	ND	↓
Integrin α v β 3	Cyclic RGD integrin inhibitor	130 μ M	ND	↑
Rhomboids	DCI	10 μ M	ND	↑
eNOS	L-NAME	1mM	NE	NE
Rac1	NSC23766	50 μ M	NE	NE
NADPH oxidase	Apocynin	10 μ M	NE	NE
ROS	SOD	100 U/ml	NE	↓
Erk 1/2	PD98059	10 μ M	NE	NE
p38	PD169316	10 μ M	↑	↑
PI3K	PI3K- α In.	2 μ M	NE	NE
Protein Tyr Kinase	Genistein	2 μ M	↑	NE

Table 4.2: Signalling components tested in the absence or presence of cyclic strain for effect on strain-induced changes in TM expression and release. The symbols used represent the following; ↑, significant increase; ↓, significant decrease; ND, not determined; NE, no effect.

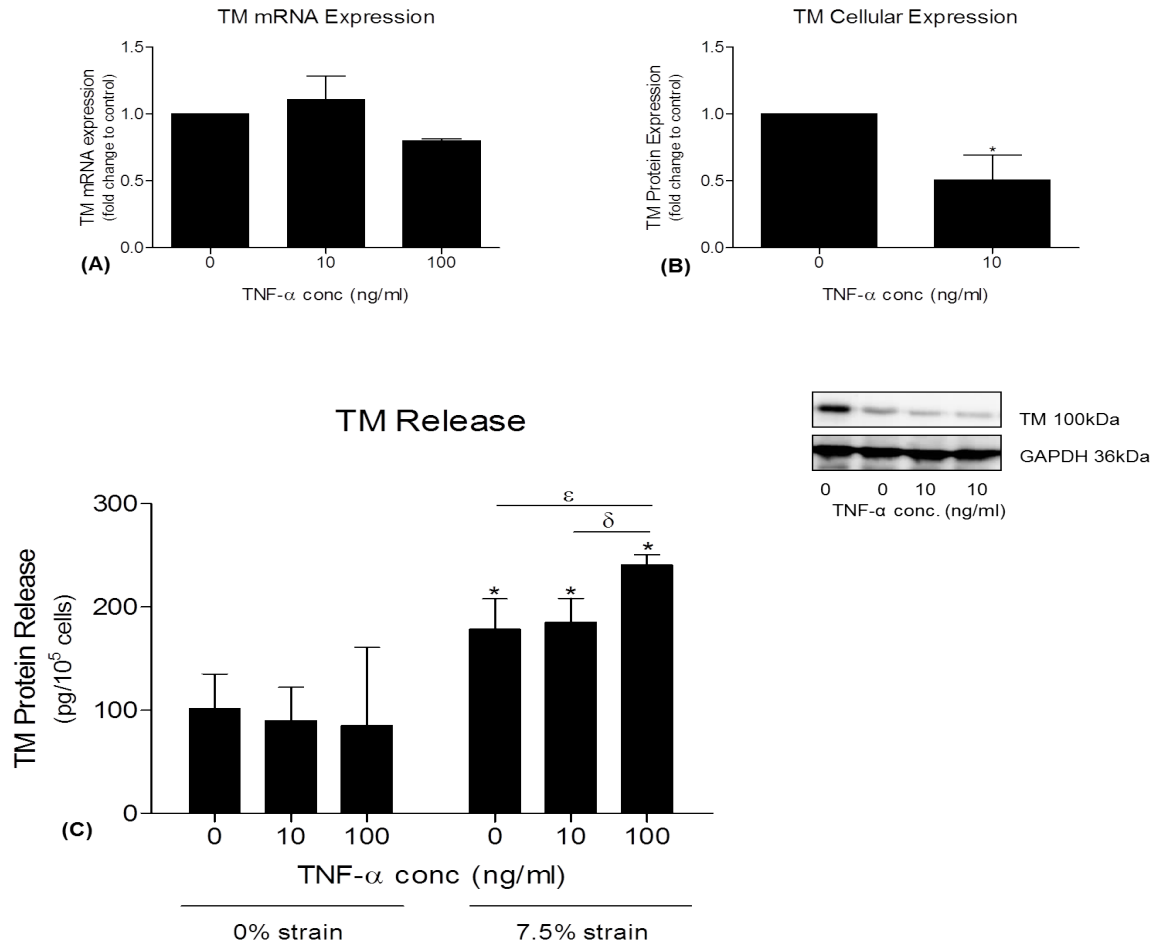


Figure 4.1: Effect of TNF- α on TM expression and release. Static HAECs were initially exposed to TNF- α (0 – 100 ng/ml for 24 hrs) and monitored for TM expression and release. **(A)** TNF- α -dependent reduction in TM mRNA levels (n=3). Histogram represents fold change in relative levels of TM mRNA normalized to untreated control (S18 primers). **(B)** TNF- α -dependent reduction in TM protein levels. Histogram represents fold change in relative levels of TM protein normalized to untreated control (GAPDH) (* $P \leq 0.05$ versus 0 ng/ml determined using 1-way ANOVA and post-hoc Dunnett's test). Blots are representative of 3 replicates. **(C)** TM release following TNF- α treatment in the absence and presence of cyclic strain (* $P \leq 0.05$ versus unstrained 0 ng/ml; $\delta P \leq 0.05$; $\epsilon P \leq 0.05$ determined using 1-way ANOVA and post-hoc Dunnett's test, n=6).

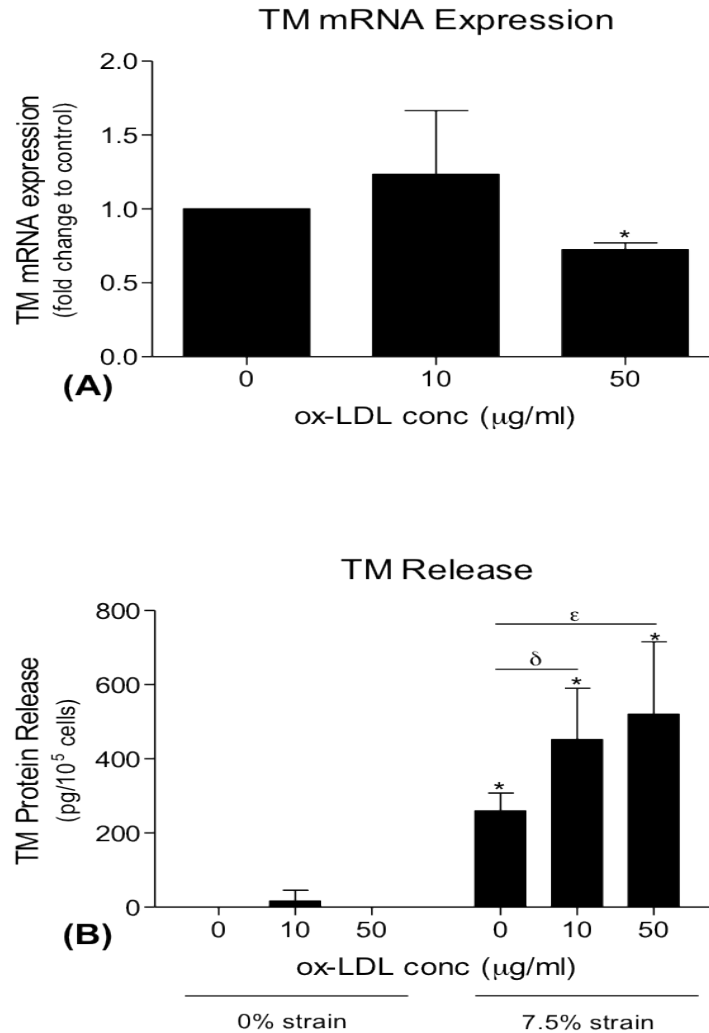


Figure 4.2: Effect of ox-LDL on TM expression and release. Static HAECs were initially exposed to ox-LDL (0 – 50 µg/ml for 24 hrs) and monitored for TM expression and release. **(A)** ox-LDL-dependent reduction in TM mRNA levels. Histogram represents fold change in relative levels of TM mRNA normalized to untreated controls (S18 primers) ($*P \leq 0.05$ versus 0 µg/ml determined using 1-way ANOVA and post-hoc Dunnett’s test, $n=3$). **(B)** TM release following ox-LDL treatment in the absence and presence of cyclic strain ($*P \leq 0.05$ versus unstrained 0 µg/ml; $\delta P \leq 0.05$; $\epsilon P \leq 0.05$ determined using 1-way ANOVA and post-hoc Dunnett’s test, $n=3$).

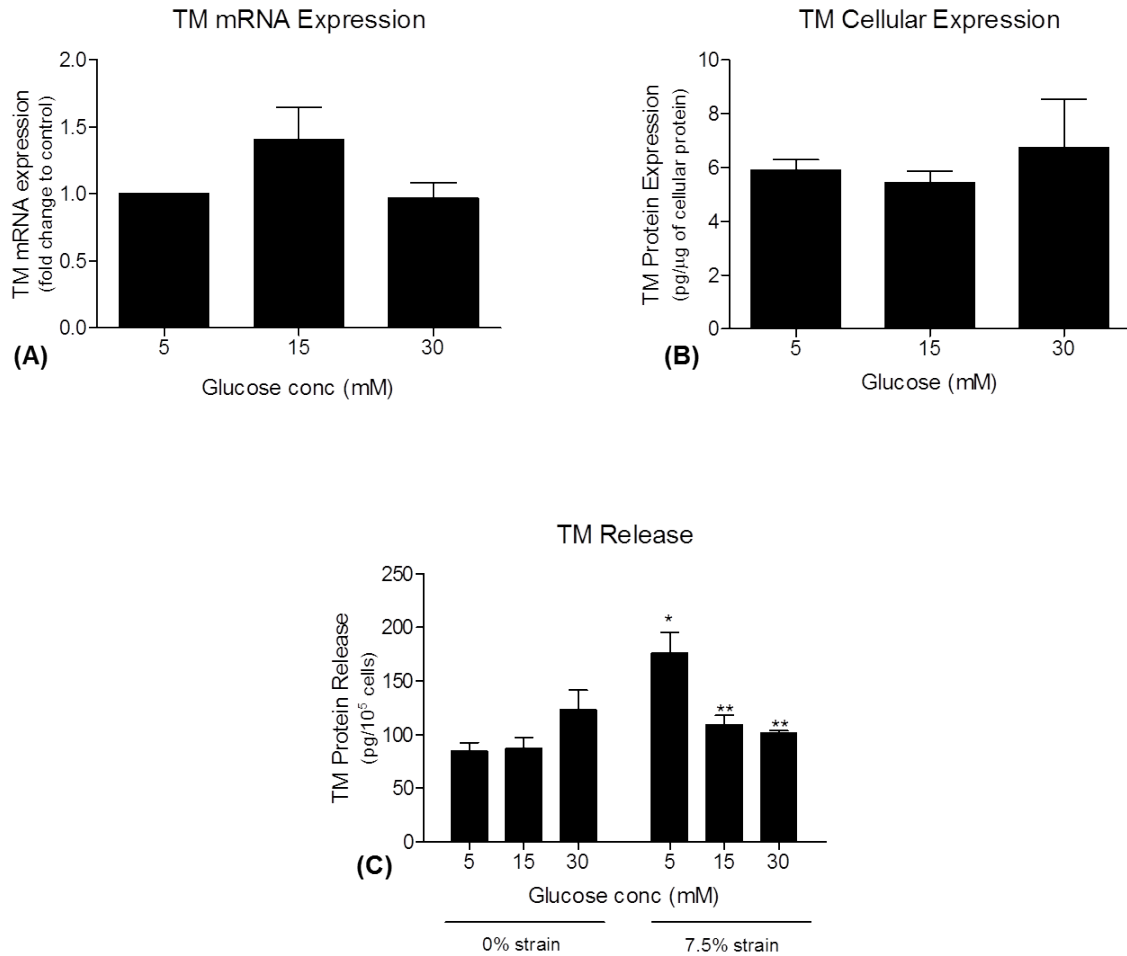


Figure 4.3: Effect of glucose on TM expression and release. Static HAECs were initially exposed to glucose (5 – 30 mM for 24 hrs) and monitored for TM expression and release. **(A)** Glucose-dependent regulation in TM mRNA levels. Histogram represents fold change in relative levels of TM mRNA normalized to untreated control (S18 primers) (n=3). **(B)** Glucose-dependent regulation of TM protein levels (n=3). **(C)** TM release following glucose treatment in the absence and presence of cyclic strain (* $P \leq 0.05$, ** $P \leq 0.01$ versus unstrained 5 mM determined using 1-way ANOVA and post-hoc Dunnett’s test, n=6).

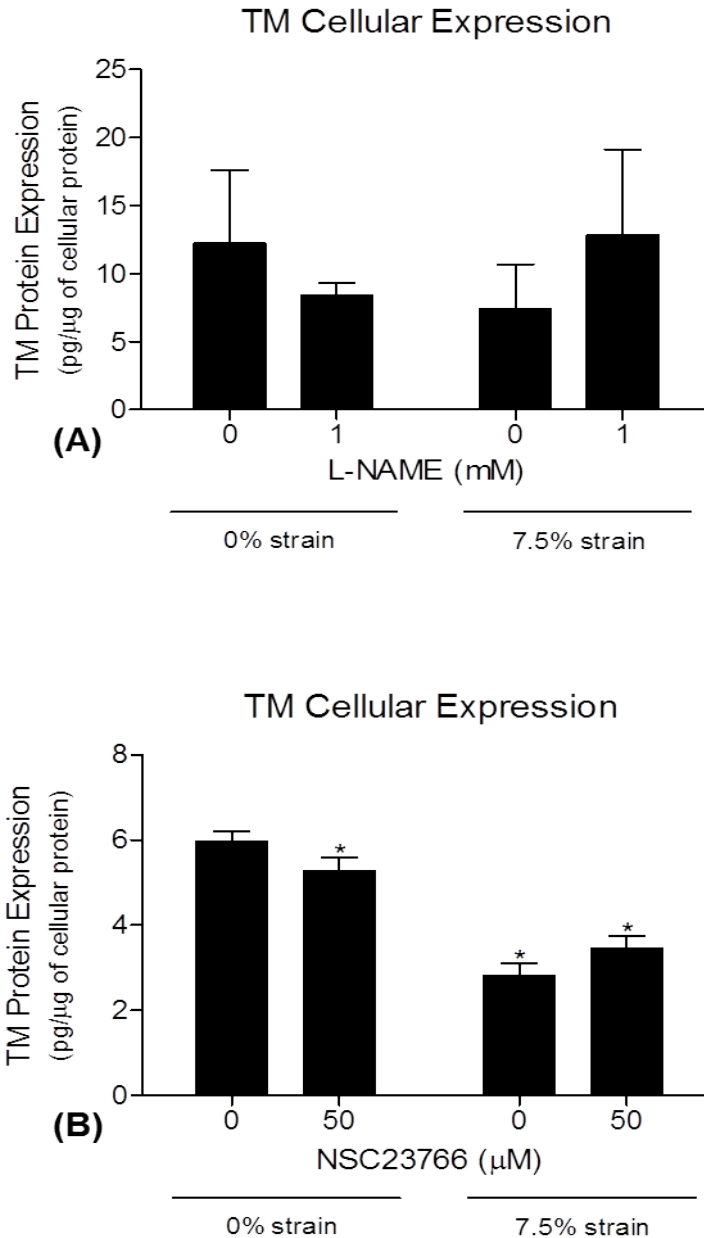


Figure 4.4: Effect of L-NAME and NSC23766 on cyclic strain-dependent TM protein expression. HAECs were pre-incubated with the relevant inhibitor for 30 mins before undergoing 7.5% cyclic strain for 24 hrs. **(A)** Effect of 1 mM L-NAME (n=12). **(B)** Effect of 50 μM NSC23766 (* $P \leq 0.05$ versus unstrained 0 μM determined using 1-way ANOVA and post-hoc Dunnett's test, n=9).

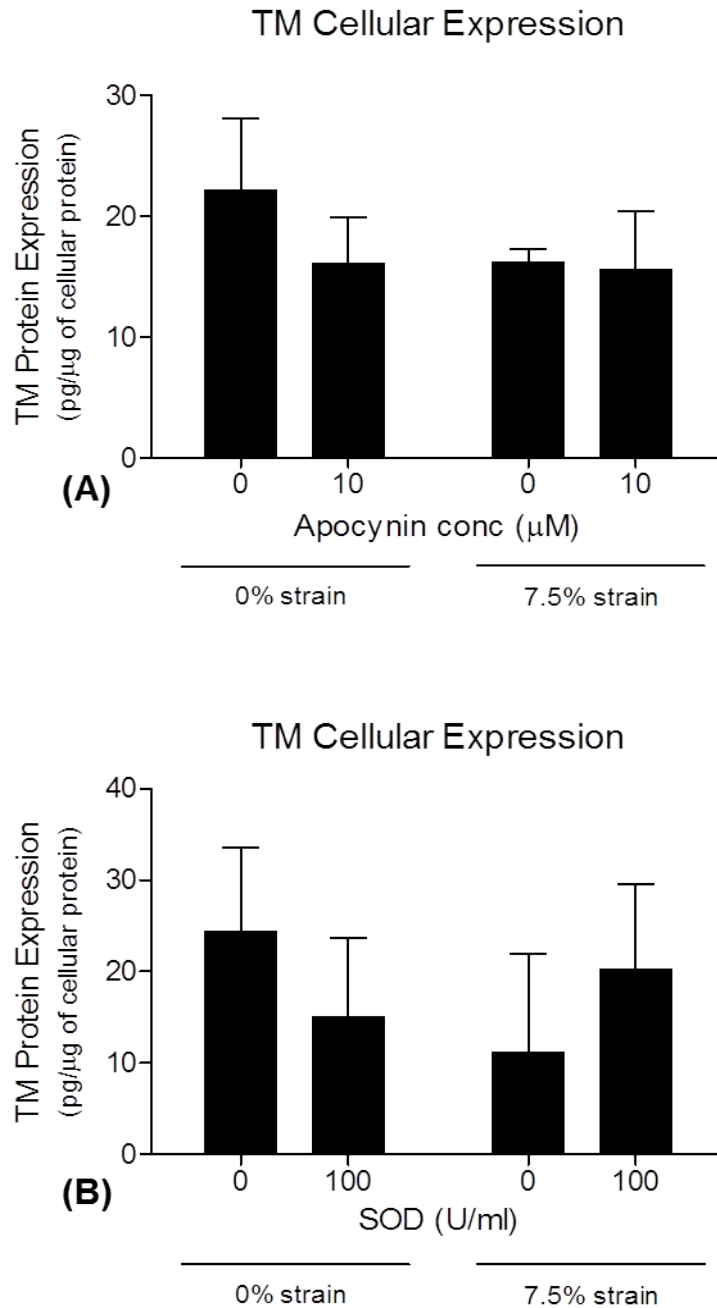


Figure 4.5: Effect of apocynin and SOD on cyclic strain-dependent TM protein expression. HAECs were pre-incubated with the relevant inhibitor for 30 mins before undergoing 7.5% cyclic strain for 24 hrs. **(A)** Effect of 10 μM apocynin (n=3). **(B)** Effect of 100 U/ml SOD (n=9).

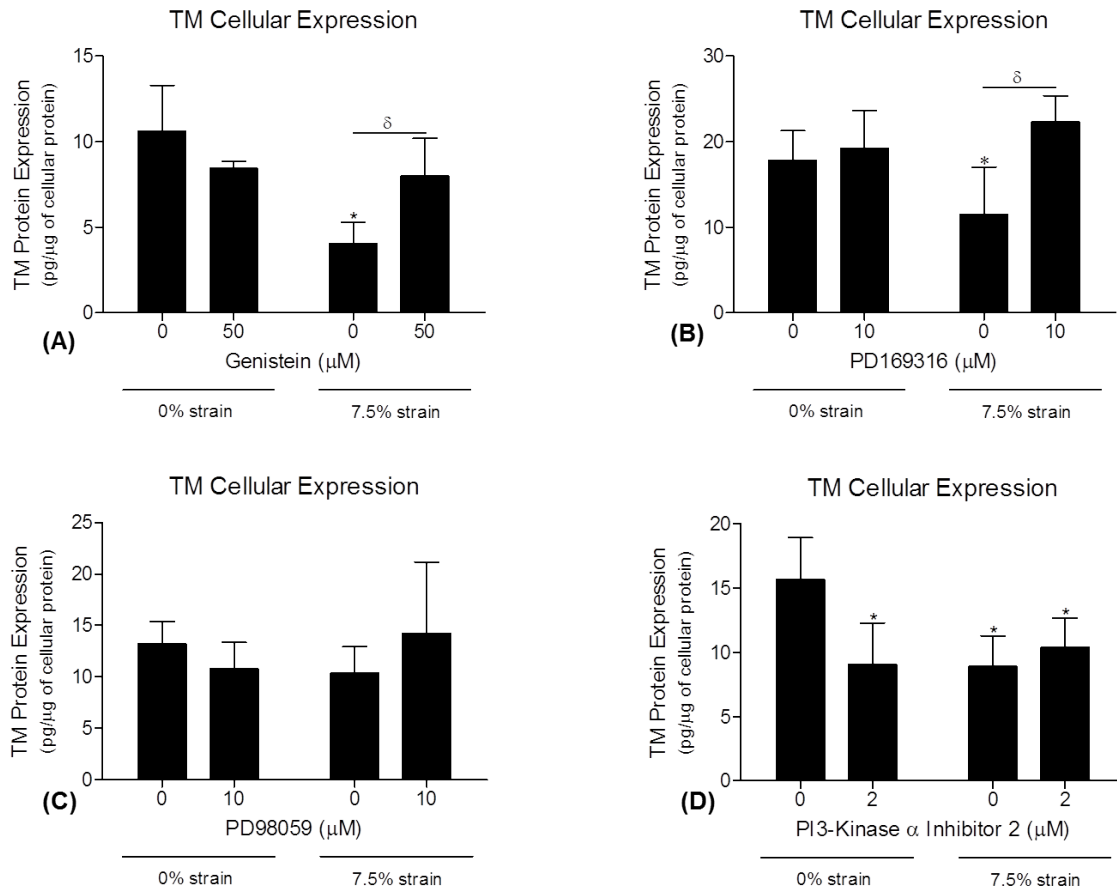


Figure 4.6: Effect of Genistein, PD169316, PD98059 and PI3K α inhibitor on cyclic strain-dependent TM protein expression. HAECs were pre-incubated with the relevant inhibitor for 30 mins before undergoing 7.5% cyclic strain for 24 hrs. **(A)** Effect of 50 μ M Genistein ($*P \leq 0.05$ versus unstrained 0 μ M, $\delta P \leq 0.05$ determined using 1-way ANOVA and post-hoc Dunnett's test, $n=3$). **(B)** Effect of 10 μ M PD169316 ($*P \leq 0.05$ versus unstrained 0 μ M, $\delta P \leq 0.05$ determined using 1-way ANOVA and post-hoc Dunnett's test, $n=6$). **(C)** Effect of 10 μ M PD98059 ($n=9$). **(D)** Effect of 2 μ M PI3K α inhibitor ($*P \leq 0.05$ versus unstrained 0 μ M determined using 1-way ANOVA and post-hoc Dunnett's test, $n=9$).

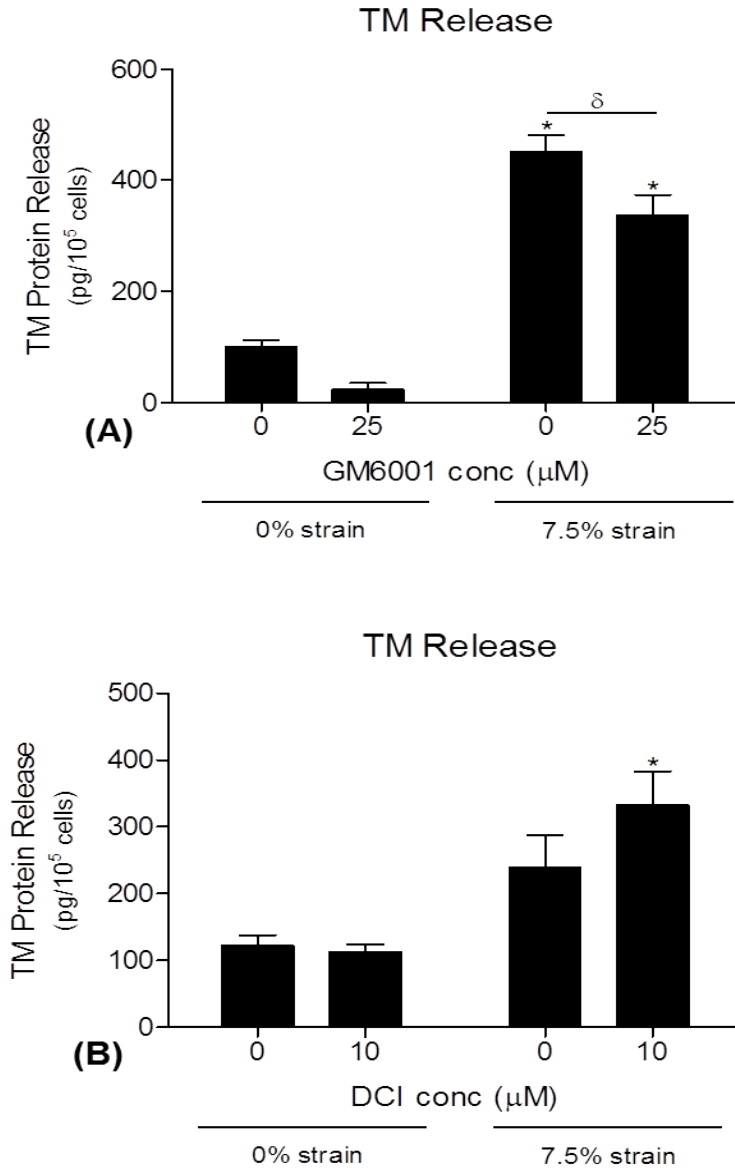


Figure 4.7: Effect of GM6001 and DCI on cyclic strain-induced TM release. HAECs were pre-incubated with the relevant inhibitor for 30 mins before undergoing 7.5% cyclic strain treatment for 24 hrs. **(A)** Effect of 25 μM GM6001 ($*P \leq 0.05$ versus unstrained 0 μM, $\delta P \leq 0.05$ determined using 1-way ANOVA and post-hoc Dunnett's test, n=6). **(B)** Effect of 10 μM DCI ($*P \leq 0.05$ versus unstrained 0 μM determined using 1-way ANOVA and post-hoc Dunnett's test, n=3).

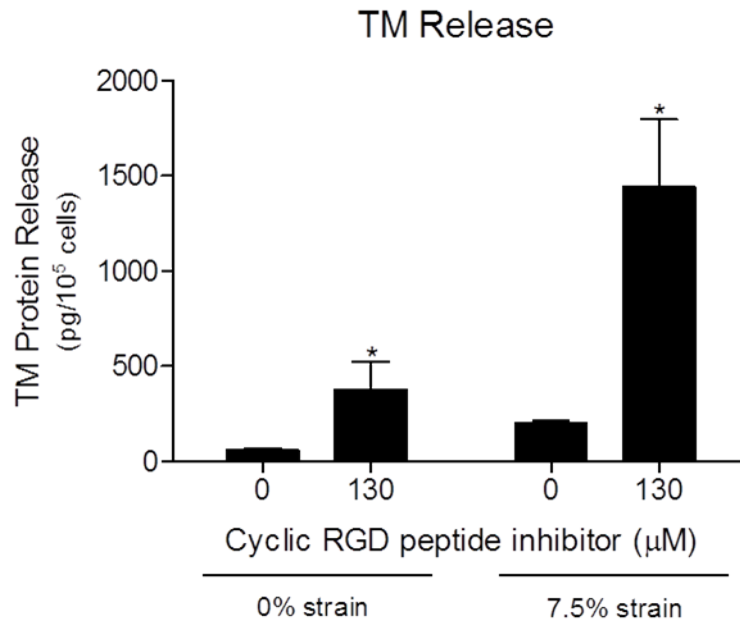


Figure 4.8: Effect of cyclic RGD peptide inhibitor on cyclic strain-induced TM release. HAECs were pre-incubated with the inhibitor for 30 mins before undergoing 7.5% cyclic strain treatment for 24 hrs. Effect of 130 μM cyclic RGD peptide inhibitor (* $P \leq 0.05$ versus unstrained 0 μM determined using 1-way ANOVA and post-hoc Dunnett's test, $n=3$).

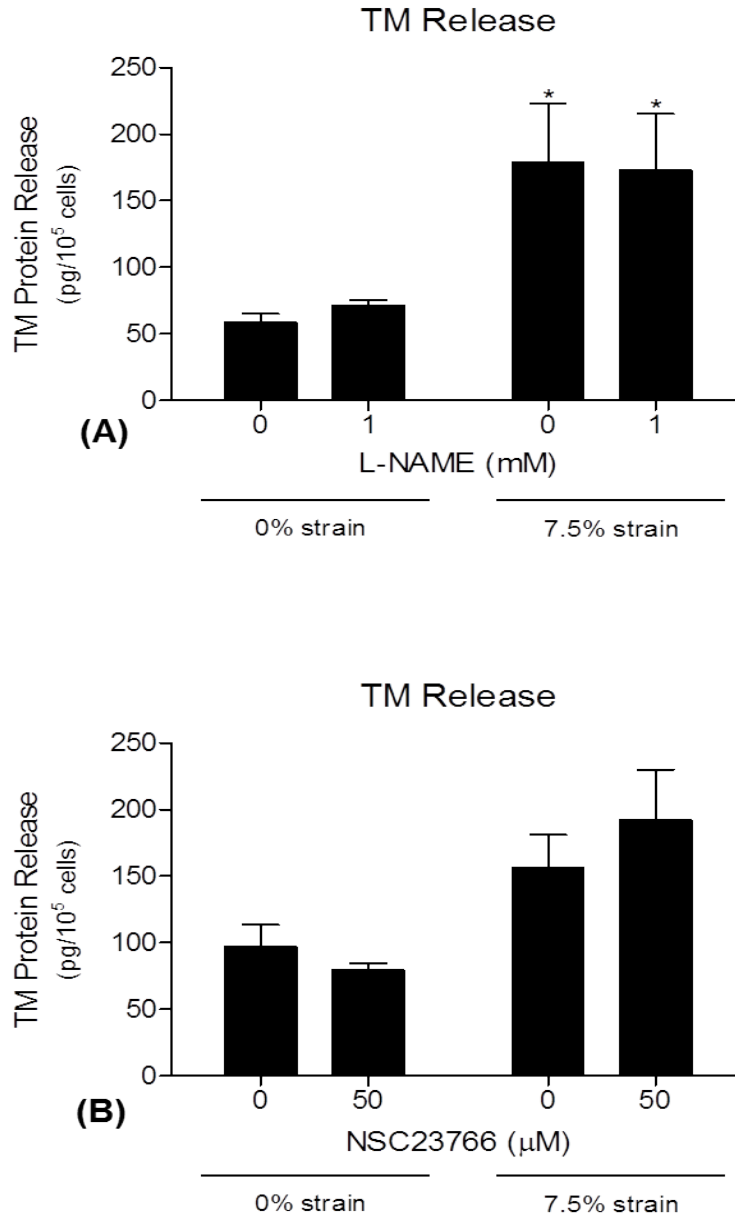


Figure 4.9: Effect of L-NAME and NSC23766 on cyclic strain-induced TM release. HAECs were pre-incubated with the relevant inhibitor for 30 mins before undergoing 7.5% cyclic strain treatment for 24 hrs. **(A)** Effect of 1 mM L-NAME ($*P \leq 0.05$ versus unstrained 0 mM determined using 1-way ANOVA and post-hoc Dunnett's test, $n=6$). **(B)** Effect of 50 μM NSC23766 ($n=3$).

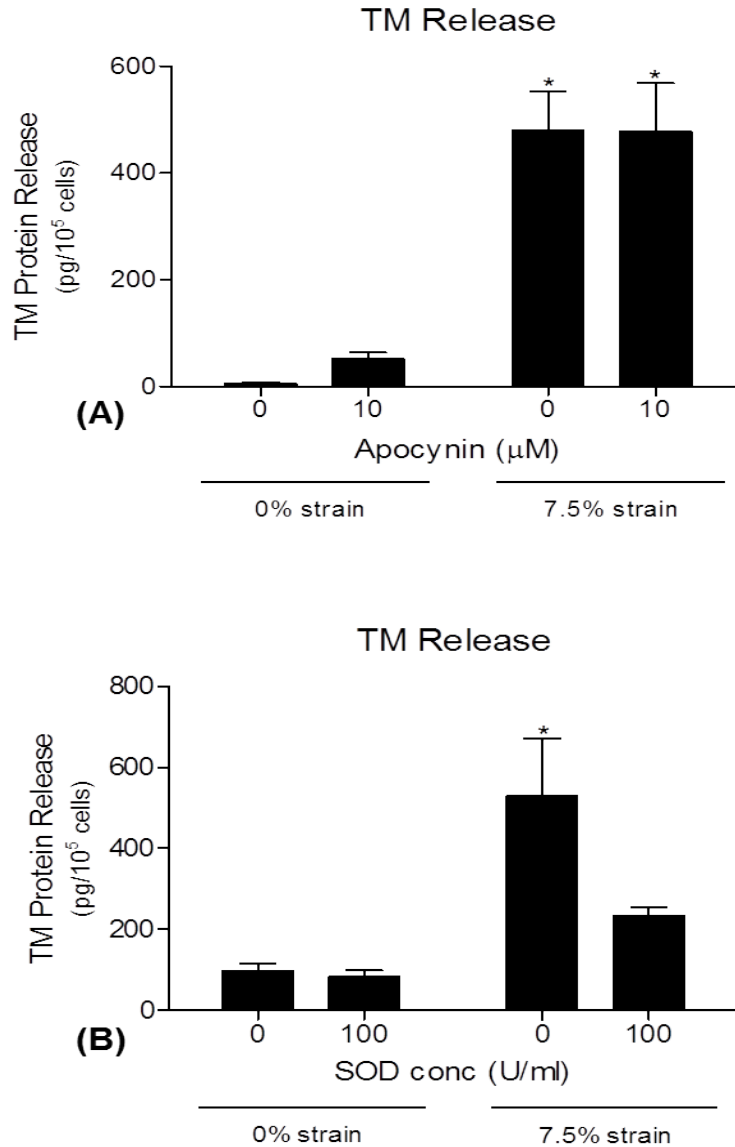


Figure 4.10: Effect of apocynin and SOD on cyclic strain-induced TM release. HAECs were pre-incubated with the relevant inhibitor for 30 mins before undergoing 7.5% cyclic strain treatment for 24 hrs. **(A)** Effect of 10 μM apocynin (* $P \leq 0.05$ versus unstrained 0 μM determined using 1-way ANOVA and post-hoc Dunnett's test, $n=6$). **(B)** Effect of 100 U/ml SOD (* $P \leq 0.05$ versus unstrained 0 U/ml determined using 1-way ANOVA and post-hoc Dunnett's test, $n=3$).

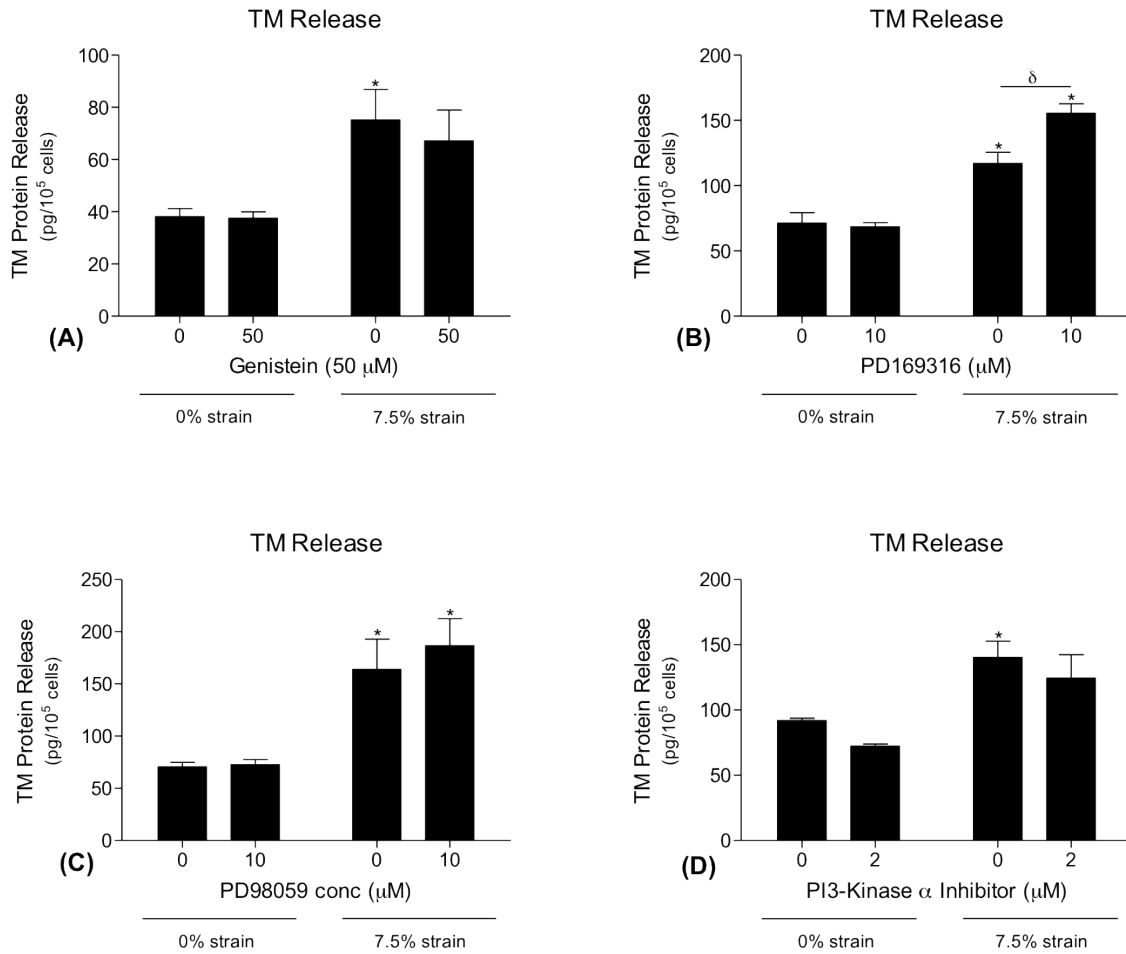


Figure 4.11: Effect of Genistein, PD169316, PD98059 and PI3K α inhibitor on cyclic strain-induced TM release. HAECs were pre-incubated with the relevant inhibitor for 30 mins before undergoing 7.5% cyclic strain treatment for 24 hrs. **(A)** Effect of 50 μ M Genistein ($*P \leq 0.05$ versus unstrained 0 μ M determined using 1-way ANOVA and post-hoc Dunnett's test, $n=3$). **(B)** Effect of 10 μ M PD169316 ($*P \leq 0.05$ versus unstrained 0 μ M, $\delta P \leq 0.05$ determined using 1-way ANOVA and post-hoc Dunnett's test, $n=3$). **(C)** Effect of 10 μ M PD98059 ($*P \leq 0.05$ versus unstrained 0 μ M determined using 1-way ANOVA and post-hoc Dunnett's test, $n=6$). **(D)** Effect of 2 μ M PI3K α inhibitor ($*P \leq 0.05$ versus unstrained 0 μ M determined using 1-way ANOVA and post-hoc Dunnett's test, $n=3$).

4.4 Discussion

The results from this chapter give a more detailed insight into the molecular signalling mechanisms putatively regulating the cyclic strain-induced change in TM expression and release from HAECs. Section 4.2.1 describes the impact of different inflammatory mediators under static and strain conditions. Atherogenic conditions typically involve “multiple” vascular parameters such as abnormal strain and shear levels, high oxLDL, high glucose, and increased levels of pro-inflammatory cytokines. We therefore decided to investigate these stimuli both in isolation and in combination with elevated strain to identify possible synergistic effects on the expression and release of TM from HAECs.

Firstly, we looked at the effect that TNF- α , a pro-inflammatory cytokine, would have on TM expression in HAECs. We were not surprised to observe a TNF- α -mediated reduction of TM protein and mRNA expression in static HAECs. This is in agreement with the literature (Bergh et al., 2009; Grey et al., 1998) as TNF- α has previously been shown to down-regulate TM expression/release in monocytes (Lin et al., 2011) via suppression of TM transcription and TM protein internalization with subsequent degradation. Subsequently, we investigated the effect TNF- α would have on TM release in HAECs in the presence and absence of cyclic strain. Interestingly, TNF- α had no significant effect on TM release in static HAECs (i.e., unstrained) but an “additive” effect at high concentrations (100 ng/ml) in the presence of 7.5% cyclic strain. There is nothing reported in the literature about the combined effect of cyclic strain and TNF- α on TM release, making this a relatively novel observation. It has been shown that TNF- α stimulation of endothelial/neutrophil co-cultures causes TM release from static endothelial cells, possibly explaining the TNF- α induced increase in serum TM levels

observed in diseases associated with elevated inflammatory signalling (Boehme et al., 1996). The same group observed that incubation of endothelial cell monocultures with TNF- α (i.e., without neutrophils) had no effect on TM release, which also agrees with our observations. These two observations of reduced TM expression and increased TM release following incubation with high concentrations of TNF- α are typical of an inflammatory stimulus.

The second inflammatory mediator we looked at in this context was ox-LDL. We first observed the effect ox-LDL had on TM mRNA expression in HAECs. We found that ox-LDL reduced TM mRNA expression in static HAECs at 50 μ g/ml. This result was consistent with the literature as ox-LDL has previously been shown to down-regulate TM mRNA expression in HUVECs (Ishii et al., 1996). This group suggested that the decrease in mRNA expression was caused by an inhibition of TM transcription, likely explaining our result. Next, we looked at the effect ox-LDL had on TM release in the presence and absence of cyclic strain in HAECs. We observed that ox-LDL had little or no effect on TM release at 10 μ g/ml in static HAECs but clearly potentiated TM release dose-dependently in the presence of 7.5% cyclic strain. Again, to our knowledge there are no reports investigating the effect that oxLDL has on TM release either in static or strained cells. Interestingly, ox-LDL produces free radicals which are cytotoxic to endothelial cells (Cominacini et al., 2000) and may stimulate TM release. This possibility and others (e.g., ox-LDL interaction with endothelial plasma membrane dynamics and vesicular production under strain) remains to be investigated as possible mechanisms. Based on these observations, we can conclude that atherogenic mediators such as TNF- α and ox-LDL may potentiate endothelial dysfunction stemming from elevated cyclic strain, leading to reduced production of TM and enhanced release by either cleavage or shedding into the circulation.

Next, we observed the effect that glucose, present at high levels in hyperglycemia and diabetes mellitus, would have on TM regulatory dynamics in HAECs. Firstly, we looked at the effect glucose would have on TM mRNA expression in static HAECs. We observed a slight (but insignificant) increase of TM mRNA expression at 15 mM glucose that returns to baseline levels at 30 mM. This is in contrast with an earlier study that reported an up-regulation of TM mRNA expression in static HAECs following incubation with 30 mM glucose for 4-6 hours (Wang et al., 2012). The difference in results may be due to different incubation times (i.e., 6 hours versus 24 hours) and perhaps glucose has an acute short-term effect on the cells but returns to homeostatic status following 24 hours. We next investigated the effect glucose would have on TM protein expression (as monitored by ELISA). We noted a small but non-significant increase in TM cellular expression after incubation with 30 mM glucose in static HAECs. These observations somewhat agree with the previous study (Wang et al., 2012) which reported a 9% increase in TM protein expression in static HAECs following 30 mM glucose application for 4 – 6 hours. We subsequently investigated the effect glucose had on TM release in HAECs in the presence and absence of cyclic strain. We observed a small, but non-significant increase in TM release at 30 mM glucose in static HAECs. Intriguingly, TM release was significantly reduced at 15 and 30 mM glucose in the presence of 7.5% cyclic strain. There is an absence of *in vitro* studies documenting this response but there is some clinical data available. Increased soluble TM antigen levels were reported in the serum and urine of streptozotocin-induced diabetes model rats (Nakano et al., 2000). High levels of TM have also been reported in the serum of diabetic patients (Aso et al., 2000), likely reflecting an impairment of renal clearance of TM from the blood. Our own results in static cells indicate that elevated glucose (30 mM) can significantly enhance TM

release, consistent with these *in vivo* observations. Elevated soluble TM levels are associated with hypercoagulability and enhanced fibrinolysis in patients with type 2 diabetes (Aso et al., 2000), although cardioprotective effects cannot be ruled out. In this regard, the reduction of TM release observed following a combination of elevated glucose with strain in our studies may reflect a reduction in cardioprotection in diabetes with combined hypertension (a feature of advanced metabolic syndrome and diabetes).

In conclusion, our data to this point suggests that atherogenic conditions may involve multiple inflammatory mediators in combination to impact endothelial homeostasis and TM levels. We observed that TNF- α reduced TM expression in static HAECs but additively potentiated TM release in HAECs undergoing 7.5% cyclic strain. Similar to TNF- α , ox-LDL decreased TM mRNA expression in static HAECs whilst significantly increasing TM release in HAECs following 7.5% strain. We also found that glucose had no effect on TM expression in static HAECs and attenuated release in HAECs undergoing 7.5% cyclic strain. This area warrants further investigation possibly by combining these three different humoral conditions with elevated cyclic strain to help better replicate the actual *in vivo* situation.

The following section (4.2.2) describes how selective blockade of key signalling components may affect the cyclic strain-dependent change in TM expression and/or release. In the first portion of this section (4.2.2.1), we investigate the effect of inhibiting these signalling components on the cyclic strain-mediated reduction in TM cellular expression. Specifically, we found that the addition of either genistein or PD169316 to block Protein Tyrosine Kinase (PTK) and p38, respectively, significantly reversed the cyclic strain-mediated reduction in TM cellular expression (Fig 4.12). Other inhibitors tested either showed no effect (NSC23766) or indeed data were generally insignificant. This may be because the

pharmacological inhibitors employed had off target effects, elicited some level of cytotoxicity or interfered with the mechanism of the ELISA.

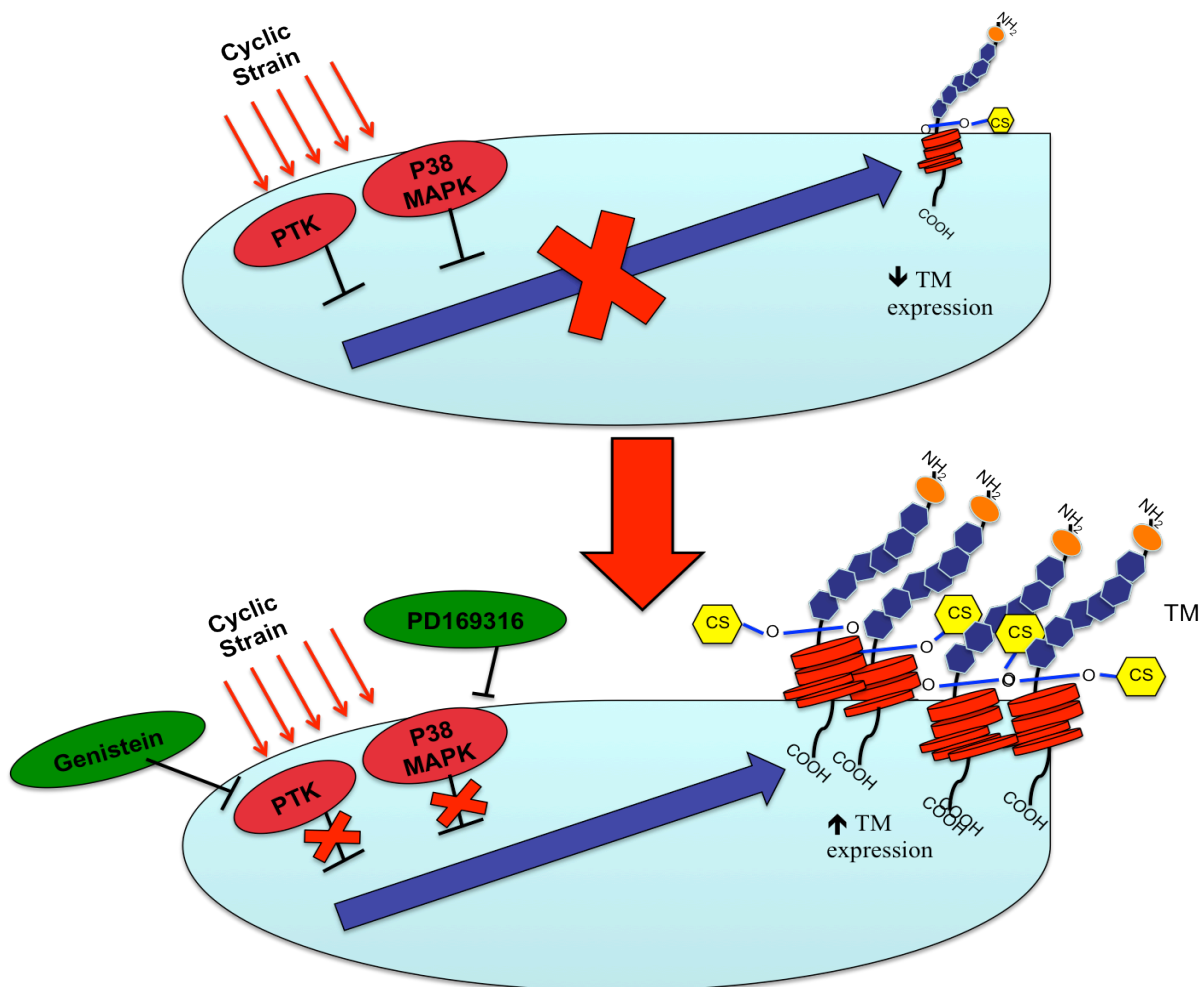


Figure 4.12: Signalling components affecting the cyclic strain-mediated TM cellular expression pathway. Cyclic strain activates PTK and p38 MAPK to dampen TM cellular expression (top diagram). Inhibition of PTK or p38 MAPK significantly reverses the cyclic strain-reduction in TM protein expression (lower diagram). Key: COOH, carboxylic acid; CS, chondroitin sulphate; MAPK, mitogen-activated protein kinase; NH₂, amine group; O, oxygen; PTK, protein tyrosine kinase; TM, thrombomodulin.

As mentioned above, the addition of genistein, a PTK inhibitor, significantly reversed the typical cyclic strain-mediated reduction in TM protein expression in HAECs. This is consistent with earlier work reporting the strain sensitivity of PTK (Cheng et al., 2002). The addition of genistein has previously been shown to reduce the strain-dependent induction of MMP-2 cellular expression in BAECs (Von Offenber Sweeney et al., 2004), indicating a role for PKT in the mechanotransduction of strain (Fig 4.12). Similarly, cyclic strain has previously been shown to stimulate monocyte chemotactic protein-1 (MCP-1) mRNA expression in smooth muscle cells through tyrosine kinase activation (Jiang et al., 1999). Due to the crucial involvement of PTK in many signal transduction cascades, it was therefore not unexpected that it had a significant effect in our TM model.

Additionally, we explored MAPK p38 by utilising PD169316 in our strain model. We determined that the addition of PD169316 significantly reversed the usual cyclic strain-dependent decrease in TM cellular expression in HAECs (Fig 4.12). p38 is known to be activated by stress stimuli and in response to various cytokines, thus mediating cellular activities including apoptosis and inflammation (Noel et al., 2008). Moreover, p38 is known to be sensitive to cyclic strain in BAECs (Von Offenber Sweeney et al., 2004) and smooth muscle cells (Li et al., 2000). In addition, p38 is involved in mediating the strain-induced expression of endothelin-1 in BAECs (Cheng et al., 2001). To our knowledge, this is the first instance in which the strain-dependent modulation of TM expression has been linked to PTK and p38 MAPK activation (note: whether these components are working in a linear fashion or via separate pathways remains to be determined however).

Also worth mentioning is the effect of NSC23766, a Rac1 inhibitor. In the presence of strain, NSC23766 failed to reverse the strain-dependent down-regulation in TM protein levels

in HAECs, suggesting lack of involvement of Rac1 in these events. Previously, pravastatin was shown to up-regulate TM expression in TNF- α treated HAECs by inhibiting the activation of Rac1/Cdc42 and NF κ B (Lin et al., 2007). This is significant as TNF- α normally has a down-regulatory effect on TM expression. Additionally, elevated strain was shown to stimulate IL-6 expression via a Rac1 signalling pathway in smooth muscle cells (Zampetaki et al., 2005). Given the pivotal role of Rac1 in the regulation of the cellular cytoskeleton in response to various stimuli (including strain), its lack of involvement in the mechanoregulation of TM expression was surprising.

In the second part of this section (4.2.2.2), we examined the outcome of blocking specific signalling components (as described above) on cyclic strain-induced TM release from HAECs. We observed a significant decrease in cyclic strain-induced TM release following the addition of GM6001 and SOD to specifically inhibit MMPs and to scavenge ROS, respectively (Fig 4.13). In addition, we noted a slight increase in cyclic strain-mediated TM release following addition of DCI and PD169316, and a very significant increase in both static and strain-mediated TM release with cyclic RGD peptide inhibitor. Results with other inhibitors were non-significant or had no effect. Additionally, it is important to note that we observed a lot of variation in the fold decrease in TM expression or increase in TM release in response to 7.5% cyclic strain. We have addressed this issue in the Appendix in Figure B.

Numerous publications have focused on the proteolytic cleavage of endothelial TM to yield a soluble released TM variant (sTM). sTM has been detected in many biological fluids including serum (Oida et al., 1990), urine (Jackson et al., 1994) and synovial fluid (Conway and Nowakowski, 1993). This proteolytic cleavage has been attributed to a number of causative elements including leukocyte-derived lysosomal proteases (Abe et al., 1994),

neutrophil-derived enzymes (Matsuyama et al., 2008), MMPs (Wu et al., 2008), cysteine proteases (Inomata et al., 2009) and serine proteases (Lohi et al., 2004). In this respect, we initially concentrated on the role MMPs and rhomboids play in relation to cyclic strain-mediated TM release. In this regard, GM6001 was incorporated into our strain experiments in order to inhibit a broad range of MMPs. MMPs were investigated based on their sensitivity to cyclic strain (Cummins et al., 2007; Hasaneen et al., 2005), and on an earlier report indicating that LPA-induced TM lectin-like domain shedding is MMP-dependent in HUVECs (Wu et al., 2008). Lysophosphatidic acid (LPA) is a bioactive lipid mediator present in biological fluids during endothelial damage or injury that can trigger MMP-dependent TM shedding. This may contribute to the exposure of its EGF-like domain for EGF receptor (EGFR) binding, thus inducing subsequent cell proliferation and possibly mediating LPA-induced EGFR transactivation. Interestingly, the lectin-like domain has anti-inflammatory properties by inhibiting NF- κ B activation and mitogen-activated protein kinase (MAPK) pathways. DCI was also included in our strain model to investigate rhomboids. It has been reported that a rhomboid-like serine protease, RHBDL2, specifically cleaves TM at the transmembrane domain for the release of soluble TM (Cheng et al., 2011). Conversely, another group observed the same affect but stated that this was not mutually exclusive as most thrombomodulin transmembrane domains (TMDs) are not rhomboid substrates (Lohi et al., 2004). We observed that the blockade of MMPs with GM6001 appeared to cause a slight decrease in the cyclic strain-induced TM release (Fig 4.13). By contrast, inhibition of rhomboids with DCI resulted in a slight increase in the cyclic strain mediated TM release. Based on these observations, we concluded that a small proportion of TM release is caused by proteolytic cleavage via MMPs (~10% following correction for baseline effects), whilst

rhomboids may be putatively involved in “slowing down” TM release (i.e., inhibition with DCI is enhancing release). However, the remainder of released sTM following strain may possibly be attributed to a different release mechanism (i.e., vesicular), which will be discussed further on.

Cyclic strain induces oxidative stress, which produces reactive oxygen species (ROS) in endothelial cells (Howard et al., 1997; Matsushita et al., 2001). This subsequently regulates gene expression, migration, proliferation, release and apoptosis (Cheng et al., 1996; Cheng et al., 2001; Hannafin et al., 2006; Kou et al., 2009; Lin et al., 2010). NADPH oxidase, a ROS producer, is implicated in atherosclerosis and vascular remodelling (Matsushita et al., 2001). NADPH oxidase was not shown in our studies to mediate cyclic strain-induced TM release (i.e., using apocynin), even though NADPH oxidase – derived ROS have previously been linked to strain-mediated MMP-2 upregulation in vascular smooth muscle cells (Grote et al., 2003) and other endothelial pathways. SOD was therefore included into our strain experiments to scavenge strain-induced superoxide (ROS) production from other cellular sources. We reported a significant decrease in cyclic strain-induced TM release with SOD (Fig 4.13), contrasting sharply with the lack of effect of apocynin. It is apparent therefore that ROS has a role in cyclic strain-induced TM release but from an NADPH oxidase-independent source. This would indicate the involvement of a strain-inducible ROS-source other than NADPH oxidase (e.g., xanthine oxidase). As mentioned already, elevated cyclic strain leads to the production of ROS (Howards et al., 1997), which is associated with hypertension (Chae et al., 2001; Goch et al., 2009). ROS have the ability to target and modify MAPK proteins and PTKs (Paravicini and Touyz, 2006), both of which we have already shown to affect cyclic strain-mediated TM cellular expression. Additionally, ROS may be working in tandem with

MMPs to stimulate proteolytic release of TM due to their ability to promote MMP-2 release in vascular smooth muscle cells (Grote et al., 2003). This question requires further answers however before the mechanism can be fully described.

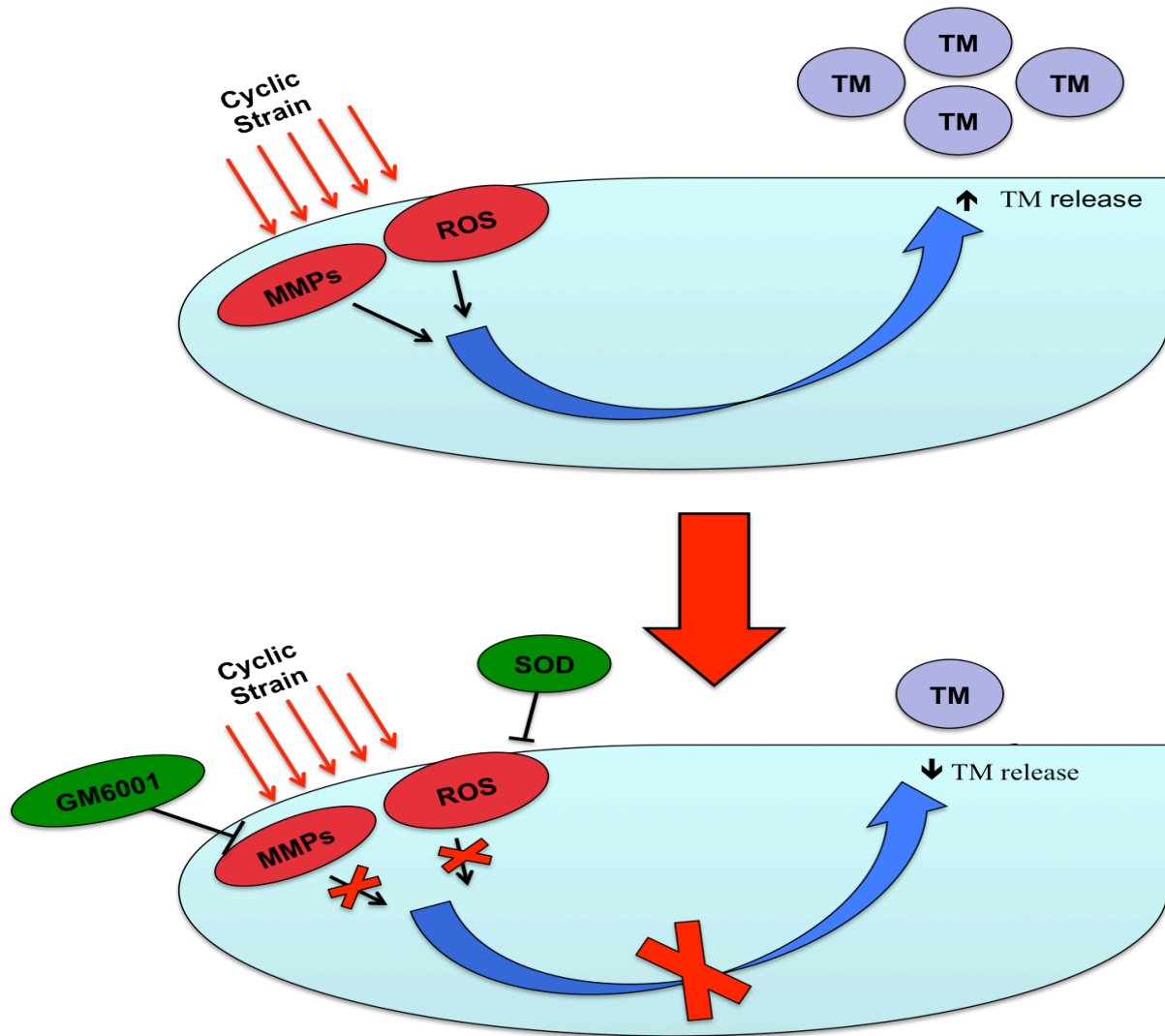


Figure 4.13: Signalling components affecting the cyclic strain-mediated TM release pathway. Cyclic strain activates MMPs and ROS to induce in-part TM release (top diagram). Inhibition of MMPs or ROS significantly reversed the cyclic strain-increase in TM release (lower diagram). Key: MMP, matrix metalloproteinase; TM, thrombomodulin; ROS, reactive oxygen species.

We next looked at integrins, transmembrane receptors known to be cyclic strain-sensitive mechanotransducers (Wilson et al., 1995; Yano et al., 1997). They mediate crucial endothelial cell functions such as migration and tube formation in response to hemodynamic forces (Thodeti et al., 2009; Von Offenberg Sweeney et al., 2005). To our knowledge, there is a complete absence of *in vitro* data documenting a role for integrins in regulating cyclic strain-mediated TM release. Integrins were previously shown to regulate cyclic strain-induced IL-6 secretion in HUVECs (Sasmoto et al., 2005) among other markers. We employed cyclic RGD peptide inhibitor to specifically block integrin $\alpha\beta3$ in our strain experiments. Interestingly, TM release was further increased very significantly under both static and strain conditions following inhibition of this integrin. This suggests that integrins “slow down” the release of TM under both basal and cyclic strain conditions (i.e., inhibition enhances release), which may reflect their typical “outside-in” signalling capacities (Hannafin et al., 2006). This possibly reveals the status of the endothelial cell to the extracellular environment as elevated sTM is a well-known injury marker for cardiovascular disorders (Thorand et al., 2007; Urban et al., 2005; Wu et al., 2003). Furthermore, integrin-mediated shedding of procoagulant microparticles from unstimulated platelets was reported (Cauwenberghs et al., 2006) which points to a possible role for microvesicles in cyclic strain-induced TM release. This study contrasts with our observations which may indicate that the response we are observing may be an endothelial-cell specific one.

Finally, we did not observe an effect on strain-induced TM release after the addition of NSC23766, genistein, PD169316 or L-NAME to inhibit rac1, PTK, MAPK p38 and eNOS, respectively. We investigated Rac1 due to its sensitivity to cyclic strain (Kumar et al., 2004) and its link to TM expression (Lin et al., 2007) but nothing has previously been reported in

relation to TM release. Interestingly, Rac1 was previously shown to regulate the release of Weibel-Palade Bodies in HAECs (Yang et al., 2004) so it was surprising that Rac1 had no role in the cyclic strain-mediated TM release. Similarly, PTK and MAPK p38, both strain-sensitive kinases (Cheng et al., 2002; Lin et al., 2000; Von Offenberg Sweeney et al., 2004) had no effect on this strain-driven event. This is despite the fact that these proteins significantly reversed the cyclic strain-induced reduction of TM protein expression (Section 4.2.2.1). Taken together, these results indicate that TM expression and release likely engage different signalling pathways.

In summary, the first portion of this chapter demonstrated that many inflammatory mediators work together to regulate endothelial homeostasis and TM dynamics. TNF- α potentiated TM release in HAECs undergoing 7.5% cyclic strain, which may reflect its ability to activate NF- κ B and MAPK pathways (Anrather et al., 1997; Li et al., 2005). Similarly to TNF- α , ox-LDL reduced TM mRNA expression in static HAECs possibly due to decreased TM transcription (Ishii et al., 1996; Ishii et al., 2003). Ox-LDL also potentiated TM release in HAECs undergoing cyclic strain although, like TNF- α , the cellular mechanisms involved are unknown at present. Lastly, we observed that glucose had no significant effect on TM expression in static HAECs despite reports suggesting the opposite in the literature (Wang et al., 2012). We also found that the addition of glucose (30 mM) enhances TM release in static HAECs. This is consistent with the *in vivo* literature, as elevated levels of TM have been reported in the serum of patients with type 2 diabetes (Aso et al., 2000). Additionally, TM release was attenuated when elevated glucose (30 mM) was combined with strain, which may suggest a decrease in cardioprotection. This observation is somewhat consistent with a second clinical study showing that levels of soluble TM were inversely correlated with the risk of

developing type 2 diabetes (Thorand et al., 2007). However, contradictory data has been reported on sTM levels (whether they are increased or decreased) and type-2 diabetes. This area warrants further investigation possibly by combining these three different humoral conditions with elevated cyclic strain to help better replicate the actual *in vivo* situation. Additionally, this would address the possible degree of commonality between these interlinked pathways (i.e., ox-LDL, TNF- α and glucose may operate through similar pathways) that these inflammatory mediators act on.

The second portion of this chapter identifies the signalling components involved in cyclic strain-mediated TM regulation. We found that inhibition of PTK and p38 MAPK increased cyclic strain-mediated TM expression (i.e., reverses the typical strain-dependent response). In respect to these two proteins, this result was not unexpected due to their strain-sensitivity (Cheng et al., 2002) and their involvement in many signal transduction pathways (Noel et al., 2008; Von Offenbergs Sweeney et al., 2004). Subsequently, we focused on cyclic strain-induced TM release. Firstly, we observed that inhibition of MMPs decreased cyclic strain-induced TM release (i.e., reverses the typical strain-dependent response). This was not unexpected as MMPs are known to be strain-sensitive and implicated in atherosclerosis and hypertension (Cummins et al., 2007). We also observed that NADPH oxidase-independent ROS plays a role in cyclic strain-induced TM release (e.g., xanthine oxidase), which was not surprising as the endothelium typically experiences oxidative stress (i.e., high levels of ROS) during CVD (Howard et al., 1997; Matsushita et al., 2001). ROS has previously been reported to target MAPK proteins and PTKs (Paravicini and Touyz, 2006), which also have a significant effect on cyclic strain-mediated TM cellular expression. We also found that inhibition of integrin $\alpha\beta 3$ causes an additional increase in TM release in both static and

strained HAECs, suggesting that integrins serve as a cellular “brake” for the release of TM, and may explain elevated TM release in pathophysiological situations wherein integrin function is compromised (e.g., atherosclerosis). Thus, a small proportion of TM release during strain is triggered by proteolytic cleavage by MMPs (~10% corrected for baseline effects), whilst the remainder of TM release may possibly proceed through a vesicular pathway (i.e., on microparticles or exosomes), which will be the focus of Chapter 5.

Chapter 5:

**Further studies on the dynamics of
cyclic strain-mediated TM “release”
from HAECs**

5.1 Introduction

In the previous chapter, we investigated the role of inflammatory mediators (e.g., TNF- α) and signaling components (e.g., p38) on cyclic strain-induced TM expression and release. For Chapter 5, we subsequently decided to focus on TM release, as it is very poorly understood in the literature, whilst soluble TM (sTM) is now widely regarded as a significant injury biomarker for endothelial dysfunction (Boehme et al., 1996). Indeed, elevated levels of sTM have been reported in the plasma of patients with atherosclerosis (Pawlak et al., 2010; Taylan et al., 2012), cardioembolic stroke (Dharmasaroja et al., 2012), obesity (Urban et al., 2005), *Lupus erythomatosus*-associated metabolic syndrome (Mok et al., 2010), pre-eclampsia (Rousseau et al., 2009), sepsis-associated disseminated intravascular coagulation (DIC) (Lin et al., 2008), and severe acute respiratory syndrome (SARS) (Liu et al., 2005). Interestingly, the beneficial effects of soluble TM have also been reported in human clinical trials (Saito et al., 2007) with the development of ART-123 (thrombomodulin alpha, ReomodulinTM), a recombinant human soluble TM shown to be extremely effective in the rapid resolution of DIC. Given the consistent release of TM (dose- and time-dependently) from HAECs by cyclic strain, and considering that only a proportion (~30%) appears to be attributable to proteolytic release, we hypothesize that cellular microvesicles (MVs) may represent a possible vehicle for a proportion of strain-dependent TM release in this model.

MVs (Section 5.2.1) (Fig 5.1) are shed from the endothelium in response to cell activation or apoptosis and are emerging as novel biomarkers with the potential to regulate inflammation and immunological processes (reviewed in more detail in Leroyer et al., 2010). Due to the fact that we have shown that elevated levels of cyclic strain stimulate TM release,

we suspect that it may in fact be causing MV shedding. Although there is nothing reported in the literature that directly links cyclic strain with MVs, it has been shown that TM activity on both monocytes and monocyte-derived microparticles is increased after treatment with lipopolysaccharide (LPS) (Satta, 1997).

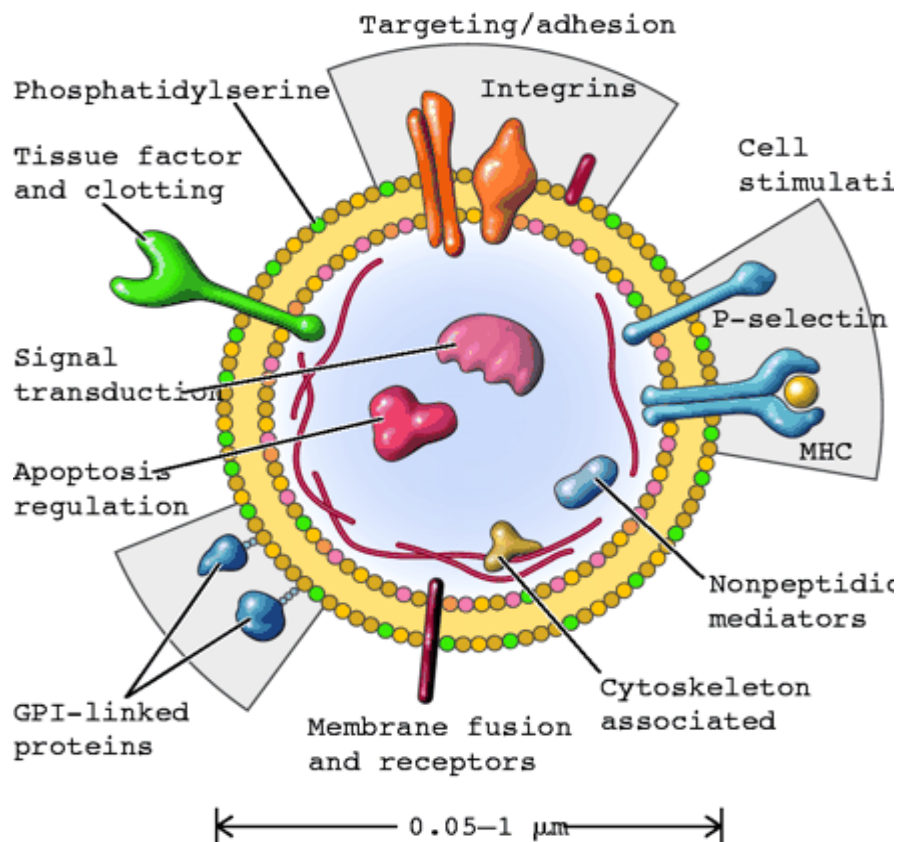


Figure 5.1: Cellular microvesicle (MV). MVs are shed from the plasma membrane of activated cells. They store membrane and cytoplasmic proteins implicating them in a wide range of vital functions. Key; MHC, major histocompatibility complex; GPI, glycosylphosphatidylinositol (Hugel, 2005).

Of the secreted membrane vesicles from endothelial cells, exosomes and microparticles (MPs) remain the most commonly studied (Azevedo et al., 2007; Vlassov et al., 2012). These differ by size, with exosomes measuring 30-100 nm (Théry et al., 2009) and MPs 100–1000 nm (Distler et al., 2005). Our aim in this chapter was to clarify whether TM released into the media (aka sTM) was present on a microvesicular structure such as a microparticle or an exosome. We therefore carried out a series of centrifugation experiments (Fig 5.3) to isolate MVs putatively released into media following strain of HAECs, with subsequent analysis of MV-associated TM levels by ELISA and Western blotting. A Total Exosome Isolation Kit was also employed for these studies.

Soluble “released” thrombomodulin (sTM), a molecular marker for assessing endothelial cell injury, has been reported to vary in size between 55 kDa to 105 kDa (Ishii and Majerus, 1985; Salem et al., 1984) although its precise functional role in release is the subject of much speculation. To date, sTM has been detected in biological fluids ranging from serum (Oida et al., 1990) and urine (Jackson et al., 1994) to synovial fluid (Conway and Nowakowski, 1993). High levels of sTM typically signify endothelial dysfunction, thus acting as a biomarker for the same. The difference in molecular weight (MW) for sTM may be explained by its release mechanism from the membrane and subsequent processing within the extracellular environment. For example, it has been reported that cellular TM can be cleaved by proteases to release low MW sTM variants (Lohi et al., 2004; Wu et al., 2008). Others have suggested microparticle (and exosome) involvement in sTM release, which would suggest up to full size TM (Bouchama et al., 2008; Ogura et al., 2004). We therefore, decided to measure the MW of the sTM released by cyclic strain *in vitro* from HAECs. Post-

strain, we harvested cell lysates and concentrated cell culture media with Amicon[®] Ultra-2 centrifugal filter devices for MW analysis of sTM by Western blotting.

Due to the elevated presence of released sTM linked to endothelial injury and dysfunction in numerous vascular disorders (Aso et al., 2000; Blann et al., 1997; Dharmasaroja et al., 2012), it is logical to presume that this released entity may have a functional role within the vasculature *in vivo*. We therefore decided to investigate in this chapter whether the TM released via cyclic strain had functional activity. Methods used to measure TM “functionality” *in vitro* are limited however, with the most common being to measure protein C (PC) activation. In this regard, one group has developed a novel technique to quantitate sTM activity *in vitro* using a human activated protein C (APC) antibody-based ELISA in order to back-calculate levels of sTM (Carnemolla et al., 2012). Interestingly, one of the most well known roles of TM is the inhibition of coagulation by neutralization of thrombin. Our lab has therefore designed a novel assay based on thrombin neutralization by sTM in cell culture media (i.e., neutralization of thrombin’s ability to induce permeabilization in reporter human aortic endothelial cell cultures). This assay was subsequently employed in this chapter to monitor the functional efficacy of released TM following static and strain conditions.

The ability of cyclic strain-conditioned media to elicit TM release in “static” reporter HAECs was also conducted as the final aspect of this chapter. This was performed in order to assess the “paracrine” impact of strain on TM release from endothelial cells. Interestingly, an earlier study showed that a cyclic strain-induced paracrine release of TGF- β (1) elicited a downregulation in TM expression in vein grafts (Kapur et al., 2011), although the signalling pathway used was unknown. Using a pan-neutralizing TGF- β 1 antibody (1D11), these authors

were able to block TM down-regulation, preserve levels of activated protein C, and reduce thrombus formation in a rabbit vein graft model. In our study, we harvested endothelial “conditioned” media from static and strained cells, incubated it with static reporter HAECs, and subsequently measured the changes in TM release from these reporter cells as an index of paracrine regulation.

5.2 Results

5.2.1 Microvesicle (MV) analysis

HAECs were subjected to 0% and 7.5% equibiaxial cyclic strain (60 cycles per min for 24 hrs). Post-experiment, cell culture serum-free media was harvested from each Bioflex well and processed for MVs by centrifugation before being analysed for TM by ELISA (protocol illustrated in Fig 5.2). Centrifugation conditions obtained from previous literature (Nieuwland et al., 1997; Théry et al., 2009).

In a preliminary experiment (Fig 5.3A), we measured the TM concentrations in the cell culture serum-free media; before (Pre-Spin) and after (Super) centrifugation at 14,400 rcf for 20 mins, as well as in the pellets. We observed that a small proportion of TM release was microvesicular (i.e., detected in the pellets) in unstrained HAECs, with slightly more TM detected in the pellet after 7.5% cyclic strain. Subsequently, the experiment was repeated with spin conditions increased to 20,000 rcf for 40 mins (Fig 5.3B) in an attempt to enhance MV enrichment in the pellet fraction. Similar results were obtained.

Interestingly, when we repeated this study in BAECs (Fig 5.4) where cell culture serum-free media was centrifuged at 14,400 rcf for 20 mins, we did not see a significant induction of TM release in response to strain, nor any slight increase in pellet-enriched TM in response to strain.

We subsequently compared the effectiveness of both microvesicle spin conditions using the “same” batch of HAEC serum-free media; 14,400 (spin A) vs 20,000 rcf (spin B) for 20 vs 40 mins, respectively (Fig 5.4A). Increasing spin speed and time was seen to decrease TM concentration in supernatants (Fig 5.5A).

MVs can be subdivided into exosomes and microparticles (MPs) based on size. With a view to further clarifying whether TM released post-cyclic strain is present on MPs or exosomes, we isolated exosomes using Total Exosome Isolation[®] (Invitrogen, The Netherlands) reagent from the cell culture serum-free media following static and strain conditions (protocol described in more detail in Fig 5.6). Total TM levels (pg) were measured in pre-spin media, supernatants and pellets (containing the enriched exosomes) by ELISA (Fig 5.7). A high level of TM was observed in the static pellets with strain stimulating significantly more release of TM into the pellet fraction.

5.2.2 Molecular size of sTM

To further investigate the molecular size of soluble TM (sTM) released into the media from HAECs, cell culture serum-free media was concentrated using Amicon[®] Ultra-2 centrifugal filter devices, determined for protein concentration with a BCA assay and subsequently, analysed for TM cellular expression by Western blotting (Fig 5.8). TM variants

were observed in cellular lysates at molecular weights ranging from 35-100 kDa. sTM variants were also detected in cell culture serum-free media faintly at 100 kDa and very strongly at 35 kDa.

5.2.3 Functional efficacy of sTM

HAECs were subjected to cyclic strain (0% and 7.5% for 24 hrs). Cell culture serum-free media was harvested post-treatment and concentrated using Amicon[®] Ultra-2 centrifugal filter devices and measured for protein via BCA assay. Conditioned serum-free medias (spiked with either vehicle buffer or thrombin, the latter a known permeability agent for endothelial cells) was incubated with reporter HAEC monolayers in transwell insert plates and the effects on HAEC barrier integrity monitored by a FITC-dextran permeability assay (Fig 5.9). We found that the sTM released into the cell culture serum-free media by cyclic strain had increased functional activity manifested as an increased ability to attenuate thrombin-induced permeability (presumably via sTM binding of thrombin).

5.2.4 Paracrine release of TM

In order to determine if cyclic strain of endothelial cells can elicit TM release in a “paracrine” manner, we conducted a series of conditioned media experiments. Serum-free media was taken from pre-strained endothelial cells (0% and 7.5% for 24 hrs) and incubated with static “reporter” HAECs for 24 hrs, after which we measured for TM release. When

basally released TM was taken into account, we noted that cyclic strain could induce media conditioning leading to paracrine induction of TM release in HAECs (Fig 5.10A).

Additionally, a time-dependent study was also carried out to identify the earliest time-point at which a paracrine-induced release of TM may be observed. In this regard, serum-free media was harvested from pre-strained endothelial cells (0% and 7.5%, 0-24 hrs) and incubated with static HAEC reporter cultures for 24 hrs, after which we measured for TM release via ELISA (Fig 5.10B). Under cyclic strain conditions, a significant sharp increase in paracrine TM release is apparent after 12 hrs.

5.3 Table and Figures

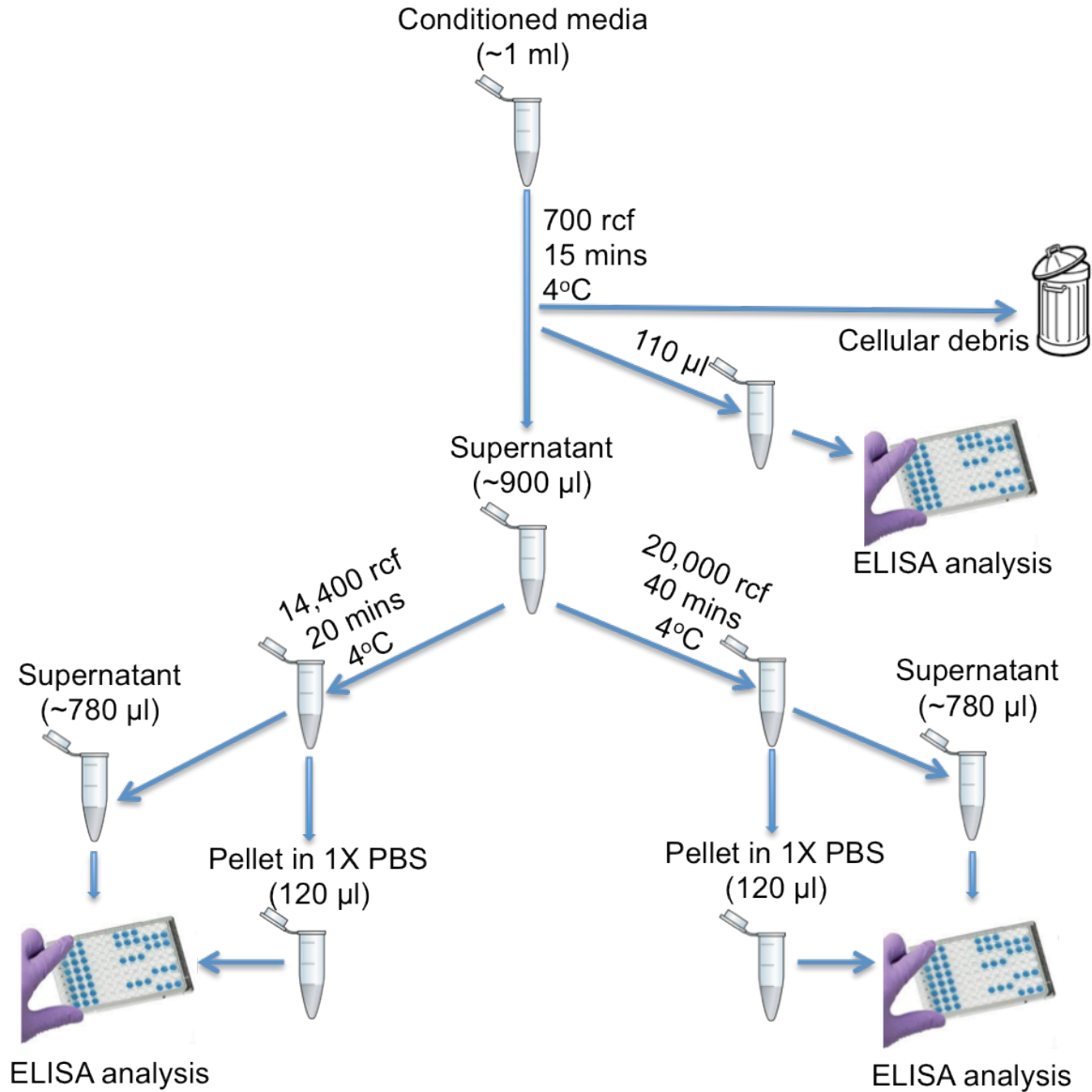


Figure 5.2: The steps involved in processing microvesicles (MVs) from cell culture media

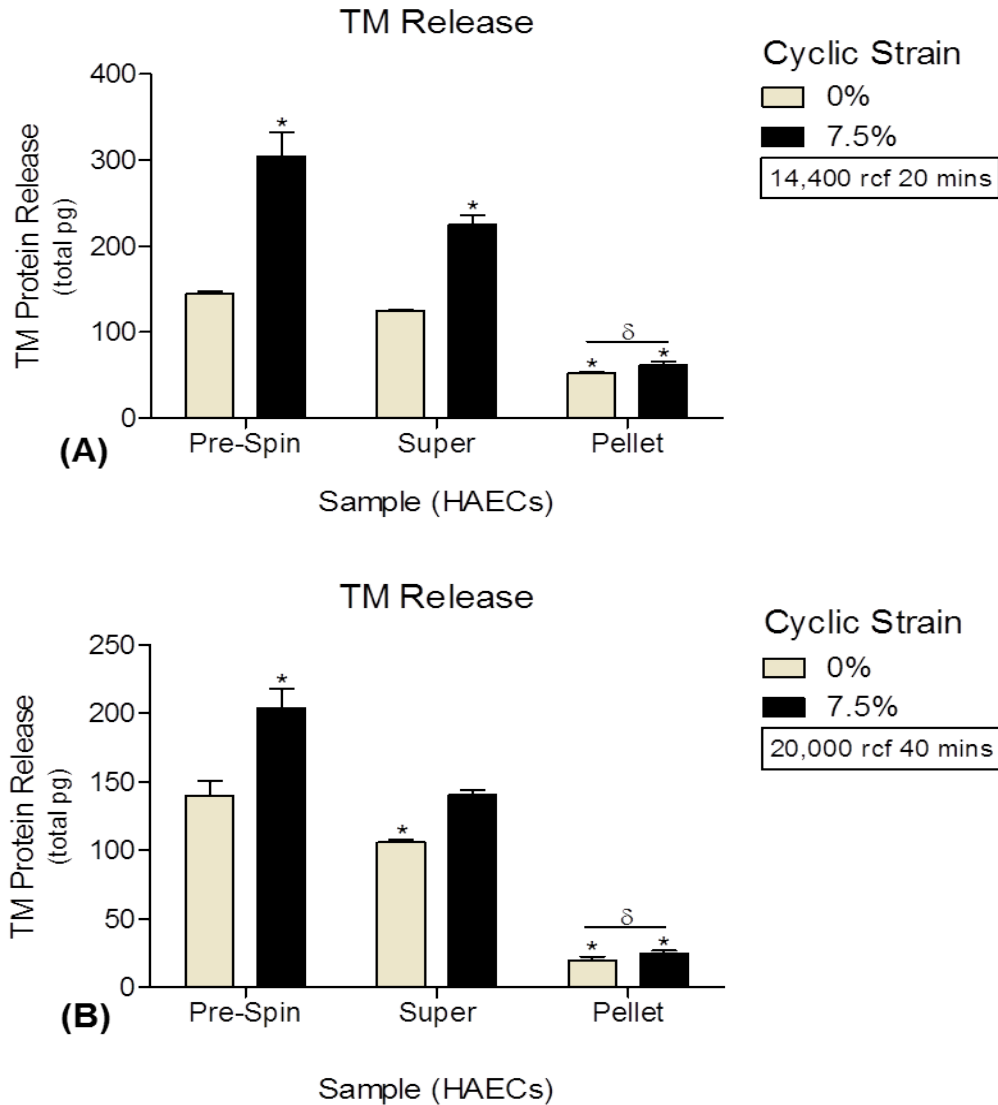


Figure 5.3: Microvesicles and TM release. HAECs were exposed to cyclic strain (0% - 7.5% for 24 hrs) and monitored for TM levels in the pre-spin media, post-spin supernatant and pellet. **(A)** HAEC media centrifuged at 14,400 rcf for 20 mins (normalised for total pg) ($\delta P \leq 0.05$; $*P \leq 0.05$ versus 0% Pre-Spin determined using 1-way ANOVA and post-hoc Dunnett's test, n=6). **(B)** HAEC media centrifuged at 20,000 rcf for 40 mins (normalised for total pg) ($\delta P \leq 0.05$; $*P \leq 0.05$ versus 0% Pre-Spin determined using 1-way ANOVA and post-hoc Dunnett's test, n=6). Key: Super, supernatant.

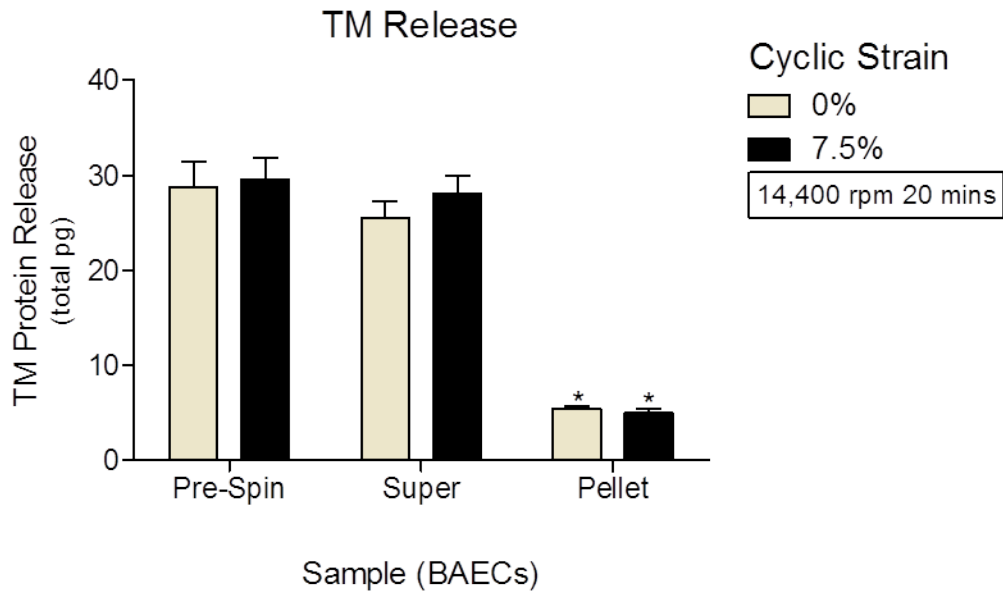
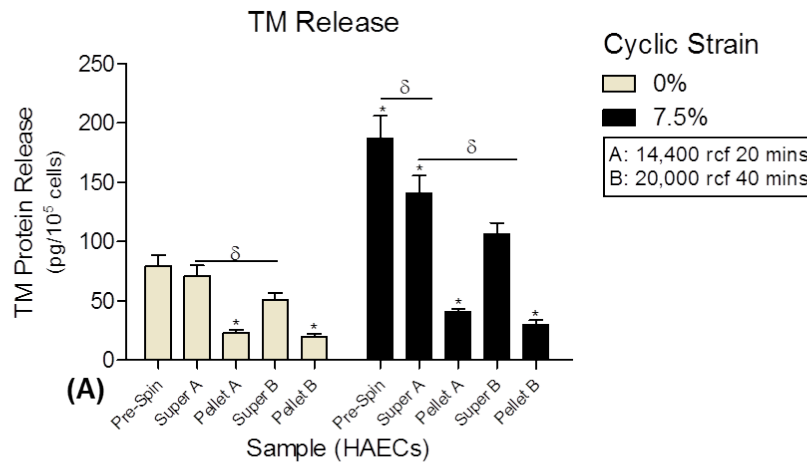


Figure 5.4: Microvesicle and TM release from BAECs. BAECs were exposed to cyclic strain (0% - 7.5% for 24 hrs) and then monitored for TM release in the pre-spin media, supernatants and pellet. BAEC media was centrifuged at 14,400 ref 20 min (normalised for total pg) (* $P \leq 0.05$ versus 0% Pre-Spin determined using 1-way ANOVA and post-hoc Dunnett's test, $n=6$). Key: Super, supernatant.



Spin	RCF	Time	Decrease in TM concentration in 0% strain media samples	Decrease in TM concentration in 7.5% strain media samples
A	14,400	20 mins	9.75%↓	35%↓
B	20,000	40 mins	33.23%↓	46.49%↓

(B)

Figure 5.5: Impact of increasing centrifugation conditions. **(A)** HAECs were exposed to cyclic strain (0% - 7.5% for 24 hrs) and then monitored for TM concentration in the pre-spin media, post-spin supernatant and pellet following centrifugation of the same batch of HAEC-conditioned media at 14,400 and 20,000 rcf for 20 and 40 mins, respectively. ($\delta P \leq 0.05$; $*P \leq 0.05$ versus 0% Pre-Spin determined using 1-way ANOVA and post-hoc Dunnett's test, $n=6$). **(B)** The percentage decrease in sTM concentration in strain-conditioned media following both consecutive spins. Key: Super, supernatant.

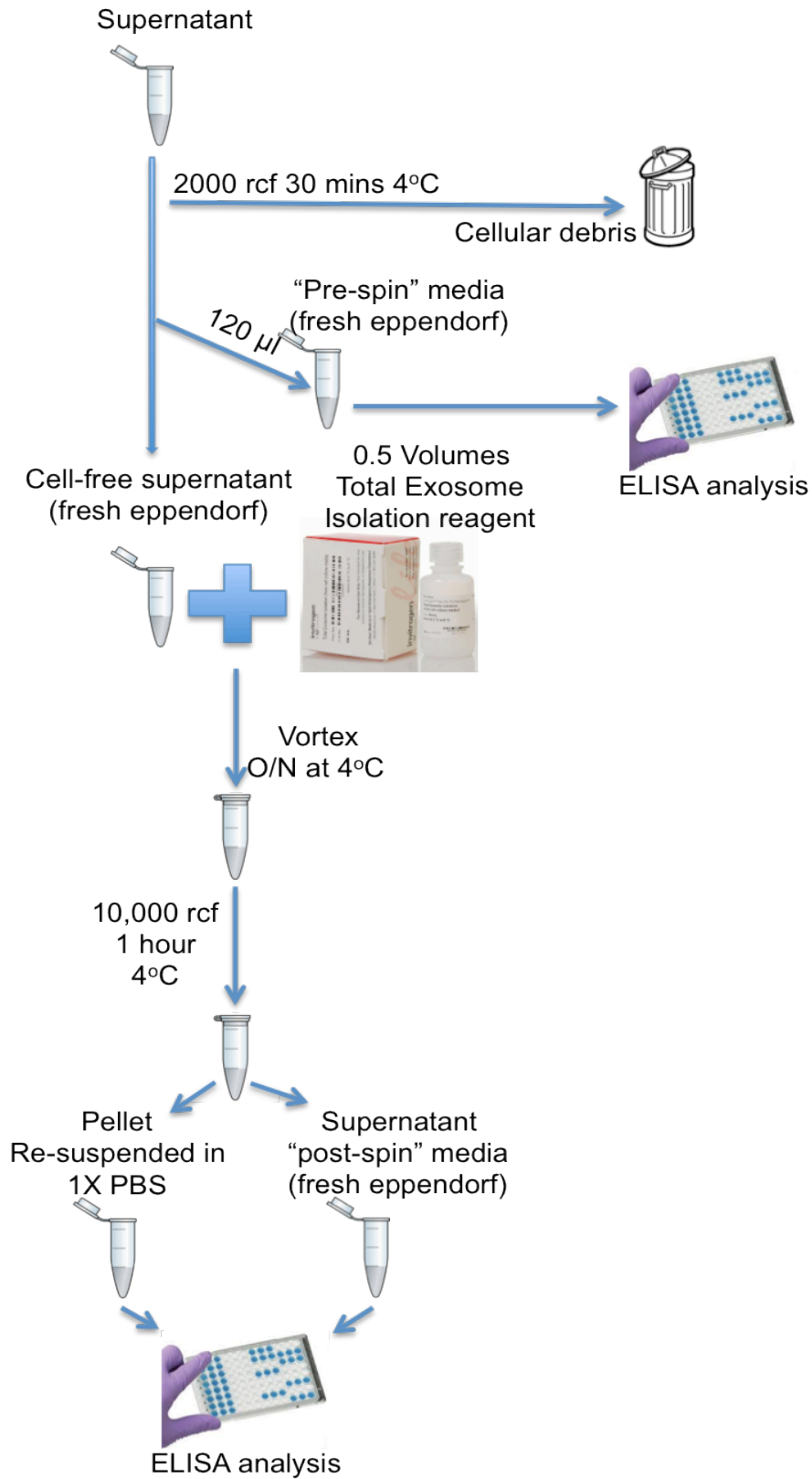


Figure 5.6: The steps involved in enriching exosomes from cell culture media.

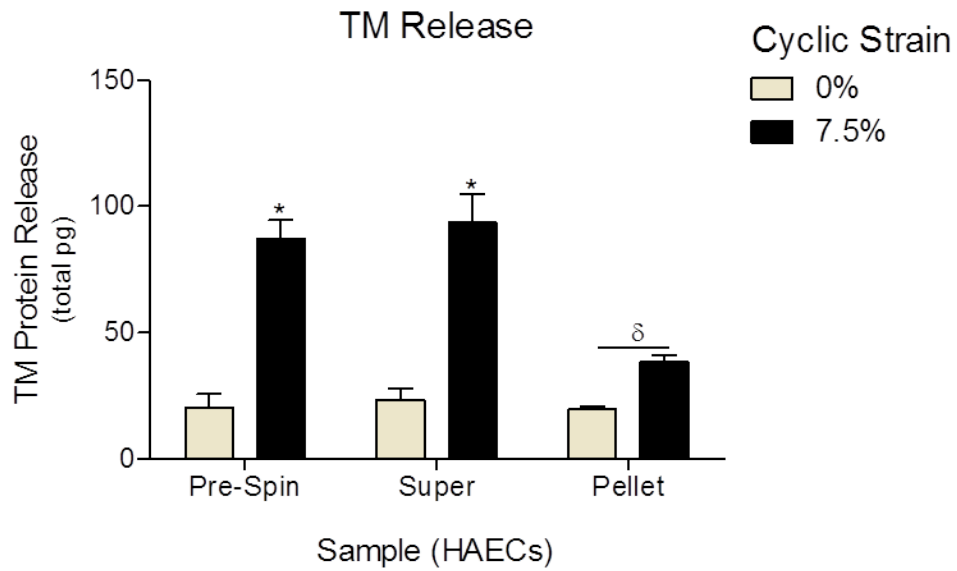


Figure 5.7: Exosome enrichment. HAECs were exposed to cyclic strain (0% - 7.5% for 24 hrs) and TM levels (normalised for total pg) were measured in the pre-spin media, supernatant and pellet (containing the enriched exosomes) via ELISA. ($\delta P \leq 0.05$; $*P \leq 0.05$ versus 0% Pre-spin Spin determined using 1-way ANOVA and post-hoc Dunnett's test, $n=6$). Key: Super, supernatant.

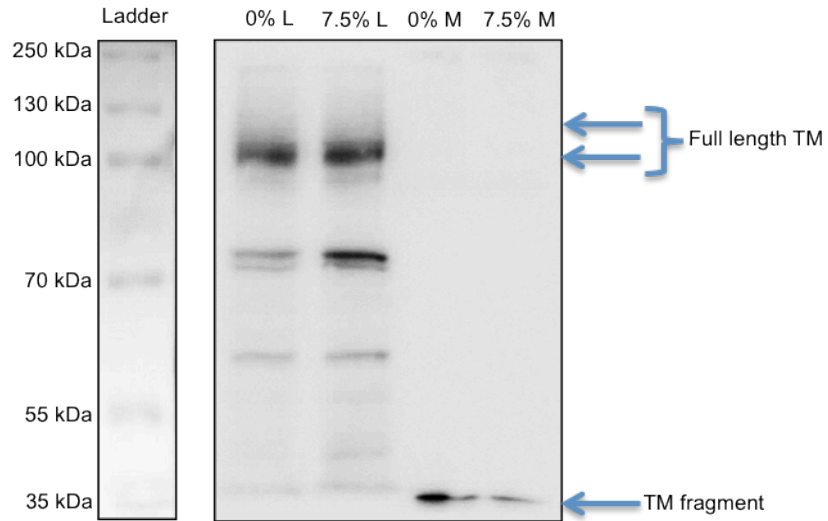


Figure 5.8: Detection of TM in cell lysates and media supernatants. HAECs were exposed to cyclic strain (0% and 7.5%, for 24 hrs). Media supernatants were concentrated using Amicon[®] Ultra-2 centrifugal filter devices and then monitored alongside cell lysates for TM by Western blotting (30 μ g/ml of protein per lane) (n=1). Key: L, lysates; M, media.

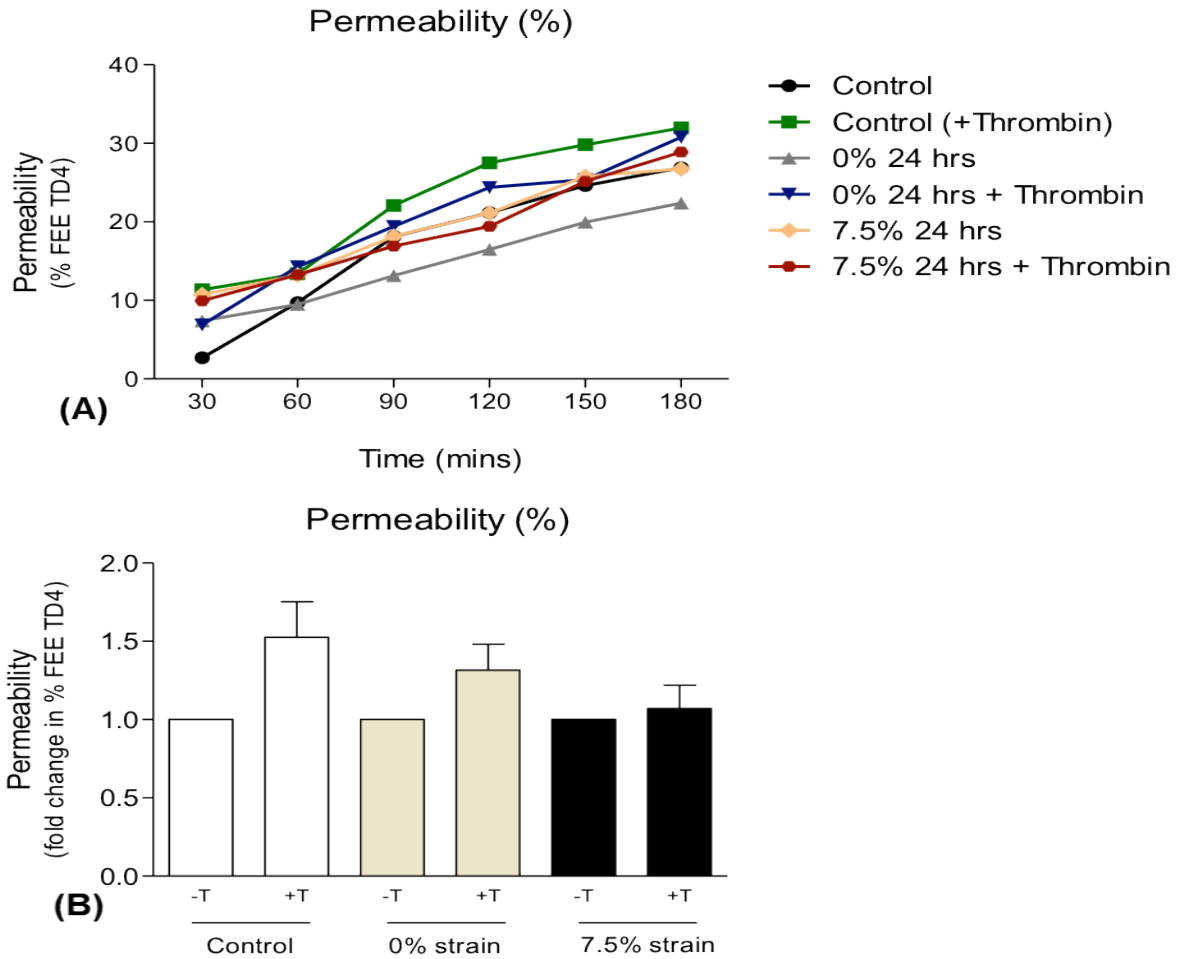


Figure 5.9: Functional efficacy of sTM. HAECs were exposed to cyclic strain (0% and 7.5%, for 24 hrs) with subsequent measurement of transendothelial permeability. Media supernatants containing sTM (harvested from static and strained HAECs) were concentrated using Amicon® Ultra-2 Centrifugal Filter Devices and then “spiked” with either buffer vehicle or thrombin (1 U/ml). Medias were then incubated into the abluminal space of transwell assays to monitor effects of permeabilization by thrombin. **(A)** Line graphs showing the fold-change in % trans-endothelial exchange of FITC-Dextran over 3 hrs (n=2). **(B)** Histogram showing the difference in permeability at the 120 min-time point (n=2). Note: control media are unconditioned media.

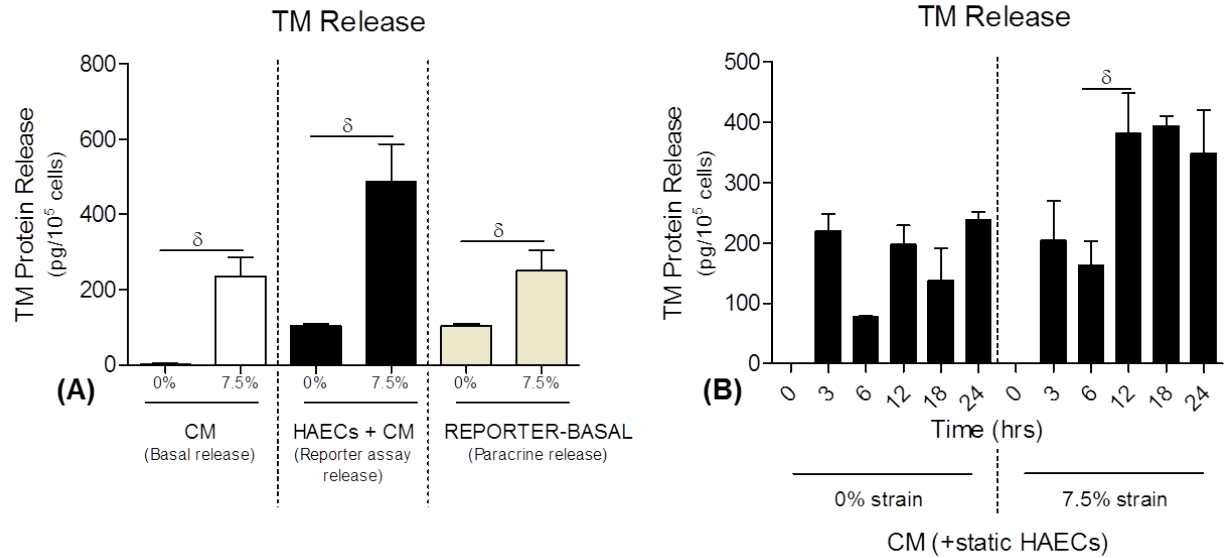


Figure 5.10: Paracrine TM release. (A) HAECs were pre-exposed to cyclic strain (0% - 7.5% for 24 hrs) and conditioned media harvested and incubated with static HAEC reporter cultures for 24 hrs. Media supernatants from reporter cultures were monitored for TM release via ELISA ($\delta P \leq 0.05$ determined using 1-way ANOVA and post-hoc Dunnett's test, $n=6$). (B) HAECs were pre-exposed to cyclic strain (0% vs 7.5%) and conditioned (strained) media supernatants were taken at varying time-points (0-24 hrs). This conditioned media was then incubated with static HAEC reporter cultures for 24 hrs and then measured for TM release via ELISA ($\delta P \leq 0.05$ determined using 1-way ANOVA and post-hoc Dunnett's test, $n=3$). Key: CM, conditioned media.

5.4 Discussion

This chapter further investigates the mechanisms associated with cyclic strain-induced TM release from HAECs. We started by investigating the possibility that TM release from HAECs in response to cyclic strain may proceed via a microvesicular vehicle, namely microparticles and/or exosomes. In this regard, we detected sTM on an enriched exosome fraction, which was increased in response to chronic cyclic strain. Endothelial MVs are complex vesicular structures shed from activated or apoptotic endothelial cells (Leroyer et al., 2010) and have roles in coagulation, inflammation, endothelial function, and angiogenesis. TM has in fact previously been linked to microvesicles as increased TM activity was shown on both monocytes and monocyte-derived microparticles following treatment with LPS (Satta et al., 1997). Additionally, endothelial MPs and sTM were found to be elevated in the plasma of patients with severe systemic inflammatory response syndrome (SIRS) (Ogura et al., 2004). In Chapter 4, we established that TM released after elevated cyclic strain is in part due to proteolysis by MMPs (~10%) but the remainder presumably advances through other pathways possibly including microparticles or exosomes. In section 5.2.1, we carried out a range of centrifugation experiments to enrich MVs within HAEC conditioned media taken from static and strained cells. Firstly, we centrifuged media at 14,400 rcf for 20 mins and analysed for TM via ELISA. We observed a significant decrease in TM levels from “pre-spin” media to supernatant fractions, within subsequent observation of TM in the pellet fraction. Moreover, the TM within the pellet fraction increased slightly (albeit significantly) in response to strain. Similar observations were made when we increased the centrifugation conditions to improve the microvesicle enrichment process. Interestingly, we did not observe a significant induction

of TM release in response to strain. When we employed BAECs (although we did observe a proportion of TM enrichment into the pellet fraction – equal for both static and strained BAECs). This may reflect a species issue between HAECs and BAECs and warrants further investigation. The lack of suitability of the human ELISA kit for the bovine cells may also be at issue here.

Taken together, these results point to a putative microvesicular involvement in TM release following elevated cyclic strain of HAECs an observation not shown in the literature to date. It is worth noting however that mechanical strain was shown to stimulate microparticle formation in human pulmonary endothelial cells (Vion et al., 2013). Interestingly, this group used a similar centrifugation protocol (20,000 rcf for 30 mins) as our study and our data is consistent with their findings. Following high levels of cyclic strain, TM may utilise MVs as an escape pathway into the circulation to act as a biomarker for endothelial dysfunction and/or a ‘SOS’ signal to communicate with adjacent healthy endothelial cells.

We next considered that the centrifugation procedure employed may only be allowing enrichment of a small proportion of the microvesicular complement in conditioned media, and may in fact not be sufficiently enriching for exosomes. MVs are small membrane-enclosed sacs (size varying from 50 nm to 1000 nm) that are sub-characterised into exosomes, circulating MVs or microparticles (MPs) (Azevedo et al., 2007). These two entities differ in size with MPs measuring 100 to 1000 nm² and exosomes, 50 -100 nm²-sized structures (György et al., 2011). We subsequently enriched for exosomes from HAEC media using a Total Exosome Isolation[®] kit. TM was subsequently measured in pre-spin media, supernatant and pellet (containing the enriched exosomes) by ELISA. Whilst we did not observe a

substantial difference between TM levels in the pre-spin media and supernatants (which may be down to reagent interference with the ELISA) , we found enrichment in TM levels in the pellet fraction, with moderately higher amounts of TM detected following 7.5% cyclic strain. This presumably indicates that a moderate proportion of sTM released post-strain may be present on exosomes. Again, this is the first time that the presence of released sTM on exosomes has been reported, and again warrants further investigation with the use of exosomal markers. A recent study showed that the release of MVs expressing an exosome marker tumor susceptibility gene (Tsg 101) decreased TM cellular expression in static HUVECs (Aharon et al., 2008). This led to increased endothelial thrombogenicity as well as a disruption in endothelial integrity and is somewhat consistent with our findings. Although the biological roles of exosomes are not clearly understood, we can speculate as to its subsequent function in this context. Exosomes are thought to function as “intercellular messengers” between adjacent cells, and in this capacity may be capable of delivering TM to other endothelial beds to help regulate vessel wall homeostasis during inflammation of the endothelium (Vlassov et al., 2012). Whilst the function of sTM *in vivo* has yet to be clarified (with opinion divided between damage biomarkers and functional efficacy), the size of the sTM variants has been shown to vary, and so we sought to examine this in the next portion of this chapter. Whilst microparticles are known to be regulated by shear stress (Vion et al., 2013), there is an absence of literature showing that exosomes are strain-sensitive. Vion and co-workers established that sustained atheroprone low shear stress induces microparticle release from endothelial cells through activation of Rho kinases and Erk1/2 pathways, whereas atheroprotective high shear stress restricts microparticle release in an NO-dependent manner. This contrasts with our findings wherein we demonstrated increased release of TM in

response to shear stress (although did not investigate the release mechanism, barring any further conclusions).

sTM has been reported to vary in size between 55 kDa – 105 kDa (Blann and Taberner, 1995; Ikegami et al., 1998; Ishii and Majerus, 1985; Salem et al., 1984; Takahashi et al., 1995) which may reflect the method of release from the membrane. The literature has mainly attributed this to proteolysis induced by leukocyte-derived lysosomal proteases (Abe et al., 1994), neutrophil-derived enzymes (Matsuyama et al., 2008), MMPs (Wu et al., 2008), cysteine proteases (Inomata et al., 2009) and rhomboids (Cheng et al., 2011; Lohi et al., 2004). Yet when we inhibited rhomboids using DCI (Fig 4.7, Chapter 4) we observed a slight but non-significant increase in the cyclic strain mediated TM release, which suggests that rhomboids may actually be involved indirectly in “slowing down” TM release (possibly via cleavage of a signalling component). Interestingly however, we found that a moderate percentage of TM release may be due to proteolytic cleavage via MMPs (~30%). To address this we concentrated HAEC media to analyse sTM via Western blotting alongside cellular lysates. We detected full length TM and fragments in the cell lysates (possibly due to cellular turnover or antibody non-specificity). In media, we identified a strong low molecular weight fragment and faint full length bands for TM. This may be due to a combination of proteolysis and MV involvement. Moreover, we cannot discount further proteolysis following full length release on MVs. This suggests that both the entire cellular TM molecule and a smaller fragment of TM are released following cyclic strain. Unfortunately, there is an absence of publications documenting biomechanical force-mediated release of sTM.

So far, we have established that TM is released following elevated cyclic strain, and so we were interested to determine if sTM had any functional activity. Techniques to measure

the activity of TM *in vitro* typically involve protein C activation (PC) assays (Carnemolla et al., 2012), which can be expensive and have long incubation times with the substrate. This led us to develop a TM functional efficacy assay based on the ability of TM to bind thrombin (and in terms of assay read-out, prevent it from causing HAEC permeabilization). Thrombin typically compromises the barrier integrity in endothelial cells (Adams and Huntington, 2006) so we employed concentrated HAEC media (presumably containing sTM) to neutralize thrombin permeabilization in a HAEC reporter transwell permeability assay using FITC-dextran labels. In this experiment, we found that the sTM in the media had the ability to inhibit thrombin activity (at 1 U/ml) with 7.5% strain-conditioned media having the maximal effect. As this media has an elevated level of released sTM, we concluded that the sTM is functional. The reason for this elevated release of sTM post-strain is still not clear although we propose, based on our observations, it may have the ability to bind thrombin to regulate both coagulation and fibrinolysis *in vivo*. It is worth noting that numerous clinical observations of CVD patients (e.g., sepsis, lupus, SARS) have reported increased levels of sTM in patient plasma, which may have a functional role in the vasculature (Aso et al., 2000; Ho et al., 2003; Ikegami et al., 1998; Liu et al., 2005; Ogawa et al., 2012).

The issue of “paracrine” TM release by cyclic strain was also considered in this chapter. In this regard, we conducted a range of conditioned media experiments involving incubation of static “reporter” HAECs with conditioned media harvested from HAECs maintained for 24 hrs under static and strain conditions. TM release from reporter HAECs was subsequently measured by ELISA. The addition of the strain-conditioned media to reporter HAECs was clearly seen to induce further TM release. Probing further into the dynamics of this event, we noted that a minimum of 12 hrs of conditioning by strain was

required to stimulate this paracrine release event. This strain-dependent “paracrine” effect of conditioned media has not previously been shown with respect to TM regulation within the endothelium, and constitutes relatively novel findings. Interestingly, another group reported that a strain-induced paracrine release of TGF- β (1) induced a reduction in TM expression in vein grafts (Kapur et al., 2011). Interestingly, it was shown that exposure of HUVECs to MVs, which include both microparticles and exosomes resulted in increased cell surface thrombogenicity with decreased levels of TM expression (Aharon et al., 2008). In this study, stimulation of a monocyte cell line by starvation or by endotoxin and calcium ionophore A23187 caused the release of MVs. These MVs were incubated with HUVECs for short (2-4 hours) or long (20 hours) periods of time. MVs were shown to rapidly induce membrane blebbing following brief exposure (2-4 hours) whereas longer incubation (20 hours) times lead to further perturbation of the endothelial haemostatic balance. Although this group did not measure TM release, this still agrees with our observations in relation to this conditioned media study and coincides with our previous observations in relation to TM expression. We hypothesize that cyclic strain-mediated TM release may be a chronic response happening *in vivo* with sTM variants stimulating a cascade of further TM release. Whether the sTM fragments stimulate this ‘extra’ release via MMP, ROS or exosomes remains to be determined. In conclusion, the purpose of this paracrine TM release may be for the benefit of the endothelial cell to regain homeostatic balance during an inflammatory challenge. Our confirmation of a degree of functional efficacy within the released sTM function would be consistent with this hypothesis.

To summarise, we observed MV involvement in the release of TM from HAECs, including the elevated release in response to high cyclic strain. Using an exosome enrichment

protocol, our data suggest that approximately one third of the TM release occurs via the exosomal pathway (with the remainder of TM release putatively attributed to microparticles and proteolytic cleavage). We further detected multiple TM size variants in both lysates and media (ranging from 35-100 kDa), which would possibly indicate proteolytic processing of TM. Next, we determined that sTM released post-strain still retained a level of functional activity (manifested on the ability to bind thrombin). Finally, we noted that strain-conditioned HAEC media serves as a “paracrine” stimulus for TM release from reporter HAECs. The vasculoprotective properties of this released sTM that we have identified *in vitro* are mirrored in the rapid development of recombinant sTM-based therapeutics (Matsusaki et al., 2008; Nakashima et al., 1998; Omichi et al., 2010). For instance, ART-123 (thrombomodulin alpha, ReomodulinTM) was approved in 2008 for human therapy in Japan (Saito et al., 2007) to treat disseminated intravascular coagulation (DIC). This therapeutic consists of the TM extracellular domains 1-3, which are crucial for the anti-inflammatory and anti-coagulant actions of the molecule.

Chapter 6:
Final Summary

6.1 Final Summary

Thrombomodulin (TM) has crucial physiological importance within the vasculature as evidenced by its functions in coagulation, inflammation and fibrinolysis (Conway, 2011). The endothelium, a continuous monolayer of flattened endothelial cells, is vital for maintaining the homeostatic integrity of the blood vessel by virtue of its ability to adapt and respond to the ever-changing environment of the vasculature (Aird, 2007). The endothelial cell exists within a pressurized fluid environment in direct contact with the circulating blood and blood-borne components. This creates blood flow-associated hemodynamic forces, namely pulsatile shear stress and cyclic circumferential strain, which exert a profound biochemical influence on the blood vessel wall (Fig 6.1) (Ando and Yamamoto, 2011). The latter force, and indeed the focus of this thesis, namely cyclic strain, describes the repetitive circumferential stretching of the vessel wall in synchronization with the cardiac cycle (Chen et al., 2008).

Cyclic strain contributes to endothelial homeostasis whilst aberrantly high and low levels are strongly associated with endothelial dysfunction (Cheng et al., 2001; Chen et al., 2008; Cummins et al., 2007). Interestingly, there are limited studies (and particularly *in vitro* studies) investigating the effects of cyclic strain upon TM expression and release. The hypothesis for this project was therefore to further understand; ***how elevated cyclic strain impacts the regulation and function of thrombomodulin (TM) in human aortic endothelial cells.*** This lack of information on TM regulation by this potent hemodynamic force has therefore framed the resultant thesis.

In **Chapter 3**, we employed an MSD[®] Multiplex ELISA to identify a profile of pro-inflammatory and vascular injury biomarkers that were responsive to elevated cyclic strain.

The most interesting result from this study showed down-regulation of TM cellular expression in combination with an increase of TM release following elevated cyclic strain. Additional studies using Western blotting and qRT-PCR both confirmed the dose-dependent decrease of TM protein and mRNA expression levels subsequent to elevated cyclic strain of HAECs. Furthermore, ELISA studies using a single-plex Duoset ELISA showed how TM release/shedding was amplified in response to cyclic strain in a dose-, frequency- and time-dependent manner. Moreover, we found that TM mRNA expression was also increased by shear stress, a hemodynamic component of blood flow known to convey an *atheroprotective* phenotype to the endothelium (Traub and Berk, 1998), an observation – quite opposite to that of cyclic strain. Additionally, shear stress up-regulated TM release in a temporal manner. These results suggest to us that cyclic strain and shear stress are most likely eliciting effects on TM regulation via different pathways.

In **Chapter 4**, we examined how elevated cyclic strain affects TM release in the presence and absence of a range of inflammatory mediators. We found that TNF- α moderately reduced TM mRNA expression in static HAECs whilst potentiating TM release in HAECs in the presence of 7.5% strain. Interestingly, ox-LDL exhibited similar effects. We did not observe a significant effect of glucose application on TM expression in static HAECs although by contrast to TNF- α and ox-LDL, it attenuated TM release in HAECs undergoing 7.5% cyclic strain. The second portion of this chapter endeavored to identify the cellular signalling components mediating the effects of cyclic strain on TM dynamics. Firstly, we focused on TM cellular expression. We found that inhibition of PTK and p38 MAPK reversed the down-regulatory effects of cyclic strain on TM expression, implying their mutual roles in this event. We also determined the role that various components may play in the cyclic strain-

induced increase in TM release. In this regard, we observed that blockade of MMPs partially decreased cyclic strain-induced TM release as well as implicating a role for NADPH. Interestingly, inhibition of integrin ($\alpha v\beta 3$) caused a very substantive increase in TM release under both static and strained conditions, suggesting that integrins may serve to “dampen” the induction of TM release by cyclic strain.

In **Chapter 5**, we further investigated mechanisms associated with strain-induced TM “release” from HAECs. We presented data to support the notion that, in addition to proteolytic release, a considerable proportion of TM release from endothelial cells under static and strain conditions proceeds through an exosomal pathway. Furthermore, we determined the sTM released post-strain still retained a level of functional efficacy. Moreover, we observed that strain-conditioning of HAECs may lead to the release of humoral components (including sTM) that can elicit a paracrine release of TM from reporter HAECs.

We have focused on TM release extensively in this thesis in-part due to its relevance to diagnostics and therapeutics. sTM is an established biomarker for a number of cardiovascular disorders (Liu et al., 2005; Ogawa et al., 2012). Moreover, the vasculoprotective properties of this released sTM are reflected in the rapid development of recombinant sTM-based therapeutics (Matsusaki et al., 2008; Omichi et al., 2010). The most successful therapeutic based on sTM so far is ART-123 (thrombomodulin alpha, ReomodulinTM). This was approved in 2008 for human therapy in Japan (Saito et al., 2007) to treat disseminated intravascular coagulation (DIC) and consists of the TM extracellular domains 1-3, which are crucial for the anti-inflammatory and anti-coagulant actions of the molecule. This therapeutic proves to be a safer and more effective inhibitor of the propagation of coagulation than the traditional low-dose heparin therapy (Nakashima et al., 1998). The

data in this thesis documents the functionality and composition of sTM following release, which adds to the growing field of MVs as diagnostic markers and therapeutic models. We have also greatly enhanced the knowledge on cyclic strain-associated disorders (i.e., hypertension). In addition, clinical studies using exosomal biomarkers could be based on this research.

The studies conducted in this thesis reflect the first comprehensive attempt to evaluate cyclic strain-dependent regulation of TM in endothelial cells *in vitro*, an important aspect of the mechanistic understanding of *in vivo* findings and clinical approaches. Naturally, several questions remain unanswered and so further studies are warranted;

- i. The role of KLF2 in the transcriptional regulation of TM in HAECs by cyclic strain. This transcription factor is inhibited by a microRNA, miR-92a that then indirectly inhibits TM (Dekker et al., 2002; Ishibazawa et al., 2011). However, the relationship between KLF2 and cyclic strain is somewhat less investigated so there may be a possibility it indirectly regulates cyclic strain-induced TM dynamics.
- ii. ROS source and function. We identified a NADPH oxidase-independent role for ROS in cyclic strain-induced TM release. This would suggest that an alternative oxidase may be involved in this event (e.g., xanthine oxidase).
- iii. Precise functions and efficacy of the released TM. This could involve further functional studies involving thrombin and Protein C assays.
- iv. Nature of release mechanism by exosomes and microparticles. We could employ FACs analysis to confirm known markers for these vesicles.

- v. Identification of conditioned-media components mediating paracrine release. This could entail knock-out experiments (i.e., eliminating one component to identify the regulator).

Biomechanical force	TM expression	TM release
Shear stress	<p>↑ (Takada 1994; Bergh 2009; Wu 2011)</p> <p>↑ (Martin et al., 2013)</p>	<p>↑ (Martin et al., 2013)</p>
Cyclic strain	<p>↑ <i>in vitro</i> (Chen et al., 2008)</p> <p>↓ in vivo vein grafts (Sperry et al., 2003)</p> <p>↓ <i>in vitro</i> (Martin et al., 2013)</p>	<p>↑ (Martin et al., 2013)</p>
Soluble TM (sTM)	NA	<p>↑ in DIC, hypertension (Lin et al., 2008; Lopes et al., 2002)</p> <p>↓ in type-2 diabetes, coronary heart disease (Thorand et al., 2007; Wu et al., 2003)</p>

Table 6.1: My contribution demonstrating the effect of hemodynamic forces on TM expression and release (shown in red). The symbols used represent the following; ↑, increased; ↓, decreased; +/-CS, in the absence or presence of cyclic strain; NA, not applicable.

These studies will no doubt contribute to a fuller understanding of these important vascular concepts and ultimately contribute to a greater mechanistic understanding of the role cyclic strain plays in vascular cell physiology and CVD. Ultimately, succeeding the completion of further *in vitro* studies we would like to measure sTM levels in human serum samples from patients with CVD (i.e., hypertension, DIC) and subsequently, test the functionality and composition of these released fragments. This could lead to the development of a new therapeutic for coagulation disorders.

Bibliography

Abe H, Okajima K, Okabe H, Takatsuki K, Binder BR. Granulocyte proteases and hydrogen peroxide synergistically inactivate thrombomodulin of endothelial cells in vitro. *J Lab Clin Med* 1994; **123**: 874-881.

Aird WC. Phenotypic heterogeneity of the endothelium: I. Structure, Function and Mechanisms. *Circ Res* 2007; **100**: 158-73.

Adams GN, LaRusch GA, Stavrou E, Zhou Y, Nieman MT, Jacobs GH, Cui Y, Lu Y, Jain MK, Mahdi F, Shariat-Madar Z, Okada Y, D'Alecy LG, Schmaier AH. Murine prolylcarboxypeptidase depletion induces vascular dysfunction with hypertension and faster arterial thrombosis. *Blood* 2011; **117**: 3929-3937.

Adams TE, Huntington JA. Thrombin-cofactor interactions: structural insights into regulatory mechanisms. *Arterioscler Thromb Vasc Biol* 2006; **26**: 1738-1745.

Aharon A, Tamari T, Brenner B. Monocyte-derived microparticles and exosomes induce procoagulant and apoptotic effects on endothelial cells. *Thromb Haemost* 2008; **100**(5): 878-885.

Akimoto S, Mitsumata M, Sasaguri T, Yoshida Y. Laminar shear stress inhibits vascular endothelial cell proliferation by inducing cyclin-dependent kinase inhibitor p21(Sdi1/Cip1/Waf1). *Circ Res* 2000; **86**: 185-90.

Alcaraz C, Diego MD, Pastor MJ, Escribano JM. Comparison of a radioimmunoprecipitation assay to immunoblotting and ELISA for detection of antibody to African swine fever virus. *J Vet Diagn Invest* 1990; **2**: 191-196.

Aleksic N, Wang YW, Ahn C, Juneja HS, Folsom AR, Wu KK. Assessment of coronary heart disease risk by combined analysis of coagulation factors. *Atherosclerosis* 2008; **198**: 294-300.

Almqvist N, Lonnqvist A, Hultkrantz S, Rask C, Telemo E. Serum-derived exosomes from antigen-fed mice prevent allergic sensitization in a model of allergic asthma. *Immunology* 2008; **125**: 21-27.

Al-Nedawi K, Meehan B, Micallef J, et al. Intercellular transfer of the oncogenic receptor EGFRvIII by microvesicles derived from tumour cells. *Nat Cell Biol* 2008; **10**: 619-624.

Ando J, Yamamoto K. Effects of shear stress and stretch on endothelial function. *Antioxid Redox Signal* 2011; **15**: 1389-403.

Andriantsitohaina R, Gaceb A, Vergori L, Martínez MC. Microparticles as regulators of cardiovascular inflammation. *Trends Cardiovasc Med* 2012; **22**: 88-92.

Anrather D, Millan MT, Palmethofer A, Robson SC, Geczy C, Ritchie AJ, Bach FH, Ewenstein BM. Thrombin activates nuclear factor-kappaB and potentiates endothelial cell activation by TNF. *J Immunol* 1997; **159**: 5620-5628.

Arazi HC, Doiny DG, Torcivia RS, Grancelli H, Waldman SV, Nojek C, Fornari MC, Badimon JJ. Impaired anti-platelet effect of aspirin, inflammation and platelet turnover in cardiac surgery. *Interact Cardiovasc Thorac Surg* 2010; **10**: 863-867.

Aso Y, Fujiwara Y, Tayama K, Takebayashi K, Inukai T, Takeemura Y. Relationship between soluble thrombomodulin in plasma and coagulation of fibrinolysis in type 2 diabetes. *Clin Chim Acta* 2000; **301**: 135-145.

Awolesi MA, Sessa WC, Sumpio BE. Cyclic strain upregulates nitric oxide synthase in cultured bovine endothelial cells. *J Clin Invest* 1995; **96**(3): 1449-1454.

Azevedo LCP, Janiszewski M, Soriano FG, Laurindo FRM. Redox mechanisms of vascular cell dysfunction in sepsis. *Endocrin Metab Immun Dis* 2006; **6**(2): 159-164.

Azevedo LCP, Pedro MA, Laurindo FRM. Circulating microparticles as therapeutic targets in cardiovascular diseases. *Recent Pat Cardio Drug Dis* 2007; **2**: 41-51.

Bajzar L. Thrombin activatable fibrinolysis inhibitor and an antifibrinolytic pathway. *Atheroscler Thromb Vasc Biol* 2000; **20**: 2511-2518.

Balda MS, Matter K. Tight Junctions. *J Cell Sci* 1998; **111**: 541-7.

Beppu T, Gil-Bernabe P, Boveda-Ruiz D, D'Alessandro-Gabazza C, Matsuda Y, Toda M, Miyake Y, Shiraki K, Murata M, Murata T, Yano Y, Morser J, Gabazza EC, Takei Y. High incidence of tumors in diabetic thrombin activatable fibrinolysis inhibitor and apolipoprotein E double-deficient mice. *J Thromb Haemost* 2010; **8**: 2514-2522.

Bergbold N, Lemberg MK. Emerging role of rhomboid family proteins in mammalian biology and disease. *BBA-Rev Biomembranes* 2013; Available at: <http://www.sciencedirect.com/science/article/pii/S0005273613000941> [Accessed: 27 May 2013].

Bergh N, Larsson P, Ulfhammer E, Jern S. Effect of shear stress, statins and TNF- α on hemostatic genes in human endothelial cells. *Biochem Biophys Res Commun* 2012; **420**: 166-171.

Bergh N, Ulfhammer E, Glise K, Jern S, Karlsson L. Influence of TNF- α and biomechanical stress on endothelial anti- and prothrombotic genes. *Biochem Biophys Res Co* 2009; **385**: 314-318.

Blann AD, Amiral J, McCollum CN. Prognostic value of increased soluble thrombomodulin and increased soluble E-selectin in ischemic heart disease. *Eur J Haematol* 1997; **59**(2): 115-120.

Blann AD, Taberner DA. A reliable marker of endothelial cell dysfunction: does it exist? *Brit J Haematol* 1995; **90**(2): 244-248.

Boehme MW, Deng Y, Raeth U, Bierhaus A, Ziegler R, Stremmel W, Nawrath PP. Release of thrombomodulin from endothelial cells by concerted action of TNF-alpha and neutrophils: in vivo and in vitro. *Immunology* 1996; **87**(1): 134-140.

Bonauer A, Boon RA, Dimmeler S. Vascular microRNAs. *Curr Drug Target* 2010; **11**: 943-949.

Bonauer A, Dimmeler S. The microRNA-17-92 cluster: still a miRacle? *Cell Cycle* 2009; **8**: 3866-3873.

Borissoff JI, Ten Cate H. From neutrophil extracellular traps release to thrombosis: an overshooting host-defense mechanism? *J Thromb Haemost* 2011; **9**: 1791-1794.

Bouchama A, Kunzelmann C, Dehbi M, Kwaasi A, Eldali A, Zobairi F, Freyssinet JM, de Prost D. Recombinant activated protein C attenuates endothelial injury and inhibits procoagulant microparticles release in baboon heatstroke. *Arterioscler Thromb Vasc Biol* 2008; **28**: 1318-1325.

Bouton MC, Venisse L, Richard B, Pouzet C, Arocas V, Jandrot-Perrus M. Protease nexin-1 interacts with thrombomodulin and modulates its anticoagulant effect. *Circ Res* 2007; **100**: 1174-1181.

Caby MP, Lankar D, Vincendeau-Scherrer C, Raposo G, Bonnerot C. Exosomal-like vesicles are present in human blood plasma. *Int Immunol* 2005; **17**: 879-887.

Califano F, Giovanniello T, Pantone P, Campana E, Parlapiano C, Alegiani F, Vincentelli GM, Turchetti P. Clinical importance of thrombomodulin serum levels. *Eur Rev Med Pharmacol* 2000; **4**: 59-66.

Calnek DS, Grinnell BW. Thrombomodulin-dependent anticoagulant activity is regulated by vascular endothelial growth factor. *Exp Cell Res* 1998; **238**: 294-8.

Carnemolla R, Patel KR, Zaitsev S, Cines DB, Esmon CT, Muzykantov VR. Quantitative analysis of thrombomodulin-mediated conversion of protein C to APC: Translation from in vitro to in vivo. *J Immunol Methods* 2012; **384**: 21-24.

Cauwenberghs S, Feijge MAH, Harper AGS, Sage SO, Curvers J, Heemskerk JWM. Shedding of procoagulant microparticles from unstimulated platelets by integrin-mediated destabilization of actin cytoskeleton. *FEBS letters* 2006; **580**(22): 5313-5320.

Chacko AM, Nayak M, Greineder CF, Delisser HM, Muzykantov VR. Collaborative enhancement of antibody binding to distinct PECAM-1 epitopes modulates endothelial targeting. *PLoS One* 2012; **7**: e34958.

Chae CU, Lee RT, Rifai N, Ridker PM. Blood pressure and inflammation in apparently healthy men. *Hypertension* 2001; **38**: 399-403.

Chen SC, Cheng JJ, Wu SE, Shen HC, Shyu KG, Wang DL. Cyclic strain-induced thrombomodulin expression in endothelial cells is mediated by nitric oxide, but not hydrogen peroxide. *Acta Cardiol Sin* 2008; **24**: 144-150.

Chen WJ, Yin K, Zhao GJ, Fu YC, Tang CK. The magic and mystery of MicroRNA-27 in atherosclerosis. *Atherosclerosis* 2012; **222**: 314-323.

Chen YT, Hsu HY. The role of thrombomodulin mediation of angiogenin in human melanoma growth. *National Yang-Ming University, Institute of Biotechnology in Medicine* 2006; Master thesis.

Cheng JJ, Chao YJ, Wang DL. Cyclic strain activates redox-sensitive proline-rich Tyrosine Kinase 2 (PTK2) in endothelial cells. *J Bio Chem* 2002; **277**: 48152-48157.

Cheng JJ, Chao YJ, Wung BS, Wang DL. Cyclic strain-induced plasminogen activator inhibitor-1 (PAI-1) release from endothelial cells involves reactive oxygen species. *Biochem Bioph Res Co* 1996; **225**(1): 100-105.

Cheng JJ, Wung BS, Chao YJ, Wang DL. Sequential activation of protein kinase C (PKC)- α and PKC- ϵ contributes to sustained Raf/Erk 1/2 activation in endothelial cells under mechanical strain. *J Bio Chem* 2001; **276**: 31368-31375.

Cheng TH, Shih NL, Chen SY, Loh SH, Cheng PY, Tsai CS, Liu SH, Wang DL, Chen JJ. Reactive oxygen species mediate cyclic strain-induced endothelin-1 gene expression via Ras/Raf/extracellular signal-regulated kinase pathway in endothelial cells. *J Mol Cell Cardiol* 2001; **33**: 1805-1814.

Cheng T, Liu D, Griffin JH, Fernández JA, Castellino F, Rosen ED, Fukudome K, Zlokovic BV. Activated protein C blocks p53-mediated apoptosis in ischemic human brain endothelium and is neuroprotective. *Nat Med* 2003; **9**: 338-342.

Cheng TL, Wu YT, Lin HY, Hsu FC, Liu SK, Chang BI, Chen WS, Lai CH, Shi GY, Wu HL. Functions of rhomboid family protease RHBDL2 and thrombomodulin in wound healing. *J Invest Dermatol* 2011; **131**: 2486-2494.

Chien S. Mechanotransduction and endothelial cell homeostasis: the wisdom of the cell. *Am J Physiol Heart Circ Physiol* 2007; **292**: H1209-H1224.

Chomczynski P, Sacchi N. Single-step method of RNA isolation by acid guanidinium thiocyanate-phenol-chloroform extraction. *Anal Biochem* 1987; **162**(1): 156-159.

Cines DB, Pollak ES, Buck CA, Loscalzo J, Zimmerman GA, McEver RP, Pober JS, Wick TM, Konkle BA, Schwartz BS, Barnathan ES, McCrae KR, Hug BA, Schmidt AM, Stern DM. Endothelial cells in physiology and in the pathophysiology of vascular disorders. *Blood* 1998; **91**: 3527-61.

Cocucci E, Racchetti G, Meldolesi J. Shedding microvesicles: artefacts no more. *Trends Cell Biol* 2009; **19**(2): 43-51.

Collins NT, Cummins PM, Colgan OC, Ferguson G, Birney YA, Murphy RP, Meade G, Cahill PA. Cyclic strain mediated regulation of vascular endothelial occludin and ZO-1. *Arterioscl Thromb Vasc Biol* 2006; **26**: 62-68.

Cominacini L, Pasini AF, Garbin U, Davoli A, Tosetti ML, Campagnola M et al. Oxidized low density lipoprotein (ox-LDL) binding to ox-LDL receptor-1 in endothelial cells induces the activation of NF-kappaB through an increased production of intracellular reactive oxygen species. *J Biol Chem* 2000; **28**(275): 12633-12638.

Conway EM. Thrombomodulin and its role in inflammation. *Semin Immunopathol* 2011; **34**: 107-25.

Conway EM, Nowakowski B. Biologically active thrombomodulin is synthesized by adherent synovial fluid cells and is elevated in synovial fluid of patients with rheumatoid arthritis. *Blood* 1993; **81**: 726-733.

Conway EM, Nowakowski B, Steiner-Mosonyi M. Human neutrophils synthesize thrombomodulin that does not promote thrombin-dependent protein C activation. *Blood* 1992; **80**: 1254-63.

Conway EM, Nowakowski B, Steiner-Mosonyi M. Thrombomodulin lacking the cytoplasmic domain efficiently internalizes thrombin via nonclathrin-coated, pit-mediated endocytosis. *J Cell Physiol* 1994; **158**: 285-98.

Conway EM, Pollefeyt S, Collen D, Steiner-Mosonyi M. The amino terminal lectin-like domain of thrombomodulin is required for constitutive endocytosis. *Blood* 1997; 89: 652-661.

Conway EM, Van deWouwer M, Pollefeyt S, Jurk K, Van Aken H, De Vriese A, Weitz JI, Weiler H, Hellings PW, Schaeffer P et al. The lectin-like domain of thrombomodulin confers protection from neutrophil-mediated tissue damage by suppressing adhesion molecule expression via nuclear factor kappaB and mitogen-activated protein kinase pathways. *J Exp Med* 2002; **196**: 565-77.

Corselli M, Chen CW, Sun B, Yap S, Rubin JP, Péault. The Tunica Adventitia of Human Arteries and Veins As a Source of Mesenchymal Stem Cells. *Stem Cells Dev* 2012; **21**(8): 1299-1308.

Cotran RS, Pober JS. Cytokine-endothelial interactions in inflammation, immunity, and vascular injury. *J Am Soc Nephrol* 1990; **1**: 225-35.

Cummins PM, Von Offenbergs Sweeney N, Killeen MT, Birney YA, Redmond EM, Cahill PA. Cyclic strain-mediated matrix metalloproteinase regulation within the vascular endothelium: a force to be reckoned with. *Am J Phys* 2007; **292**(1): H28-H42.

Dahlbäck B, Villoutreix BO. Regulation of blood coagulation by the protein C anticoagulant pathway: novel insights into structure-function relationships and molecular recognition. *Arterioscler Thromb Vasc Biol* 2005; **25**: 1311-1320.

Dashwood MR, Loesch A. The saphenous vein as a bypass circuit: the potential role of vascular nerves in graft performance. *Curr Vasc Pharmacol* 2009; **7**(1): 47-57.

Deanfield JE, Halcox JP, Rabelink TJ. Endothelial function and dysfunction. *Circulation* 2007; **115**: 1285-1295.

Dekker RJ, van Soest S, Fontijn RD, Salamanca S, de Groot PG, VanBavel E, Pannekoek H, Horrevoets AJ. Prolonged fluid shear stress induces a distinct set of endothelial cell genes, most specifically lung Krüppel-like factor (KLF2). *Blood* 2002; **100**: 1689-1698.

Delekta PC, Apel IJ, Gu S, Siu K, Hattori Y, McAllister-Lucas LM, Lucas PC. Thrombin-dependent NF- κ B activation and monocyte/endothelial adhesion are mediated by the CARMA3·Bcl10·MALT1 signalosome. *J Biol Chem* 2010; **285**: 41432-41442.

Delvaeye M, Noris M, De Vriese A, Esmon CT, Esmon NL, Ferrell G, Del-Favero J, Plaisance S, Claes B, Lambrechts D, Zoja C, Remuzzi G, Conway EM. Thrombomodulin mutations in atypical hemolytic-uremic syndrome. *N Engl J Med* 2009; **361**: 345-357.

Dharmasaroja P, Dharmasaroja PA, Sobhon P. Increased plasma soluble thrombomodulin levels in cardioembolic stroke. *Clin Appl Thromb Hemost* 2012; **18**: 289-293.

Distler JH, Pisetsky DS, Huber LC, Kalden JR, Gay S, Distler O. Microparticles as regulators of inflammation: novel players of cellular crosstalk in the rheumatic diseases. *Arthritis Rheum* 2005; **52**(11): 3337-3348.

Dittman WA, Kumada T, Sadler JE, Majerus PW. The structure and function of mouse thrombomodulin: phorbol myristate acetate stimulates degradation and synthesis of thrombomodulin without affecting mRNA levels in human fibroblasts. *J Biol Chem* 1988; **263**: 15815-22.

Donato AJ, Pierce GL, Lesniewski LA, Seals DR. Role of NF κ B in age-related vascular endothelial dysfunction in humans. *Aging* 2009; **1**: 678-680.

Duchemin J, Ugo V, Ianotto JC, Lecucq L, Mercier B, Abgrall JF. Increased circulating procoagulant activity and thrombin generation in patients with myeloproliferative neoplasms. *Thromb Res* 2010; **126**: 238-242.

Dusse L, Godoi L, Kazmi RS, Alpoim P, Petterson J, Lwaleed BA, Carvalho M. Sources of thrombomodulin in pre-eclampsia: renal dysfunction or endothelial damage? *Semin Thromb Hemost* 2011; **37**(2): 153-157.

Ebnet K, Vestweber D. Molecular mechanisms that control leukocyte extravasation: the selectins and the chemokines. *Histochem Cell Biol* 1999; **112**: 1-23.

Edano T, Kumai N, Mizoguchi T, Ohkuchi M. The glycosylation sites and structural characteristics of oligosaccharides on recombinant human thrombomodulin. *Int J Biochem Cell Biol* 1998; **30**: 77-88.

El-Hamamsy I, Chester AH, Yacoub MH. Cellular regulation of the structure and function of aortic valves. *J Adv Res* 2010; **1**(1): 5-12.

Ensley AE, Nerem RM, Anderson DE, Hanson SR, Hinds MT. Fluid shear stress alters the hemostatic properties of endothelial outgrowth cells. *Tissue Eng Part A* 2012; **18**: 127-36.

Esmon CT, Owen WG. The discovery of thrombomodulin. *J Thromb Haemost* 2004; **2**: 209-213.

Esmon CT. The Protein C Pathway. *Chest* 2003; **124**: 26S-32S.

Espinosa R 3rd, Sadler JE, Le Beau MM. Regional localization of the human thrombomodulin gene to 20p12-cen. *Genomics* 1989; **5**: 649-50.

Fang Y, Davies PF. Site-specific microRNA-92a regulation of Kruppel-like factors 4 and 2 in atherosusceptible endothelium. *Arterioscler Thromb Vasc Biol* 2012; **32**: 979-987.

Fang Y, Shi C, Manduchi E, Civelek M, Davies PF. MicroRNA-10a regulation of proinflammatory phenotype in athero-susceptible endothelium in vivo and in vitro. *Proc Natl Acad Sci USA* 2010; **107**: 13450-13455.

Feng Y, Yang JH, Huang H, Kennedy SP, Turi TG, Thompson JF, Libby P, Lee RT. Transcriptional profile of mechanically induced genes in human vascular smooth muscle cells. *Circ Res* 1999; **85**: 1118-23.

Fleissner F, Goerzig Y, Haverich A, Thum T. Microvesicles as novel biomarkers and therapeutic targets in transplantation medicine. *Am J Transplant* 2012; **12**: 289-297.

Foley JH, Petersen KU, Rea CJ, Harpell L, Powell S, Lillicrap D, Nesheim ME, Sørensen B. Solulin increases clot stability in whole blood from humans and dogs with hemophilia. *Blood* 2012; **119**: 3622-3628.

Freedman JE. Thrombin, thrombomodulin and extracellular signal-regulated kinases regulating cellular proliferation. *Circ Res* 2001; **88**: 651-653.

Fujiwara M, Jin E, Ghazizadeh M, Kawanami O. Antisense oligodeoxynucleotides against thrombomodulin suppress the cell growth of lung adenocarcinoma cell line A549. *Pathol Int* 2002; **52**: 204-13.

Fu Q, Wang J, Boerma M, Berbée M, Qiu X, Fink LM, Hauer-Jensen M. Involvement of heat shock factor 1 in statin-induced transcriptional upregulation of endothelial thrombomodulin. *Circ Res* 2008; **103**: 369-77.

Furchgott RF, Zawadzki JV. The obligatory role of endothelial cells in the relaxation of arterial smooth muscle by acetylcholine. *Nature* 1980; **288**: 373-6.

Geiger H, Pawar SA, Kerschen EJ, Nattamai KJ, Hernandez I, Liang HP, Fernández JA, Cancelas JA, Ryan MA, Kustikova O et al. Pharmacological targeting of the thrombomodulin-activated protein C pathway mitigates radiation toxicity. *Nat Med* 2012; **18**: 1123-1129.

Glaser CB, Morser J, Clarke JH, Blasko E, McLean K, Kuhn I, Chang RJ, Lin JH, Vilander L, Andrews WH. Oxidation of a specific methionine in thrombomodulin by activated neutrophil products blocks cofactor activity. A potential rapid mechanism for modulation of coagulation. *J Clin Invest* 1992; **90**: 2565-2573.

Goch A, Banach M, Mikhailidis DP, Rysz J, Goch JH. Endothelial dysfunction in patients with non-complicated and complicated hypertension. *Clin Exp Hypertens* 2009; **31**: 20-30.

Golledge J, Turner RJ, Gosling M, Powell JT. Rapid changes in the coagulant proteins on saphenous vein endothelium in response to arterial flow. *Angiology* 1999; **50**: 693-701.

Gosling M, Golledge J, Turner RJ, Powell JT. Arterial flow conditions downregulate thrombomodulin on saphenous vein endothelium. *Circulation* 1999; **99**: 1047-1053.

Gracia-Sancho J, Russo L, García-Calderó H, García-Pagán JC, García-Cardena G, Bosch J. Endothelial expression of transcription factor Kruppel-like factor 2 and its vasoprotective target genes in the normal and cirrhotic rat liver. *Gut* 2011; **60**: 517-524.

Grey ST, Csizmadia V, Hancock WW. Differential effect of tumor necrosis factor-alpha on thrombomodulin gene expression by human monocytoid (THP-1) cell versus endothelial cells. *Int J Hematol* 1998; **67**: 53-62.

Grey ST, Tsuchida A, Hau H, Orthner CL, Salem HH, Hancock WW. Selective inhibitory effects of the anticoagulant activated protein C on the responses of human mononuclear phagocytes to LPS, IFN-gamma, or phorbol ester. *J Immunol* 1994; **153**: 3664-3672.

Groarke, D.A., Drmota, T., Bahia, D.S., Evans, N.A., Wilson, S. and Milligan, G. Analysis of the C-terminal tail of the rat thyrotropin-releasing hormone receptor-1 in interactions and co-internalization with β -arrestin 1-green fluorescent protein. *Molecular Pharmacology* 2001; **59**(2): 375-385.

György B, Módos K, Pállinger É, Pálóczi K, Pásztói M, Misják P, Deli MA, Sipos Á, Szalai A, Voszka I et al. Detection and isolation of cell-derived microparticles are compromised by protein complexes resulting from shared biophysical parameters. *Blood* 2011; **117**(4): e39-e48.

Grote K, Flach I, Luchtefeld M, Akin E, Holland SM, Drexler H, Schieffer B. Mechanical stretch enhances mRNA expression and proenzyme release of matrix metalloproteinase-2 (MMP-2) via NAD(P)H oxidase-derived reactive oxygen species. *Circ Res* 2003; **92**: e80-e86.

Hagiwara S, Iwasaka H, Goto K, Ochi Y, Mizunaga S, Saikawa T, Noguchi T. Recombinant thrombomodulin prevents heatstroke by inhibition of high-mobility group box 1 protein in sera of rats. *Shock* 2010; **34**: 402-406.

Hahn C, Schwartz MA. Mechanotransduction in vascular physiology and atherogenesis. *Nat Rev Mol Cell Biol* 2009; **10**: 53-62.

Hannafin JA, Attia EA, Henshaw R, Warren RF, Bhargava M. Effect of cyclic strain and plating matrix on cell proliferation and integrin expression by ligament fibroblasts. *J Orthop Res* 2006; **24**(2): 149-158.

Hansson GK. Inflammation, atherosclerosis, and coronary artery disease. *N Eng J Med* 2005; **352**: 1685-1695.

Han Y, Pan J, Wang X, Qi Y, Wang S, Yan Z. Cyclic strain promotes migration and proliferation of human periodontal ligament cell via PI3K signaling pathway. *Cell Mol Bioeng* 2010; **3**(4): 369-375.

Hasaneen NA, Zucker S, Cao J, Chiarelli C, Panettieri RA, Foda HD. Cyclic mechanical strain-induced proliferation and migration of human airway smooth muscle cells: role of EMMPRIN and MMPs. *Faseb J* 2005; **19**: 1507-1509.

Hearts.vcu.edu. *Clinical Services and Programs – VCU Division of Cardiothoracic Surgery* 2012; [Online] Available at: <http://www.hearts.vcu.edu/clinical/aortic/index2.html> [Accessed: 16 May 2013].

He Y, Duraiswamy N, Frank AO, Moore JE, Jr. Blood flow in stented arteries: a parametric comparison of strut design patterns in three dimensions. *J Biomech Eng* 2005; **127**: 637-647.

Howard AB, Alexander RW, Nerem RM, Griending KK, Taylor WR. Cyclic strain induces an oxidative stress in endothelial cells. *Am J Physiol Cell Physiol* 1997; **272**(2): C421-C427.

Ho CY, Wong CK, Li EK, Tam LS, Lam CWK. Elevated plasma concentrations of nitric oxide, soluble thrombomodulin and soluble vascular cell adhesion molecule-1 in patients with systemic lupus erythematosus. *Rheumatology* 2003; **42**: 117-122.

Hsiai TK, Wu JC. Hemodynamic forces regulate embryonic stem cell commitment to vascular progenitors. *Curr Cardiol Rev* 2008; **4**(4): 269-274.

Hugel B, Martínez MC, Kunzelmann C, Freyssinet JM. Membrane microparticles: two sides of the coin. *Physiology* 2005; **20**(1): 22-27.

Hussain MU. Micro-RNAs (miRNAs): genomic organisation, biogenesis and mode of action. *Cell Tissue Res* 2012; **305**: 409-413.

Ikegami K, Suzuki Y, Yukioka T, Matsuda H, Shimazaki S. Endothelial cell injury, as quantified by the soluble thrombomodulin level, predicts sepsis/multiple organ dysfunction syndrome after blunt trauma. *J Trauma* 1998; **44**(5): 789-795.

Ikezoe T, Takeuchi A, Taniguchi A, Togitani K, Yokoyama A. Recombinant human soluble thrombomodulin counteracts capillary leakage associated with engraftment syndrome. *Bone Marrow Transplant* 2010; **46**: 616-618.

Inomata M, Ishihara Y, Matsuyama T, Imamura T, Maruyama I, Noguchi T, Matsushita K. Degradation of vascular endothelial thrombomodulin by arginine- and lysine-specific cysteine proteases from *Porphyromonas gingivalis*. *J Periodontol* 2009; **80**: 1511-1517.

Inoue N, Ramasamy S, Fukai T, Nerem RM, Harrison DG. Shear stress modulates expression of Cu/Zn superoxide dismutase in human aortic endothelial cells. *Circ Res* 1996; **79**: 32-37.

Irani K. Crippling of Krüppel (like factor 2) by bad flow portends a miRky day for endothelial function. *Circulation* 2011; **124**: 541-543.

Isermann B, Hendrickson SB, Zogg M, Wing M, Cumiskey M, Kisanuki YY, Yanagisawa M, Weiler H. Endothelium-specific loss of murine thrombomodulin disrupts the protein C anticoagulant pathway and causes juvenile-onset thrombosis. *J Clin Invest* 2001; **108**: 537-546.

Ishibazawa A, Nagaoka T, Takahashi T, Yamamoto K, Kamiya A, Ando J, Yoshida A. Effects of shear stress on the gene expressions of endothelial nitric oxide synthase, endothelin-1, and thrombomodulin in human retinal microvascular endothelial cells. *Invest Ophthalmol Vis Sci* 2011; **52**(11): 8496-8504.

Ishii H, Kizaki K, Horie S, Kazama M. Oxidized low density lipoprotein reduces thrombomodulin transcription in cultured human endothelial cells through degradation of the lipoprotein in lysosomes. *J Biol Chem* 1996; **271**: 8458-8465.

Ishii H, Majerus PW. Thrombomodulin is present in human plasma and urine. *J Clin Invest* 1985; **76**(6): 2178-2181.

Ishii H, Tezuka T, Ishikawa H, Takada K, Oida K, Horie S. Oxidized phospholipids in oxidized low-density lipoprotein down-regulate thrombomodulin transcription in vascular

endothelial cells through a decrease in the binding of RARbeta-RXRalpha heterodimers and Sp1 and Sp3 to their binding sequences in the TM promoter. *Blood* 2003; **101**: 4765-74.

Ito T, Maruyama I. Thrombomodulin: protectorate God of the vasculature in thrombosis and inflammation. *J Thromb Haemost* 2011; **9**: 168-173.

Izumi Y. Therapeutical potential of microvesicles in cardiovascular diseases. *J Genet Syndr Gene Ther* 2012; **3**:3.

Jackson DE, Tetaz TJ, Salem HH, Mitchell CA. Purification and characterization of two forms of soluble thrombomodulin from human urine. *Eur J Biochem* 1994; **221**: 1079-1087.

Jiang MJ, Yu YJ, Chen YL, Lee YM, Hung LS. Cyclic strain stimulates monocyte chemoattractant protein-1 mRNA expression in smooth muscle cells. *J Cell Biochem* 1999; **76**: 303-310.

Joner M, Nakazawa G, Finn AV, Quee SC, Coleman L, Acampado E, Wilson PS, Skorija K, Cheng Q, Xu X, Gold HK, Kolodgie FD, Virmani R. Endothelial cell recovery between comparator polymer-based drug-eluting stents. *J Am Coll Cardiol* 2008; **52**: 333-342.

Joyce DE, Gelbert L, Ciaccia A, DeHoff B, Grinnell BW. Gene expression profile of antithrombotic protein c defines new mechanisms modulating inflammation and apoptosis. *J Biol Chem* 2001; **276**: 11199-11203.

Jun P, Huangqing C, Xiaoheng L, Ruheng L, Xiaohong Z. Effects of shear stress on protein C activation, EPCR expression and TM expression in endothelial cells. *Sheng Wu Yi Xue Gong Cheng Xue Za Zhi* 2009; **26**: 303-9.

Kapur NK, Bian C, Lin E, Deming CB, Sperry JL, Hansen BS, Kakouros N, Rade JJ. Inhibition of transforming growth factor- β restores endothelial thromboresistance in vein grafts. *J Vasc Surg* 2011; **54**: 1117-1123.

Kapur NK, Deming CB, Kapur S, Bian C, Champion HC, Donahue JK, Kass DA, Rade JJ. Hemodynamic modulation of endocardial thromboresistance. *Circulation* 2007; **115**: 67-75.

Karakas M, Baumert J, Herder C, Rottbauer W, Meisinger C, Koenig W, Thorand B. Soluble thrombomodulin in coronary heart disease: lack of an association in the MONICA/KORA case-cohort study. *J Thromb Haemost* 2011; **9**: 1078-1080.

Kawano N, Yoshida S, Ono N, Himeji D, Nagahiro Y, Sayaka Kawano, Yamashita K, Ikeda N, Uezono S, Ochiai H, Kawano F, Kikuchi I, Ishikawa F, Shimoda K, Ueda A, Akashi K. Clinical features and outcomes of 35 disseminated intravascular coagulation cases treated with recombinant human soluble thrombomodulin at a single institution. *J Clin Exp Hematop* 2011; **51**: 101-107.

Kim AY, Walinsky PL, Kolodgie FD, Bian C, Sperry JL, Deming CB, Peck EA, Shake JG, Ang GB, Sohn RH, Esmon CT, Virmani R, Stuart RS, Rade JJ. Early loss of thrombomodulin expression impairs vein graft thromboresistance. *Circ Res* 2002; **90**: 205-212.

Kobayashi H, Sadakata H, Suzuki K, She MY, Shibata S, Terao T. Thrombomodulin release from umbilical endothelial cells initiated by preeclampsia plasma-induced neutrophil activation. *Obstet Gynecol* 1998; **92**: 425-430.

Kokame K, Zheng X, Sadler JE. Activation of thrombin-activable fibrinolysis inhibitor requires epidermal growth factor-like domain 3 of thrombomodulin and is inhibited competitively by protein C. *J Biol Chem* 1998; **273**: 12135-12139.

Kou B, Zhang J, Singer DRJ. Effects of cyclic strain on endothelial cell apoptosis and tubulogenesis are dependent on ROS production via NAD(P)H subunit p22phox. *Microvasc Res* 2009; **77**(2): 125-133.

Koyama T, Parkinson JF, Sié P, Bang NU, Müller-Berghaus G, Preissner KT. Different glycoforms of human thrombomodulin. Their glycosaminoglycan-dependent modulatory effects on thrombin inactivation by heparin cofactor II and antithrombin III. *Eur J Biochem* 1991; **198**: 563-570.

Krukemyer JJ, Talbert RL. Lovastatin: a new cholesterol-lowering agent. *Pharmacotherapy* 1987; **7**: 198-210.

Kumar A, Hoffman TA, Dericco J, Naqvi A, Jain MK, Irani K. Transcriptional repression of Kruppel like factor-2 by the adaptor protein p66shc. *FASEB J* 2009; **23**: 4344-4352.

Kumar A, Murphy R, Robinson P, Wei L, Boriek AM. Cyclic mechanical strain inhibits skeletal myogenesis through activation of focal adhesion kinase, Rac-1 GTPase, and NF-kappaB transcription factor. *FASEB J* 2004; **18**(13): 1524-1535.

Laemmli UK. Cleavage of structural proteins during the assembly of the head of bacteriophage T4. *Nature* 1970; **227**(5259): 680-685.

Laplace, E. A new forceps for intestinal anastomosis. *Annals of Surgery* 1899; **29**(3): 297-305.

Lehoux S. Endothelial strain and stress in atherosclerosis. *Clin Hemorheol Micro* 2007; **37**: 47-55.

Leroyer AS, Anfosso F, Lacroix R, Sabatier F, Simoncini S, Njock SM, Jourde N, Brunet P, Camoin-Jau L, Sampol J, Dignat-George, F. Endothelial-derived microparticles: Biological conveyors at the crossroad of inflammation, thrombosis and angiogenesis. *Thromb Haemost* 2010; **104**: 456-463.

Leung LL, Nishimura T, Myles T. Regulation of tissue inflammation by thrombin-activatable carboxypeptidase B (or TAFI). *Adv Exp Med Biol* 2008; **632**: 61-69.

Li C, Hu Y, Sturm G, Wick G, Xu Q. Ras/Rac-dependent activation of p38 mitogen-activated protein kinases in smooth muscle cells stimulated by cyclic strain stress. *Arterioscl Thromb Vas* 2000; **20**: e1-e9.

Li D, Yang P, Xiong Q, Song X, Yang X, Liu L, Yuan W, Rui YC. MicroRNA-125a/b-5p inhibits endothelin-1 expression in vascular endothelial cells. *J Hypertens* 2010; **28**: 1646-1654.

Li JM, Singh MJ, Itani M, Vasiliu C, Hendricks G, Baker SP, Hale JE, Rohrer MJ, Cutler BS, Nelson PR. Recombinant human thrombomodulin inhibits arterial neointimal hyperplasia after balloon injury. *J Vasc Surg* 2004; **39**: 1074-1083.

Li YH, Hsieh CY, Wang DL, Chung HC, Liu SL, Chao TH, Shi GY, Wu HL. Remodeling of carotid arteries is associated with increased expression of thrombomodulin in a mouse transverse aortic constriction model. *Thromb Haemost* 2007; **97**: 658-64.

Li YP, Chen Y, John J, Moylan J, Jin B, Mann DL, Reid MB. TNF-alpha acts via p38 MAPK to stimulate expression of the ubiquitin ligase atrogin1/MAFbx in skeletal muscle. *FASEB J* 2005; **19**(3): 362-370.

Liddy P, Ridker PM, Hansson GK. Progress and challenges in translating the biology of atherosclerosis. *Nature* 2011; **473**: 317-325.

Light DR, Glaser CB, Betts M, Blasko E, Campbell E, Clarke JH, McCaman M, McLean K, Nagashima M, Parkinson JF, Rumennik G, Young T, Morser J. The interaction of thrombomodulin with Ca²⁺. *Eur J Biochem* 1999; **262**: 522-533.

Lim SS, Vos T, Flaxman AD, Danaei G, Shibuya K, Adair-Rohani H et al. A comparative risk assessment of burden of disease and injury attributable to 67 risk factors and risk factor

clusters in 21 regions, 1990-2010: a systematic analysis for the Global Burden of Disease Study 2010. *Lancet*, 2012, **380**(9859): 2224–2260.

Lin FY, Tsai YT, Lee CY, Lin CY, Lin YW, Li CY, Shih CM, Huang CY, Chang NC, Tsai JC et al. TNF- α -decreased thrombomodulin expression in monocytes is inhibited by propofol through regulation of tristetraprolin and human antigen R activities. *Shock* 2011; **36**(3): 279-288.

Lin JH, McLean K, Morser J, Young TA, Wydro RM, Andrews WH, Light DR. Modulation of glycosaminoglycan addition in naturally expressed and recombinant human thrombomodulin. *J Biol Chem* 1994; **269**: 25021-25030.

Lin PY, Shen HC, Chen CJ, Wu SE, Kao HL, Huang JH, Wang DL, Chen SC. The inhibition in tumor necrosis factor-alpha-induced attenuation in endothelial thrombomodulin expression by carvedilol is mediated by nuclear factor-kappaB and reactive oxygen species. *J Thromb Thrombolysis* 2010; **29**: 52-59.

Lin SJ, Chen YH, Lin FY, Hsieh LY, Wang SH, Lin CY, Wang YC, Ku HH, Chen JW, Chen YL. Pravastatin induces thrombomodulin expression in TNF α -treated human aortic endothelial cells by inhibiting Rac1 and Cdc42 translocation and activity. *J Cell Biochem* 2007; **101**(3): 642-653.

Lin SJ, Hsieh FY, Chen YH, Lin CC, Kuan II, Wang SH, Wu CC, Chien HF, Lin FY, Chen YL. Atorvastatin induces thrombomodulin expression in the aorta of cholesterol-fed rabbits and in TNF α -treated human aortic endothelial cells. *Histol Histopathol* 2009; **24**: 1147-1159.

Lin SM, Wang YM, Lin HC, Lee KY, Huang CD, Liu CY, Wang CH, Kuo HP. Serum thrombomodulin level relates to the clinical course of disseminated intravascular coagulation, multiorgan dysfunction syndrome, and mortality in patients with sepsis. *Crit Care Med* 2008; **36**: 683-689.

Liu PL, Tsai JR, Chiu CC, Hwang JJ, Chou SH, Wang CK, Wu SJ, Chen YL, Chen WC, Chen YH, Chong IW. Decreased expression of thrombomodulin is correlated with tumor cell invasiveness and poor prognosis in nonsmall cell lung cancer. *Mol Carcinogen* 2010; **49**: 874-881.

Liu ZH, Wei R, Wu YP, Lisman T, Wang ZX, Han JJ, Ren DL, Chen B, Xia ZL, Chen B, Zhu Z, Zhang Y, Cui X, Hu HT, de Groot PG, Xu WB. Elevated plasma tissue-type plasminogen activator (t-PA) and soluble thrombomodulin in patients suffering from severe acute respiratory syndrome (SARS) as a possible index for prognosis and treatment strategy. *Biomed Environ Sci* 2005; **18**: 260-264.

Livak KJ, Schmittgen TD. Analysis of relative gene expression data using real-time quantitative PCR and the 2(-delta delta C(T)) method. *Methods* 2001; **25**(4): 402-408.

Lohi O, Urban S, Freeman M. Diverse substrate recognition mechanisms for rhomboids; thrombomodulin is cleaved by Mammalian rhomboids. *Curr Biol* 2004; **14**: 236-241.

MacGregor IR, Perrie AM, Donnelly SC, Haslett C. Modulation of human endothelial thrombomodulin by neutrophils and their release products. *Am J Respir Crit Care Med* **1997**; **155**: 47-52.

Maillard C, Berruyer M, Serre CM, Amiral J, Dechavanne M, Delmas PD. Thrombomodulin is synthesized by osteoblasts, stimulated by 1,25-(OH)₂D₃ and activates protein C at their cell membrane. *Endocrinology* 1993; **133**: 668-74.

Malek AM, Izumo S. Molecular aspects of signal transduction of shear stress in the endothelial cell. *J Hypertens* 1994; **12**: 989-999.

Malek AM, Jackman R, Rosenberg RD, Izumo S. Endothelial expression of thrombomodulin is reversibly regulated by fluid shear stress. *Circ Res* 1994; **74**: 852-860.

Mann HJ, Short MA, Schlichting DE. Protein C in critical illness. *Am J Health-Syst Ph* 2009; **66**(12): 1089-1096.

Mao SS, Holahan MA, Bailey C, Wu G, Colussi D, Carroll SS, Cook JJ. Demonstration of enhanced endogenous fibrinolysis in thrombin activatable fibrinolysis inhibitor-deficient mice. *Blood Coagul Fibrinolysis* 2005; **16**: 407-415.

Marchetti M, Vignoli A, Bani MR, Balducci D, Barbui T, Falanga A. All-trans retinoic acid modulates microvascular endothelial cell hemostatic properties. *Haematologica* 2003; **88**: 895-905.

Maruyama I, Majerus PW. The turnover of thrombin-thrombomodulin complex in cultured human umbilical vein endothelial cells and A549 lung cancer cells. Endocytosis and degradation of thrombin. *J Biol Chem* 1985; **260**: 15432-15438.

Matsushita H, Lee K, Tsao PS. Cyclic strain induces reactive oxygen species production via an endothelial NAD(P)H oxidase. *J Cell Biochem* 2001; **81**(S36): 99-106.

Matsuyama T, Izumi Y, Shibata K, Yotsumoto Y, Obama H, Uemura M, Maruyama I, Sueda T. Expression and activity of thrombomodulin in human gingival epithelium: in vivo and in vitro studies. *J Periodontal Res* 2000; **35**: 146-57.

Matsusaki M, Omichi M, Maruyama I, Akashi M. Physical adsorption of human thrombomodulin (ART-123) onto polymeric biomaterials for developing an antithrombogenic blood-contacting material. *J Biomed Mater Res A* 2008; **84**: 1-9.

Matsuyama T, Tokuda M, Izumi Y. Significance of thrombomodulin release from gingival epithelial cells in periodontitis patients. *J Periodontal Res* 2008; **43**: 379-385.

McKinley MP, O'Loughlin VD. *Human anatomy* 2006. McGraw-Hill Higher Education.

Menschikowski M, Hagelgans A, Eisenhofer G, Tiebel O, Siegert G. Reducing agents induce thrombomodulin shedding in human endothelial cells. *Thromb Res* 2010; **126**: e88-93.

Michiels C. Endothelial cell functions. *J Cell Physiol* 2003; **196**: 430-43.

Mishra N, Vercauteren E, Develter J, Bammens R, Declerck PJ, Gils A. Identification and characterisation of monoclonal antibodies that impair the activation of human thrombin activatable fibrinolysis inhibitor through different mechanisms. *Thromb Haemost* 2011; **106**: 90-101.

Mok CC, Poon WL, Lai JP, Wong CK, Chiu SM, Wong CK, Lun SW, Ko GT, Lam CW, Lam CS. Metabolic syndrome, endothelial injury, and subclinical atherosclerosis in patients with systemic lupus erythematosus. *Scand J Rheumatol* 2010; **39**: 42-49.

Moore J, Jr, Berry JL. Fluid and solid mechanical implications of vascular stenting. *Ann Biomed Eng* 2002; **30**: 498-508.

Morser J. Thrombomodulin links coagulation to inflammation and immunity. *Curr Drug Targets* 2012; **13**: 421-431.

Morser J, Gabazza EC, Myles T, Leung LL. What has been learnt from the thrombin-activatable fibrinolysis inhibitor deficient mouse? *J Thromb Haemost* 2010; **8**: 868–876.

Mosnier LO, Bouma BN. Regulation of fibrinolysis of thrombin activatable fibrinolysis inhibitor, an unstable carboxypeptidase B that unites the pathways of coagulation and fibrinolysis. *Arterioscler Thromb Vasc Biol* 2006; **26**: 2445-2453.

Motley ED, Eguchi K, Patterson MM, Palmer PD, Suzuki H, Eguchi S. Mechanism of endothelial nitric oxide synthase phosphorylation and activation by thrombin. *Hypertension* 2007; **49**: 577-583.

Muralidharan-Chari V, Clancy JW, Sedgwick A, D'Souza-Schorey C. Microvesicles: mediators of extracellular communication during cancer progression. *J Cell Sci* 2010; **123**: 1603-1611.

Nakagami H, Kaneda Y, Ogihara T, Morishita R. Endothelial dysfunction in hyperglycemia as a trigger of atherosclerosis. *Curr Diabetes Rev* 2005; **1**: 59-63.

Nakano M, Furutani M, Hiraishi S, Ishii H. Characterization of soluble thrombomodulin fragments in human urine. *Thromb Haemost* 1998; **79**: 331-7.

Nakano M, Furutani M, Shinno H, Ikeda T, Oida K, Ishii H. Elevation of soluble thrombomodulin antigen levels in the serum and urine of streptozotocin-induced diabetes model rats. *Thromb Res* 2000; **99**(1): 83-91.

Nakashima M, Uematsu T, Umemura K, Maruyama I, Tsuruta K. A novel recombinant soluble human thrombomodulin, ART-123, activates the protein C pathway in healthy male volunteers. *J Clin Pharmacol* 1998; **38**: 540-544.

Nanayakkara PWB, Gaillard CAJM. Vascular disease and chronic renal failure: new insights. *Neth J Med* 2010; **68**: 5-10.

Nan B, Yang H, Yan S, Lin PH, Lumsden AB, Yao Q, Chen C. C-reactive protein decreases expression of thrombomodulin and endothelial protein C receptor in human endothelial cells. *Surgery* 2005; **138**: 212-222.

Nara H, Okamoto H, Minota S, Yoshio T. Mouse monoclonal anti-human thrombomodulin antibodies bind to and activate endothelial cells through NF-kappaB activation in vitro. *Arthritis Rheum* 2006; **54**: 1629-1637.

Nesheim M. Thrombin and fibrinolysis. *Chest* 2003; **124**: 33-39.

Nesheim M, Wang W, Boffa M, Nagashima M, Morser J, Bajzar L. Thrombin, thrombomodulin and TAFI in the molecular link between coagulation and fibrinolysis. *Thromb Haemost* 1997; **78**: 386-391.

Nieuwland R, Berckmans RJ, Rotteveel-Eijkman RC, Maquelin KN, Roozendaal KJ, Jansen PGM, Have KT, Eijnsman L, Hack CE, Sturk A. Cell-derived microparticles generated in patients during cardiopulmonary bypass are highly procoagulant. *Circ* 1997; **96**: 3534-3541.

Noel JK, Crean S, Claffin JE, Rawganathan G, Linz H, Lahn M. Systemic review to establish the safety profiles for direct and indirect inhibitors of p38 mitogen-activated protein kinases for treatment of cancer. *Med Onco* 2008; **25**(3): 323-330.

Nomura E, Kohriyama T, Kozuka K, Kajikawa H, Nakamura S, Matsumoto M. Significance of serum soluble thrombomodulin level in acute cerebral infarction. *Eur J Neurol* 2004; **11**: 329-334.

Ogawa S, Shreeniwas R, Brett J, Clauss M, Furie M, Stern DM. The effect of hypoxia on capillary endothelial cell function: modulation of barrier and coagulant function. *Br J Haematol* 1990; **75**: 517-24.

Ogawa Y, Yamakawa K, Ogura H, Kiguchi T, Mohri T, Nakamori Y, Kuwagata Y, Shimazu T, Hamasaki T, Fujimi S. Recombinant human soluble thrombomodulin improves mortality and respiratory dysfunction in patients with severe sepsis. *J Trauma* 2012; **72**(5): 1150-1157.

Ogura H, Tanaka H, Koh T, Fujita K, Fujimi S, Nakamori Y, Hosotsubo H, Kuwagata Y, Shimazu T, Sugimoto H. Enhanced production of endothelial microparticles with increased binding to leukocytes in patients with severe systemic inflammatory response syndrome. *J Trauma* 2004; **56**: 823-831.

Oida K, Takai H, Maeda H, Takahashi S, Tamai T, Nakai T, Miyabo S, Ishii H. Plasma thrombomodulin concentration in diabetes mellitus. *Diabetes Res Clin Pract* 1990; **10**: 193-196.

Okada M, Matsumori A, Ono K, Furukawa Y, Shioi T, Iwasaki A, Matsushima K, Sasayama S. Cyclic stretch upregulates production of interleukin-8 and monocyte chemoattractant and activating factor/monocyte chemoattractant protein-1 in human endothelial cells. *Arterioscler Thromb Vasc Biol* 1998; **18**: 894-901.

Okamoto T, Tanigami H, Suzuki K, Shimaoka M. Thrombomodulin: A bifunctional modulator of inflammation and coagulation in sepsis. *Critical Care Research and Practice* 2012; **2012**: article ID 614545.

Omichi M, Matsusaki M, Kato S, Maruyama I, Akashi M. Enhancement of the blood compatibility of dialyzer membranes by the physical adsorption of human thrombomodulin (ART-123). *J Biomed Mater Res B Appl Biomater* 2010; **95**: 291-297.

Paravicini TM, Touyz RM. Redox signaling in hypertension. *Cardio Res* 2006; **71**: 247-258.

Park R, Song J, An SSA. Elevated levels of activated and inactivated thrombin-activable fibrinolysis inhibitor in patients with sepsis. *Korean J Hematol* 2010; **45**(4): 264-268.

Pawlak K, Myśliwiec M, Pawlak D. Kynurenine pathway - a new link between endothelial dysfunction and carotid atherosclerosis in chronic kidney disease patients. *Adv Med Sci* 2010; **55**: 196-203.

Pearson JD. Endothelial cell function and thrombosis. *Baillieres Best Pract Res Clin Haematol* 1999; **12**: 329-41.

Pober JS, Min W, Bradley JR. Mechanisms of endothelial dysfunction, injury and death. *Annu Rev Pathol Mech Dis* 2009; **4**: 71-95.

Pries AR, Secomb TW, Gaehtgens P. The endothelial surface layer. *Pflugers Arch* 2000; **440**: 653-66.

Qin B, Yang H, Xiao B. Role of microRNAs in endothelial inflammation and senescence. *Mol Biol Rep* 2012; **39**: 4509-4518.

Rajashekhar G, Gupta A, Marin A, Friedrich J, Willuweit A, Berg DT, Cramer MS, Sandusky GE, Sutton TA, Basile DP, Grinnell BW, Clauss M. Soluble thrombomodulin reduces inflammation and prevents microalbuminuria induced by chronic endothelial activation in transgenic mice. *Am J Physiol Renal Physiol* 2012; **302**: F703-712.

Ran XZ, Ran X, Zong ZW, Liu DQ, Xiang GM, Su YP, Zheng HE. Protective effect of atorvastatin on radiation-induced vascular endothelial cell injury in vitro. *J Radiat Res* 2010; **51**: 527-533.

Recomodulin.com. Mechanism of Action. About Recomodulin™ (ART-123). The world's first recombinant human thrombomodulin. *Asahi Kasei Pharma Corporation*; Available at: <http://www.recomodulin.com/en/recomodulin/mechanism.html> [Accessed: 27 May 2013].

Redl H, Schlag G, Schiesser A, Davies J. Thrombomodulin release in baboon sepsis: its dependence on the dose of *Escherichia coli* and the presence of tumor necrosis factor. *J Infect Dis* 1995; **171**: 1522-1527.

Rezaie AR. The occupancy of endothelial protein C receptor by its ligand modulates the par-1 dependent signaling specificity of coagulation proteases. *IUBMB Life* 2011; **63**: 390-396.

Riewald M, Petrovan RJ, Donner A, Ruf W. Activated protein C signals through the thrombin receptor PAR1 in endothelial cells. *J Endotoxin Res* 2003; **9**: 317-321.

Rijneveld AW, Weijer S, Florquin S, Esmon CT, Meijers JC, Speelman P, Reitsma PH, Ten Cate H, van der Poll T. Thrombomodulin mutant mice with a strongly reduced capacity to generate activated protein C have an unaltered pulmonary immune response to respiratory pathogens and lipopolysaccharide. *Blood* 2004; **103**: 1702-1709.

Rossi J, Jonak P, Rouleau L, Danielczak L, Tardif JC, Leask RL. Differential response of endothelial cells to simvastatin when conditioned with steady, non-reversing pulsatile or oscillating shear stress. *Ann Biomed Eng* 2011; **39**: 402-413.

Rossi J, Rouleau L, Tardif JC, Leask RL. Effect of simvastatin on Kruppel-like factor2, endothelial nitric oxide synthase and thrombomodulin expression in endothelial cells under shear stress. *Life Sci* 2010; **87**: 92-99.

Rousseau A, Favier R, Van Dreden P. Elevated circulating soluble thrombomodulin activity, tissue factor activity and circulating procoagulant phospholipids: new and useful markers for pre-eclampsia? *Eur J Obstet Gynecol Reprod Biol* 2009; **146**: 46-49.

Ryang YM, Dang J, Kipp M, Petersen KU, Fahlenkamp AV, Gempt J, Wesp D, Rossaint R, Beyer C, Coburn M. Solulin reduces infarct volume and regulates gene-expression in transient middle cerebral artery occlusion in rats. *BMC Neurosci* 2011; **12**: 113.

Sabiosciences.com. *Adhesion molecules and mechanotransduction in vascular physiology and disease* 1997; [online] Available at: <http://www.sabiosciences.com/pathwaymagazine/minireview/Adhesionmoleculesmechanotransduction.php> [Accessed: 16 May 2013].

Saito H, Maruyama I, Shimazaki S, Yamamoto Y, Aikawa N, Ohno R, Hirayama A, Matsuda T, Asakura H, Nakashima M, Aoki N. Efficacy and safety of recombinant human soluble thrombomodulin (ART-123) in disseminated intravascular coagulation: results of a phase III, randomized, double-blind clinical trial. *J Thromb Haemost* 2007; **5**: 31-41.

Sakai M, Ikezoe T, Bandobashi K, Yokoyama A. Successful treatment of thrombotic thrombocytopenic purpura associated with systemic lupus erythematosus with recombinant human soluble thrombomodulin. *Thromb Res* 2010; **126**: e392-393.

Salem HH, Maruyama I, Ishii H, Majerus PW. Isolation and characterization of thrombomodulin from human placenta. *J Bio Chem* 1984; **259**: 12246-12251.

Salomaa V, Matei C, Aleksic N, Sansores-Garcia L, Folsom AR, Juneja H, Chambless LE, Wu KK. Soluble thrombomodulin as a predictor of incident coronary heart disease and symptomless carotid artery atherosclerosis in the Atherosclerosis Risk in Communities (ARIC) Study: a case-cohort study. *Lancet* 1999; **353**: 1729-1734.

Sambrook J, Fritsch E, Maniatis T. Molecular cloning: a laboratory manual. *New York: Cold Spring Harbor Laboratory Press* 1989.

Sasmoto A, Nagino M, Kobayashi S, Naruse K, Nimura Y, Sokabe M. Mechanotransduction by integrin is essential for IL-6 secretion from endothelial cells in response to uniaxial continuous stretch. *Am J Physiol Cell Physiol* 2005; **288**(5): C1012-C1022.

Satta N, Freyssinet JM, Toti F. The significance of human monocyte thrombomodulin during membrane vesiculation and after stimulation by lipopolysaccharide. *Brit J Haematol* 1997; **96**: 534-542.

Schaper, W. Collateral circulation: past and present. *Basic Research in Cardiology* 2009; **104**(1):5-21.

Schiffrin, E. Reactivity of small blood vessels in hypertension: relation with structural changes. State of the art lecture. *Hypertension* 1992; **19**(2):1-9.

Séguin C, Abid MR, Spokes KC, Aird WC. Thrombin downregulates thrombomodulin expression and activity in primary human endothelial cells. *Endothelium* 2008; **15**: 143-8.

Sen-Banerjee S, Mir S, Lin Z, Hamik A, Atkins GB, Das H, Banerjee P, Kumar A, Jain MK. Kruppel-like factor 2 as a novel mediator of statin effects in endothelial cells. *Circulation* 2005; **112**: 720-726.

Senet P, Peyri N, Berard M, Dubertret L, Boffa MC. Thrombomodulin, a functional surface protein on human keratinocytes, is regulated by retinoic acid. *Arch Dermatol Res* 1997; **289**: 151-57.

Sharfuddin AA, Sandoval RM, Berg DT, McDougal GE, Campos SB, Phillips CL, Jones BE, Gupta A, Grinnell BW, Molitoris BA. Soluble thrombomodulin protects ischemic kidneys. *J Am Soc Nephrol* 2009; **20**: 524-534.

Shi CS, Shi GY, Chang YS, Han HS, Kuo CH, Liu C, Huang HC, Chang YJ, Chen PS, Wu HL. Evidence of human thrombomodulin domain as a novel angiogenic factor. *Circulation* 2005; **111**: 1627-1636.

Shi J, Wang J, Zheng H, Ling W, Joseph J, Li D, Mehta JL, Ponnappan U, Lin P, Fink LM, Hauer-Jensen M. Statins increase thrombomodulin expression and function in human endothelial cells by a nitric oxide-dependent mechanism and counteract tumor necrosis factor alpha-induced thrombomodulin downregulation. *Blood Coagul Fibrinolysis* 2003; **14**: 575-585.

Shyu KG, Wang BW, Lin CM, Chang H. Cyclic stretch enhances the expression of Toll-like receptor 4 gene in cultured cardiomyocytes via p38 MAP kinase and NF- κ B pathway. *J Biomed Sci* 2010; **17**: 1-13.

Smith PK, Krohn RI, Hermanson GT, Mallia AK, Gartner FH, Provenzano MD, Fujimoto EK, Goeke NM, Olsen BJ, Klenk DC. Measurement of protein using bicinchoninic acid. *Anal Biochem* 1985; **150**(1): 76-85.

Soff GA, Jackman RW, Rosenberg RD. Expression of thrombomodulin by smooth muscle cells in culture: different effects of tumor necrosis factor and cyclic adenosine monophosphate on thrombomodulin expression by endothelial cells and smooth muscle cells in culture. *Blood* 1991; **77**: 515-8.

Sohn RH, Deming CB, Johns DC, Champion HC, Bian C, Gardner K, Rade JJ. Regulation of endothelial thrombomodulin expression by inflammatory cytokines is mediated by activation of nuclear factor-kappa B. *Blood* 2005; **105**: 3910-3917.

Soltsez P, Bereczki D, Szodoray P, Magyar MT, Der H, Csipo I, Hajas A, Paragh G, Szegedi G, Bodolay E. Endothelial cell markers reflecting endothelial cell dysfunction in patients with mixed connective tissue disease. *Arthritis Res Ther* 2010; **12**: R78.

Spanier T, Oz M, Levin H, Weinberg A, Stamatis K, Stern D, Rose E, Schmidt AM. Activation of coagulation and fibrinolytic pathways in patients with left ventricular assist devices. *J Thorac Cardiovasc Sur* 1996; **112**(4): 1090-1097.

Sperry JL, Deming CB, Bian C, Walinsky PL, Kass DA, Kolodgie FD, Virmani R, Kim AY, Rade JJ. Wall tension is a potent negative regulator of *in vivo* thrombomodulin expression. *Circ Res* 2003; **92**: 41-47.

Stanková J, Rola-Pleszczyński M, D'Orléans-Juste P. Endothelin 1 and thrombin synergistically stimulate IL-6 mRNA expression and protein production in human umbilical vein endothelial cells. *J Cardiovasc Pharmacol* 1995; **26**: S505-S507.

Staszal T, Zapala B, Polus A, Sadakierska-Chudy A, Kiec-Wilk B, Stepień E, Wybrańska I, Chojnacka M, Dembińska-Kiec A. Role of microRNAs in endothelial cell pathophysiology. *Pol Arch Med Wewn* 2011; **121**: 361-366.

Stearns-Kurosawa DJ, Kurosawa S, Mollica JS, Ferrell GL, Esmon CT. The endothelial cell protein C receptor augments protein C activation by the thrombin-thrombomodulin complex. *Proc Natl Acad Sci USA* 1996; **93**: 10212-10216.

Stites WE, Froude JW 2nd. Does the oxidation of methionine in thrombomodulin contribute to the hypercoagulable state of smokers and diabetics? *Med Hypotheses* 2007; **68**: 811-821.

Su EJ, Geyer M, Wahl M, Mann K, Ginsburg D, Brohmann H, Petersen KU, Lawrence DA. The thrombomodulin analog Solulin promotes reperfusion and reduces infarct volume in a thrombotic stroke model. *J Thromb Haemost* 2011; **9**: 1174-1182.

Suarez Y, Fernandez-Hernando C, Pober JS, Sessa WC. Dicer dependent microRNAs regulate gene expression and functions in human endothelial cells. *Circ Res* 2007; **100**: 1164-1173.

Sun X, Icli B, Wara AK, Belkin N, He S, Kobzik L, Hunninghake GM, Vera MP, Blackwell TS, Baron RM, Feinberg MW. MicroRNA-181b regulates NF- κ B-mediated vascular inflammation. *J Clin Invest* 2012; **122**: 473-490.

Suzuki K, Nichioka J, Hayaoni T, Kosaka Y. Functionally active thrombomodulin is present in human platelets. *J Biochem* 1988; **104**: 628-32.

Svenungsson E, Cederholm A, Jensen-Urstad K, Fei G-Z, Faire U, Frostega J. Endothelial function and markers of endothelial activation in relation to cardiovascular disease in systemic lupus erythematosus. *Scand J Rheumatol* 2008; **37**: 352-359.

Tabit CE, Chung WB, Hamburg NM, Vita JA. Endothelial dysfunction in diabetes mellitus: molecular mechanisms and clinical implications. *Rev Endocr Metab Disord* 2010; **11**: 61-74.

Taddei A, Giampietro C, Conti A, Orsenigo F, Breviario F, Pirazzoli V, Potente M, Daly C, Dimmeler S, Dejana E. Endothelial adherens junctions control tight junctions by VE-cadherin-mediated up-regulation of claudin-5. *Nat Cell Biol* 2008; **10**: 923-34.

Takada Y, Shinkai F, Kondo S, Yamamoto S, Tsuboi H, Korenaga R, Ando J. Fluid shear stress increases the expression of thrombomodulin by cultured human endothelial cells. *Biochem Biophys Res Commun* 1994; **205**(2): 1345-1352.

Takagi T, Taguchi O, Toda M, Ruiz DB, Bernabe PG, D'Alessandro-Gabazza CN, Miyake Y, Kobayashi T, Aoki S, Chiba F, Yano Y, Conway EM, Munesue S, Yamamoto Y, Yamamoto H, Suzuki K, Takei Y, Morser J, Gabazza EC. Inhibition of allergic bronchial asthma by thrombomodulin is mediated by dendritic cells. *Am J Respir Crit Care Med* 2011; **183**: 31-42.

Takahashi Y, Hosaka Y, Niina H, Nagasawa K, Naotsuka M, Sakai K, Uemura A. Soluble thrombomodulin purified from human urine exhibits a potent anticoagulant effect in vitro and in vivo. *Thromb Haemostasis* 1995; **73**(5): 805-811.

Takeda N, Maemura K, Horie S, Oishi K, Imai Y, Harada T, Saito T, Shiga T, Amiya E, Manabe I, Ishida N, Nagai R. Thrombomodulin is a clock-controlled gene in vascular endothelial cells. *J Biol Chem* 2007; **282**: 32561-32567.

Takemoto M, Liao JK. Pleiotropic effects of 3-hydroxy-3-methylglutaryl coenzyme a reductase inhibitors. *Arterioscler Thromb Vasc Biol* 2001; **21**: 1712-1719.

Taylan A, Sari I, Kozaci DL, Yildiz Y, Bilge S, Coker I, Maltas S, Gunay N, Akkoc N. Evaluation of various endothelial biomarkers in ankylosing spondylitis. *Clin Rheumatol* 2012; **31**: 23-28.

Tazawa R, Hirosawa S, Suzuki K, Hirokawa K, Aoki N. Functional characterization of the 5'-regulatory region of the human thrombomodulin gene. *J Biochem* 1993; **113**: 600-6.

Theofilopoulos AN, Koundouris S, Kono DH, Lawson BR. The role of IFN- γ in systemic lupus erythematosus: a challenge to the Th1/Th2 paradigm in autoimmunity. *Arthritis Res* 2001; **3**: 136-141.

Théry C, Ostrowski M, Segura E. Membrane vesicles as conveyors of immune responses. *Nat Rev Immunol* 2009; **9**(8): 581-593.

Thodeti CK, Matthews B, Ravi A, Mammoto A, Ghosh K, Bracha AL, Ingber DE. TRPV4 channels mediate cyclic strain-induced endothelial cell reorientation through integrin-to-integrin signaling. *Circ Res* 2009; **104**: 1123-1130.

Thorand B, Baumert J, Herder C, Meisinger C, Koenig W. Soluble thrombomodulin as a predictor of type 2 diabetes: results from the MONICA/KORA Augsburg case-cohort study, 1984-1998. *Diabetologia* 2007; **50**: 545-548.

Thumbs.dreamstime.com. *Royal Free Stock Photography: Vascular system* 2008; [online] Available at: http://thumbd.dreamstime.com/thumblarge_281/12139130173V71Nj.jpg [Accessed: 16 May 2013].

Tineli RA, Viaro F, Dalio MB, Reis GS, Basseto S, Vicente WV, Rodrigues AJ, Evora PR. Mechanical forces and human saphenous veins: coronary artery bypass graft implications. *Rev Bras Cir Cardiovasc* 2007; **22**: 87-95.

Towbin H, Staehelin T, Gordon J. Electrophoretic transfer of proteins from polyacrylamide gels to nitrocellulose sheets: Procedure and some applications. *PNAS* 1979; **76**: 4350-4354.

Traub O, Berk BC. Laminar shear stress: mechanisms by which endothelial cells transduce an atheroprotective force. *Arterioscler Thromb Vasc Biol* 1998; **18**: 677-85.

Tsai CS, Tsai YT, Lin CY, Lin TC, Huang GS, Hong GJ, Lin FY. Expression of thrombomodulin on monocytes is associated with early outcomes in patients with coronary artery bypass graft surgery. *Shock* 2010; **34**(1): 31-39.

Urban M, Wojtkielewicz K, Głowińska B, Peczyńska J. Soluble thrombomodulin: a molecular marker of endothelial cell injury in children and adolescents with obesity. *Endokrynol Diabetol Chor Przemiany Materii Wieku Rozw* 2005; **11**: 73-77.

Uszyński M, Sztenc S, Zekanowska E, Uszyński W. Thrombomodulin in human gestational tissues: placenta, fetal membranes and myometrium. *Adv Med Sci* 2006; **51**: 312-5.

Van den Berg CW, Gonçalves-de-Andrade RM, Magnoli FC, Tambourgi DV. *Loxosceles* spider venom induces the release of thrombomodulin and endothelial protein C receptor: implications for the pathogenesis of intravascular coagulation as observed in loxoscelism. *J Thromb Haemost* 2007; **5**(5): 989-995.

Van de Wouwer, Collen D, Conway EM. Thrombomodulin-protein EPCR system: integrated to regulate coagulation and inflammation. *Arteriocler Thromb Vasc Biol* 2004; **24**(8): 1374-1383.

Van Iersel T, Stroissnig H, Giesen P, Wemer J, Wilhelm-Ogunbiyi K. Phase I study of Solulin, a novel recombinant soluble human thrombomodulin analogue. *Thromb Haemost* 2011; **105**: 302-312.

Vanhoutte PM, Perrault L, Vilaine J. *Endothelial dysfunction and vascular disease* 2007.

Vanhoutte PM. Endothelial dysfunction: the first step toward coronary arteriosclerosis. *Circ J* 2009; **73**(4): 595-601.

Vasa-Nicotera M, Chen H, Tucci P, Yang AL, Saintigny G, Menghini R, Mahè C, Agostini M, Knight RA, Melino G, Federici M. miR-146a is modulated in human endothelial cell with aging. *Atherosclerosis* 2011; **217**: 326-330.

Vion AC, Birukova AA, Boulanger CM, Birukov KG. Mechanical forces stimulate endothelial microparticle generation via caspase-dependent apoptosis-independent mechanism. *Pulm Circ* 2013; **3**(1): 95-99.

Vion AC, Ramkhelawan B, Loyer X, Chironi G, Devue C, Loirand G, Tedgui A, Lehoux S, Boulanger CM. Shear stress regulates endothelial microparticle release. *Circ Res* 2013; **112**: 1323-1333.

Virdis A, Ghiadoni L, Giannarelli C, Taddei S. Endothelial dysfunction and vascular disease in later life. *Maturitas* 2010; **67**: 20-24.

Vlassov AV, Magdaleno S, Setterquist R, Conrad R. Exosomes: current knowledge of their composition, biological functions, and diagnostic and therapeutic potentials. *BBA-Gen Subjects* 2012; **1820**: 940-948.

Voellenkle C, Rooij Jv, Guffanti A, Brini E, Fasanaro P, Isaia E, Croft L, David M, Capogrossi MC, Moles A, Felsani A, Martelli F. Deep-sequencing of endothelial cells exposed to hypoxia reveals the complexity of known and novel microRNAs. *RNA* 2012; **18**: 472-484.

Von Offenberg Sweeney N, Cummins PM, Birney YA, Cullen JP, Redmond EM, Cahill PA. Cyclic strain-mediated regulation of endothelial matrix metalloproteinase-2 expression and activity. *Cardio Res* 2004; **63**(4): 625-634.

Von Offenberg Sweeney N, Cummins PM, Cotter EJ, Fitzpatrick PA, Birney YA, Redmond EM, Cahill PA. Cyclic strain-mediated regulation of vascular endothelial cell migration and tube formation. *Biochem Bioph Res Co* 2005; **329**(2): 573-582.

Wakabayashi H, Natsuka S, Honda M, Naotsuka M, Ito Y, Kajihara J, Hase S. Structural analysis of the sugar chains of human urinary thrombomodulin. *J Biochem* 2001; **130**: 543-552.

Wang HJ, Huang HC, Chuang YC, Liao PJ, Yang DM, Yang WK, Huang H. Modulation of tissue factor and thrombomodulin expression in HAECs incubated with high glucose. *Acta Diabetol* 2012; **49**: 125-130.

Wang HJ, Lu TL, Huang H, Huang HC. Paclitaxel induces thrombomodulin downregulation in human aortic endothelial cells. *Tex Heart Inst J* 2011; **38**: 20-26.

Wang JH, Thampatty BP. An introductory review of cell mechanobiology. *Biomechan Model Mechanobiol* 2006; **5**: 1-16.

Wang W, Nagashima M, Schneider M, Morser J, Nesheim M. Elements of the primary structure of thrombomodulin required for efficient thrombin-activable fibrinolysis inhibitor activation. *J Biol Chem* 2000; **275**: 22942-22947.

Wang YX, Wu C, Vincelette J, Martin-McNulty B, Alexander S, Larsen B, Light DR, McLean K. Amplified anticoagulant activity of tissue factor-targeted thrombomodulin: in-vivo validation of a tissue factor-neutralizing antibody fused to soluble thrombomodulin. *Thromb Haemost* 2006; **96**: 317-324.

Ware LB, Fang X, Matthay MA. Protein C and thrombomodulin in human acute lung injury. *Am J Physiol-Lung C* 2003; **285**(3): L514-L521.

Weiß S, Szymczak H, Meißner A. Fatigue and endurance of coronary stents. *Materialwissenschaft und Werkstofftechnik* 2009; **40**: 1-2.

Wei HJ, Li YH, Shi GY, Liu SL, Chang PC, Kuo CH, Wu HL. Thrombomodulin domains attenuate atherosclerosis by inhibiting thrombin-induced endothelial cell activation. *Cardiovasc Res* 2011; **92**: 317-327.

Welters I, Menges T, Ballesteros M, Knothe C, Ruwoldt R, Görlach G, Hempelmann G. Thrombin generation and activation of the thrombomodulin protein C system in open heart surgery depend on the underlying cardiac disease. *Thromb Res* 1998; **92**: 1-9.

Wen DZ, Dittman WA, Ye RD, Deaven LL, Majerus PW, Sadler JE. Human thrombomodulin: complete cDNA sequence and chromosome localization of the gene. *Biochemistry* 1987; **26**: 4350-7.

Weiler H, Isermann BH. Thrombomodulin. *J Thromb Haemost* 2003; **1**: 1515-1524.

Wilson E, Sudhir K, Ives HE. Mechanical strain of rat vascular smooth muscle cells is sensed by specific extracellular matrix/integrin interactions. *J Clin Invest* 1995; **96**(5): 2364-2372.

Wolf P. The nature and significance of platelet products in human plasma. *Br J Haematol* 1967; **13**: 269-288.

Wong G, Li JM, Hendricks G, Eslami MH, Rohrer MJ, Cutler BS. Inhibition of experimental neointimal hyperplasia by recombinant human thrombomodulin coated ePTFE stent grafts. *J Vasc Surg* 2008; **47**: 608-615.

Wood MJ, Becvar LA, Prieto JH, Melacini G, Komives EA. NMR structures reveal how oxidation inactivates thrombomodulin. *Biochemistry* 2003; **42**: 11932-11942.

Wood MJ, Helena Prieto J, Komives EA. Structural and functional consequences of methionine oxidation in thrombomodulin. *Biochim Biophys Acta* 2005; **1703**: 141-147.

Wood SC, Tang X, Tesfamariam B. Paclitaxel potentiates inflammatory cytokine-induced prothrombotic molecules in endothelial cells. *J Cardiovasc Pharmacol* 2010; **55**: 276-285.

Wu HL, Lin CI, Huang YL, Chen PS, Kuo CH, Chen MS, Wu GCC, Shi GY, Yang HY, Lee H. Lysophosphatidic acid stimulates thrombomodulin lectin-like domain shedding in human endothelial cells. *Biochem Biophys Res Commun* 2008; **367**: 162-168.

Wu KK. Soluble thrombomodulin and coronary heart disease. *Curr Opin Lipidol* 2003; **14**(4): 373-375.

Wu MH, Kouchi Y, Onuki Y, Shi Q, Yoshida H, Kaplan S, Viggers RF, Ghali R, Sauvage LR. Effect of differential shear stress on platelet aggregation, surface thrombosis, and endothelialization of bilateral carotid-femoral grafts in the dog. *J Vasc Surg*. 1995; **22**: 382-90.

Wu W, Xiao H, Laguna-Fernandez A, Villarreal G Jr, Wang KC, Geary GG, Zhang Y, Wang WC, Huang HD, Zhou J, Li YS, Chien S, Garcia-Cardena G, Shyy JY. Flow-dependent regulation of Krüppel-like factor 2 is mediated by microRNA-92a. *Circulation* 2011; **124**: 633-641.

Yang SX, Yan J, Deshpande SS, Irani K, Lowenstein CJ. Rac1 regulates the release of Weibel-Palade Bodies in human aortic endothelial cells. *Chinese Med J-Peking* 2004; **117**(8): 1143-1150.

Yano Y, Geibel J, Sumpio BE. Cyclic strain induces reorganization of integrin $\alpha_5\beta_1$ and $\alpha_2\beta_1$ in human umbilical vein endothelial cells. *J Cell Biochem* 1997; **64**(3): 505-513.

Yano Y, Saito Y, Narumiya S, Sumpio BE. Involvement of rho p21 in cyclic strain-induced tyrosine phosphorylation of focal adhesion kinase (pp125^{FAK}) morphological changes and migration of endothelial cells. *Biochem Biophys Res Commun* 1996; **224**(2): 508-515.

Yao A, Wang J, Fink LM, Hardin JW, Hauer-Jensen M. Molecular cloning and sequence analysis of the 5'-flanking region of the Sprague-Dawley rat thrombomodulin gene. *DNA Seq* 1999; **10**: 55-60.

Ye J, Esmon CT, Johnson AE. The chondroitin sulfate moiety of thrombomodulin binds a second molecule of thrombin. *J Biol Chem* 1993; **268**: 2373-2379.

Yin R, Bao W, Xing Y, Xi T, Gou S. MiR-19b-1 inhibits angiogenesis by blocking cell cycle progression of endothelial cells. *Biochem Biophys Res Commun* 2012; **417**: 771-776.

Yerkovich ST, Roponen M, Smith ME, McKenna K, Bosco A, Subrata LS, Mamessier E, Wikström ME, Le Souef P, Sly PD, Holt PG, Upham JW. Allergen-enhanced thrombomodulin (blood dendritic cell antigen 3, CD141) expression on dendritic cells is associated with a TH2-skewed immune response. *J Allergy Clin Immunol* 2009; **123**: 209-16.

Yun JK, Anderson JM, Ziats NP. Cyclic strain-induced endothelial cell expression of adhesion molecules and their roles in monocyte-endothelial interaction. *J Bio Mat Res* 1999; **44**(1): 87-97.

Zaitsev S, Kowalska MA, Neyman M, Carnemolla R, Tliba S, Ding BS, Stonestrom A, Spitzer D, Atkinson JP, Poncz M, Cines DB, Esmon CT, Muzykantov VR. Targeting recombinant thrombomodulin fusion protein to red blood cells provides multifaceted thromboprophylaxis. *Blood* 2012; **119**: 4779-4785.

Zampetaki A, Zhang Z, Hu Y, Xu Q. Biomechanical stress induces IL-6 expression in smooth muscle cells via Ras/Rac1-p38 MAPK-NF- κ B signalling pathways. *Am J Physiol Heart Circ Physiol* 2005; **288**: H2946-H2954.

Zhao L, Buckman B, Seto M, Morser J, Nagashima M. Mutations in the substrate binding site of thrombin-activatable fibrinolysis inhibitor (TAFI) alter its substrate specificity. *J Biol Chem* 2003; **278**: 32359-32366.

Zycinska K, Wardyn KA, Zielonka TM, Krupa R, Lukas W. Clinical implications of serum thrombomodulin in PR3-ANCA-associated vasculitis. *Eur J Med Res* 2009; **14**: 268-70.

Appendix

BCA assay standard curve

The bicinchoninic acid assay (BCA) assay is a biochemical assay for colorimetric detection and quantitation of total protein. In this method, protein reduces Cu^{+2} to Cu^{+1} under alkaline conditions, which in turn reacts with bicinchoninic acid to produce a complex (purple) that absorbs light at 562 nm. Results of standards and unknown samples are then graphed to calculate protein concentration (Fig A).

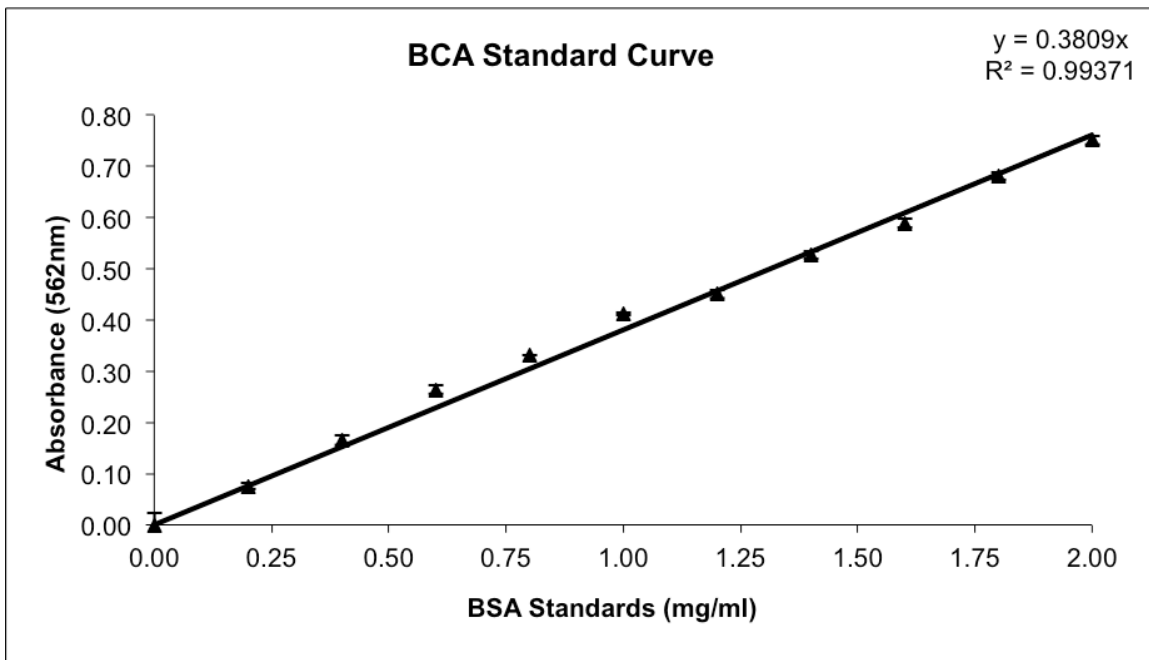


Figure A: Typical standard curve for a BCA assay, with absorbance on the Y-axis and concentration on the X-axis.

Unpublished results

Baseline response from signalling component studies

There is a lot of variation in the fold decrease in TM cellular expression and increase in TM release between 0% and 7.5% strain in the signalling component studies. To address this, we merged all baseline data from these experiments to show that there is a significant decrease in TM cellular expression and increase in TM release following 7.5% cyclic strain (Fig B).

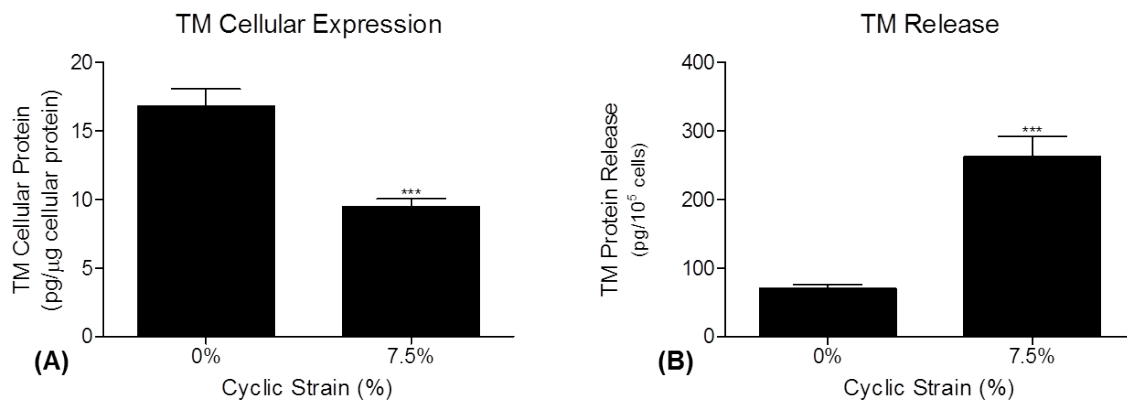


Figure B: Effect of cyclic strain on TM expression and release. Baseline response data from signalling components studies showing effect of cyclic strain on (A) TM cellular expression and (B) TM release. ($P \leq 0.0001$ determined by unpaired Student's t test).

Further microvesicle analysis

To further investigate the molecular size of soluble TM (sTM) post-strain, cell culture media was concentrated using Amicon[®] Ultra-2 centrifugal filter devices, determined for protein concentration with a BCA assay and subsequently, analysed for TM cellular expression via Western blotting (Fig B). TM was observed in cellular lysates at different molecular weights including 100 kDa. sTM was detected in cell culture media at 50, 60, 70 and 100 kDa. This suggests that a portion of TM release may be on a microvesicle and another proportion may be due to proteolytic cleavage (e.g., by MMPs).

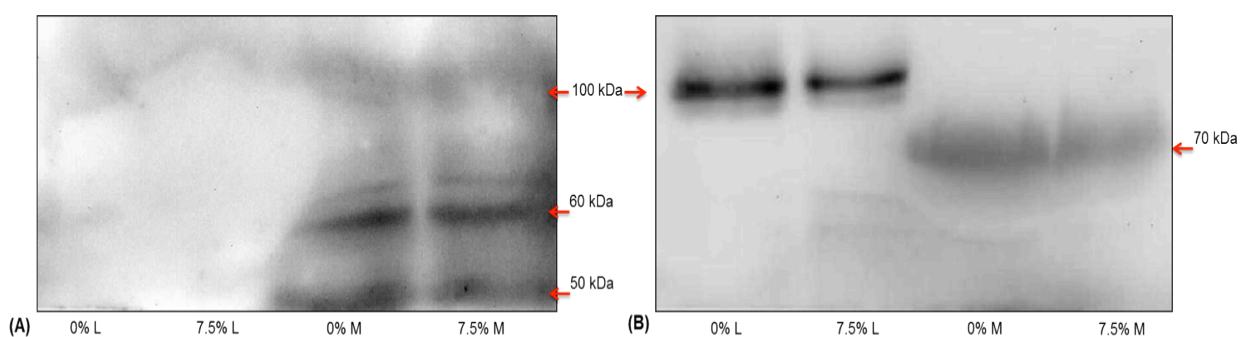


Figure C: Detection of TM in cell lysates and media supernatants. HAECs were exposed to cyclic strain (0% and 7.5%, for 24 hrs). Media supernatants were concentrated using Amicon[®] Ultra-2 centrifugal filter devices and then monitored alongside cell lysates for TM by Western blotting. TM was detected in cell lysates at 100 kDa and in media supernatants at 50, 60, 70 and 100 kDa. Key: L, lysates; M, media.

Further conditioned media analysis

Cell culture media was harvested from HAECs post-cyclic strain (0% and 7.5%, 0-48 hrs), incubated with static “reporter” HAECs for 24 hrs and then cell lysates were harvested. TM cellular expression was subsequently measured via ELISA (Fig C). We observed a downward trend in TM cellular expression following incubation with conditioned “strained” media. Nevertheless, there was no substantial affect noted.

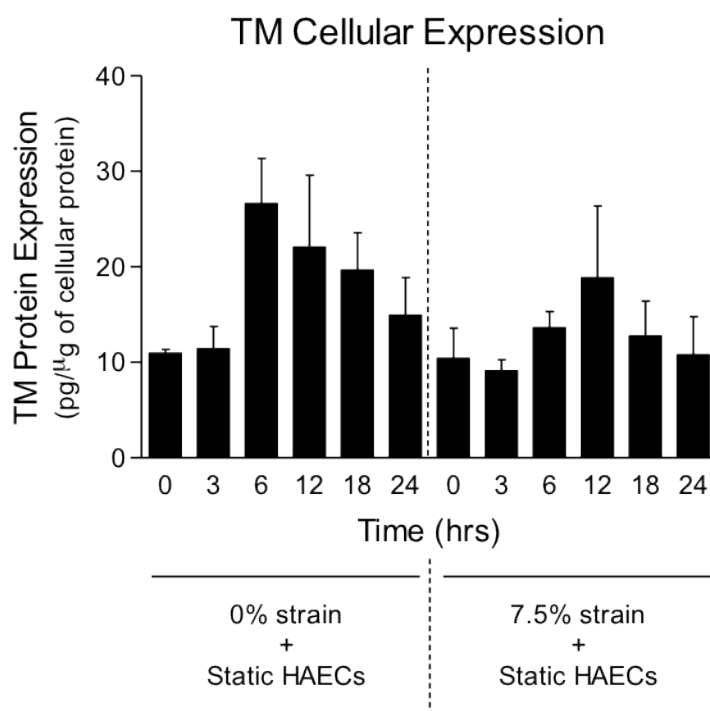


Figure D: Conditioned media and TM cellular expression. HAECs were pre-exposed to cyclic strain (0% - 7.5% for 24 hrs) and cell culture media was harvested. Static “reporter” HAECs were incubated with this conditioned (strained) media for 24 hrs. Subsequently, cell lysates were harvested and measured for TM cellular expression by ELISA.

KLF2 mRNA expression

As already mentioned in Chapter 1 (Section 1.2.3), TM levels are regulated by transcription factor Krüppel-like factor 2 (KLF2), which is shear stress sensitive (Kumar et al., 2009). This transcription factor is inhibited by a microRNA, miR-92a that then indirectly inhibits TM (Dekker et al., 2002; Ishibazawa et al., 2011). The relationship between KLF2 and laminar flow has been studied extensively (Bonauer and Dimmeler, 2009; Dekker et al., 2002; Irani, 2011; Ishibazawa et al., 2011; Gracia-Sancho et al., 2011; Wu et al., 2011) but cyclic strain is somewhat less investigated.

Dose response studies were carried out on HAECs to examine the effect of cyclic strain on KLF2 mRNA expression levels. For mRNA studies, two wells were harvested per sample post-cyclic strain (0% and 7.5%) and then analysed using qPCR with a 7900HT Fast real-time PCR system (Applied Biosystems, CA USA) (Fig D). Firstly, primers designed to target KLF2 for PCR amplification and then visualized on an agarose gel to ensure correct band size. To determine the specificity of my primers, I carried out a melt curve analysis to generate a dissociation curve for my primers for KLF2. We found that KLF2 was increased dose-dependently in response to cyclic strain, which may potentially be related to TM regulation. Further experiments, will provide statistical clarity and also, identify if KLF2 indirectly regulates TM expression in HAECs.

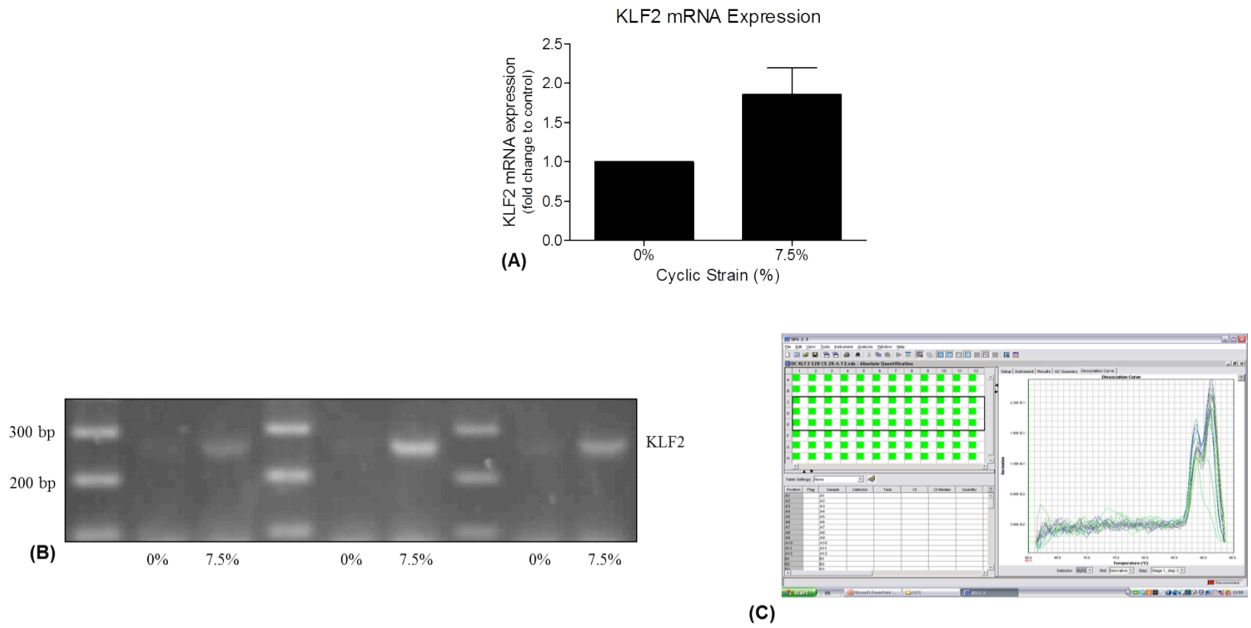


Figure E: Dose-dependent effect of cyclic strain on KLF2 mRNA expression. **(A)** Following application of cyclic strain (0% and 7.5% for 24 hrs) to HAECs, mRNA KLF2 expression was measured using qPCR (n=3). **(B)** The same samples were monitored for KLF2 expression by standard PCR and visualised on an agarose gel (n=3). **(C)** Melt curve analysis was carried out on the KLF2 primers to determine their specificity.

Recipes

Coomassie stain

Coomassie Brilliant Blue R250 0.25g

Methanol:dH₂O (1:1 v/v) 90 ml

Glacial Acetic acid 10ml

Filter the Coomassie stain using a 0.25 µm filter

Coomassie destain solution

Methanol:Acetic acid mixed in a 50:50 ratio

10X Phosphate buffered saline (PBS)

NaCl 80 g

Na₂HPO₄ 14.5 g

KH₂PO₄ 2 g

KCL 2 g

pH adjusted to 7.3 with HCL and volume adjusted to 1 L with dH₂O

TBS-T

1X TBS 1L

Tween 20 1 ml

1.28X RIPA Lysis buffer(50 mls)

Hepes	0.7625 g (64 mM)
NaCl	0.561 g (192 mM)
20% Triton X-100 stock	3.2 ml (1.28% v/v)
10% Sodium deoxycholate stock	3.2 ml (0.64% v/v)
10% SDS stock	0.64 ml (0.128% v/v)

Volume adjusted to 50 mls with dH₂O and stored at 4°C

1X RIPA (1 ml)

Protease inhibitors (25X)	40 µl
1.28X RIPA	780 µl
0.5M sodium fluoride	20 µl
0.5M EDTA (ph 8.0)	10 µl
0.1M sodium phosphate	100 µl
10mM sodium orthovanadate	100 µl

1X Tris buffered saline (TBS)

Tris base	6.1 g
NaCL	8.8 g
dH ₂ O	800 ml

pH adjusted to 7.5 with HCL and volume adjusted to 1 L